Cape Peninsula
University of Technology

VOLTAGE CONTROL USING DEMAND-SIDE RESOURCES IN ACTIVE DISTRIBUTION NETWORKS

by

WILLIAM NORMAN MURRAY

Thesis submitted in fulfilment of the requirements for the degree.

Doctor of Engineering: Electrical Engineering

in the Faculty of Engineering

at the Cape Peninsula University of Technology

Supervisor: Dr. Marco Adonis
Co-supervisor: Prof. Atanda Raji

Bellville
Date submitted: August 2022

CPUT copyright information

The dissertation/thesis may not be published either in part (in scholarly, scientific, or technical journals), or (as a monograph), unless permission has been obtained from the University.

DECLARATION

I, William Norman Murray, declare that the contents of this dissertation/thesis represent my own unaided work, and that the dissertation/thesis has not previously been submitted for academic examination towards any qualification. Furthermore, it represents my own opinions and not necessarily those of the Cape Peninsula University of Technology.

28/09/22

Signed **Date**

ABSTRACT

The demand for electricity is projected to increase over the next few years, driven by economics, population growth and electrification. The need for alternative energy resources, especially at distribution level, will find greater traction in the future, based on this demand, a rise in electricity pricing and a decreased carbon footprint may result. It is projected that renewable energy will account for 38% of energy demand by 2050 in South Africa. This increasing demand for renewable energy, especially at distribution level, will change the traditional passive grid into an active grid and create a challenge for optimal voltage regulation in real-time. Given the above, it is projected that the distribution grid will have a more active role, driven by advancement in power electronics and distributed energy technologies.

The control of voltage is an important aspect in modern power systems. The current technology deployed in local distribution networks will not be able to respond to technical challenges that will be imposed by the future grid. A lack of adequate voltage control will limit the widespread adoption of distributed energy resources (DER) in the future grid if not addressed properly. A revision of the control strategy is required to integrate DER into the grid, considering South Africa's commitment to reduce CO_2 emissions by 2035 to 350-420 million metric tons. A substantial level of grid intelligence is required to meet the energy demand increase, projected by 2050. A control strategy must be implemented that takes advantage of available technologies, control techniques, monitoring and communication that mitigates grid stability problems. The South African electrical power industry is at an exciting crossroad of transformation, with the imminent unbundling of the generation and supply authority and the possibility of deregulation, that might provide a way out, for the cash-strapped parastatal.

The work in this thesis focused on control strategies that could be implemented in the future distribution network, to deal with the voltage control problem. These control strategies used the integration of distributed energy resource (DER), to mitigate the voltage control problem. The work can broadly be categorized into five parts:

Firstly, existing voltage control strategies based on control techniques, strategies and optimization methods were reviewed. The literature showed that an increase in DER penetration causes dynamic and transient voltages to exceed the prescribed limits, which results in damage to electrical equipment. Conventional voltage control devices are unable to respond fast and effectively to bidirectional power flow caused by DER. New control strategies, based on intelligent control are needed to deal with the voltage control problem in distribution networks. Secondly, specific gaps and opportunities in the current control strategy in the South African distribution grid were identified. It was shown that the South African transmission and

distribution system is characterised by a centralized unidirectional, demand driven control with no intelligence at the distribution level. Voltage quality parameters are covered by NRS (National Rationalised Specifications**)** 048 in South Africa. The aim of these standards is to set and provide acceptable voltage quality limits at the point of common coupling (PCC). The current specifications, which this study was based on, places restrictions on control functions for DER with a power output of less than 100kVA. This limits the participation of domestic and light commercial rooftop solar PV for voltage regulation. Opportunities exist for intelligent control using the reactive power capability of DER for voltage regulation in the future distribution grid. Thirdly, a test network was developed, which included DER. Phasor models were developed to test and implement specific voltage control methods. The results showed that an increase in DER penetration causes dynamic and transient voltages to exceed the prescribed limits at low penetration levels, which is greater than 25% but less than 50%. At higher penetration levels i.e., 50% and greater, the violations are severe. It was shown that power factor control of inverter-based DER based on load demand can be used to mitigate these voltage violations. Injecting or absorbing reactive power during a 24hour cycle based on the load demand proved an effective way to limit voltage violations and decrease the number of tap operations of the On-load Tap Changing (OLTC) transformer. Lastly, a discrete model comprising of a 6.5kW residential solar PV system was developed using reactive and active power control. This model was tested on a developed test feeder using OPAL-RT, a real-time simulation software package. The software uses a hardware-in-the-loop concept that incorporates digital real-time simulators. The results showed that reactive power of the solar PV inverter can be used for local voltage control.

Key words

Voltage control, distributed energy resources, demand response, active distribution network

ACKNOWLEDGEMENTS

I would like to express my sincere gratitude to my supervisors, Dr. Marco Adonis, and Professor Atanda Raji for the guidance during this research. Your help in making sure that the objectives of the research were well constructed and coherent is highly valued. I am very grateful for the time spent in reading the document and your valuable feedback and suggestions.

I would like to thank my employer, ACTOM Electrical Products for supporting my ambition to undertake this research. I want to especially thank my CEO for the financial support.

The financial assistance of the National Research Foundation towards this research is acknowledged as well.

Lastly, but most importantly, I want to thank my darling wife, Nikki, parents-in-law, and my two beautiful daughters, Bella, and Sienna for the emotional and moral support when I needed it the most. I owe everything I've achieved to my loving wife and daughters.

DEDICATION

To

My darling wife, Nikki and

Our beautiful daughters, Bella, and Sienna

TABLE OF CONTENTS

LIST OF ABBREVATIONS

AMI	Advanced metering infrastructure
ATC	Autonomous Tap Control
AVR	Automatic Voltage Regulator
CO_2	Carbon Dioxide
DER	Distributed Energy Resources
DR	Demand Response
DS	Distribution Storage
DSI	Demand Side Integration
DSM	Demand Side Management
DSR	Demand Side Resources
DSTATCOM	Distributed Static Compensator
EMS	Energy management systems
ESS	Energy Storage Systems
GA	Genetic Algorithm
HAN	Home area network
ICT	Information and Communication Technology
IVVC	Integrated Volt/Var Control
LP	Linear Programming
MAS	Multi-Agent Systems
MPC	Model Predictive Control
NLP	Non-Linear Programming
OLTC	On-load Tap Changer
OPF	Optimal Power Flow
PEV	Plug-in Electric Vehicles
PHEV	Plug-in Hybrid Electric Vehicles
PV	Photovoltaic
PSO	Particle Swarm Optimization
SC	Shunt Capacitor
SCADA	Supervisory Control and Data Acquisition
STATCOM	Static Compensator
SVC	Static Var compensators
SVR	Step voltage regulator
TOU	Time of use
VVC	Volt/Var Control
WAN	Wide-area network

LIST OF FIGURES

LIST OF TABLES

CHAPTER ONE
INTRODUCTION

1.1 Introduction

Electricity generation shortages experienced in 2007/08 caused major financial loss to the South African economy and exposed the country's dependence on the electricity supply authority. Significant capital has since been invested to address generation constraints during the subsequent years. At distribution level, distributed energy resources (DER) have been deployed to help mitigate loss of supply. Despite the benefits of local DER deployment, an increased penetration could lead to stability problems within the distribution grid, which must be mitigated. Integration of demand-side resources (DRS) and demand response (DR) programmes can be used to improve the energy efficiency and quality of supply. Integration of DER is effective at: (i) decreasing the total energy demand from the utility, (ii) expanding the use(DG) and (iii) addressing stability problems such as voltage violations in distribution networks. The aim of this research is to develop and model a test feeder that can be used to test voltage control strategies and methods using DER based on future scenarios. This chapter presents the awareness of the research problem in 1.2, statement of the research problem in 1.3, rationale/background to the problem in 1.4, research questions in 1.5, delimitations of research in 1.6, assumptions in 1.7, significance of the research in 1.8, aims and objectives in 1.9, research methodology in 1.10 and outline of the thesis in 1.11.

1.2 Awareness of the research problem

The global demand for electricity is projected to increase by 33% from 2020 to 2035 (IEA, 2018). New power generation plants will have to be built based on this projection. According to the Department of Energy in South Africa (DOE), the average demand for electricity is projected to increase by 59% from 2017 to 2050 (DOE, 2018). To meet the forecasted demand, it is expected that DER will play a greater role in the energy mix. DER, such as DG and DS, however, present significant challenges to the stability of the future grid. The ageing infrastructure, which has served the distribution network for decades, will not be able to cope with the technical demands presented by the future grid. To address grid stability problems, particularly voltage control, a coordinated operation of DER is needed at distribution level. Active demand management and Volt/Var optimization can reduce peak demand and defer expensive investment in large fossil-fuel based power plants and expenditure on the transmission and distribution network.

1.3 Statement of research problem

The integration of non-dispatchable energy resources and distributed storage is creating a challenge for optimal voltage regulation in real-time. The current grid and technology deployed

in distribution networks cannot respond to technical challenges imposed by the future grid. Voltage schemes, which operate in real-time, will need to be improved to support the changing network requirements of the future.

1.4 Rationale/Background

South Africa made a firm commitment to reduce carbon emissions by 2035, but this commitment will not be realized without the integration of RE and substantial improvement in grid intelligence, especially in the distribution network (Department of Energy, 2017). In South Africa, the current electricity generation capacity is 51,309 megawatts (MW) (USAID, 2018). Eskom, the state owned, vertically integrated company, generates approximately 91.2% of this capacity from thermal power stations. The balance is generated from renewable energy sources (USAID, 2018). Since its establishment in 1923, Eskom, has enjoyed the monopoly of power generation and transmission (Newbery & Eberhard, 2008). The energy mix is slowly changing, but Eskom, once an asset to the government, has become a major liability, with debt levels approaching R500bn (Naidoo, Goko & Cohen, 2019). Any large-scale investment in transmission and distribution infrastructure development would be unrealistic, given Eskom's levels of debt.

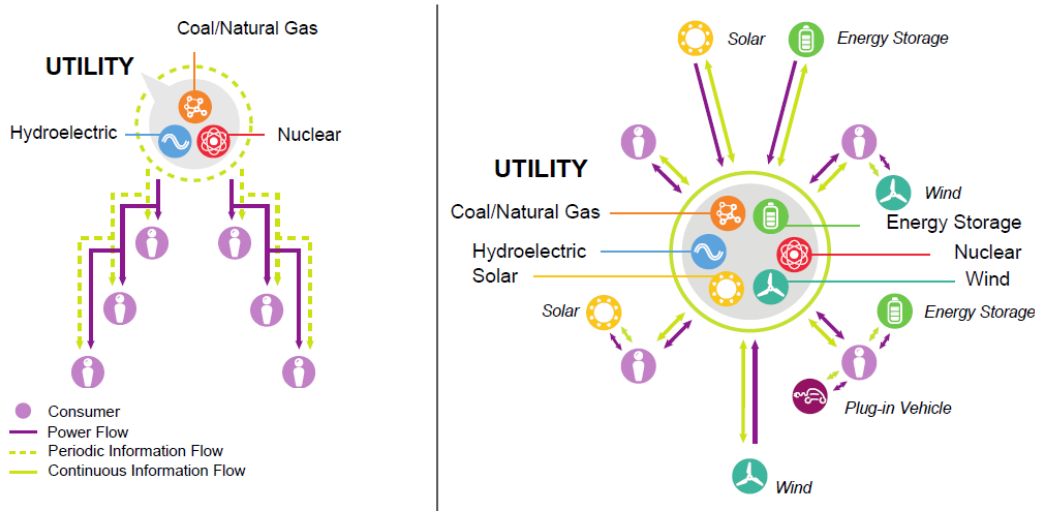

Figure 1.1. Evolution of the existing (left) to the future (right) distribution grid (Department of Energy, 2017)

The electrical infrastructure was designed several decades ago based on simplistic power generation and supply requirements. The design was based on power generation at large central power station, which is fed via the transmission and distribution networks to the end user, several hundred kilometres away via overhead conductors, substations, and distribution transformers (Ekanayake et al, 2012). Power flow was based on a simplistic unidirectional principle, where primary control was executed at the point of generation. The generation (coal,

nuclear, hydro, etc) and transmission, which includes “HV” and “MV” substations are linked via a good communication system to ensure stability and reliability. In contrast, the distribution system, which was largely passive, has little communication between the power system and load (Ekanayake et al, 2012).The current electricity distribution system in Southern Africa is in the process of changing from a passive to an active distribution grid based on consumer’s drive for energy conservation, plug-in electric vehicles (PEV) and greater consumer involvement (Department of Energy, 2017). The ageing infrastructure, which has served the electrical power system for almost 100 years, is now struggling to cope with the changing 21st century demands. The existing distribution grid is evolving into a smart grid as illustrated in figure 1.1, where intelligent control between generator and consumer is deployed to deliver efficient and secure electrical supply.

Due to the large R/X ratio of LV networks, intermittent, non-linear, non-dispatchable renewable energy sources and DS such as energy storage devices (ESS) and PEV, cause voltage deviations on distribution feeders (Siewierski, Szypowski, & Andrzej, 2018). The adverse effect of DER on the voltage profile of distribution networks is well documented in various publications (Wallings et al, 2008; Viawan, 2008; Caples, Boljevic & Conlon, 2011; Petinrin & Shaaban, 2016). Conventional VVC devices, which are designed to keep the voltage at various buses within 5% of nominal values during steady-state conditions, are unable to respond timeously to voltage violations in the distribution grid (Lai, Lu, Tang, Li, & Dong, 2019). The development in power electronics and Information and Communication Technologies (ICT’s) have created opportunities for utilities to develop flexible control schemes to deal with voltage violations (Antoniadou-plytaria et al., 2017). Various solutions to the voltage control problem have been proposed in literature i.e. (i) optimal dispatch of DER, (ii) load control, (iii) control of the PV/PEV inverters, (vi) matching the PEV charging periods to peak PV outputs and (v) the use of distributed energy storage. According to the Department of Energy’s Strategic National Smart Grid Vision for the Electricity Supply Industry, a coordination between DR and distribution level generation is needed to address the challenges presented by the future grid (Department of Energy, 2017). In the current generation supply crisis context, integration of DSR could be an effective tool to reduce the overall demand on the supply authority and address voltage violations, simultaneously.

1.5 Research questions

It is hypothesized that the voltage control problem in the future South African distribution network can be mitigated by a coordinated operation and integration of DER, using intelligent control strategies.

Several questions emerge as a result:

a. What are the currently employed methods or solutions to address voltage control in distribution networks, locally?
b. What are the methods or strategies adopted by utilities globally, to deal with voltage control?
c. Based on technical and economic considerations, what is the most suitable coordination strategy for voltage control, locally?
d. What optimization methods have been applied globally, to solve the voltage control problem?
e. How can international best practices be adopted locally?
f. Could DER be used locally as an effective strategy to improve energy efficiency, quality of customers' supply and simultaneously address voltage control?

1.6 Delimitations of the research

a. DER modelling is restricted to wind and solar PV only.
b. Distributed storage is restricted to ESS and PEV only.
c. Only three phase symmetrical networks are considered.
d. Voltage control is limited to MV and LV distribution network.
e. Distribution networks are limited to radial networks.
f. MATLAB/SIMULINK® is used for off-line modelling. OPAL-RT is used for real-time simulation.
g. OPAL-RT's OP5410 real-time simulator only has one core activated. ARTEMiS is not loaded on the simulator.
h. Only non-dispatchable renewable resources are considered.

1.7 Assumptions

a. OPAL-RT is used for real-time simulations.
b. For local control, the operating information within each zone is not shared with the others, but controlled by a dedicated single device.
c. Active and reactive power set points of DER are used.

1.8 Significance of research

The study is based on future scenarios and therefore provides an insight into the future distribution grid. The South African electricity system is on the brink of being unbundled and deregulation of the electricity market could become a reality within the next few years. The developed testbed and results of the study could be valuable to:

a. Utilities, parastatals, and academia to understand the impact of DER on the future South African distribution network.
b. Determine the maximum allowable penetration given the Department of Energy's RE projection by 2050.
c. Understand how DER, which are the cause of voltage control problem could be used to mitigate the problem in the future.

1.9 Aim and objectives

The aim of this research is to develop a testbed to study existing and improved voltage control strategies in real-time based on future scenarios in local distribution networks.

The objectives are to:

1. Conduct a comprehensive literature review of voltage control in active distribution networks with respect to control techniques, strategies, and optimization methods based on global experience.

2. Give an overview of current local control strategies. Identify specific gaps and opportunities in the current control strategy in the South African distribution grid

3. Present a mathematical overview of distribution level voltage control with conventional voltage control devices and DER control. For inverter-based DER, present two strategies used to control the voltage at the local bus.

4. Develop a test feeder, which includes phasor models for variable loads, solar PV, and Wind energy systems. The testbed will be used to study electromechanical oscillations based on a phasor solution as the study is concerned with changes in currents and voltage magnitudes only.

5. Propose control strategies using inverter-based DER to regulate the voltage at the central substation and local bus. Propose solutions to the voltage control problem in the future South African network.

6. Develop a simulation platform based on discrete models. Develop and model a 6.5kW grid-tied solar PV system and static loads, which will be tested with OPAL-RT's real-time simulator. The results will be based on steady state and transient voltage stability analysis.

1.10 Research Methodology

The research methodology, aimed at achieving the objectives, is illustrated in figure 1.2.

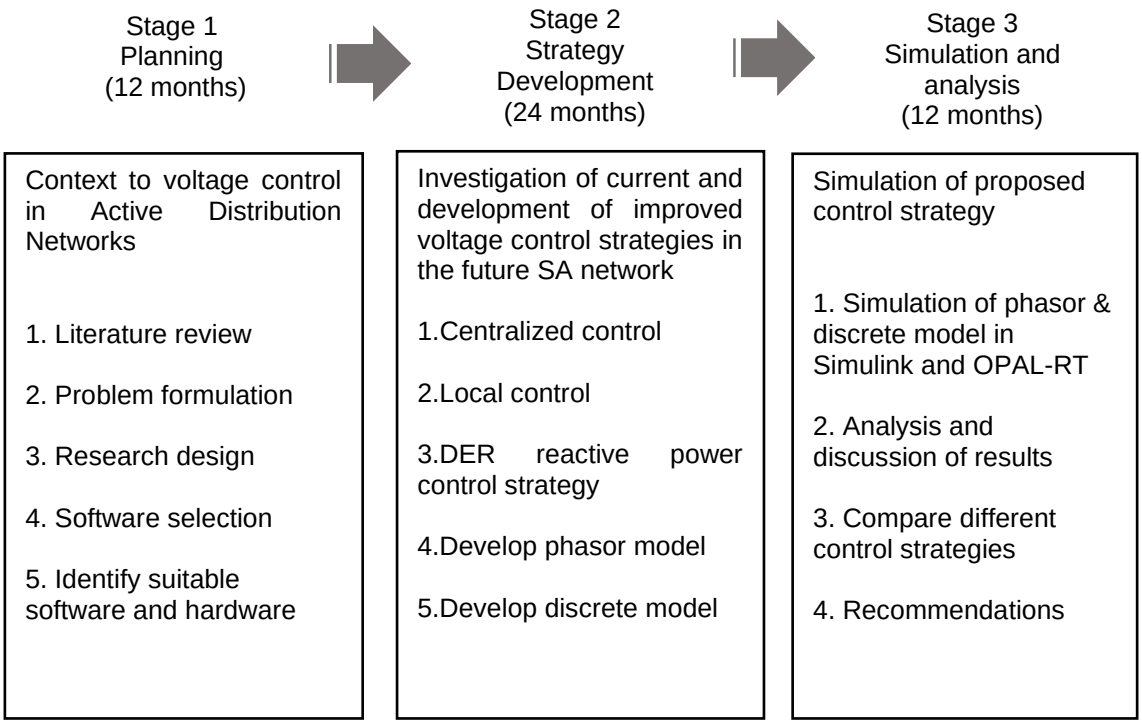

Figure 1.2. Research methodology

1.11 Outline of the thesis

Chapter 1 provides the introduction to the thesis, which includes the motivation, background, aim and objectives

Chapter 2 presents a comprehensive literature review of the voltage control problem using DSR. A statement of the voltage control problem is presented, followed by a discussion of control strategies and optimization algorithms used to solve the voltage control problem.

Chapter 3 provides the technical analysis with mathematical models of voltage control in distribution networks.

Chapter 4 comprises of the selection of simulations software and development of a phasor model for off-line simulation testing and verification.

Chapter 5 presents the selection of software and hardware for real-time simulation and testing. Development of a test feeder for steady state and transient voltage stability analysis

Chapter 6 presents the discussion, conclusion, and recommendations.

CHAPTER TWO
LITERATURE REVIEW

2.1 Introduction

Traditional electric power systems, which were designed several decades ago, consist of generation, transmission, and distribution. These grids are characterised by a centralized unidirectional, demand driven control. The high voltage grid is equipped with intelligent control, but the distribution network has largely been neglected. The electrical distribution network in South Africa, is likely to change over the next few years, based on demand for DG, distributed energy storage and greater customer involvement. A large penetration of DER could lead to reverse power flow, which affects the stability of the network. The distribution infrastructure is ageing and needs modernization to accommodate the complexities of reverse power flow. Financial investment in new electrical infrastructure is estimated to be several billion Rand, which cannot be afforded at present. In South Africa particularly, integration of DSR could be used as a mechanism to control the growing demand for electricity, defer investment in large generating plants and deal with instability problems, such as voltage violations in distribution networks. The objective of this chapter is to review current literature on active distribution network management with reference to voltage control. A total of 151 references were considered as illustrated in Figure 2.1. Of these, 96 scientific papers have been reviewed that specifically deal with the voltage control problem.

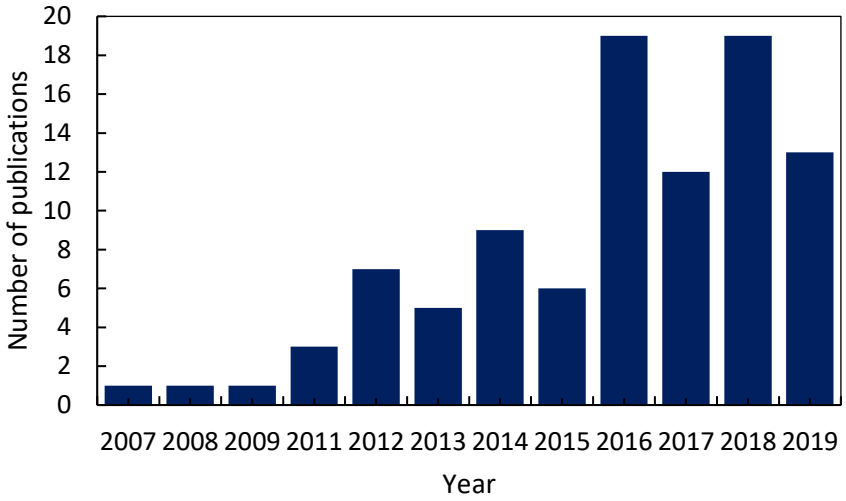

Figure 2.1. Publications trend related to active distribution network management

Table 2.1. Voltage control techniques

Control Technique	Reference	Key characteristics	Number of publications
Centralized	(Nasiri et al., 2016); (Olival, Madureira, & Matos, 2017); (Paula, Mello, Lopes, & Pinheiro, 2017); (Mokhtari et al., 2013); (Siewierski et al., 2018); (Mokgonyana, Zhang, Zhang, & Xia, 2016); (Khalid et al., 2018); (Anderson & Narayan, 2011); (Yi et al., 2012); (Kulmala & Repo, 2014); (Zakariazadeh, Homaee, Jadid, & Siano, 2014); (Behravesh, Keypour, & Foroud, 2019); (Hashemi, Aghamohammadi, & Sangrody, 2018); (Davarzani, Pisica, & Taylor, 2017); (Yi et al., 2012); (Rathbun et al, 2018); (C. Li, Disfani, Pecenak, Mohajeryami, & Kleissl, 2018); (Farina, Guagliardi, Mariani, Sandroni, & Scattolini, 2015); (Haque, Nguyen, Vo, & Bliek, 2017); (Oshiro et al., 2011); (Jung, Onen, Arghandeh, & Broadwater, 2014); (Quijano & Padilha-feltrin, 2019); (Cagnano & Tuglie, 2015); (Ji et al., 2018); (Efkarpidis, Rybel, & Driesen, 2016); (Abessi, Vahidinasab, & Ghazizadeh, 2016); (Takahashi & Hayashi, 2012); (Nimpitiwan & Chaiyabut, 2014); (Jiongcong, Nanhua, Xiaoping, & Xudong, 2014); (Y. Yang et al., 2014); (Xie, 2017); (Kawamura, 2013); (Kadurek, Sarab, Cobben, & Kling, 2012); (Xiangqi et al., 2017); (Karthikeyan, Pokhrel, Pillai, Bak-jensen, & Frederiksen, 2017); (Abraham, Marzooghi, & Terzija, 2017); (Y. Dong et al., 2018); (Bayat, Sheshyekani, Member, & Hamzeh, 2016); (Yujun & Petit, 2013)	• Voltage regulation from the substation to the rest of the network • Wide range of communication systems to coordinate different devices in the systems such as OLTC, Voltage Regulators, Switched Capacitors, etc. • Data is obtained by sensors along the feeders. • The control system is relatively complex and expensive • Can make full use of various voltage control. devices to regulate globally. • Require a reliable communication channel	39
Decentralized	(Fazio, Fusco, & Russo, 2013); (Rashidi & Moshtagh, 2014); (Guo, Zheng, Lin, & Yan, 2016); (Villacci, 2019); (Li et al.,2019); (Fallahzadeh-abarghouei, Hasanvand, & Nikoobakht, 2018); (Joelle, Torre, & Pedrasa, 2016); (Wu, Huang, & Ding, 2017); (Y. Liu et al., 2018); (Christakou, Tomozei, & Boudec, 2014); (Diaz et al., 2016); (Mufaris & Baba, 2015); (Davarzani et al., 2017); (Y. Li, Li, Peng, & Zou, 2019), (Pournazarian, Karimyan, Gharehpetian, & Abedi, 2019); (Hashemi et al., 2018); (Fallahzadeh-abarghouei et al., 2018); (Islam, Muttaqi, et al., 2015); (Calderaro et al, 2014); (Calderaro et al,, 2012); (Mehrjerdi, Lefebvre, Saad, & Asber,	• Local control using local information to independently control voltage. • Able to provide local voltage support. • Each unit is controlled by its local controller that is not fully aware of the system-wide disturbances and is independent of other controllers.	50

	2013); (Fazio et al., 2013); (Gu et al, 2017); (Feng, Li, & Shahidehpour, 2018); (H. J. Liu, Shi, & Zhu, 2017); (Islam, Sutanto, & Muttaqi, 2015); (Yorino, Zoka, & Watanabe, 2015); (Lai et al., 2019); (Hashemi et al., 2018); (Mufaris & Baba, n.d.); (Takayama & Ishigame, 2018); (Tanaka, 2009); (Cagnano & Tuglie, 2016); (Zeraati, Esmail, Golshan, & Guerrero, 2019); (Zeraati, Golshan, & Guerrero, 2018); (Ssekulima & Hinai, 2016); (Y Wang et al., 2016); (Bode, Shigenobu, Ooya, Senjyu, & Motin, 2019); (Zimann, Batschauer, Mezaroba, & Neves, 2019); (X. Dong et al., 2018); (Bahramipanah, Cherkaoui, & Paolone, 2016); (Bahramipanah et al., 2016); (Shaoyun, Fournier, & Andri, 2019); (Kabir, Mishra, Ledwich, Xu, & Bansal, 2014); (Jamroen, Pannawan, & Sirisukprasert, 2018); (Mocci, Natale, Pilo, & Ruggeri, 2015); (Zecchino & Marinelli, 2018); (Cardona, López, & Rider, 2018); (Swain & De, 2019); (Horoufiany, 2012);	• Coordination is poor, and some devices may be activated frequently. • Communication with other DER's is not necessary, which enables plug and play capability. • Cost-effective • Don't require extensive deployment of sensors and communication equipment. • Cannot achieve global optimization	
Distributed	(Arshad, Ekström, & Lehtonen, 2018); (B. Li et al., 2018); (Mahmud & Zahedi, 2016)	• Local controllers work together to achieve a common decision. • Communication link between the local controllers is required. • Global grid information is not required. • providing "plug and play" capability.	3
Hybrid	(H. J. Liu, Shi, & Zhu, 2019); (Efkarpidis et al., 2016)	• Combining characteristics and advantages of central and local control	2

2.2 Distributed Energy Resources (DER)

DER refers to distributed generation (DG) and distributed storage (DS) as illustrated in Figure 2.2. One of the common goals of supply authorities is to reduce or defer expenditure on large generation plants. One way of achieving this objective is through the integration of DER (Guo, Fang & Khargonekar, 2017). The key to the successful integration of DER in the future South African distribution network is a coordinated management of these technologies using available intelligence.

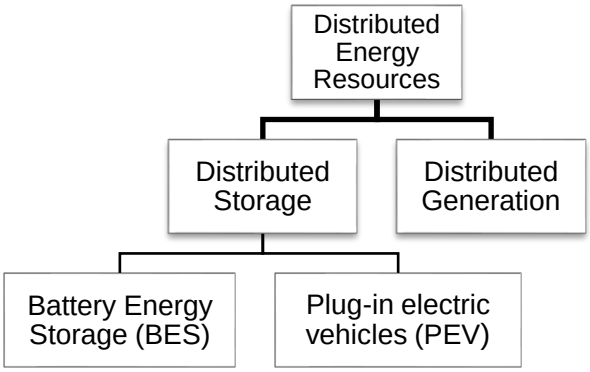

Figure. 2.2. - Distributed Energy Resources

2.2.1 Distributed Generation

Prior to the establishment of large power generation plants, power was supplied by DG at or close to the point of consumption (Jenkins, 2010). Rooftop solar PV, wind turbines, diesel generators, small hydro turbines and biogas are classified as decenetralized power sources and are usually connected behind the customer's meter (Akorede, Hizam, & Pouresmaeil, 2010). Small-scale embedded gneration like rooftop solar PV, are modular and typically range between 1 to 10 kW (Azzopardi, 2017). Other DG technologies include, geothermal, biomass, biogas, hydrogen fuel cell, micro-turbine, biogas-based internal combustion engine, geo-thermal heat pump, micro-hydro generator, reciprocating engine and small-scale cogeneration plants (Lip, Shiun, Shin, Hashim, & Tin, 2017). The popularity of DG, especially residential and commercial PV in South Africa is due to the supply authority's inability to supply reliable power and escalating cost of coal-based electricity. Many developed countries have popularized the adoption of RE through government driven targets and incentives. Feed-in tariffs have encouraged users to generate their own electricity for economic benefit. The main challenge of PV and wind grid integration is its unpredictability due to its dependence on weather conditions (Funabashi, 2016).

Power sources that generate DC voltage such as PV, fuels cells and batteries are typically connected to the grid by power electronic devices. PV systems consist of a DC/DC converter to keep the DC voltage constant and a DC/AC converter, which connects to the grid. Figure 2.3 shows a simple PV system connected to the grid. In wind systems, the rectifier converts AC power with variable frequency to DC power and then converts this DC to AC via a DC/AC inverter. Real, reactive power, voltage and frequency can be controlled using local feedback applied to the inverter. V and E are the voltage at the inverter and grid, respectively and X represents the passive filter.

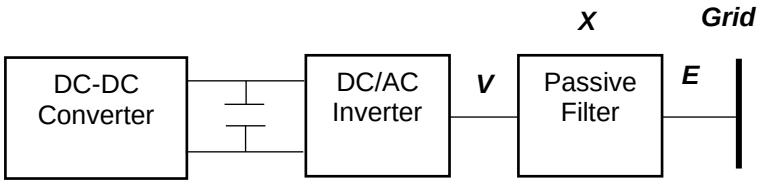

Figure. 2.3. Solar PV system (Funabashi, 2016)

2.2.2 Distributed Storage

In the context of this review, only small-scale battery energy storage systems (BESS) and plug-in electric vehicles (PEV) have been considered. Both technologies are connected behind the customer's meter. According to a recent analysis, the cost of lithium-ion battery technology is becoming more affordable (Melhem, 2013). Since its commercialization in 1991, lithium-ion batteries have become very popular in power and electronic applications (Du & Lu, 2015). The most suitable application is in PEVs. This is due to their efficiencies, which is over 95%, higher energy density of 200 Wh/g, and smaller self-discharge capabilities (Takana, 2009). PV generation occurs during midday hours and doesn't coincide with maximum load demand. Like PV solar, wind energy is intermittent in nature as well and is highly dependent on weather conditions. A possible solution to overcome this, is to store extra energy generated from PV and wind during maximum generation and use this stored energy when RE resources are not available (Kim, 2017, IRENA, 2017, Gelazanskas & Gamage, 2014). Based on research, this method would be more promising than curtailing the active power of PV system (Jung, et al, 2014).

An energy storage system (ESS), converts electricity into a stored form by means of an electrochemical process and usually consists of a management and control system (Das, Bass, Kothapalli, Mahmoud, & Habibi, 2019). Interface between the systems and the networks consist of a controller and converter, which manages P & Q setpoints. Electrical energy storage, which constitutes a small part of the overall energy storage systems in use, can be beneficial to (i) meeting peak load demands, (ii) solving intermittent RE generation, (iii) improving power quality, and (iv) supply remote loads (Luo et al. 2015).

2.2.1.1 Battery Energy Storage Systems (BESS)

Rechargeable batteries are a commonly used technology generally used in power quality, energy management and transportation systems (Luo, Wang, Dooner, & Clarke, 2015). Batteries are rated based on energy, power output, efficiency, lifespan, operating temperature, depth of discharge, self-discharge, and energy density. BESS is a controllable device with a fast output, that can operate as a load or generator. The application of BESS in LV networks has increased in recent years due to their fast responses to transients (Takana, 2009). ESS technologies include (i) lead acid batteries, (ii) lithium-ion (Li-ion) batteries, (iii) Nickel–metal Hydride (NiMH), (iv) Sodium–sulfur (NaS) and (v) Nickel–cadmium (NiCd) (Luo et al, 2015). Li-ion batteries are used in utility RE plants around the world and are extensively used in hybrid and full electric vehicles (Luo et al., 2015). Distributed storage devices usually consist of a management and control system, which manages active and reactive power setpoints. BESS can operate at leading or lagging power factor, depending on the charging/discharging requirement. Depending on the grid requirment, it can inject or absorb reactive power. BESS is connected to the grid via a bidirectional-type DC/AC converter (Basak, et al, 2012). In most instances, DER operate in parallel to the supply utility, providing back-up power when required.

In a distribution feeder, overvoltage is experienced due to an increased penetration of PV. Conversely, undervoltage is experienced due to peak loading on the feeder. A common method to mitigate over and undervoltage based on the literature reviewed, is reactive power control of PV inverters and battery energy storage. In networks with high R/X ratios, however, DG reactive power compensation may be insufficient to deal with the voltage problem (Shaoyun et al., 2019). A decentralized community-based participation integrated PV and Battery Storage (IPVBS) is proposed in (Kabir et al., 2014) using a probabilistic analysis to deal with the voltage profile issue. The study used a sensitivity analysis and highlights the opportunity of using BES to increase the penetration of PV by using droop-based BES. The energy generated by the PV system is stored for used when required for voltage regulation. In (Shaoyun et al., 2019), the reactive power of PV and active power of BES based on an adaptive particle swarm optimization algorithm (APSO) is used for voltage control. The charge/discharge characteristics of the BES is used to solve the voltage control problem. Shaoyun et al (2019), proposed a decentralized control approach to mitigate the shortcomings of the centralized control system by dividing the network into semi-autonomous entities. A distributed zonal control method is proposed based on a multi-agent system, which is typically used in large scale systems. In the decentralized method, two control methods i.e. Thévenin-based" and "Top-down sweep" are used to determine the BESS active and reactive power set-points. In (Zimann et al., 2019), an active and reactive power injection control scheme is proposed at the point of common coupling (PCC), where reactive power is given priority. The solution is based on the study proposed by (Kabir et al., 2014) but focuses on the search for

the least amount of active power required for voltage control. In (Bode et al., 2019), optimal capacity of active and reactive power compensation was used with BESS based on PSO. A voltage source converter is used to control the active and reactive power independently. The objective function of the study was an improvement in the voltage line index and the constraints were identified as power systems and voltage stability. In (Wang et al., 2016), a distributed and localized method of ESS is proposed based on consensus algorithm to deal with the voltage regulation problem. For the distributed method, the consensus algorithm estimates the ESS power output and for local control, state of charge (SoC) regulates individual ESS's.

2.2.1.2 Plug-in Electric Vehicles (PEVs)

The global uptake of PEV during the past few years has mainly been driven by a reduction in carbon footprint and the depletion of fossil fuels (Dong et al., 2018). The global sales of EVs have increased from 1 million units in 2015 to 7 million in 2019 (Greencape, 2019). The uptake of EVs have been slower in South Africa, compared to developed countries, but the drive towards the reduction in carbon footprint, remains a common objective. The present limitations in South Africa are cost and operating range. The technology will mature over the next few years, driven by demand, which will reduce cost and increase operating range (Taghavipour, Vajedi, & Azad, 2019). One of the major advantages of using electric vehicles is that it reduces the dependence on the volatile petroleum market, but creates extra demand on the electrical infrastructure, especially during night-time charging (Gelazanskas & Gamage, 2014). The local drivers for EVs can be attributed to (i) rising fuel costs, (ii) energy storage innovations, (iii) falling cost of electric vehicles (iv) increased driving range (Greencape, 2019).

Plug-in electric vehicles can be classified as hybrid or all-electric. The hybrid vehicle consists of two energy sources i.e. chemical fuel and rechargeable electrochemical battery storage devices (Onori, 2016). The efficiency of full electric vehicles is 70% compared to internal combustion engines at only 30% (Taghavipour, Vajedi, & Azad, 2019.). PHEV and PEVs are viable long-term options for carbon reductions and future transport challenges.

The batteries of PEVs and PHEVs could be used as energy storage devices and provide vehicle-to-grid services (V2G), which could deal with generation constraints and voltage control problems (Veneri, 2017). The successful integration of EVs depends on various factors including two-way communication, smart meters and most importantly, the charging schedule, which has a direct impact on the commercialization of the technology. It is therefore important to conduct studies to determine the effect of charging demand on the distribution system. The charging strategies can be divided into controlled/coordinated and uncontrolled/uncoordinated (Veneri, 2017). Figure 2.4 shows a flow chart of PEV charging strategies.

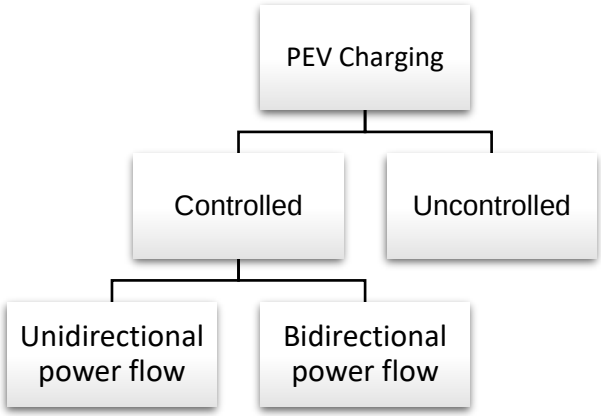

Figure 2.4. PEV charging strategies (Veneri, 2017)

- Controlled charging - This strategy is characterized by a centrally controlled scheme, where the utility is responsible for the coordinated charging of multiple PHEVs. Based on driving habits and parking times, the utility would incorporate these loads into the power demand forecast and dispatch generation based on forecasted demand, whilst minimizing generation cost. This strategy would be ideal for utilities from a demand/supply balance perspective but could lead to owner discomfort.

- Uncontrolled charging - In this decentralized strategy, the user charges PHEVs whenever it is parked. Uncontrolled charging based on a high penetration could lead to a peak in load and violation of the prescribed voltage limits. A decentralized charging strategy could be an effective mechanism, as it would give users control over charging times, based on price incentives from the utility.

The control strategies of EVs can be classified into (i) online and (ii) offline (Enang & Bannister, 2017). Online control strategies are implemented in real time. For offline control strategies, mixed-integer linear programming (MILP) and PSO algorithms have been applied to solve the global voltage control problem. In (Cardona et al., 2018), a decentralized charging strategy is used based on user priority. The strategy, which uses an algorithm based on current and historical voltage measurements is developed to avoid voltage and capacity violations. The results are compared to a centralized approached based on MILP. In (Feshki, 2017), the role of PEVs in reducing of voltage unbalance factor (VUF) is analysed using PSO. Online control can be categorized as (i) rule-based control strategies or, (ii) online optimisation based. Rule-based is based on mathematical models, whilst online optimization, such as artificial neural networks, PSO and MPC, aims to reduce a global optimization problem into various local problems

2.3 Demand-side resources (DSR)

One of the common goals for supply authorities is to reduce or defer expenditure on large generation plants (Kakran & Chanana, 2018). One way of achieving this objective is through demand-side management (DSM) programs, illustrated in igure 2.5. DSM has been used since the early 1980s to achieve different load shaping objectives. The intermittent nature of DER makes supply and demand balancing difficult. The difficulty of the task is enhanced by the increased deployment of DER over the past few years. The execution of this task is made more complex, due to:

- Generation uncertainty - the generation uncertainty of non-dispatchable energy resources is influenced by weather conditions. The peak load demand does not necessarily coincide with peak RE generation.
- DER complexity - the technology ranges from inverter-based DG to smart loads. All these technologies have different characteristics.
- Lack of visibility - utilities may not have visibility to individually installed DER and are not able to control customer loads. The lack of intelligence between the utility and the customer makes customer involvement difficult. It would be difficult for customers to respond to power shortages or peaks in demand if they don't know the status of the grid.

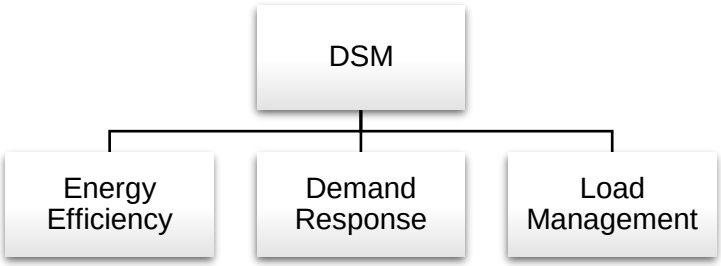

Figure 2.5. DSM Strategies (Bagher, Moshtagh, Shafie-khah, & Catalão, 2018)

The use of DSM techniques, however, can reduce the demand at peak times and increase the efficiency of the network (Gelazanskas & Gamage, 2014). In the future grid with smart meters, communication and control, DSM could be a useful tool.

2.3.1 Demand response

DR can be defined as the manipulation of the load, based on price incentive from the utility. Utilities enter into an agreement with consumers to change their electricity consumption patterns in response to incentives (Rabiee & Mohseni-bonab, 2019; Gilson & Ferreira,2019). By implementing adjustment to the consumption patterns in conjunction with using DER at peak times, the customer may benefit financially (Siano, 2014). DR strategies are gaining increasing popularity based on technological advances in AMI and smart appliances. Shifting loads from peak to off-peak could be seen as a viable option for utility and consumer, but it could merely transfer the peaks to another time, which does not solve the initial problem (Li, 2017). Consumers can change the use of electricity consumption in three ways (Gelazanskas & Gamage, 2014; Saino, 2014) i.e., (i) load reduction/curtailment strategies, (ii) moving consumption to different times and (iii) using DER sources to reduce demand on the utility. DR methods can be broadly classified into two groups i.e., price-based, or incentive-based as illustrated in figure 2.6. The effectiveness of DR programs is dependent on advanced metering infrastructures (AMI), which is installed at the end user's site (Jordehi, 2019).

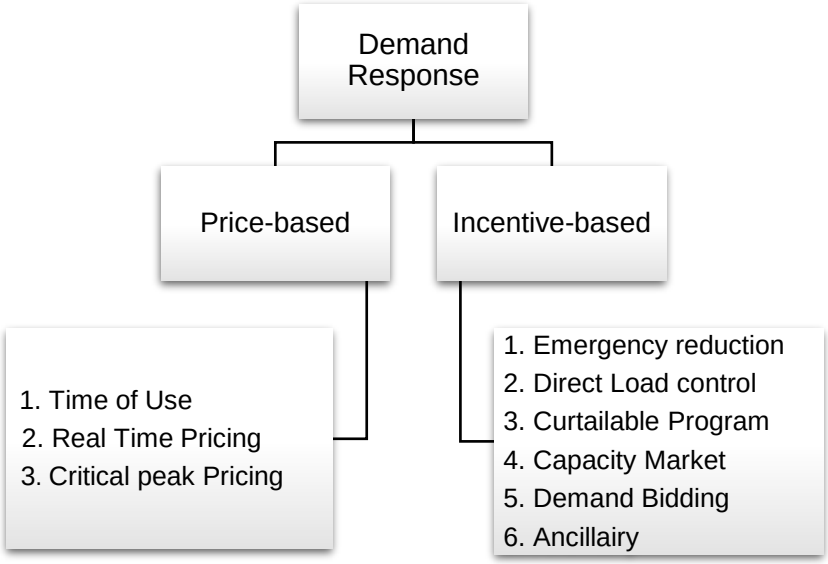

Figure 2.6. DR techniques (Bagher et al., 2018)

2.3.1.1 Price-based DR

In price-based DR, the tariffs vary relative to the actual or standard price of electricity (Law et al, 2012). Time of use (TOU), critical peak pricing and real time pricing are considered as price based. In TOU, which is common in many developed countries, prices are charge based on off-peak, standard, and peak blocks, per day and season (Gelazanskas & Gamage, 2014). France has the most successfully implemented TOU pricing scheme in the world, with 30 million customers connected to the scheme (World Bank, 2005). In 2018, 84,4% or 13.7 million households were connected to the electrical infrastructure in South Africa (STATSSA, 2018).

An effective DR strategy, which incorporates these households could relieve the burden on demand. There are 278 municipalities in South Africa, but very few offer TOU pricing scheme for households. TOU, in South Africa, has largely been focused on industrial consumers in the past. In critical peak, consumers are notified of critical peaks in demand, during which the price is increased, relative to standard tariffs. In real time pricing, customers are notified of tariffs that vary on an hourly basis on a day-ahead or hourly-ahead basis. In a price-based DR system, customers will decrease their demand, based on signals from the utility (Kadurek et al., 2012).

2.3.1.2 Incentive-based DR

In incentive-based DR, either the consumer or utility controls load shaping. The consumer is incentivised by the utility for participating in load reduction strategies (Jordehi, 2019). Various load control or load curtailment strategies could be used to reduce demand on the utility. Different incentive-based DR programmes are illustrated in figure 2.6. Some are briefly discussed below (Jordehi, 2019);

- Direct load control - the utility and consumer enter into an agreement where the customer is compensated for load reduction. The agreement consists of a contract that gives the utility the control over the controllable appliances, via power line carriers or WiFi (Rahman, Are, Sha, & Hettiwatte, 2018).
- Load curtailment - the user is compensated by the utility for curtailing their load as and when required by the utility.
- Demand bidding - this mainly applies to large consumers, typically greater than 1MW. The utility would encourage these consumers to reduce their load during peak times or change their consumption patterns based on a specific bid price.

2.3.1.3 Demand Response Optimization

The DR optimisation problem can be classified into two broad categories i.e., (i) classic and (ii) metaheuristic. In the reviewed literature, the classic method consists of linear and non-linear optimization and for metaheuristics, Particle Swarm Optimization and Genetic algorithm. DR problems are generally solved by the classic methods i.e., linear and non-linear optimization. In (Christakou et al., 2014) a study was conducted to determine the potential of a large aggregation of small thermostatic loads on primary control, using a low overhead DR decentralized control scheme. Linear programming was used by providing a low bit control signal, which provides an ON-OFF action on the appliance that is equipped with a programmable controller, for direct load control. It must be noted that the utility does not control each individual load, but rather send a unique signal to each bus in the network via power line

communication. In emergency situations, such as grid disturbances, the utility can use tap changers at the substation to stabilize the voltage. In (He & Petit, 2016), a centralized control strategy is proposed where the voltage problem has been formulated into a MILP. The objective of the study is to find the total cost associated with the voltage control using tap changers, reactive and active control of DG and demand response. The study concludes that the cost of DR is cheaper than DG active curtailment and provides a more robust voltage support if the demand increases.

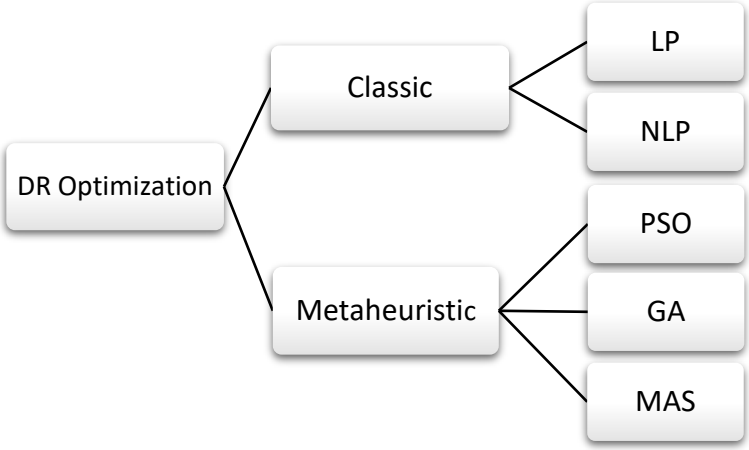

Figure 2.7. DR Optimization algorithms. dapated from (Jordehi, 2019)

Metaheuristics is another good method to solving DR problems as they can handle discrete and constrained problems (Jordehi, 2019). From the literature, seven publications used metaheuristics to solve the DR problem. These are PSO and GA as illustrated in figure 2.7. In (Petinrin & Shaaban, 2014), GA is used to consider the optimum energy scheduling of appliances to reduce voltage deviations on a feeder, considering wind power participation. The problem was modelled as a non-linear optimization problem. The advantage of this method over traditional techniques, is that it is population based, rather than a single solution. The aim of the proposed solution in this study is to minimize the voltage deviation through customer load scheduling. In this price-based scheme, the utility sends electricity pricing to consumers via AMI's. The customer responds by scheduling elastic loads at different time intervals. The study proves that DR techniques, improves the voltage profile along the feeders, as the customer participation increases. In (Xie, 2017), a centralized control scheme is proposed based on a day-ahead load scheduling and real-time load scheduling to solve the overvoltage problems in LV networks, caused by penetration of PV and PEV. GA is used to solve the day-ahead load scheduling. In the solution, Home Energy Management (HEM) and Community Energy Management (CEM) systems are developed to screen and control scheduled loads. The day-ahead load scheduling aims to increase customer profits and reduce voltage violations in the network.

In (Hashemi et al., 2018), a corrective DR control action is implemented based on minimum load reduction. PSO is used to find the optimal load reduction based on DR participation to maintain the voltage security in the network. In this study, the threshold voltage and optimal load reduction pattern is estimated, which triggers DR response. Rahman et al, (2018), used a modified particle swarm optimisation algorithm (MPSO) to determine the optimal switching combination of household appliances and OLTC tap positions in unbalanced LV systems. MPSO is chosen to deal with premature convergence and lack of guarantee in global convergence. The optimisation aims to determine the optimal size of DR and OLTC tap position for effective voltage control. In (Bayat et al., 2016), a multi-objective problem is formulated by DR and DER participation in a microgrid and solved by PSO. In the proposed method, a centrally controlled energy management system (EMS) assigns the real and reactive power setpoints for the local DER's and reactive power compensators as well as power to be curtailed through the controllable loads for voltage management.

Multi-agent systems (MAS) is a very popular method to solve DR optimization problems. An agent is an autonomous and intelligent component that acts on behalf of its user and is able of making autonomous decisions (Byrski & Kisiel-Dorohinicki, 2017). The study conducted by (Anderson & Narayan, 2011), uses the MAS method to solve the voltage problem by integrating demand response with distribution Volt/Var control. It considers the role of an aggregator in DR. In (Davarzani et al., 2017), a MAS framework is proposed that mitigates local overloading of networks by controlling domestic loads. The aim of the framework is to reduce the total active power at the distribution transformer during emergency conditions by using four different DR participants, which are modelled as agents. In (Solanki, Venkatesan & Khushalani, 2012), MAS framework is used to coordinate DR with VVC during peak loads.

2.3.2 Load management

Different load shaping techniques are illustrated in figure 2.8. Peak clipping is implemented to reduce the power demand during peak hours. It is especially useful when the demand exceeds the supply and capacity is insufficient. Valley filling is used to obtain greater load factors in predefined time margins. By doing so, the utility may increase its profit. In load shifting, consumers are encouraged to use cheaper tariffs during off-peak times.

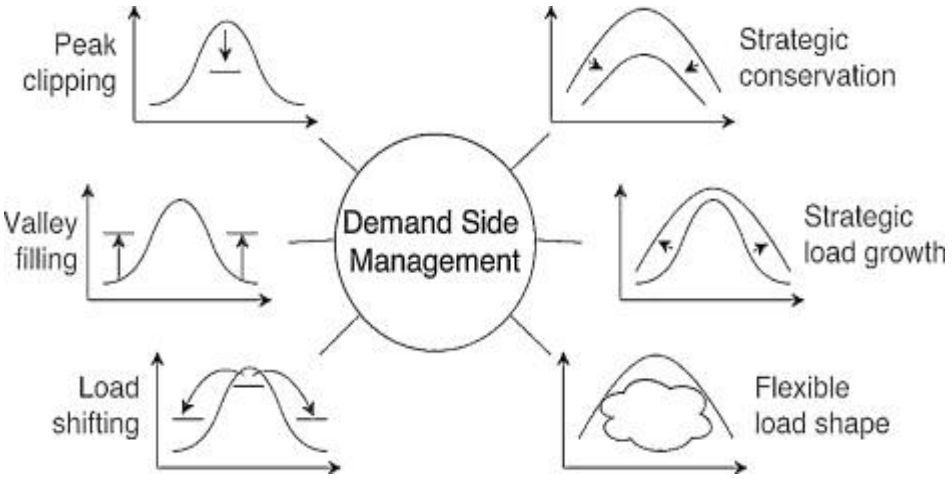

Figure 2.8. Load shaping techniques (Gelazanskas & Gamage, 2014)

2.4 Distribution network voltage control

In traditional distribution networks, power flows from the substation transformer to the loads. With DER connected to the network, power flows in both directions, which raises the voltage levels along the feeders. It is the responsibility of supply authorities to keep dynamic and transient voltage levels of distribution networks within their prescribed limits and to reduce reactive power losses (Jenkins, 2010). It is beneficial for utilities and consumers to have a voltage profile that meets statutory requirement as it reduces network power losses and improves the quality of supply. Voltage control can be done through control measures taken at the substation and feeders. Distribution systems, are however, difficult to monitor, analyse and control in real-time due to their topology, which changes as it expands; limited communication and their unknown complex loads (Ekanayake et al, 2012). There are various methods adopted by utilities globally, to deal with the voltage control problem. These range from the conventional centrally controlled substation transformer management to local control of DER (Jenkins, 2010). Various papers have highlighted the use of reactive capacity of inverters to limit voltage rise in networks (Fazio et al, 2013; Calderaro et al, 2012; Wu et al, 2017, Islam et al, 2015, Rashidi & Moshtagh, 2014 & Villacci, 2019). Mahmud & Zahedi (2016) presents a comprehensive review of voltage control strategies in the presence of smart networks with high renewable energy penetration. Extensive research has been done to understand and address the voltage violation problem in active distribution networks. The development in advanced metering infrastructure (AMI) and power electronics have created new possibilities for voltage control with flexible control schemes.

One of the primary objectives of supply authorities is to keep voltage levels of distribution networks within their prescribed limits, typically within 5% of nominal values (Jenkins, 2010). With high penetration of DER at distribution level, safe voltage levels are being exceeded. It is critical to keep the dynamic and transient voltages within the prescribed limits to avoid damage

to electrical equipment (Tabatabaei, Aghbolaghi, Bizon & Blaabjerg, 2017). Distribution systems, however, are difficult to monitor, analyse and control (Ekanayake et al, 2012), This can be attributed to:

- Their radial topology
- Unbalanced three phase systems.
- Limited communication
- Network structure, which changes as it expands.
- Large R/X ratio, which is higher than transmission networks.

Traditionally, the use of reactive power to control voltage in a power grid is done by using transformer on-load tap-changers (OLTC), capacitor banks (CB), voltage regulators (VR), static synchronous compensator (STATCOM), and static Var compensators (SVC) (Fallahzadeh-abarghouei et al., 2018). These conventional Volt-Var compensation (VVC) devices are unable to respond timeously to voltage violations in the distribution grid during reverse power flow. Extensive research has been done to understand and address the voltage violation problem in active distribution networks and networks with a large DER penetration. The proposed solutions suggested by researchers to deal with voltage rise due to increased penetration of RE sources in LV network are summarized by (Petinrin & Shaaban, 2014):

- Network upgrading - this includes resizing conductors, which is not economically feasible for utilities.
- Continuous changing of transformer tap setting - the intermittent nature of renewable energy generation makes this method ineffective.
- Demand-side Resources - the use of DG and controllable devices (PEV, smart loads and storage units). It is hypothesized that the voltage problem can be mitigated by the effective utilization of DSR. The core focus of this research is based on this assumption.

2.4.1 Voltage control strategies in Distribution Networks

There are various methods adopted by utilities globally, to deal with voltage control. These range from the conventional centrally controlled substation transformer management to local control of DER (Petinrin & Shaaban, 2014). Voltage control schemes can be broadly divided into communication-based and local (autonomous) control (Antoniadou-plytaria et al., 2017). Autonomous control is based on local measurements at the point of common coupling (PCC). Communication based schemes are sub-divided into (i) local (ii) centralized, (iii) decentralized (iv) distributed and (v) hybrid (combination of centralized and local).

2.4.1.1 Centralised control architecture

Voltage control in transmission systems is done by adjusting the generator reactive power output. At distribution level, this is traditionally done by automatic voltage regulation (AVR) and feeder-level voltage regulation (Melhem, 2013). AVR systems uses on-load tap-changers (OLTC) and shunt capacitors (SC) at the primary substation. OLTC uses transformer tap positions to regulate voltage at the substation, whereas SC inject reactive power (Zhao, Wang & Zhang, 2018). In a traditional network, these control measures would be adequate as voltage setpoints are predetermined based on load flow calculations. The addition of DER to the network changes voltage levels, which creates a challenge for conventional voltage control devices. Some of the key components of the centralized control architecture is illustrated in figure 2.9 and briefly discussed below, where CC, SVR, CB, represents central controller, step voltage regulator and capacitor bank, respectively.

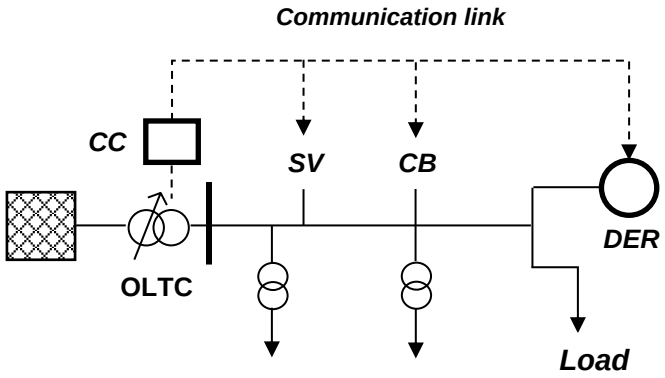

Figure 2.9. Centralized control architecture

Centralized control is used for global system optimization but becomes a problem when global information is not available (Ji et al., 2018). The disadvantage of central control, which has to deal with a large amount of data and monitoring devices, is its single point of failure (Arshad et al., 2018). Various studies have been conducted based on conventional centralized methods. In (Paula et al., 2017), a central controlled algorithm was developed based on fuzzy logic that coordinates voltage regulators, capacitors banks and reactive power injected by DG. In this study, an optimization problem for VVC is defined and a solution is developed to solve the shortcomings of local voltage control. The central controller receives information from the remote terminal units (RTU's) of devices and sends a control action back based on the developed optimization algorithm. In (C. Li et al., 2018), a central optimization of the OLTC tap position is proposed to minimize voltage deviations on the feeder. The objective of the optimization model is to minimize the voltage on the feeder and to reduce the number of tap changes. An optimal tap control (OTC) method is proposed to regulate OLTC. The results show that; compared to autonomous tap control (ATC), which is the conventional OLTC operation, OTC, which is the optimal tap control method can accommodate around 67% more

PV without over-voltage issues. Mokhtari et al (2013), proposes a localized and centralized control strategy to avoid voltage limit violations in LV networks. In this study, each user is controlled by its own energy management device. This device acts as a central controller for all controllable devices, such as PV, ESS, PEV and controllable loads. The local controller is used to coordinate real and reactive power of the PV and wind power. In this study, the voltage rise due to active power injection is mitigated by reactive power absorption.

In centralized control schemes, advanced methods have been used to mitigate the shortcomings of conventional voltage control (Mahmud & Zahedi, 2016). The control scheme is characterized by local DER, load controllers and smart meters that are linked via a communication system to the central controller. SCADA control is considered as another advanced voltage control scheme. In SCADA control, all the conventional devices are monitored and controlled by the SCADA substation system (Padullaparti et al., 2016). The SCADA system determines the control actions based on measurements and pre-determined rules, which is communicated to VVC devices along the feeder. The predetermined rules are based on unidirectional power flow in network studies. The limitation with this type of control is that it is not flexible to accommodate any change in feeder configuration as the rules are predetermined. Integrated VVC (IVVC) control compensates for the shortcomings of the SCADA controlled systems in that it can adapt to feeder reconfigurations. It uses real time measurements to run power flow results, which is fed into an optimization engine to determine the optimal set of control actions (Padullaparti et al., 2016). Various intelligent algorithms have been used in the literature to deal with voltage control based on DG penetration. The advantage of using intelligent control is that the solution can be adapted based on varying conditions and demand.

In (Nasiri et al., 2016), a centralized scheme is used to coordinate active/reactive power control from PV with OLTC in low voltage feeders, interfaced with back-to-back converters. An algorithm is devised that supply/consumes reactive power from the PV units based on voltage limitations. If these limitations are not met, tap changer of the transformer will be activated. Various other publications reviewed, which focused on centralized control, used a similar methodology. In (Farina et al., 2015), a three-layer hierarchical method is applied to deal with voltage violations in the MV network. An MPC-based algorithm for control of the network is used in this centrally controlled system.

- Central Controller

In conventional distribution networks, VVC devices are switched on and off based on load variations, as well as local voltage and current measurements. These devices are independently controlled based on local information and do not require a communication link

between devices. This strategy addresses the local voltage problem independently but does not address the entire network voltage problem. To solve this problem, a central controller, which links VVC devices by a communication link is used. The controller collects data from devices and controls the power flow and bus voltage profiles by algorithms in the network (Berger & Iniewski, 2012). The central controller adjusts voltage settings of the OLTC controller and is responsible for determining and sending the voltage and frequency set points to VVC devices and DER controllers (Behravesh et al, 2019; Yazdanian & Mehrizi-sani, 2014). DER local controller and other demand side resources is manged by a central controller by giving instruction to these devices based on predetermined set points (Yazdanian & Mehrizi-sani, 2014). The main controller acts as the central point of control and is responsible for determining and sending the voltage and frequency set points to local controllers (Azzopardi, 2017). Central control is the most common control method in traditional networks but has several drawbacks. As the distribution network is not equipped with ICT systems, real time information is not always available. In most cases, estimated measurements and historical data is used during planning. Some of the drawbacks include the cost associated with high-bandwidth communication infrastructure and the ability to control large systems (Wu, Rangan & Zhang, 2013). This strategy is the most common control method in traditional networks. It can be divided into (i) rule based, applied to transformer tap changer operations and (ii) optimization-based algorithms (Arshad et al., 2018). Frequent tap changing may lead to decrease lifespan of the transformer, so the optimization-based algorithm was improved by applying DER real and reactive power control. Optimization-based algorithms are discussed extensively in (Sarimuthu, Ramachandaramurthy, Agileswari, & Mokhlis, 2016). A summary of the advantages and disadvantages in given in table 2.3.

- Volt/Var Control (VVC) devices

Autonomous control uses conventional VVC devices such as OLTC of the transformer in HV/MV substations, step voltage regulator (SVR) and shunt capacitors (SC). These devices, which are classified as slow regulating, are used in unidirectional power flow based on the assumption that the voltage decreases as the distance from the transformer increases.

(i) On load tap changes (OLTC) - OLTC is the most used method to maintain secondary voltage. The main controller, based at the substation uses local or remote measurements as input values (Siewierski et al., 2018). The OLTC transformer uses a moving connection point to automatically adjustable taps and are widely used in voltage regulation (C. Li et al., 2018). The ratio of the secondary voltage changes with respect to the primary voltage by changing the tap position. The automatic voltage setting consists of a set-point and deadband. The former is

the desired voltage at the transformer and the latter represents the margin of tolerance, which keeps the voltage within the desired levels (Mokgonyana et al., 2016).

(ii) Step Voltage Regulator (SVR) - The step voltage regulator consists of an autotransformer and a load tap changing mechanism with adjustable steps. The change in voltage is achieved by changing the series winding of the autotransformer.

(iii) Shunt Capacitor (SC) - The shunt capacitor, which can be installed at the substation or along the feeder, generates reactive power. Control is done independently using local current and voltage measurements (Padullaparti, Nguyen, & Santoso, 2016).

(iv) Static compensators (STATCOMs) - STATCOMs inject reactive power at or near the load, especially in lines with inductive impedance. DSTATCOMs are used for distribution lines (Zimann et al., 2019).

- Communication technologies

The existing distribution network lacks the capability to do real-time monitoring and control. Such intelligence and control are reserved for generation and transmission. The intelligence, monitoring and control must be extended to the future distribution network based on real-time data and communication. The role of the communication infrastructure is to connect devices like VVC, DER and other controllable devices and exchange information (Budka, Deshpande & Thottan, 2014) The requirements of a good communication infrastructure are: latency - time it takes for information to travel; bandwidth - maximum transmitted data in bits per second and data rate - maximum data transmitted (Azzopardi, 2017). Communication at distribution level is referred to as local area network (LAN) or Neighbour hood area network (NAN). LAN serves field sensors, CBs, and VRs on feeders. Wide area network (WAN) and home are network (HAN) serve generation/transmission and consumers only. Monitoring of active distribution networks is achieved by smart meters, advanced metering infrastructure (AMI) and energy management systems (EMS) (Siano, 2014). A comparison of communication technologies is presented in table 2.2.

Table 2.2. Communication technologies (Azzorpardi, 2017; Berger & Iniewski, 2012)

Technology	**Data rate**	**Range**
PLC	1-500 Kbps	>150 km
Zigbee	<250 Kbps	<100 m
Wimax	< 1 Gbps	<10 km
Wifi	<600 Mbps	<1 km
Bluetooth	<720 Kbps	<100 m

Smart meters have two functions i.e., measurement and communication and should have the capability to (i) measure energy consumed on a time interval basis, (ii) have two-way communication, (iii) store time interval data and transfer it remotely and (iv) perform remote load management. A smart meter performs advanced current, voltage and frequency measurements, including their magnitudes. According to the Department of Energy in South Africa, all consumers who use more than 1000kWh/m, should have a smart meter installed. According to Regulation 773 of the Energy Regulation Act, a utility should be able to remotely control controllable loads as part of the DSM programme. Signals between users and utilities are sent via two-way communication such as radio, internet, PLC, and GSM.

2.4.1.2 Decentralized control architecture

In centralized systems, the continuous tap changing because of intermittent DER, may lead to equipment failure. An alternative option is to use the reactive and active power capabilities of DER to control the voltage at local buses and reduce distribution losses. The local controller receives data from sensors and smart meters and makes control decisions based on local measurements (Mahmud & Zahedi, 2016). Control decisions can be made locally and in conjunction with neighbouring controllers, via a communication link (Fazio et al., 2013). In this way, controllers work together to achieve a global solution. DER inverters generally operate below rated power, which means that reactive power will always be available. This power depends on the apparent power (S) and active power (P) output. DER controllers use local measurements and information to control the voltage independently at a given bus, based on localized voltage issues. In a decentralized control approach, the voltage problem is decomposed and sub-divided into smaller semi-autonomous areas, which simplifies the optimization solution. In this way, the problem is managed locally without any communication link with the central controller. One of the major advantages of decentralized control is that it can provide voltage support at local level. A typical decentralized system is illustrated in figure 2.10, where DG inverter at each bus can provide local voltage support.

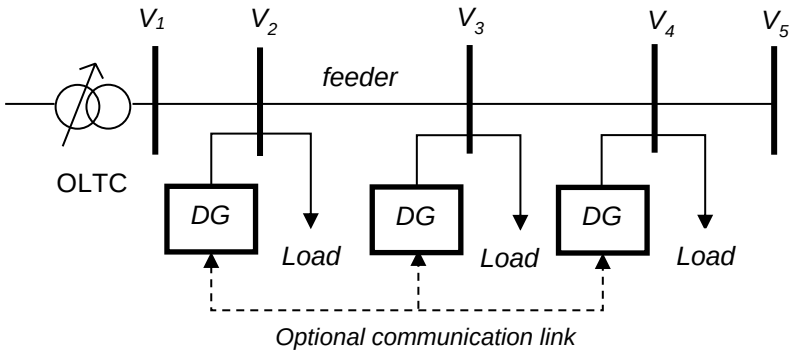

Figure 2.10. Decentralized control architecture

Multi-agent has been proposed as a solution to decentralized voltage control in (Mahmud & Zahedi, 2016). In this decentralized method, the voltage control problem is sub-divided by segregating the network into smaller zones or semi-autonomous areas (Islam, Sutanto, & Muttaqi, 2015). One of the major advantages of decentralized control is that it can provide voltage support at local level. Some of these methods will briefly be reviewed below.

- Reactive Power Control - Voltage can be controlled by allowing the synchronous generators to absorb reactive power and inverter-based DG to dispatch reactive power. Other devices include STATCOM, which provides a faster response time and SVC, which provides control with tight parameters. The other conventional method to inject reactive power into the distribution line is via SCs (Tengku, Mohamed, & Shareef, 2012).

- Active Power Control - This method can be achieved either by DG active power curtailment or curtailment of controllable loads (Siewierski et al., 2018). Voltage rise can be limited by reducing the active power from intermittent resources. In these methods the central controller sends predetermined values to the inverter. This is seen as a last resort, as curtailment of power from PV and wind energy, is not an ideal option for owners, as it reduced profits.

- Energy Storage - Energy storage devices consists of battery energy storage (BES) devices and plug-in electric vehicles (PEV). Both use conversion systems, which control charging and discharging (Xu & Taylor, 2008). Energy storage devices can inject or consume active and reactive power depending on network requirements.

Table 2.3. Comparison between voltage control methods (Bahramipanah et al., 2016)

Method	Advantage	Disadvantage
Centralized	i. Wide coordination ii. Ease of hardware implementation iii. Robust iv. Possibility to ensure global and local objectives	i. Requires reliable communication. ii. High investment iii. Extensive control iv. Subject to single point failures v. Extremely sensitive to system failure vi. Computation complexity vii. Difficulties when global information is not available. viii. Network control is lost when central supervisor is lost
Decentralized	i. No coordination ii. Cost saving - limiting the need for large investment. iii. Control actions are locally determined. iv. Not reliant on the wide area communication system v. Able to provide voltage support. vi. Avoids the need for complex data management	i. Limited coordination ii. Ignores global objective. iii. Focuses on the local objective. iv. Possibility of conflicts when several local controls exist

2.5 Voltage control in South African distribution networks

Voltage quality parameters are covered by NRS 048 in South Africa (NERSA, 2003). The aim of these standards is to set and provide acceptable voltage quality limits at the point of common coupling (PCC). The standard connection voltage for low voltage (LV) customers is 400 V, phase to phase and 230 V, phase to neutral (NERSA, 2003)

The local voltage control strategy is based on a centralized system where control is executed at the HV/MV substation. The strategy uses traditional voltage regulation equipment like power transformers, equipped with on-load tap changers (OLTCs) to regulate the secondary voltage at the substation. This secondary voltage is usually regulated at 103% of nominal voltage with tap change bandwidth settings typically set at 1.4% or 1.5%. Voltage regulators are used on long MV feeders to increase the voltage when required (Carter-Brown, 2010). Local utilities use a combination of VRs and OLTCs to regulate the voltage on MV feeders (Van Zyl & Gaunt,

2003). The majority of OLTC and VRs use line drop compensator (LDC), but this is not common in South African distribution networks due to higher load density ((Van Zyl & Gaunt, 2003). Capacitors are used on local distribution feeders for reactive power compensation and to reduce the voltage drop along the line. Capacitor sizes used on local distribution networks are rated for 1.5-13 kV and 300kVAr per can with a rated voltage of 110% of the nominal system ((Van Zyl & Gaunt,C.T.,2003). The local supply authority uses single phase capacitors connected in ungrounded star, which provides a path for zero sequence currents.

The primary application of DER is to inject active power into the grid but can also be used for reactive power and voltage control. Renewable Power Plants (RPP) in SA are classified under 3 categories. Category A, which is connected on the LV side of the distribution transformer, is divided into 3 sub-categories. Whilst categories A1 and A2 have similar characteristic except for power output, A1 is reserved for residential customers and A2 is connected at commercial and light industrial level. RPP categories and connection requirements are given in table 2.4.

Table 2.4. Grid connection requirements (SAGC,2012)

Category	Power Output	**Voltage Level (V)**	**Voltage limit (%)**	**PF range**	**Control functions**
A1	0 kVA ≤ x ≤ 13.8 kVA	< 500	-15+10	> 0.98	N/A
A2	13.8 kVA < x < 100 kVA	< 500	-15+10	> 0.98	N/A
A3	100 kVA ≤ x < 1 MVA	< 500	-15+10	0.95 lagging & 0.95 leading	PF control
B	1 MVA ≤ x < 20 MVA	≥ 500	± 5	0.975 lagging & 0.975 leading	Q, PF & V control
C	20 MVA ≤ x.	≥ 500	± 5	0.95 lagging & 0.95 leading	Q, PF & V control

According to [SAGC], DER should have the following functionality, based on size**:**

- Reactive power control - Only DER with a power output greater than 100 kVA are able to control reactive power at the point of common coupling (PCC). This limits the reactive power contribution of residential and light commercial DER. For DER with power output greater than 1 MVA and operating between 5% and 100% of rated power, reactive power support is allowed. The reactive power setpoints and gradients are set by the local supply authority and controlled via a centralized controller. This setpoint received from the central controller shall have an accuracy of 1kVar. The reactive power control *(Q)* function controls the reactive power supply and absorption at the PCC.

- Power Factor control - DER with output power of 0-100kVA shall operate above 0.98 PF or at unity PF. The PF should be improved to unity, where PF control at the PCC is possible. The PF control is used to control *Q,* proportional to the acive power *(P)* at the connection point. For DER output power between 100 kVA and 1 MVA and operating between 20% and 100% of rated power, the PF range should be 0.95 lagging and 0.95 leading.

- Voltage control - Voltage setpoints are determined by the supply authority. Based on regulations, these setpoints shall be within ±0.5% of nominal voltage and within ±2% of *Q* according to droop characteristics.

- Active power constraint - Active power curtailment functionality is limited to DER with output power of 100 kVA and greater. The setpoint is issued by the supply authority to limit the active power at the PCC.

2.6 Optimization Methods

An optimization problem consists of (i) an objective function, which is the output that is, either being minimized or maximized, (ii) the input variables, and (iii) constraints of inequality and equality, which places limitations on the variables (Kuroda & Magori, 2015). The main challenge with renewable energy incorporation into the grid is unpredictability, due to its intermittent nature. This challenge can be expressed and solved as an optimization problem, which consists of a constraint. The solution to the optimization problem must satisfy this constraint. Different types of optimization problems exist. Some have constraints and some do not; some have one variable, and some have multiple, which can be discrete or continuous. Optimization problems can be static or dynamic, whilst some systems can be deterministic or stochastic. In distribution networks, the optimization problem is usually modelled as a non-linear mathematical optimization problem, which involves various variables (Resener, Haffner, Pereira, & Pardalos, 2018). In power systems, the optimization problem can be categorized as single and multi-objective (Kuroda & Magori, 2015).

- Single-objective optimization problem - an optimization problem based on solving a single objective and is mathematically defined as:

$$\min f(x) \tag{2.1}$$

Subject to.

$$g_j(x) \leq 0 \qquad j = 1,2 \ldots., q \tag{2.2}$$

$$h_j(x) = 0 \qquad j = q+1, q+2, \dots, m \tag{2.3}$$

$$k_i \le x_i \le l_i \qquad i = 1,2, \dots, n \tag{2.4}$$

Where:

$f(x)$	= objective function
$x = (x_1, x_2, \dots \dots x_n)$	= the n-dimensional vector
$g_j(x) \le 0$	= inequality constraints
$h_j(x) = 0$	= equality constraints
l_i & k_i	= upper and lower bounds of x_i ,respectively

- Multi-objective optimization problem - an optimization problem based on solving multiple objectives, simultaneously. In the real world, optimization problems are in competition with each other and must be solved simultaneously. The optimization problem is mathematically defined as:

$$f(x) = [f_1(x), \dots, f_n(x)] \tag{2.5}$$

Subject to.

$$g_i(x) \le 0, \qquad i = (1, \dots, m) \tag{2.6}$$

$$h_i(x) = 0, \qquad j = (1, \dots, p) \tag{2.7}$$

Where:

$g_i(x) \le 0$		= inequality constraint
$h_i(x) = 0$		= equality constraint
n		= number of objective functions.
$k_i \le x_i \le l_i$	$i = 1,2, \dots, k$	= upper and lower limits

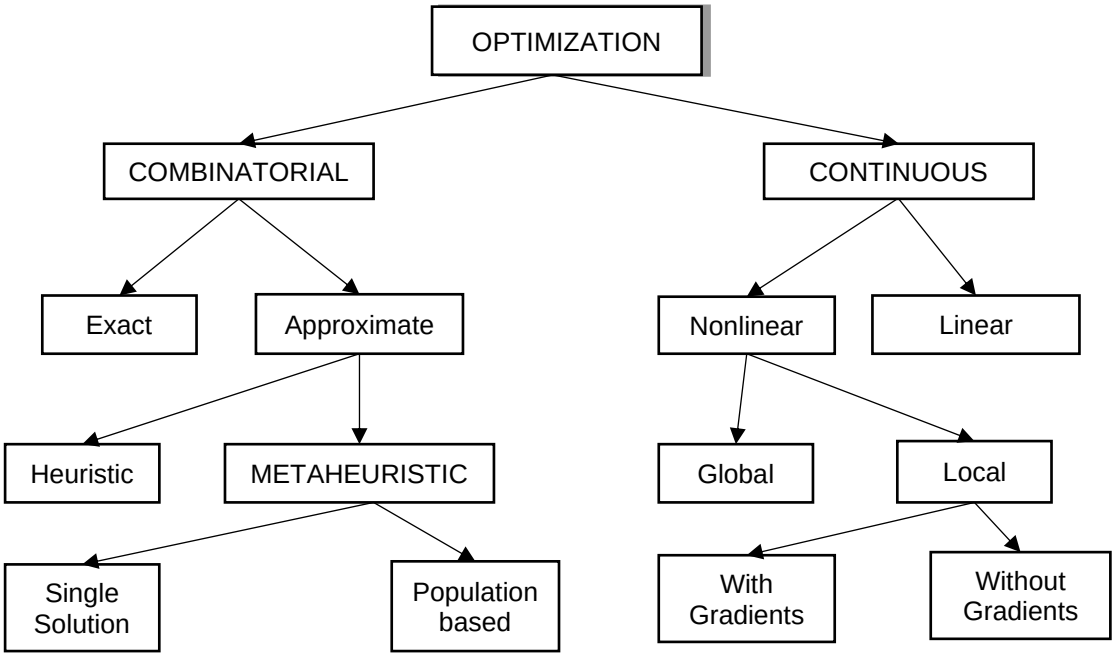

Figure 2.11. Mono-objective optimization methods adapated from (Dreo at al, 2006)

Conventional and intelligent optimization methods can be used to solve voltage and demand-side management problems in active networks. Some of these are discussed and summarized in table 2.5.. For this review, optimization methods are divided into conventional and intelligent methods. These can be categorized into distributed and decentralized methods as well. Based on the reviewed literature, the multiobjective optimization problem is formulated from the voltage profile, which is considered with other network constraints. In the centralized control architecture, the minimization of system losses is a common objective, with various constraints such as reactive powers supplied by inverters, transformer taps SVRs and other VVC devices. In decentralised systems, minimizing grid loss, voltage deviation, total cost, and maximizing DER owner benefit can be formulated as the main objective function.

2.6.1 Conventional methods

The conventional method uses a numerical equation based on a mathamatical analysis. The approach has been successfully applied to improve voltage profile in networks (Abdmouleh, Gastli, Ben-brahim, Haouari, & Al-emadi, 2017). Some of the commonly used conventional methods are:

- Sensitivity Analysis (SA) - In SA, certain parameters are changed to determine the impact on the results. Based on the literature, SA is a popular method used for PV and wind analysis. Sensitivity analysis reduces computational time and has been used extensively for voltage profile calculation (Gu, W., Lou, G., Tan, W., & Yuan, X..2017). Khalid et al (2018) uses a sensitivity-based method to address overvoltage in LV

networks using reactive power of PV inverters. In the study the Jacobian matrix is used for sensitivity analysis with real and reactive power. Di Fazio et al (2019) used a Jacobian-based method for sensitivity analysis of nodal voltages based on active and reactive power injection from DER. The study is based on a centralized voltage method and aims to divide the large network into voltage control zones as defined in Antoniadou-Plytaria et al (2019), based on similar electrical distances. This method is used to overcome the computational inefficiency presented by the Jacobian matrix and is proposed to simplify the voltage control problem and to cope with large decision variables.

- Linear and Non-Linear Programming (LP & NLP) - Linear Programming uses a linear mathematical method to solve a linear problem, where the objective function and constraints are linear, and the decision variables are continuous. In practice, constraints and objectives are linear. The general linear programming problem can be mathematically expressed as:

  minimize $\mathbf{c}^T\mathbf{x}$
  subject to $\mathbf{Ax} = \mathbf{b} \;\; and \; \mathbf{x} \geq \mathbf{0}$

  where, $\mathbf{x}$ is an *n*-dimensional column vector, $\mathbf{c}^T$ is an *n*-dimensional row vector, $\mathbf{A}$ is an *m x n* matrix and $\mathbf{b}$ is an m-dimensional column vector. The study by Di Fazio et al (2019), used a linear method for steady state analysis of distribution systems based on a Jacobian-based method. The linear method proposes an evaluation of the initial condition of the distribution network without DER and then evaluates sensitivity coefficients from the contribution of active and reactive power from DER at various nodal points. The closed loop expression is obtained from the sensitivity coefficients based on DER power injection or absorption. From the results, this linear method shows an increase in the computational efficiency when compared to other linear methods.

  For Non-Linear Programming, the objective function and constraints are non-linear, and the variables are continuous (Kenny et al, 2016) The general non-linear program problems can be mathematical express as:

  minimize $f(\mathbf{x})$
  subject to $\mathbf{h}(\mathbf{x}) = 0, \; \mathbf{g}(\mathbf{x}) \leq 0$
  $x \in \Omega$

where, $\mathbf{h}(\mathbf{x}) = 0,\ \mathbf{g}(\mathbf{x}) \leq 0$ is the functional constraint and $x \in \Omega$ is the set constraint.

Christakou et al (2014) conducted a study to determine the potential of a large aggregation of small thermostatic loads on primary control, using a low overhead DR decentralized control scheme. Linear programming was used by providing a low bit control signal, which provided an ON-OFF action on the appliance that was equipped with a programmable controller, for direct load control. It must be noted that the utility does not control each individual load, but rather sends a unique signal to each bus in the network via power line communication. In emergency situations, such as grid disturbances, the utility can use tap changers at the substation to stabilize the voltage. He & Petit (2016)] proposes a centralized control strategy where the voltage problem has been formulated into a MILP. The objective of the study is to find the total cost associated with the voltage control using tap changers, reactive and active control of DG and demand response. The study concluded that the cost of DR is cheaper than DG active curtailment and provides a more robust voltage support if the demand increases.

- Model Predictive Control (MPC) - MPC is used for control of large process plants (Yazdanian & Mehrizi-Sani, 2014)

- Optimal Power Flow (OPF) - OPF has been extensively used and researched in power systems engineering. The aim of OPF is to minimize the total operating cost and total losses in the network, subjected to many constraints, such voltage profile. The method is used to solve DG allocation and sizing problem, based on economic considerations. OPF problem is a non-linear, large-scale and non-convex problem due to the presence of non-linear (AC) power flow equality constraints. Vovos et al (2006) used OPF method to determine the DG hosting capacity using a centralized and distributed voltage control scheme. The objective function can be mathematically presented by:

$$min\ F\ (u, x) \tag{2.8}$$

Subject to.

$$h\ (u, x)\ \leq 0 \tag{2.9}$$

$$g\ (u, x) = 0 \tag{2.10}$$

$$u^{min}\ \leq u\ \leq u^{max} \tag{2.11}$$

Where:

$min\ F\ (u, x)$ = objective function

$g\ (u, x) = 0$ = non-linear equality constraint

$h\ (u, x)\ \leq 0$ = non-linear inequality constraint

u = controllable quantities

x = set of dependent variables

- Fuzzy logic (FL) - FL was used in 1979 for the first time to deal with uncertain problems. Power system problems, allocation and sizing of DG and enhancing voltage profile in distribution networks have been solved by FL. The technique is derived from fuzzy set theory dealing with reasoning that is approximate rather than precise. Fuzzy control has been used in several studies to solve non-linear problems such as the relationship between power injected from DG and voltage at a certain bus (Mehrjerdi et al., 2013).

- Consensus-based - the goal of consensus is to have different DER units converge to a single value.

- Multi-Agent Systems (MAS) - MAS is a network of loosely-coupled autonomous intelligent agents, who can process data and perform actions (Bahramipanah et al., 2016). MAS is viewed as a distributed problem, where the global problem is decomposed into sub-problems, solved and later converged (Byrski & Kisiel-Dorohinicki, 2017). The algorithm has been used in distributed control in LV networks with DER (Mocci et al., 2015). The major advantage of MAS is that it suited to large scale complex systems.

2.6.2 Intelligent methods

Heuristic-based techniques, also referred to as computational intelligence methods, are inspired by nature or social inspirations and can be used to solve large complex problems (Byrski & Kisiel-Dorohinicki, 2017). Intelligent methods consist of algorithms that are simplistic and speed up the process of finding an optimal solution. The algorithms discussed below are classified as metaheuristic and are often nature inspired.

- Genetic Algorithm (GA) - GA is a search and optimization method, simulating natural selection and genetics. J. Holland pioneered GA in the 1960's, based on Darwin's evolution of the species (Yang, 2014). In 1989, D.E. Goldberg popularized the field after the publication of his book entitled "*Genetic Algorithms in Search, Optimization*

and Machine Learning" (Dreo et al, 2006). The aim of GA is to find the optimal solution to a problem (Abdmouleh et al., 2017). The program continually re-adjusts, reorganizes, and even mutates, to continually find a better solution as illustrated in figure 2.12.

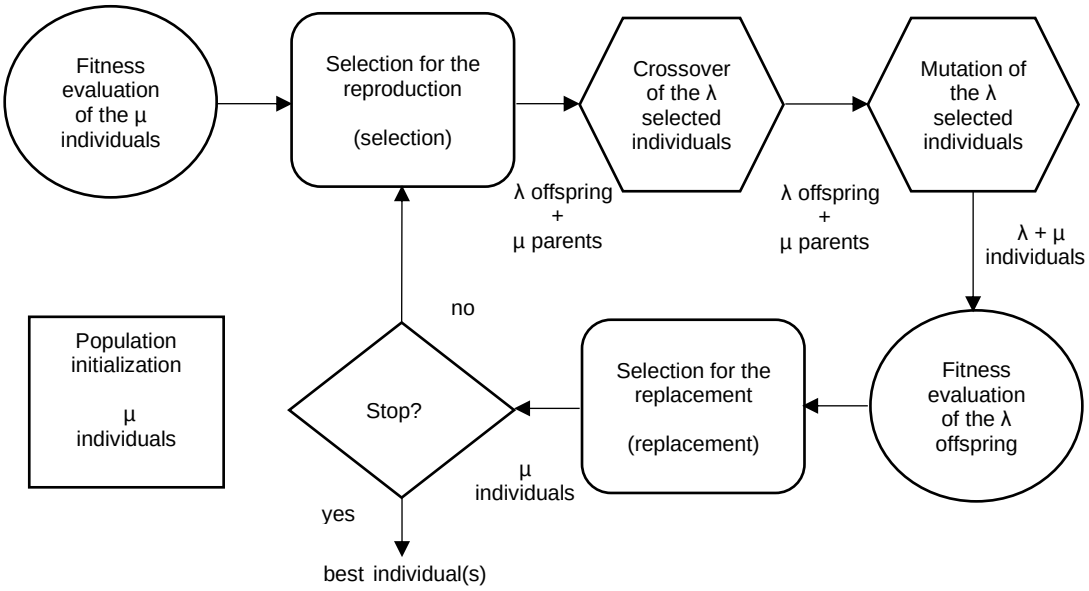

Figure 2.12. The Genetic Algorithm (Dreo et al, 2006)

- Particle Swarm Optimization (PSO) - PSO is a meta-heuristic optimization algorithm that was firstly introduced by Kennedy and Eberhart in 1995 (Dreo et al, 2006). It is like GA, but differs in selection of population of individuals, rather than one individual. PSO is a population-based stochastic optimization technique inspired by the social behaviour of bird flocking or fish schooling (Abdmouleh et al., 2017). The algorithms try to find a near-optimal solution with a limited computational burden. It can handle constrained and discrete optimisation problems with large decision variables. The method works in three simple steps i.e., evaluate, compare, and imitate and is based on a group of particles moving in a search space. Each particle is influenced by its own experience, known as *p*best and learning from others, known as *g*best.(Bansal, Singh, & Pal, 2019). The movement of the particle with respect to magnitude and direction is known as the velocity. The movement of the particle, relative to its neighbours is influenced by its direction and speed. The particle $\boldsymbol{i}$ can be represented as an object with several characteristics. The velocity and position update is given by 2.13 and 2.14, respectively (Bansal, Singh, & Pal, 2019):

$$v_{id}^{t+1} = v_{id}^{t} + c_1 r_1 (p_{id}^{t} - x_{id}^{t}) + c_2 r_2 (p_{gd}^{t} - x_{id}^{t}) \quad (2.12)$$

$$x_{id}^{t+1} = x_{id}^{t} + v_{id}^{t+1} \quad (2.13)$$

Where:

$x_i^t = (x_{i1}^t, x_{i2}^t, \dots, x_{iD}^t)$ = *i*th particle at time step t

$v_i^t = (v_{i1}^t, x_{i2}^t, \dots, v_{iD}^t)$ = velocity of particle at time step t

$p_i^t = (p_{i1}^t, p_{i2}^t, \dots, p_{iD}^t)$ = previous best position of *i*th particle

g = index of the best particle

$d = 1,2, \dots D$ = dimensions

$i = 1,2, \dots S$ = particle index

c_1, c_2 = acceleration coefficients

r_1, r_2 = random number

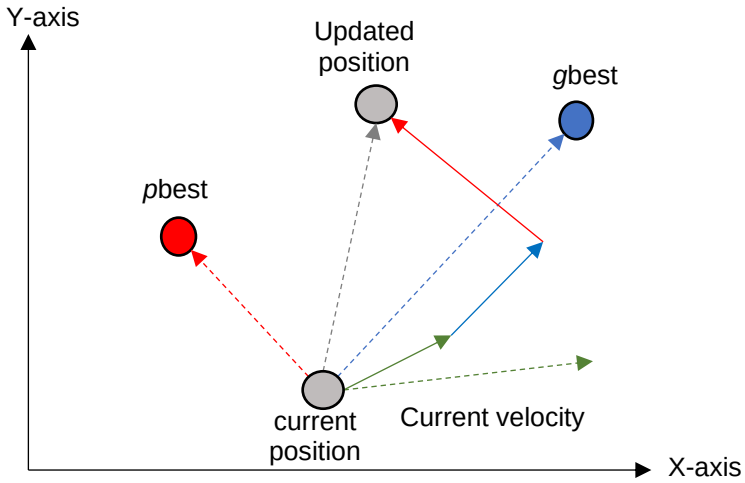

Figure 2.13. Geometric illustration of particle's movement in PSO (Bansal, Singh, & Pal, 2019)

Figure 2.13 is an illustration of a particle's movement in a 2-dimensional space. PSO has been used extensively in location and sizing of DG and can handle non-linear functions. It has the advantage of being robust and has excellent global convergence properties (Feshki, 2017).

- Cuckoo Search (CS) – this nature-inspired search algorithm was developed by Yang and Deb in 2009. It is based on the specific breeding and egg laying behaviour of some cuckoo species, who lay their eggs in the nests of a host birds. The algorithm uses the so-called Lévy flights, which is not based on random walks. The Lévy flights is used, which is more efficient and generates a larger search space. Using the Lévy flights, new solutions are formed according to:

$$x_i^{t+1} = x_i^t + \alpha \otimes Lévy(\lambda), \tag{2.14}$$

Where, α > 0 is the step size; α = 1 can be used for most cases and $Lévy \sim u = t^{-1}, 1 < \lambda \leq 3$. A comparative study between cuckoo search and other meta heuristic algorithms showed that cuckoo search is more efficient and can satisfy global convergence (Yang, 2014). Civicioglu & Beshok (2014) conducted a comparitive study using CS. A deterministic algorithm is used for voltage control in distribution networks based on current and future scenarios. The determinstic algorithm may only achieve local optimal solutions, whilst CS could achieve global optimal solutions.

2.6.3 Demand response Optimization

The DR optimisation problem can be classified into two broad categories i.e. (i) classic and (ii) Meta-heuristic. In the reviewed literature, the classic method consists of linear and non-linear optimization and for metaheuristics, Particle Swarm Optimization and Genetic algorithm. DR problems are generally solved by the classic methods i.e., linear, and non-linear optimization. In (He & Petit, 2016), a centralized control strategy is proposed where the voltage problem has been formulated into a MILP. The objective of the study is to find the total cost associated with the voltage control using tap changers, reactive and active control of DG and demand response. The study concludes that the cost of DR is cheaper than DG active curtailment and provides a more robust voltage support if the demand increases.

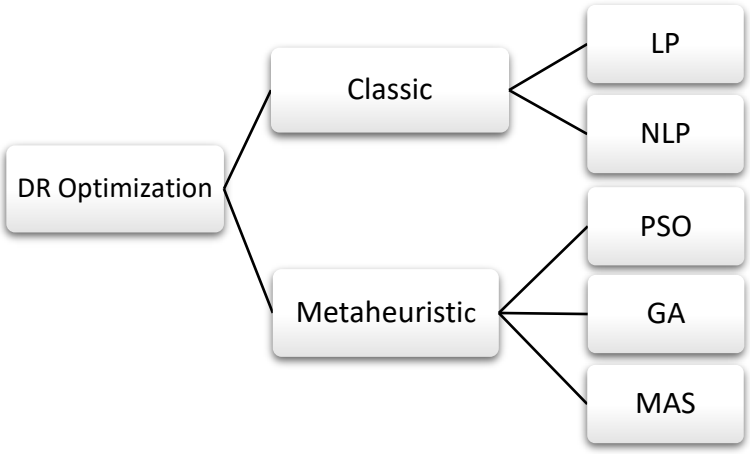

Figure 2.14. DR Optimization algorithms. dapated from (Jordehi, 2019)

Meta-heuristics is another good method to solving DR problems as they can handle discrete and constrained problems (Jordehi, 2019). From the literature, seven publications used metaheuristics to solve the DR problem. These are PSO and GA as illustrated in figure 2.14. In (Petinrin & Shaaban, 2014), GA is used to consider the optimum energy scheduling of appliances to reduce voltage deviations on a feeder, considering wind power participation. The problem was modelled as a non-linear optimization problem. The advantage of this method over traditional techniques, is that it is based on population based, rather than a single solution. The procedure for finding the optimum solution though GA is illustrated in figure 2.6, which shows the general flowchart. The aim of the proposed solution in this study is to minimize the voltage deviation through customer load scheduling. In this price-based scheme, the utility sends electricity pricing to consumers via AMI's. The customer responds by scheduling elastic loads at different time intervals. The study proves that DR techniques improves the voltage profile along the feeders, as the customer participation increases. In (Xie, 2017), a centralized control scheme is proposed based on a day-ahead load scheduling and real-time load scheduling to solve the overvoltage problems in LV networks caused by penetration of PV and PEV. GA is used to solve the day-ahead load scheduling. In the solution, Home Energy Management (HEM) and Community Energy Management (CEM) systems are developed to screen and control scheduled loads. The day-ahead load scheduling aims to increase customer profits and reduce voltage violations in the network.

In (Hashemi et al., 2018), a corrective DR control action is implemented based on minimum load reduction. PSO is used to find the optimal load reduction based on DR participation to maintain the voltage security in the network. In this study, the threshold voltage and optimal load reduction pattern is estimated, which triggers DR response. Rahman et al, (2018), used a modified particle swarm optimisation algorithm (MPSO) to determine the optimal switching combination of household appliances and OLTC tap positions in unbalanced LV systems. MPSO was chosen to deal with premature convergence and lack of guarantee in global convergence. The optimisation aims to determine the optimal size of DR and OLTC tap position for effective voltage control. In (Bayat et al., 2016), a multi-objective problem is formulated by DR and DER participation in a microgrid and solved by PSO. In the proposed method, a centrally controlled energy management system (EMS) assigns the real and reactive power setpoints for the local DERs and reactive power compensators as well as power to be curtailed through the controllable loads for voltage management.

MAS is an extremely popular method to solve DR optimization problems. An agent is an autonomous and intelligent component that acts on behalf of its user and is capable of making autonomous decisions (Byrski & Kisiel-Dorohinicki, 2017). The study conducted by (Anderson & Narayan, 2011), uses the MAS method to solve the voltage problem by integrating DR with

distribution VVC control. It considers the role of an aggregator in DR. In (Davarzani et al., 2017), a MAS framework is proposed that mitigates local overloading of networks by controlling domestic loads. The aim of the framework is to reduce the total active power at the distribution transformer during emergency conditions by using four different DR participants, which are modelled as agents. In (Solanki, Venkatesan & Khushalani, 2012), MAS framework is used to coordinate DR with VVC during peak loads.

Table 2.5. Review of optimization methods

Optimization Method	**Goal**	**Advantage**	**Disadvantage**	**No of publications**
Sensitivity Analysis (SA)	The changing of some parameters to see the impact of the result	i. In-depth analysis ii. Helps in the proper allocation of resources. iii. Helps in quality checks	i. Based on assumptions ii. It is not relative in nature	14
Fuzzy logic (FL)	Predictive technique to solving complex stochastic problems	i. High precision ii. Rapid operation iii. Method of non-linear control iv. The rules are set in natural language	i. Lacks real time response. ii. Restricted number of input variables	4
Optimal Power Flow (OPF)	The goal is to define the optimum economic operating cost or minimize the cost of generation	i. High precision factor ii. Computational time efficiency	i. Difficult to include different aspects into calculation	4
Model Predictiive Control (MPC)	To guarantee stability of system and to improve the operation of a process and productivity of a plant	i. Handling of multivariable control problems ii. Ease of tuning iii. Ability to handle constraints. iv. Robust control	i. Computational cost ii. Cannot deal with plant model uncertainties	2
Linear and Non-Linear Programming (LP & NLP)	LP and NLP are used to determine an optimization problem where the constrains are linear and non-linear respectively	i. Exact solutions are determined. ii. High precision factor	i. Large number of decision variable ii. Long computational time	5

Consensus Algorithm (CA)	The goal is to have different units converge to a single value or achieve an agreement on a single data value	i. Can be extendable and scalable. ii. Does not need a dedicated control unit between single units	i. Computing takes a long time	9
Multi-Agent Systems (MAS)	Components or agents of the grid interact with each other to serve consumers	i. Flexible. ii. Low cost iii. Time saving approach. iv. Suitable for large complex systems. v. Reduced costs. vi. Computational efficiency and speed	i. Difficult to interoperate with other systems. ii. Maintenance cost can be high.	16
Genetic Algorithm (GA	Solving constrained and unconstrained optimization problems	i. Can be used for wide variety of optimization problems. ii. Does not require derivatives. iii. Good method to solve large scale combinatorial optimization problem	i. Can be time consuming for large and complex problems. ii. Can be inaccurate. iii. Can suggest bad solutions	8
Particle Swarm Optimization (PSO)	Optimal solution through continuous iteration	i. Simple to implement. ii. Can converge fast. iii. Have shorter computational time.	i. Difficult to define initial design parameters. ii. Cannot work out the problems of scattering. iii. Can converge prematurely	8

Table 2.6. Taxonomy of reviewed articles relating to DG

Reference	Objective function	Control technique	Solution Methodology	Variables	Case Study	Optimization methods
(Mehrjerdi et al., 2013)	Elimination of Voltage violations	Decentralized	Partitioning of network into regions. Reactive power injection at selected buses to control voltage	DG	IEEE 118-bus network	Fuzzy logic
(Calderaro et al., 2014)	Local voltage control	Decentralized	DG reactive and active power exchange	DG	20-kV, 4 feeder distribution system	Sensitivity Analysis
(Fazio et al., 2013)	Voltage minimization	Decentralized	Setpoint voltage design. DG reactive and active power control	PV & Wind	MV distribution system with multiple feeder	Sensitivity Analysis
(Calderaro et al., 2012)	Voltage limitation	Decentralized	Active and reactive power control of DG	Wind	20-kV, 4 feeder distribution system	Sensitivity Analysis & Fuzzy Logic
(Gu et al., 2017)	Average voltage restoration	Decentralized	DG reactive power sharing	DG	Micro grid test system with 3 DG's	State estimation
(Feng et al., 2018)	Voltage violation mitigation	Decentralized	Primary control via local DG active/reactive power. Secondary control coordination of DG active/reactive power	DG	110 kV, 72 nodes network	Second-order cone relaxation
(Islam, Muttaqi & Sutanto, 2015)	Control of voltage collapse	Decentralized	Shunt capacitors for injecting reactive power and load cuts	SC & Controllable loads	IEEE-57 bus system	Multi Agent System
(Yorino et al., 2015)	Voltage minimization	Decentralized	Management agents for monitoring and local agents for real-time control	OLTC & SVR	radial 6.6-kV test system	Multi Agent System

(Rashidi & Moshtagh, 2014)	Voltage minimization	Decentralized	DG reactive power control	DG	IEEE 33- bus system (unbalanced)	Genetic Algorithm
(Villacci, 2019)	Voltage regulation	Decentralized	DG reactive power control	DG	IEEE 30-bus test system	MAS & Consensus Algorithm
(Li et al., 2019)	Voltage management	Local & Decentralized	Combined local and decentralized control based on SOP	PV & Wind	69-node & modified IEEE 123-node distribution system	Not mentioned
(Fallahzadeh-abarghouei et al., 2018)	Voltage management	Decentralized	DG reactive power control based on network partitioning	PV & Wind	34-bus test system & PG&E 69-bus distribution system	Sensitivity Analysis
(Joelle et al., 2016)	Voltage control using local controllers	Decentralized	Fuzzy logic based controller for DG active & reactive power control combined with OLTC and capacitor control	DG, OLTC, Capacitors	IEEE 33-bus test network	Fuzzy Logic
(Wu et al., 2017)	Voltage minimization	Distributed	Adjustment of DG and shunt capacitors outputs according to different network states	DG, Shunt capacitors	10KV distribution network with 3 feeders and 40 buses	Multi Agent Systems
(Swain & De, 2019)	Voltage minimization	Decentralized	Controlling of DG output based on a proximity index	DG and flexible loads	IEEE 33 bus and 69 bus	Proximity index
(Yujun & Petit, 2013)	Voltage limitation	Hybrid	OLTC switching via VR and setpoint of DG reactive power injection	DG and OLTC	63kV/20kV, 3 feeder distribution network	Sensitivity Analysis

(Horoufiany, 2012)	Voltage limitations	Hybrid	Local load controller coordinate with local DER controllers, which coordinate with central controller	Loads & DER	IEEE 69-bus network	Not mentioned
(Nasiri et al., 2016)	Voltage limitations	Centralized	Voltage management of feeders via OLTC, B2B converters and PV reactive power	PV and OLTC	CIGRE European distribution model	Not mentioned
(Y. Liu et al., 2018)	Voltage limit satisfaction	Decentralized	PV active and reactive power control based on voltage amplitude and line impedance	PV	LV distribution network	Sensitivity Analysis
(Olival et al., 2017)	Voltage minimization	Centralized	Using PV & load controllers for short-term load and PV forecasting	PV, ESS & controllable loads	33 bus, 32 branches LV grid	EPSO
(Paula et al., 2017)	Minimization of the voltage violations	Centralized	Central controller coordinates VR's, SC's and DG based on real-time applications	VR, SC & DG	IEEE 34 node test feeder	Fuzzy Logic
(Mokhtari et al., 2013)	Voltage support	Local & Centralized	Local PV active & reactive power injection. Central control, which control local controllers	PV	Single-phase LV network with 12 customers	Consensus Algorithm
(Siewierski et al., 2018)	Solving voltage static rise problems	Local & Centralized	Adjustment of OLTC, PV active & reactive power control, load curtailment	PV, Load, OLTC	LV feeder supplying 18 residential customers	Sensitivity Analysis
(Mokgonyana et al., 2016)	Reduction of voltage deviations	Centralized	Feeder Capacitors dispatch schedule using reactive power set-points.	OLTC, SC	14 & 69-bus system	MPSO

(Khalid et al., 2018)	Voltage regulation	Local & Centralized	Two-stage control based on tap setting and DG reactive power flow	OLTC, SC, Wind & PV	IEEE 37- node test feeder	Genetic Algorithm
(Kulmala & Repo, 2014)	Feeder voltage limitation	Centralized	Two-stage SCADA control based on tap setting and DG reactive power flow	OLTC, DG	Finnish distribution network consisting of 2 x 20kV feeders	MINL
(Jiongcong et al., 2014)	Closed loop voltage control	Centralized	Cooperation between feeder voltage controller and central substation controller based on local DG measurements	DG, OLTC	20kV network with two feeders and 5 DERs	Sensitivity Analysis
(Behravesh et al., 2019)	Voltage profile improvement	Centralized	Combined local and central control of customer resources & OLTC	PV, Wind, BES	LV network with 60 single-phase residential houses	Sensitivity Analysis
(Y. Li et al., 2019)	Voltage deviation minimization	Decentralized	Using EV's for reactive power control	EV	19-bus LV radial distribution system	MPC
(Pournazarian et al., 2019)	Voltage drop minimization	Decentralized	Two stage inverter-based DG droop control and PHEV reactive power control	DG & PHEV's	14-bus test microgrid	Intelligent droop control
(Takayama & Ishigame, 2018)	Voltage minimization	Decentralized	PV reactive control through reinforcement learning (trial and error)	PV	LV grid consisting of 12 consumers	Multi Agent Systems
(Rathbun et al, 2018)	Over voltage minimization	Centralized	PV reactive power dispatch	PV	IEEE 132 test feeder	Multi Agent Systems
(Arshad et al., 2018)	Voltage violation limitation	Distributed	Reactive power control and active power curtailment of PV	PV	20kV, 126 nodes network	Multi Agent Systems
(Cagnano & Tuglie, 2016)	Voltage control at nodal point	Decentralized	Voltage control of nodal points/buses via reactive power injection of PV	PV	20 kV distribution network with 20 nodes	Sensitivity Analysis

(Tanaka, 2009)	Voltage minimization	Decentralized	Reactive power control of DG based on local voltage control references	DG	MV feeder with 15 buses	GA
(C. Li et al., 2018)	Over-voltage limitation	Centralized	Optimal OLTC regulation. Reduction of tap operations by PV generation forecasting.	PV & OLTC	Typical distribution feeders	SA
(Farina et al., 2015)	Voltage minimization	Centralized	Central controller control setpoints of DG reactive power and transformer tap settings	OLTC & DG	Rural radial network with two feeders	OPF
(Haque et al., 2017)	Voltage violation limitation	Local & Centralized	Local voltage control of PV with a centralized congestion management scheme	PV & Electric Heat Pumps	10/0.4 kV, 100 kVA MV/LV network with 20 households	Multi Agent Systems
(Oshiro et al., 2011)	Reduction of voltage deviations	Centralized	Central control by calculation of optimal set points for DG and OLTC tap settings	LRT's and SVR's	Sample feeder with 21 buses	GA
(Jung et al., 2014)	Optimum voltage profile maintenance	Centralized	Control of capacitors, VR's and PV reactive and active power	SC, VR's & PV inverter	13.2 kV, circuit with 2751 residential customer and 111 industrial customers	SA
(Quijano & Padilha-feltrin, 2019)	Conservation voltage reduction	Centralized	Two stage model. First stage is based on load demand and DG production. Second stage regulates DG active and reactive power and coordinates with OLTC & VR's	DG, VR & OLTC	33-bus & 135 bus test system	OPF
(Cagnano & Tuglie, 2015)	Minimization of voltage deviations	Centralized	Central controller based. PV reactive power is injected based on set points	PV	20kV test feeder with 22 buses	SA

(Ji et al., 2018)	Voltage violation minimization	Local & Centralized	DG inverters reactive and active power curtailment based on local measurements is controlled by central controller.	DG	Modified PG&E 69-node distribution system	MISOCP
(Efkarpidis et al., 2016)	Voltage minimization	Hybrid	Hybrid approach where central controller controls OLTC and local controller for PV active and reactive power management	OLTC & PV	Typical Belgian LV network	SA
(Abessi et al., 2016)	Voltage violation limitation	Centralized	Central control & reactive power injection of DG at selected buses	DG	IEEE 33 and 69 bus test systems	GA
(Takahashi & Hayashi, 2012)	Voltage correction	Centralized	Central control of D-STATCOM with dead band	D-STATCOM	4 distribution lines	Numerical simulation
(Nimpitiwan & Chaiyabut, n.d.)	Minimization of voltage fluctuations	Centralized	Central coordination of OLTC, AVR, SC & DG	OLTC, AVR, SC & DG	Modified IEEE 14-bus test system	GA
(Vovos, Kiprakis, Wallace, & Harrison, 2007)	Minimization of voltage variation and violations	Central & distributed	Voltage and reactive power control of the DG	DG	Generic 12-bus 14-line distribution network presented	OPF
(H. J. Liu et al., 2019)	Voltage mismatch minimization	Hybrid	Development of local and distributed voltage control using reactive power of DG	DG	IEEE 123-bus test case	Primal-dual gradient
(Bedawy & Mahmoud, 2017)	Voltage limitations	Decentralized	Optimal operation of the voltage control devices based on the available data where each regulator acts autonomously	OLTC & VR's	IEEE 123-node test feeder	Multi Agent Systems

Table 2.7. Taxonomy of articles relating to DR

Reference	Objective	Control technique	Solution Methodology	Variables	Case Study	Optimization methods
(Petinrin & Shaaban, 2014)	Reduction of voltage deviations	Centralized	24hour DR customer participation	Wind & customer loads	IEEE 123 test feeder	Genetic Algorithm
(Anderson & Narayan, 2011)	Conservation voltage reduction	Local & Centralized	Volt/Var controller that adjusts the tap settings and DR controller that monitors loads	Loads & OLTC	13-node residential feeder	MAS
(Yi et al., 2012)	Steady state voltage limitation	Local & Centralized	Collaborative controller controls ESS output and DR controllers	ESS, loads & EV's	N/A	Sensitivity Analysis
(Christakou et al., 2014)	Primary voltage control	Decentralized	Control of loads via low bit signals from utility to load controllers	Controllable loads	IEEE 13 bus feeder	Linear Programming
(Davarzani, Pisica, & Taylor, 2015)	Voltage control support	Centralized	Integration of home energy management systems with DR for voltage control	Controllable loads	Not mentioned	MAS
(Davarzani et al., 2017)	Voltage control in feeders	Decentralized	Power control at local level	Controllable loads	19 bus LV network	MAS
(Rabiee et al., 2019)	Corrective/Emergency voltage control	Centralized	Active and reactive power dispatch of DG with demand-side participation	Controllable loads	IEEE 118-bus system	Sensitivity Analysis
(Zakariazadeh et al., 2014)	Real-time voltage control	Local & Centralized	Load curtailment based on emergency demand response	Controllable loads, OLTC	22 bus 20-kV radial test system	Sensitivity Analysis
(Hashemi et al., 2018)	Evaluating voltage security margin (VSM)	Decentralized	Minimum load reduction DR	Controllable loads	IEEE 39-bus network	PSO

(Rahman et al., 2018)	Voltage management in unbalanced networks	Local & Centralized	Identification of the optimal switching combination of household appliances and OLTC tap positions	OLTC + domestic loads	23 bus LV network	MPSO
(Lai et al., 2019)	Voltage instability management	Decentralized	Development of a robust distributed voltage control scheme based on consensus protocol	Smart loads	Autonomous microgrid system	Consensus Algorithm & Sensitivity Analysis
(Yi et al., 2012)	Steady state voltage violation limitation	Centralized	Control using DSR and ESS based on future PHEV & DER penetration	Loads + ESS	20kV, 3 feeder networks	Sensitivity Analysis
(Mufaris & Baba, 2015)	Voltage violation mitigation	Decentralized	Determination of line drop compensator (LDC) parameter. Selection of dead band of VR. Load shifting of HPWH used as back-up	VR's & HPWH	6.6kV network with 479 consumers	Conventional measured values
(Solanki, Venkatesan, & Khushalani, 2012)	Voltage minimization	Centralized	DR agents send information to VVC agents, which enables VVC agents to control nodes	Loads + VVC devices	12.47 KV distribution feeders	MAS
(Xie, 2017)	Voltage rise mitigation	Centralized	Day-ahead load scheduling and voltage control of OLTC and community energy management system (CEMS)	Controllable loads	1800 customer distribution model	GA
(He & Petit, 2016)	Voltage control cost minimization	Centralized	Using DR with DG and tap settings in central control	OLTC, DG, & loads	IEEE 34-node distribution	MILP
(Kawamura, 2013)	Voltage rise limitations	Centralized	DR application based on PV penetration levels	PV, Controllable loads	6.6kV feeder with 2250 consumers	SA

(Kadurek et al., 2012)	Voltage minimization	Decentralized	Central voltage control at the substation (OLTC) via reduction in load	Controllable loads	LV feeder supplying 240 users	Monte Carlo
(Xiangqi et al., 2017)	Managing of feeder voltage profiles	Centralized	Managing voltage profiles based on PV penetration. Real and reactive power adjustment	Controllable loads	Not mentioned	Voltage load sensitivity matrix
(Karthikeyan et al., 2017)	Voltage-rise limitations	Centralized	DR power alterations and power curtailment from PV sources based on market price signal on an hour-ahead basis	PV & Controllable loads	LV radial feeder with 25 buses	MPC
(Abraham, Marzooghi, & Terzija, 2017)	Voltage reduction	Centralized	Voltage controlled demand response using a modified OLTC controller	OLTC, Controllable loads	9-bus Network	SA
(Y. Dong et al., 2018)	Improvement of short-term voltage stability	Local & Centralized	DR-based preventive voltage control to improve short-term voltage stability based on the day-ahead forecast	Controllable loads, shunt capacitors	220 kV, thirteen 35 kV bus system	OPF
(Bayat, Sheshyekani & Hamzeh, 2016)	Voltage deviation minimization	Local & Centralized	Energy management system, which assigns the real and reactive power setpoints for the local DER's, reactive power compensators and controllable loads	Controllable loads & DER	20-kV, five radial feeders	PSO

Table 2.8. Taxonomy of reviewed articles relating Distributed Storage

Reference	Objective	Control technique	Solution Methodology	Variables	Case Study	Optimization methods
(Zeraati et al., 2019)	Voltage rise mitigation	Local & Decentralized	Coordinated control of PEV and active power curtailment of PV	PEV & PV	IEEE LV test feeder with 55 loads	Consensus Algorithm
(Zeraati, Golshan, & Guerrero, 2018)	Voltage rise mitigation	Local & Decentralized	Local droop control of BES	BES & PV	7-bus LV radial feeder with 33 loads	Consensus Algorithm
(Ssekulima & Hinai, 2016)	Coordinated Voltage Control	Decentralized	MPPT control of PV. Injecting or absorbing surplus power through BES	PV & BES	4.16kV feeder	Incremental conductance
(Y Wang et al., 2016)	Voltage rise minimization	Local and Distributed	Discharge of stored energy for voltage support during peak load period.	ESS	17-bus distribution network	Consensus Algorithm
(Y. Yang et al., 2014)	Voltage rise minimization	Centralized	EMS, which consist of main controller controls BESS, load and PV	BESS, Load, PV, OLTC & SVR	Modified GE distribution power system	Sensitivity Analysis
(Bode et al., 2019)	Voltage stability analysis and improvement	Decentralized	Real and reactive compensation from BESS under continuous P–Q load increase.	BESS	IEEE 14 Bus system	PSO
(Kennedy et al., 2016)	Voltage rise mitigation	Centralized	Central controller controls OLTC and send signal to the BES to commence charging in order to shave the peak load.	ESS	Feeder with 5 buses and 4 DG's	Linear Programming

(Zimann et al., 2019)	Voltage drop limitation	Decentralized	Reactive power injection and active power minimization of ESS	ESS	N/A	Sensitivity Analysis
(X. Dong et al., 2018)	Voltage minimization	Decentralized	Charging pricing strategy of EV by minimizing voltage deviation and cost	EV	IEEE 33 bus distribution network	Graph theory & Monte Carlo Algorithm
(Marinelli, 2016)	Voltage deviation limitation	Evaluation of voltage deviations	Voltage dependent EV reactive power control	EV	400 V feeder with 43 loads	Droop control
(Bahramipanah et al., 2016)	Voltage minimization	Decentralized	Control of active and reactive power set points of a DESS in a partitioned network	ESS	IEEE 13 & 123 buses test feeders	MAS
(Shaoyun et al., 2019)	Voltage violation limitation	Decentralized	Active-reactive voltage control of ESS	ESS	IEEE 33 bus system	APSO
(Kabir et al., 2014)	Overvoltage limitation	Decentralized	Reactive control from PVs or coordi- nated control of PVs and BES	BES	Residential feeder with 12 loads	Probabilistic analysis
(Jamroen et al., 2018)	Over-voltage violation limitation	Decentralized	Control of BESS to charge or consume active power from PV in order to regulate voltage problems.	BESS	Simplified LV microgrid with 1 feeder	Fuzzy Logic
(B. Li et al., 2018)	Voltage rise limitation	Distributed	Feeder voltage estimation by applying back/forward algorithm. Calculation output power demand via estimation	ESS	IEEE 33-bus distribution network	Consensus Algorithm
(Mahmud & Zahedi, 2016)	Voltage limitations	Distrubted	Event-triggered control among adjacent BESS's for voltage control	BESS	5-bus radial distribution feeder	Multi Agent System

(Mocci et al., 2015)	Voltage limitations	Decentralized	MAS optimization based on local information. Master Agent and agents control responsive loads and EV recharging stations.	EV	LV network with 8 feeders, 63 buses and 193 loads	Multi Agent System
(Zecchino & Marinelli, 2018)	Voltage limitation	Decentralized	Reactive power control via EV	EV	LV feeder with 6 buses	Sensitivity Analysis
(Yu Wang, John, & Xiong, 2019)	Voltage rise/drop mitigation	Local & Distributed	Two-level coordinated voltage control scheme to utilize real and reactive power	EV	17-bus distribution network	Consensus Algorithm
(Cardona et al., 2018)	Voltage limitation	Decentralized	Decentralized EV charging algorithm, based on local current and historical measurements	EV	radial network with 178 nodes	Monte Carlo Algorithm & Mixed-integer linear programming
(Feshki, 2017)	Voltage unbalance	Decentralized	Use of PEV to reduce VUF	PEVs	LV feeder with134 single-phase loads	PSO

2.7 Summary of reviewed literature

The voltage control problem in distribution networks, which is a result of the widespread integration of demand side resources has been investigated in the literature from different perspectives. This section provides a summary of the reviewed literature, which considers (i) voltage control strategies, (ii) optimization methods and (iii) demand-side resources.

2.7.1 Voltage control strategies

Voltage control can broadly be classified as communication-based or autonomous. The former is characterized by a reliant communication link between monitoring and control devices. The latter is characterized by a local decision-making strategy, where control is independent from the central control system and based on localised voltage issues. Historically, most of the literature focused on central control strategies, based on voltage control using conventional VVC devices. During the last decade, with rapid deployment of DER and development in smart technologies, new control strategies have evolved. Various literature reviewed, focused on local or decentralized voltage control strategies, which offers various advantages over the traditional approach.

- Central control - Centralized or coordinated control strategy provides voltage regulation from the substation to the rest of the network. It uses a wide range of communication systems to coordinate different devices such as OLTC and voltage regulators. In this strategy, data is obtained by sensors along the feeders. In (Zakariazadeh et al., 2014) a centrally controlled SCADA scheme is used where data is obtained from various remote terminal units (RTU's) in the field. A coordinated centrally controlled voltage management strategy of OLTC and reactive power of PV in a LV network is used in Nasiri et al (2016). In Paula et al (2017), a central controller coordinates VR's, SC's and DG based on real-time applications. The study conducted by (Kulmala & Repo, 2014) uses a centrallly based two-stage SCADA control method using transformer tap setting and DG reactive power injection. Various other scientific papers used a centrally controlled strategy where the central controller received signals from various remote terminal units along the feeder or a local DER controller. In many applications, the reactive power capabilities of conventional VVC devices and DER are exploited for real-time voltage control. The disadvantage of centralized schemes is that it may not be able to operate under the significantly increased number of DER units (Yazdanian et al., 2014). The reasons include the following: (i) communication needs, due to the geographical span, (ii) difficulty of sharing data, (iii) frequent redesign requirements, since a change in one unit affects the central controller, (vi) reliability and security vulnerability of the central controller as a common point of failure. Geographically large systems cannot be controlled easily through

centralized control. One major obstacle is the cost of communication. Should a change be needed in one part of the system; the whole plant must be shut down. Tuning of each subsystem requires readjustment of the controller of the whole system, instead of changes to the local controller.

- Decentralized control - Decentralized control uses local information to independently control voltage at a particular bus where measurement and communication is limited. Local voltage support can be provided. The problem of faults in communication lines and slow response to rapid voltage variations could be overcome. In a fully decentralized control, each unit is controlled by its local controller. Decentralized control proposes to decompose the voltage problem by dividing it into sub-sections, which simplifies the optimization solution. Fifty scientific papers have been reviewed that deal with local or decentralized voltage control. In (Howlader, Sadoyama, Roose, & Sepasi, 2018) a local control strategy is used, where voltage control is done by injecting reactive power and active power curtialment of DG sources. This scheme has a faster response time to DER variability but lacks communication with the utility's voltage control strategy. Pournazarian et al (2019), uses a decentralized scheme with intelligent droop control on inverter-based DG and PHEV participation. Each unit is controlled by its local controller that is not fully aware of the system-wide disturbances and is independent of other controllers. A key feature of decentralized control is that communication with other DER units is not necessary. The common objective in almost all the papers reviewed, is the application of DER reactive power for voltage control at the point of common coupling.

2.7.2 Optimization Methods

Optimization methods were classified as conventional and intelligent. The conventional methods are subdivided into sensitivity analysis, Fuzzy logic (FL), Optimal Power Flow, Model Predictiive Control , Linear and Non-Linear Programming, Consensus Algorithm and Multi-Agent Systems. The intelligent methods are subdivided into genetic algorithm and PSO derivatives. The most used conventional method is Multi-Agent Systems, followed by Sensitivity Analysis. MAS has proven to be an effective method to solving distributed problems and is easy to implement in distribution networks. The system decomposes a task into smaller ones, which is easier to solve. The individual solutions are later combined to find a global solution. Davarzani et al (2013), used a distributed scheme where a MAS framework is used to achieve flexible demand response by controlling the power flow at local residential level. In this scheme, all intelligent devices work together to obtain a common goal. The relationship between power injected from DG and voltage at a certain bus is nonlinear. Non-linear programming may not be an effective solution based on the large number of decision variables

and long computational time. The voltage problem is non-linear, non-differential and non-convex with more than one local optimum. In centralized voltage control, the problem therefore is a multi-objective, non-linear programming one. Consensus Algorithm (CA) was applied by Mokhtari et al (2013) on an LV network where a local energy management system (EMS) controlled PV and controllable loads. Load management and voltage control was achieved based on a consenus reached between various residential users. This is a very effective demand response tool. Heuristic-based techniques are used to deal with the inefficiencies of conventional methods. Genetic Algorithms applied to load management with incentive schemes have been applied successfully in literature. In South Africa, incentive schemes can only be applied to customers based on time-of-use tariffs. These are predominantly industrial customers. In the future grid, with greater customer participation, incentive schemes based on load shifting or load curtailment could be applied. Customer comfort has to be considered for direct or indirect load control scheme. PSO has been applied successfully in various studies ranging from optimal size and location of DG to the use of PEV's to minimize voltage unbalance by optimally selecting the state of charging or discharging. In Rahman et al (2018), PSO was used to identify the optimal switching combination of household appliances and OLTC tap positions. PSO is simple to implement, have shorter computational time and have a fast conversion rate. The results of PSO show that this algorithm is highly effective in dealing with large-scale non-linear optimization problems.

2.7.3 Voltage control with DSR

In the literature, voltage control was achieved using various distributed generation resources. These were subdivided into (i) DG, (ii) DR and (iii) distributed storage.

- Distributed Generation - Almost all the papers reviewed used either wind or solar or a combination of both renewable technologies. A common method for voltage control used, is reactive power control or active power curtailment. It has been proven in the literature that placement of reactive power devices at predetermined locations in distribution systems, especially along the feeder or at the end of the feeder, prevents voltage instability (Tabatabaei et al., 2017). In (Mehrjerdi et al., 2013; Calderaro et al., 2012; Rashidi & Moshtagh, 2014; Villacci,2019; Fallahzadeh-abarghouei et al., 2018; Y. Liu et al., 2018; Mokhtari et al., 2013), DG inverters were used to inject reactive power for voltage control. DG inverter reactive capabilities can be used in a centralized or decentralized control strategy. In (Nasiri et al., 2016; Siewierski et al., 2018; Khalid et al., 2018; Kulmala & Repo, 2014; C. Li et al., 2018; Nimpitiwan & Chaiyabut, n.d), a central control strategy was used based on reactive power capabilities of DG with tap control of the substation transformer. In (Calderaro et al., 2014; Fazio et al., 2013; Feng et al., 2018; Swain & De, 2019; Rathbun et al, 2018; Cagnano & Tuglie, 2016), reactive

power of DG was used based on decentralized strategy. Reactive power generation technologies can be used to provide voltage control and deal with stability issues in distribution networks.

- Demand Response - Twenty-three papers dealing with voltage control, using demand response, were reviewed. The aim of DR programmes is to decrease the peak load, which provides network stability. From the reviewed papers, it was proved that DR could be an effective tool to deal with voltage control problems but depends on 2-way communication between the utility and the customer. The successful implementation depends on the installation of advanced metering infrastructures (AMI) at the consumers' site, which allows the user to measure energy consumption patterns at various intervals and allows the utility to retrieve the data to execute DR programmes. Most of the studies use a centralized control strategy. He & Petit (2016), used a centralized strategy to control the tap settings of the substation transformer based on DG parameters and controllable loads. Hashemi et al (2018), proposed an improvement on the voltage security margin based on a decentralized control stragegy by adopting a load-to-source impedance ratio (ZL/XTh). The study proposed a two-state algorithm for solving load reduction. Incentives should be made available to customers, who could participate in load management strategies, whether load shifting from peak hours or curtailment during peak hours. In South Africa, most municipal tariffs for domestic users are based on a flat kWh rate. By adopting a TOU tariff, users could be enticed to participate in demand response, which could aid in voltage control. What is needed to motivate customers to participate in DR programmes is an understanding of the process and benefits.

- Distributed Storage - Distributed storage is subdivided into energy storage and plug-in electric vehicles. In most of the reviewed papers, the voltage is controlled by active and reactive power set points of storage devices. A central controller, which controls transformer tap settings is used to send signal to the BES to commence charging in order to shave the peak load (Kennedy et al., 2016). Vaious studies use BES for peak load shaving and to regulate voltage through active power injection and absorption. The increased penetration of PEV's in the future, presents a load demand problem, but their battery packs could also provide vehicle-to-grid services (V2G), which can improve grid stability and deal with voltage violations. The unregulated charging of PEV's can lead to an increase in load, which causes heat circulation in the transformer winding. A comprehensive study to determine the suitability of a centralized or decentralized charging strategy is required for voltage control based on South African conditions. A centralized charging strategy has the advantage of utility control, which

will reduce its impact on the network and meet peak demand. The disadvantage is that user charging patterns are neglected, which could cause user discomfort. The literature proved that centralized and decentralized PEV's control could be used to mitigate the intermittent nature of RE and improve voltage stability. Very few scientific papers, however, address reactive power control (RPC) from electric vehicles.

2.8 Summary

In this chapter, the voltage control problem in active distribution networks was presented. Based on literature reviewed, it was proven that an increase in distributed energy resources cause dynamic and transient voltages to exceed the prescribed limits, which results in damage to electrical equipment. Conventional VVC devices, designed to deal with voltage control in unidirectional power flow, is unable to respond fast and effectively to bidirectional power flow caused by DER. New control strategies, based on intelligent control is needed to deal with voltage control problem in active distribution networks. These control strategies are broadly divided into communication based and autonomous. In order to solve the voltage control problem, optimization algorithms, which can be broadly divided into conventional and intelligent are proposed. Some of these algorithms decompose the task into smaller local problems, which can be solved individually and later converge into a global solution. DER, which encompass DG, DR and DS can be used at distribution level to deal with the voltage violation problem. The literature suggests that DG reactive and DS active power, is an effective tool to deal with voltage issues. DR is another effective method that can be used for peak shaving and load reduction and is a promising method to deal with voltage limitations in the future grid. Very few studies include the combination of DSR to solve the voltage problem.

CHAPTER THREE
VOLTAGE CONTROL – MATHEMATICAL MODELING

3.1 Introduction

Voltage control in distribution systems can be achieved by central control, i.e., at the substation or locally. In this chapter, voltage control methods with traditional VVC devices and DER are discussed from a mathematical perspective. Both methods are used to manage voltage regulation to maintain the desired voltages at the substation or local bus in the distribution network within statutory requirements. The chapter will focus on voltage control using (i) conventional VVC devices such as OLTC transformers at the substation and feeder-level control, which includes step voltage regulators and switched/shunt capacitor (SC) banks and (ii) inverter-based DER for control of active and reactive power.

3.2 Voltage drop calculation in conventional networks

Figures 3.1 and 3.2 represent a single line diagram and the corresponding phasor diagram of the voltage drop in a distribution network, respectively. In this simplistic 2-bus example, the voltage in the feeder is automatically controlled at the substation by adjusting the transformer taps. The voltage in the feeder decreases as the distance from the distribution transformer increases. The voltage level in the network is influenced by the load ($P + jQ$) and the balance between the reactive power supplied and consumed.

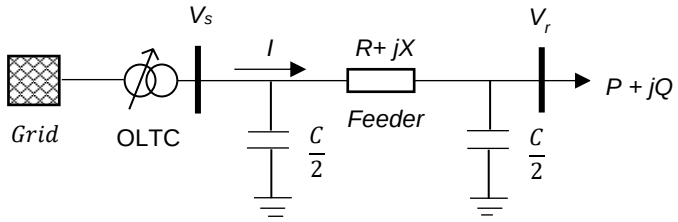

Figure 3.1. Single line diagram of 2-bus distribution network

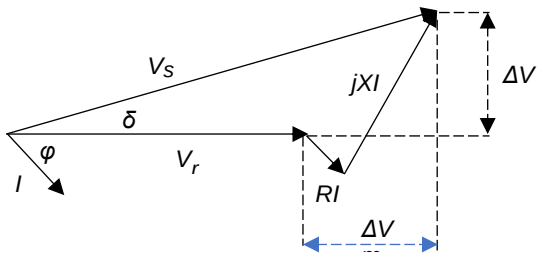

Figure 3.2. Phasor diagram of the voltage drop in a 2-bus distribution network.

The sending voltage (V_s) can be approximated by:

$$Vs = Vr + (R + jX)I \tag{3.1}$$

where:

$$I = \frac{(P - jQ)}{Vr} \tag{3.2}$$

$$Vs = \left[Vr + \frac{(RP + XQ)}{Vr}\right] + \left[\frac{j(XP - PQ)}{Vr}\right] \tag{3.3}$$

The sending voltage (*Vs*) is given by:

$$Vs = Vr + \Delta Vm + j\Delta Vp \tag{3.4}$$

From the phasor diagram,

$$\Delta Vp = \frac{XP - RQ}{Vr} \tag{3.5}$$

$$\Delta Vm = \frac{RP + XQ}{Vr} \tag{3.5}$$

The phase angle δ is sufficiently small, hence:

$$\Delta Vp < Vr + \Delta Vm \tag{3.6}$$

The sending voltage (*Vs*) can be approximated as:

$$Vs = Vr + \frac{RP + XQ}{Vr} \tag{3.7}$$

And the voltage drop (ΔV) is given by:

$$\Delta V = \frac{RP + XQ}{Vr} \tag{3.8}$$

where:

P = $Active\ Power$

Q = $Reactive\ Power$

Vs = $sending\ voltage$

Vr = $receiving\ voltage$

R+jX = $line\ impedance$

Line losses are given by:

$$Line\ losses = \left[\frac{P^2 + Q^2}{V^2 r}\right] R \tag{3.9}$$

3.3 Centralized voltage control

Traditionally, voltage control is achieved by controlling reactive power in a power grid. This is done with (i) shunt capacitor banks (SC), voltage regulators (VR) along the feeder and (ii) automatic voltage control using OLTC at the substation. In many distribution systems, a combination of feeder shunt capacitors and OLTC are used to maintain voltage regulation. The voltage levels in the network are usually predetermined based on load flow calculation and setpoints (Zhao, Wang & Zhang, 2018). The objective of these Volt/Var control devices (VVC) are to improve efficiency, reduce technical losses and control load demand in the network.

3.3.1 OLTC control

One of the common methods of voltage regulation in distribution networks is a centralized method, using an on-load tap changing (OLTC) transformer at the central substation (Berger & Iniewski, 2012). A basic transformer consists of a primary and secondary winding. The turns ratio determines the ratio of voltages across the primary and secondary windings. The taps may be positioned on the primary or secondary winding.

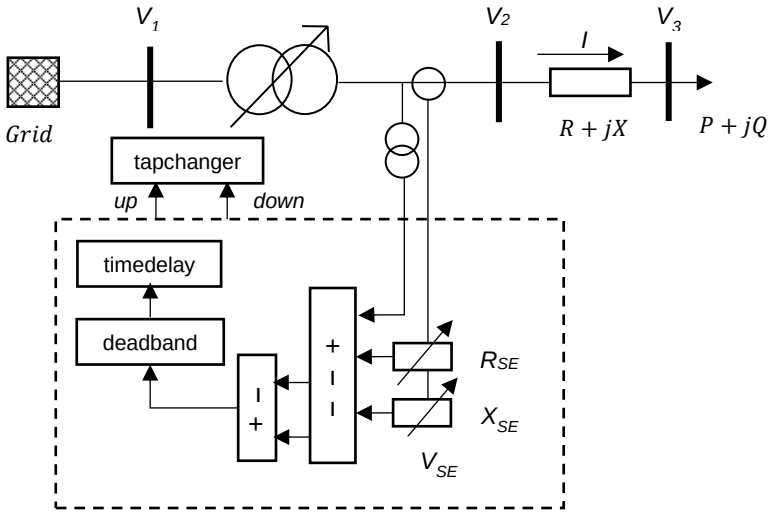

Figure 3.3. OLTC schematic with LDC

Voltage control is achieved by these taps, which change the secondary transformer turns ratio in relation to the primary voltage (Bayliss & Hardy, 2012). These tap changers are classified as no-load (NLTC) or on-load (OLTC) and can be manually or automatically operated. Figure 3.3 shows the schematic diagram of OLTC with line drop compensation (LDC).

The components of the control systems are discussed separately, below.

- Tap changer - A mechanical device is used to change the tap position in steps from 0 (zero) to N_{max} (maximum position). A change in the tap position is given by:

$$n_i = n_{i-1} + \Delta_n \tag{3.10}$$

where:

n_i = *present tap position*

n_{i-1} = *previous tap position*

Where Δ_n , is defined by:

$$\Delta_n = \begin{cases} 0 & for \ \ t \leq T_m \ \ : b = arbitrary \\ 1 & for \ \ t \geq T_m \ \ : b = -1 \\ -1 & for \ \ t > T_m \ \ : b = 1 \end{cases} \tag{3.11}$$

where:

T_m = *mechanical time delay required by motor driver*

b = *control signal applied to tap-changing mechanism*

- Time delay - a time delay is used to prevent unnecessary tap changes caused by transient voltages. Figure 3.4 shows the time delay principle of operation. After the voltage drops below U_{min} the first tap change commences with Δt_1 time delay of 60 seconds to compensate for the transient voltage variations. This is followed by a Δt_2 time delay, which is 10 seconds.

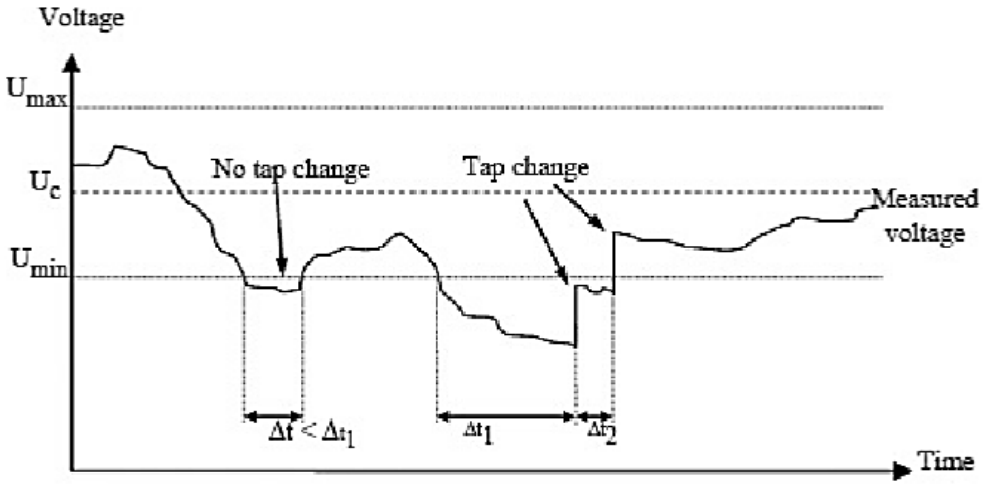

Figure 3.4. OLTC time delay principle

From equation 3.11, *b* is given by*:*

$$b = \begin{cases} 0 & for \;\; t \leq T_d \;\; : e = arbitrary \\ 1 & for \;\; t \geq T_d \;\; : e = -1 \\ -1 & for \;\; t > T_d \;\; : e = 1 \end{cases} \tag{3.12}$$

where:

T_d = *time delay from the central controller*

e = *output of hysteresis controller*

From equation 3.12, *e* is given by*:*

$$e = \begin{cases} 0 & for \;\; |\Delta V| \leq DB \\ 1 & for \;\; \Delta V > DB \\ -1 & for \;\; \Delta V < -DB \end{cases} \tag{3.13}$$

where:

ΔV = *voltage error*

DB = *controller dead band*

- Dead-band - defined as the range between the upper and lower setpoints of the controller where no tap changing is taking place. The lower and upper levels could be 0.95pu and 1.05pu voltage respectively, which represent the maximum allowable voltage limit in the distribution network. The maximum and minimum voltage range with respect to V_2 is given by:

$$V_{min} \leq V_2 \leq V_{max} \quad (3.14)$$

where:

V_{min} = $V_{set} - 0.5\, V_{db}$

V_{max} = $V_{set} + 0.5\, V_{db}$

V_{set} = $set\ point\ voltage$

V_{db} = $deaband\ voltage$

- Line drop compensator - LDC is used for voltage control at a remote bus without a communication link. From figure 3.3, a feeder impedance, composed of resistance (*R*) and reactance (*X*) exists between the transformer and the load. The LDC estimates the voltage drop between the feeder and the transformer and operates the OLTC when the voltage level is outside the dead-band setting. R_{SET} and X_{SET} are settings on the LDC used for resistive and reactive compensation, respectively. The R and X dial settings can be determined from 3.15 and 3.16, respectively.

$$R_{set} = \frac{CT_P}{PT_N} x\, R_{eff} \quad (3.15)$$

where:

CT_P = CT primary rating

PT_N = potential transformer's turns ratio

R_{eff} = feeder resistance (Ω)

$$X_{set} = \frac{CT_P}{PT_N} x\, X_{eff} \quad (3.16)$$

where:

X_{eff} = reactance of feeder (Ω)

The model in figure 3.5 below is an illustration of a simple three-phase delta connected feeder with a three-phase voltage source, OLTC transformer, neutral grounding transformer and 3.5MW mixed-variable load with a lagging power factor (PF) of 0.90. The profile consists of 40% residential and 60% industrial loads. The voltage per tap is set to 0.0125pu with a dead-band of 0.025pu.

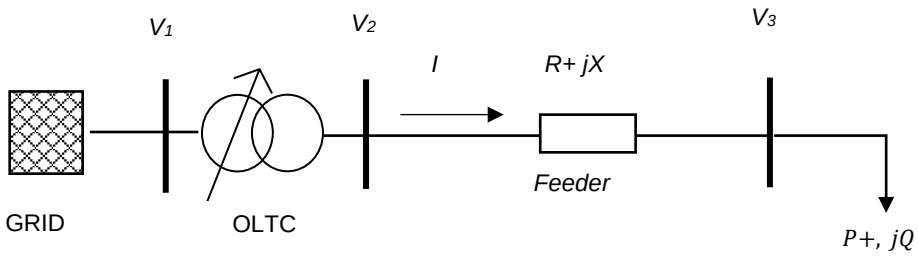

Figure 3.5. Three-bus model with OLTC transformer

Figure 3.6 shows the tap position, which follows the load profile over a 24-hour period. The voltage is measured at V_2. The input voltage to the OLTC transformer is the magnitude of the positive-sequence voltage at V_2.

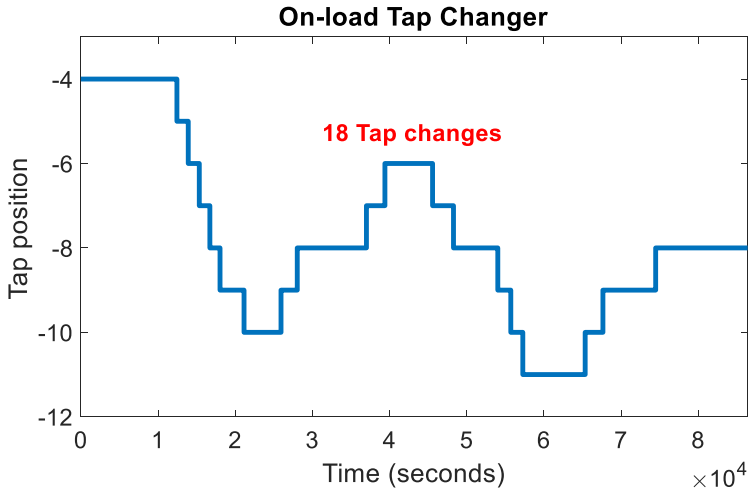

Figure 3.6. Schematic diagram of OLTC

3.3.2 Feeder-level control

For feeder-level control, additional control measures are taken along the feeder, which include Step voltage regulators (SVRs) and Shunt Capacitors (SCs) connected at the secondary side of the transformer.

- Shunt Capacitors (SC) - Distribution networks and loads consume reactive power. Capacitors are the most economical way to supply reactive power and regulate the voltage on long distribution feeders (Gers, 2014). Capacitors are classified as series or parallel, based on the type of connection and are widely used in distribution networks to generate reactive power (Berger & Iniewski, 2012). SCs can be controlled in three ways i.e., (i) sequential - time regulation according to the variation in load; (ii) voltage - regulation based on the feeder voltage; (iii) reactive power compensation - compensation based on reactive power required by feeders and loads

(Zhao, Wang & Zhang, 2018). Capacitors are versatile and can be switched on and off depending on the amount of reactive power required and to reduce voltage drops along the feeder (Baggini, 2008). SCs inject reactive power to the system according to equation 3.17.

$$Q_c = Q_{C,rat} V_C^2 \tag{3.17}$$

where:

Q_c = $Reactive\ power\ injected\ by\ the\ capacitor\ in\ kVAr$

V_c = $Applied\ volatge$

$Q_{c,rat}$ = $kVAr\ rating\ of\ the\ capacitor$

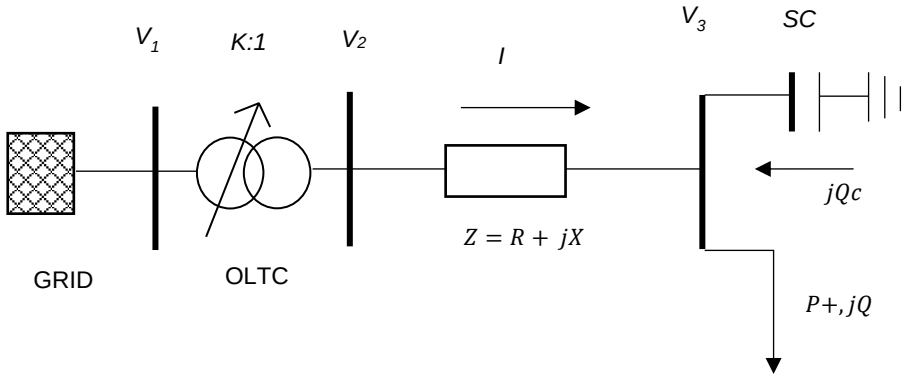

Figure 3.7. Single line diagram of 3-bus distribution network with capacitor

Some of the main advantages of SCs are low maintenance requirement, their ability to reduce electrical losses and improvement of the voltage profile, especially in long feeders (Petinrin & Shaaban,2016). Figure 3.7 is an illustration of a simple single line diagram with a shunt capacitor connected at V_3. The voltage drop on the feeder can then be approximated as:

$$\Delta V \approx \frac{R_L P_L + X(Q - Q_C)}{V_3} \tag{3.18}$$

From equation 3.18, the capacitor improves the voltage profile at V_3. The compensation in reactive power by the capacitor will decrease the feeder current, I, which will reduce the feeder power losses based on equation 3.20.

$$I = \sqrt{\frac{P_L^2 + (Q_L - Q_C)^2}{V_2}} \tag{3.19}$$

$$P_{loss} = I^2 R_L \tag{3.20}$$

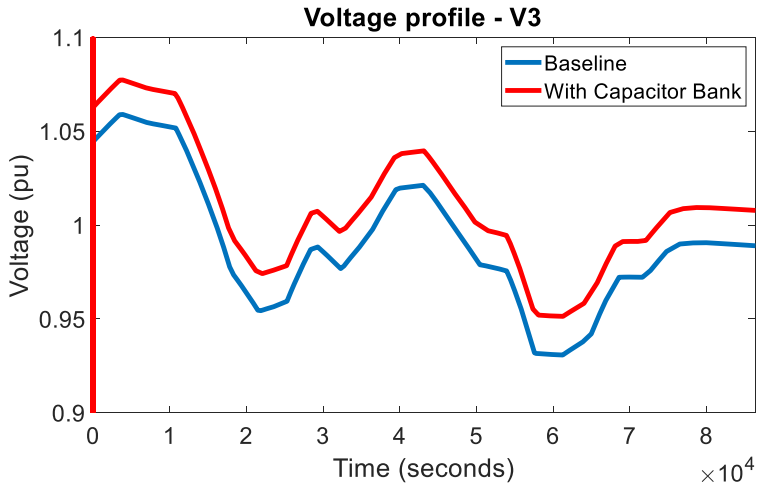

Figure 3.8. Voltage profile at V_3 with SCs

Figure 3.8 shows the voltage profile at V_3 with capacitor switching. In distribution networks, shunt capacitor may need to be switched ON and OFF during high and low load consumption. Different conventional controls can be used to control switched capacitors based on time or voltage support. Time controlled is used when the capacitor switching time is known but lacks flexibility to respond to load variations. Voltage controlled capacitors are used for voltage regulation. The capacitors are switched when voltage support is required.

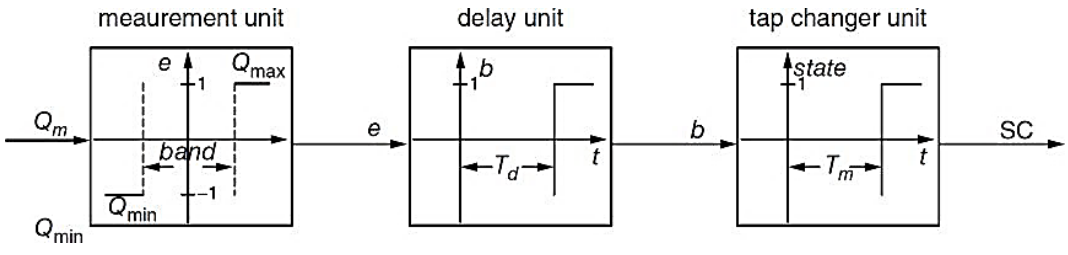

Figure 3.9. Shunt capacitor control block diagram

Figure 3.9 shows the discrete shunt capacitor block diagram. Based on the control function, the capacitors connected to V_3 will be energized when Q_m is larger than Q_{max}. Figure 3.10 shows the impact of switched capacitors on OLTC tap movement.

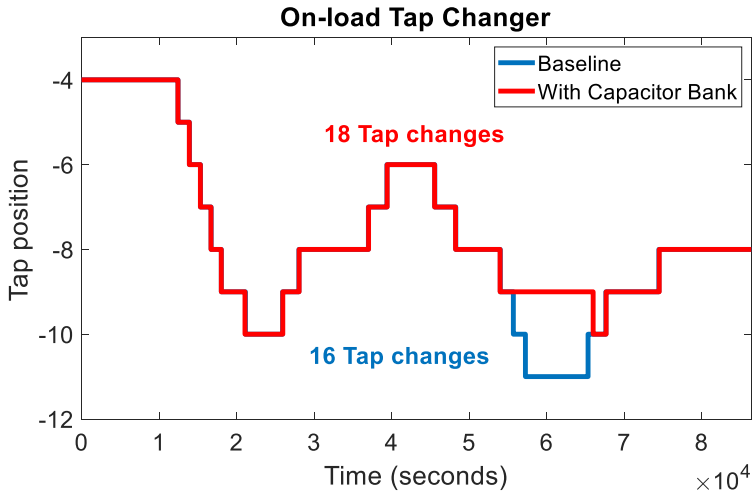

Figure 3.10. Impact of Capacitor Banks on OLTC

3.3.1.1 Case study

Reactive power devices like SCs are used on distribution lines or close to the point of consumption because reactive power cannot be transferred over long distances. In distribution systems, SCs improve the power factor and reduces I^2R power losses. In this study, minimization of losses is considered as the objective function subject to (i) voltage constraints and (ii) on-load tap minimization. The objective function is mathematically expressed as

$$f = P_{loss} = \sum_{i=1}^{Nb} I^2 R \tag{3.21}$$

where:

P_{loss} = $Total\ power\ loss$

N_b = $number\ of\ branches$

I = $Line\ current$

R = $Resistance\ of\ the\ branch$

The minimization of losses in the distribution systems is subject to operational constraints. These constraints are:

i. Voltage constraints – the voltage constraint is expressed as

$$V_m^{min} \leq V_m \leq V_m^{max}, m = 1 \ldots N_m \tag{3.22}$$

Where V_m are the operating voltage at the mth bus and V_m^{min} and V_m^{max} is the minimum and maximum operating voltage at the mth bus, which represents 0.95 and 1.05pu, respectively.

ii. Transformer tap constraints.

$$Ti_{min} \leq T_k \leq Ti_{max} \tag{3.23}$$

Where Ti_{min} and Ti_{max} are the minimum and maximum range of ratio of tap changing transformer at bus i.

iii. Capacitor constraints

$$Qci_{min} \leq Qc_i \leq Qci_{max} \tag{3.24}$$

Where Qci_{min} and Qci_{max} are the minimum and maximum allowable output of shunt capacitors at bus i.

Other methods that will be employed for SC control below, are:

(i) sequential - time regulation according to the variation in load. The capacitor bank will be switched ON/OFF depending on the time-of-the-day

(ii) voltage - regulation based on the feeder voltage, which is achieved by voltage sensing relays. The capacitor banks along the feeder will be switched ON/OFF based on the measured voltage.

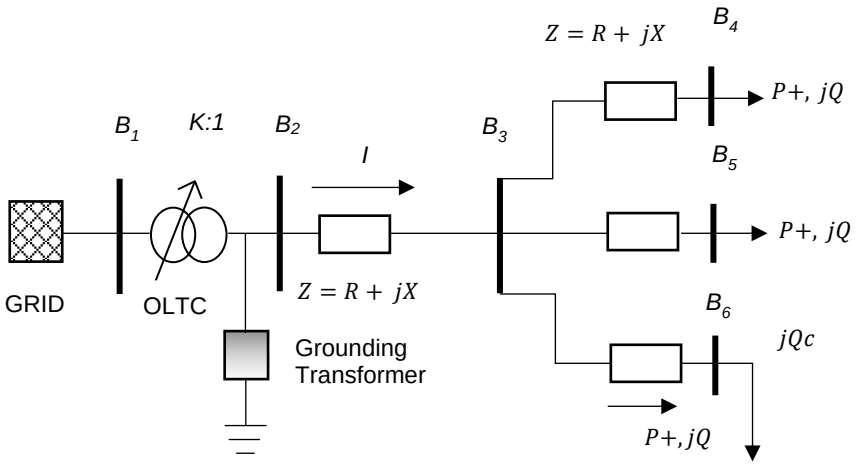

Figure 3.11. 6 Bus single line diagram

Table 3.1. Unbalanced network parameters

Description	Data
OLTC	$S_{base} = 5MVA, V_{prim} = 66kV, V_{sec} = 3.3kV$ $V_{step/tap}$= $0.0125pu, V_{ref} = 1.05pu, Tap_{min/max} = -16, +16$
Grounding transformer	$S_n = 500kVA$
Industrial load	$P_n = 1.25MW, PF = 0.85$
Commercial load	$P_n = 1.0MW, PF = 0.90$
Unbalanced residential load	$P_a = 120kW, P_b = 200kW, P_c = 85kW$ $PF = 1.0$

Figure 3.12 shows the profile of the balanced industrial and commercial loads. The commercial profile follows typical profile, where the bulk of the power is consumed around 07h00-16h00. The industrial load profile is based on a mineral iron smelter. The actual data is scaled down for the purpose of this study.

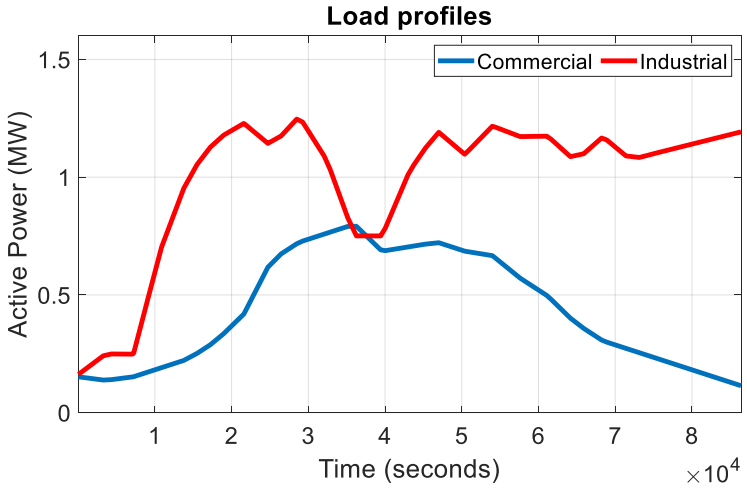

Figure. 3.12. Three-phase balanced industrial and commercial load profiles

Figure 3.13 shows the Simulink® load block, which is converted by grounding phases A and B. The input to P & Q is driven by 1-D lookup tables.

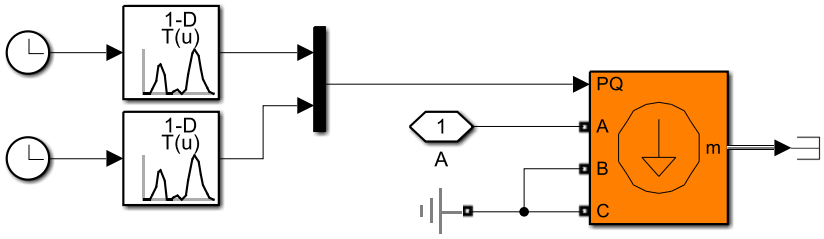

Figure. 3.13. Single-phase dynamic load block conversion

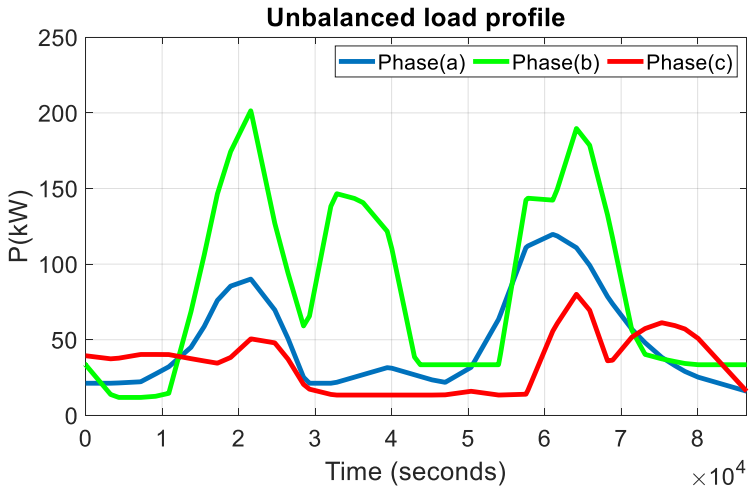

Figure. 3.14. Unbalanced residential load profiles

3.3.2.2 Simulation results

Figures 3.15 and 3.16 show the active, reactive power and power factor profile of the network, respectively.

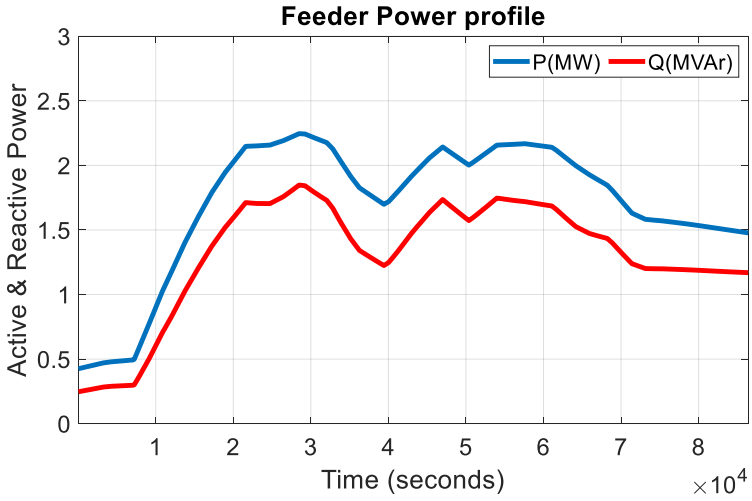

Figure. 3.15. Feeder load profile

Figures 3.17 – 3.19 shows the voltage profiles at bus 4 – 6 before compensation. The voltage at bus 4 and bus 6 have exceeded the lower limit.

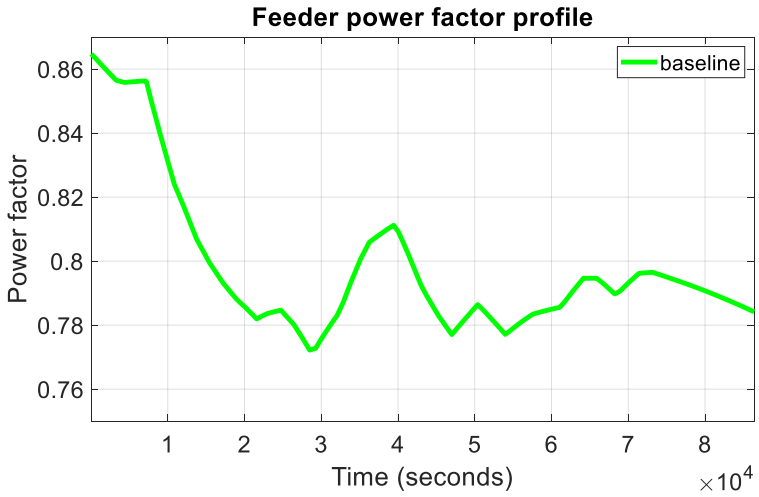

Figure. 3.16. Feeder power factor profile

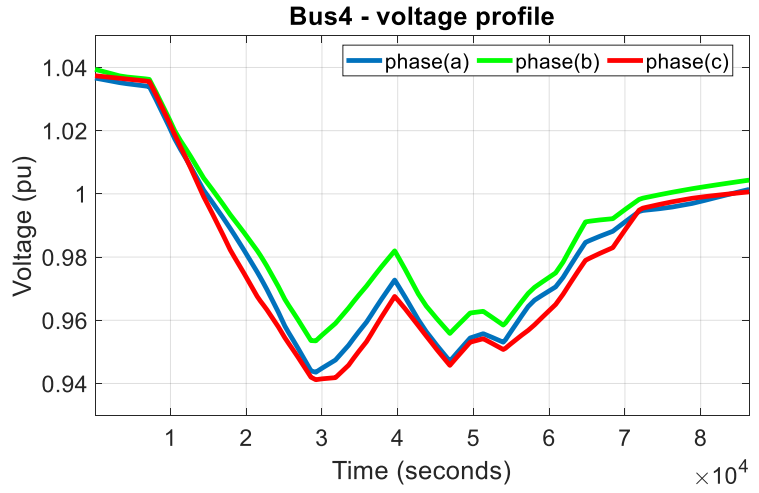

Figure. 3.17. Bus 4 voltage profile

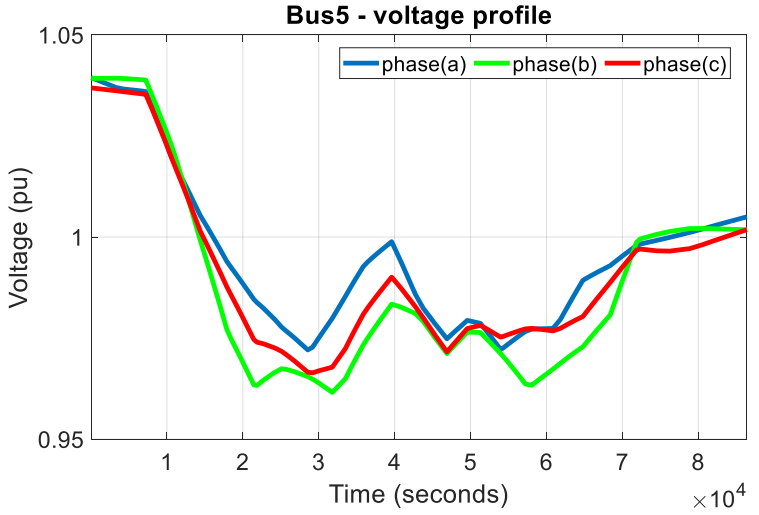

Figure. 3.18. Bus 5 voltage profile

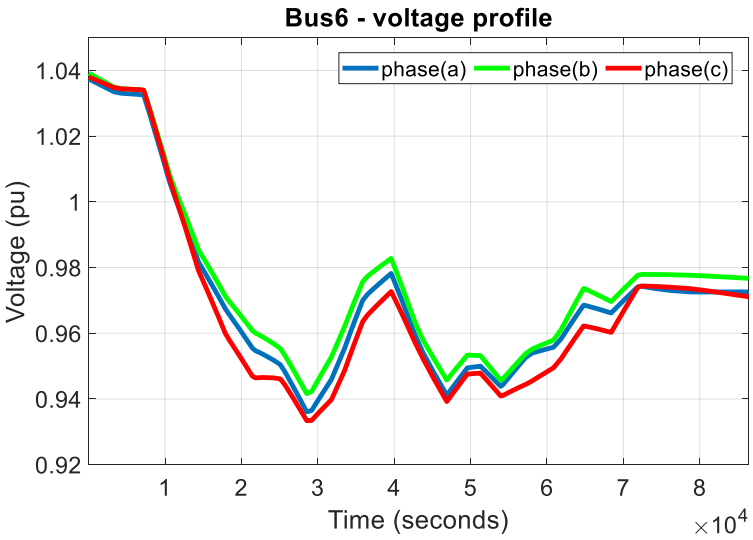

Figure. 3.19. Bus 6 voltage profile

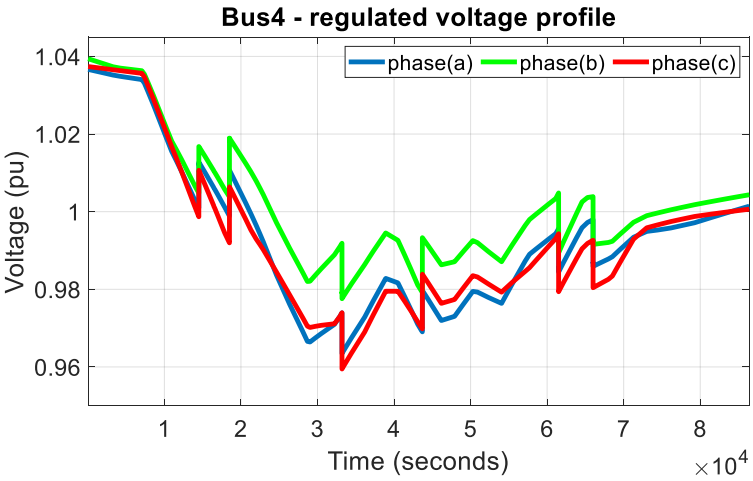

Figure. 3.20. Bus 4 compensated voltage profile

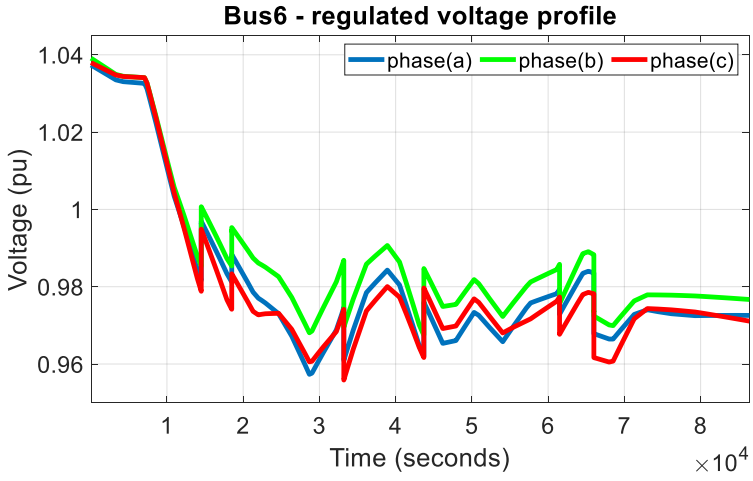

Figure. 3.21. Bus 6 compensated voltage profile

Figures 3.20 and 3.21 show the compensated voltage profiles,which are based on a predetermined switching sequence. Table 3.2 is a summary of the bus voltages at bus 4-

6, before and after voltage regulation. Phase c, at bus 4, phases b and c at bus 5 and all phases at bus 6 have exceeded the minimum limits.

The capacitor ON and OFF switching times are calculated based on the load variation, which influences the variation in voltage in the feeder. Figure 3.22 and table 3.3 show the proposed scheduling times when the SCs will be activated.

Time based control - This type of control mechanism switches the capacitor into service at pre-determined time intervals. The ON/OFF times of the capacitors are estimated from the known load profiles of the loads that are connected to the network to which the Capacitor is connected. This may of course have its drawbacks due to the fact that the networks often feed different load mixes with different loading characteristics, which cause the load profiles to be unpredictable at times. The new loads that are added to the networks also bring another complication to predicting an overall accurate load profile for the network of concern.

Table 3.2. Summary of voltage profiles

Location	**Voltage (pu)**					
	Min/Max			**Min/Max**		
	Before compensation			**After compensation**		
	A	**b**	**c**	**a**	**b**	**c**
Bus2	0.984/1.043	0.984/1.043	0.982/1.043	0.998/1.043	1.004/1.043	0.996/1.043
Bus3	0.972/1.041	0.971/1.041	0.969/1.041	0.989/1.041	0.997/1.043	0.986/1.042
Bus 4	0.944/1.041	0.955/1.041	**0.942/**1.041	0.964/1.037	0.978/1.039	0.962/1.037
Bus 5	0.972/1.039	**0.962/1.039**	**0.967/**1.039	0.993/1.039	0.973/1.039	0.980/1.039
Bus 6	**0.936/1.037**	**0.942/1.037**	**0.933/**1.037	0.957/1.037	0.968/1.037	0.961/1.037

Table 3.3. Capacitor switching schedules

Description	**Ideal Capacitor size**	**Schedule – Time (s)**	
		ON	**OFF**
Shunt Capacitor 1	300kVAr	14500	33200
		43700	66000
Shunt Capacitor 2	200KVAr	18500	61500

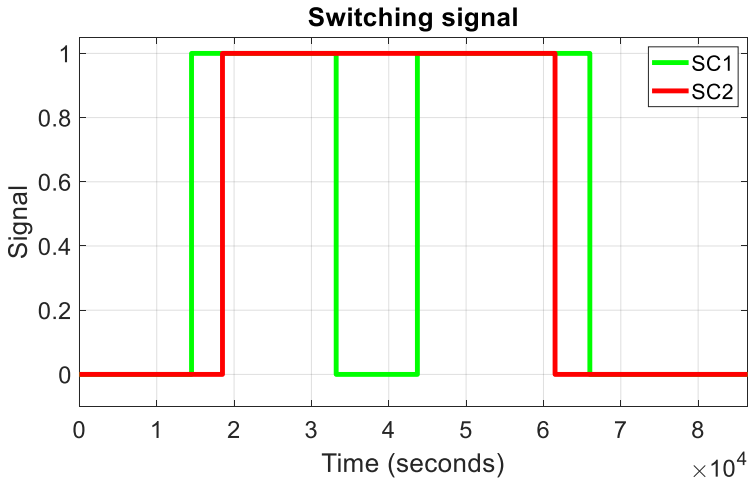

Figure. 3.22. Shunt capacitor switching signal

Figure 3.23 shows the profile at bus 6. Only phase c will be regulated as the other phases are within statutory limits. The regulated voltage profile, which is shown in figure 3.23 shows phase c, which is regulated based on the switching schedule in figure 3.22. For ease of illustration only phase c is shown. The basline for all the phases is shown in in figure 3.19.

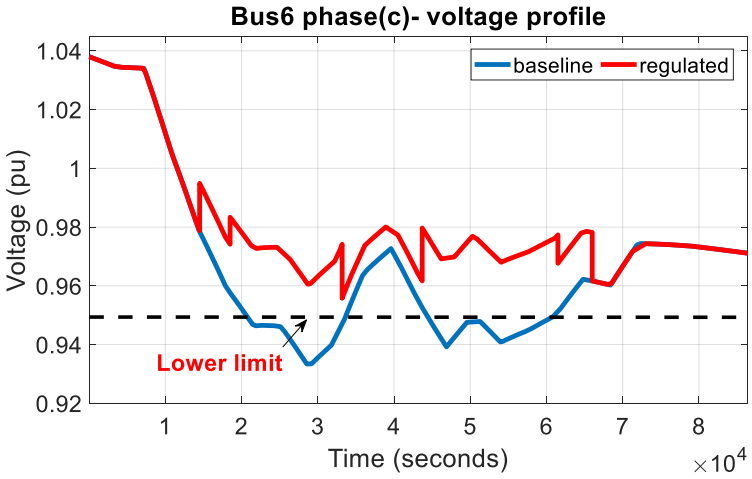

Figure. 3.23. Bus 6 phase (c) voltage profile

Figure 3.24 shows the regulated phase at bus 4. The switching cycle in figure 3.22 is applied to the capacitor connected to bus 4. The results show an improvement in the profile at bus 4.

Figure 3.25 shows the OLTC base profile. The effect of the switching cycle on the taps of the OLTC transformer is shown in figure 3.26. A brief summary, which compares the basline to the controlled SC switching is givn in table 4.5. An improvement in the voltage profile and reduction in the taps of the OLTC transformers is evident.

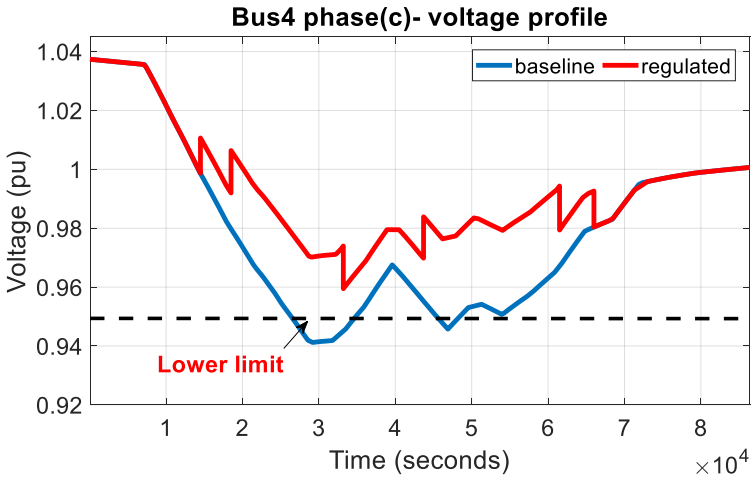

Figure. 3.24. Bus 4 phase (c) voltage profile

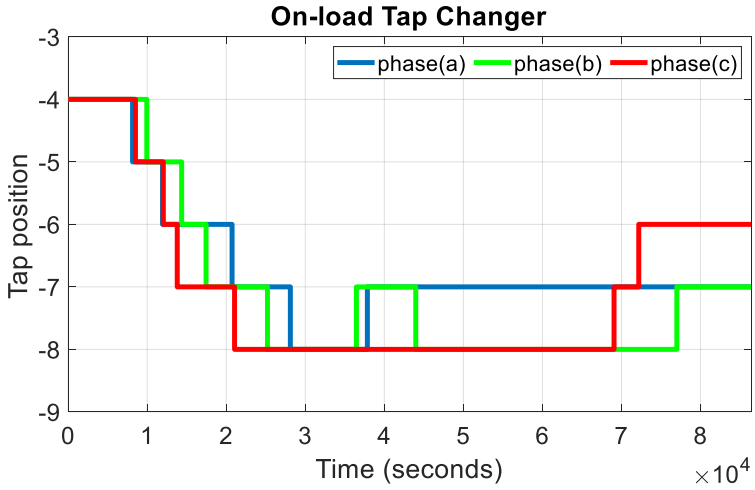

Figure. 3.25. OLTC - baseline profile

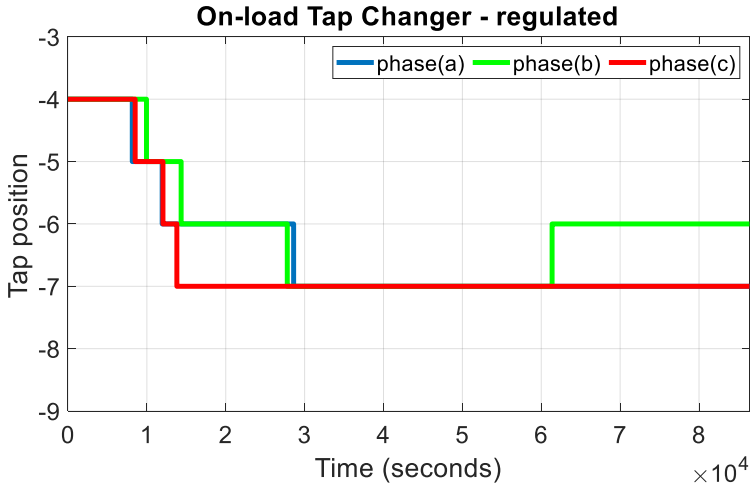

Figure. 3.26. OLTC regulated profile

Table 3.4. OLTC operations

Description	Phase		
	a	b	c
Baseline	5	7	6
SC control	3	4	3

- Step Voltage Regulator (SVR) - SVRs are installed along the feeder to keep the voltage close to constant. VRs are less expensive than upgrading the conductors along the feeder (Sclater & Traister, 2003). A voltage regulator consists of a single-phase auto transformer with automatically adjustable tap changing capability as depicted in figure 3.37 (Bayliss & Hardy, 2012). Single-phase step-voltage regulators, like SCs are common in distribution systems. They typically have a total of 16 steps, which gives +-10% single phase regulation at 0.625% per step. Their time delay is typically 15 to 30 seconds longer than that of any upstream tap changing devices. VRs are designed to provide rated voltage regulation, at rated current, with a power factor of 0.8 lagging.

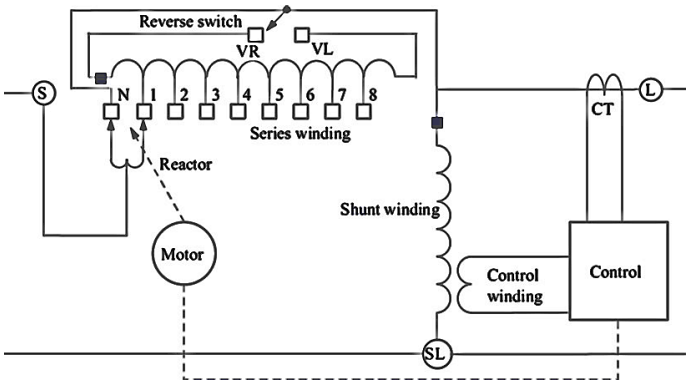

Figure 3.27. Schematic diagram of a single phase 32-step voltage regulator (Gers, 2014)

3.3.3 Other voltage regulating devices.

Other voltage regulating devices include Static Var compensator (SVC) and Static Synchronous compensators (STATCOMs). These are briefly reviewed below.

- Static Var compensator (SVC) - SVC consists of parallel connected thyristor-switched capacitor banks and thyristor-controlled inductors as illustrated in figure 3.28 (Bayliss & Hardy, 2012). SVCs deliver capacitive power by generating capacitive VArs to boost the voltage profile or inductive reactive power by generating lagging VArs to minimize the voltage on the feeder.

- Static Synchronous compensators (STATCOMs) - A STATCOM, illustrated in figure 3.28 consists of a voltage source convertor (VSC), a capacitor, and a coupling transformer. The STATCOM generates capacitive reactive power when the voltage at the bus is less than the pre-set voltage and conversely generates inductive reactive power when the bus voltage is higher than the pre-set voltage (Bayliss & Hardy, 2012). In this way, over and undervoltage in the distribution network can be controlled.

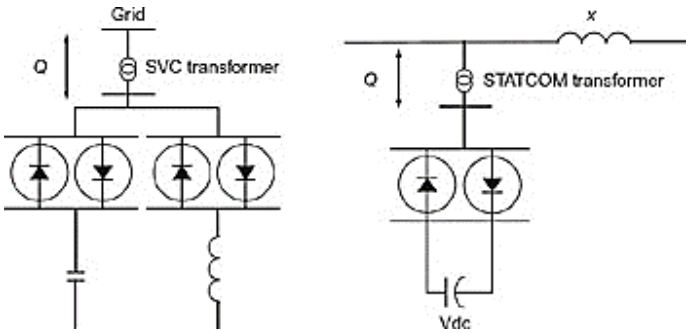

Figure 3.28. SVC (left)and STATCOM (right) diagram (Bayliss & Hardy, 2012)

3.4 Local voltage control

A centralized control method based on predefined values as described above, is classified a discrete control measure, and cannot regulate the network voltages continuously (Zhao, Bo, et al, 2017). A decentralized method, using multiple DG inverters at the local level can potentially address this problem. Theoretically, many PVs can be used to participate in voltage regulation based on their reactive power contribution when required. The effect of bidirectional power flow as illustrated in Figure 3.29, needs to be addressed to allow DGs to participate in voltage regulation at the point of common coupling (PCC).The factors that influence the voltage level in the distribution networks can be attributed to capacity and location of the DG (Zhao, Wang & Zhang, 2018).

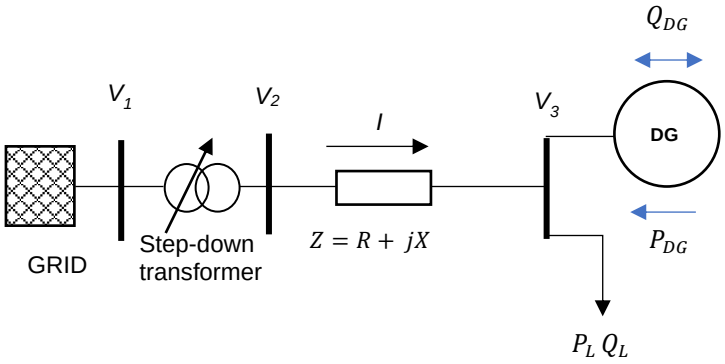

Figure 3.29. Single line diagram of 2-bus distribution network with DG

The voltage drop based on figure 3.29 can mathematically be expressed as:

$$V_2 - V_3 = \Delta V = I\ x\ (R + jX) \tag{3.25}$$

where:

$$I = \frac{(P_L - P_{DG})R + jX(Q_L - Q_{DG})}{V_1} \tag{3.26}$$

The voltage at V_2 when the demand is higher than generation, can be written as:

$$V_2 = V_3 - \frac{(P_L - P_{DG})R + (Q_L - Q_{DG})X}{V_1} \tag{3.27}$$

Conversely, when DG generation exceeds demand, power flows towards V_2 , which causes the voltage to rise at V_3. The equation is written as:

$$V_3 = V_2 + \frac{(P_L - P_{DG})R + (Q_L - Q_{DG})X}{V_1} \tag{3.28}$$

From equations 3.27 and 3.28, the reactive power generated by the DG has a significant influence of the voltage at the PCC, especially where the power generated by the DG exceeds the power required by the load. Figure 3.30 shows the impact of PV generation on the local bus voltage.

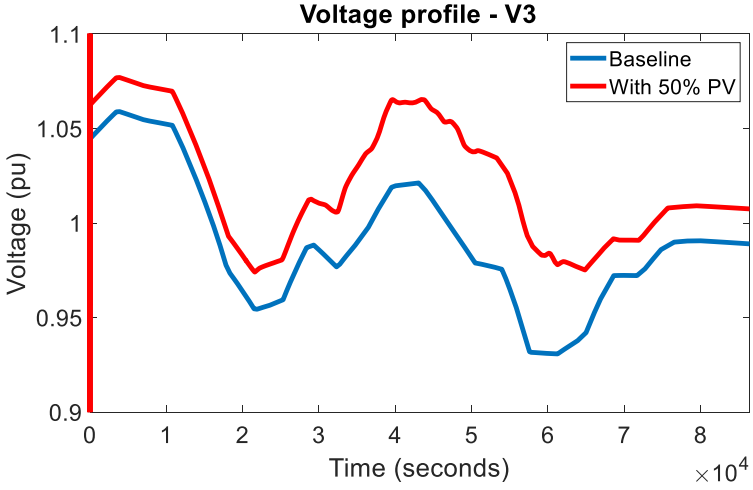

Figure 3.30. PCC voltage profile with 50% PV

3.4.1 Voltage control with PV

Historically, conventional synchronous generators have supplied reactive power to the grid, but these are being replaced by solar-PV systems, which is not able to supply the same levels of reactive power (Bansal, 2017). PV inverters, which are interfaced to the grid, are used to control the voltage in distribution networks. These inverters have the ability of absorbing and injecting reactive power. The standard inverter is oversized by approximately 10% of its rating, which means that it can still produce reactive power above its maximum active power rating (Bansal, 2017). The relationship between the inverter capacity (S_i), active power (P_i) and reactive power (Q_i) is given by:

$$\sqrt{P_i^2 + Q_i^2} \leq S_i \tag{3.29}$$

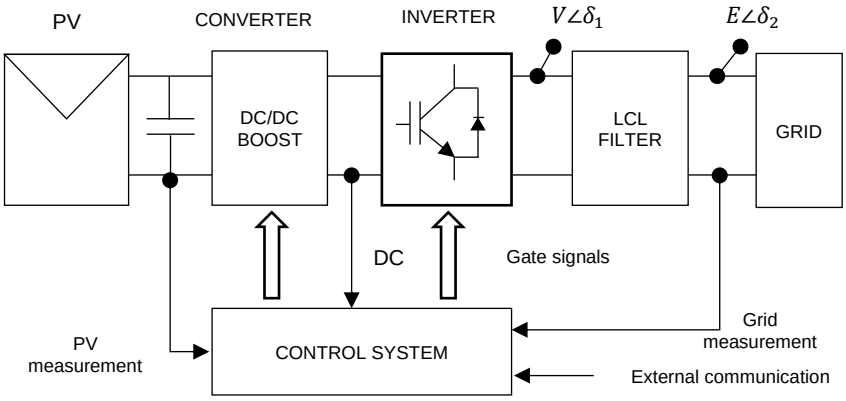

Figure 3.31. Solar PV system

Figure 3.31 shows a basic PV system, which includes PV panels, passive input filter and a capacitor. The input filter is followed by a buck or boost DC–DC converter, which is used to keep the DC voltage constant and to perform the maximum power point tracking (MPPT) of the PV system. The MPP depends on the solar irradiation and temperature of the module, which varies in time. PV arrays have an optimum operating point called the maximum power point (MPP), which is dependent on solar irradiation and PV module temperature as illustrated in Figure 3.32. The MPP adjusts the panel's output voltage to increase the maximum energy that can be transferred from the PV systems to the grid (Rashid, 2015). The DC–DC converter is connected through a DC link to the DC–AC converter, which converts DC to AC power. The function of the inverter is to: (i) control the active power delivered to the grid, (ii) control and regulate reactive power, (iii) perform grid synchronization (Hassaine, Olias, Quintero, & Haddadi, 2009). The DC-AC converter or PV inverter is connected to the grid via an output filter, which is usually made of a combination of inductors and capacitors (Abu-Rub, Malinowski & Al-Haddad, 2014).

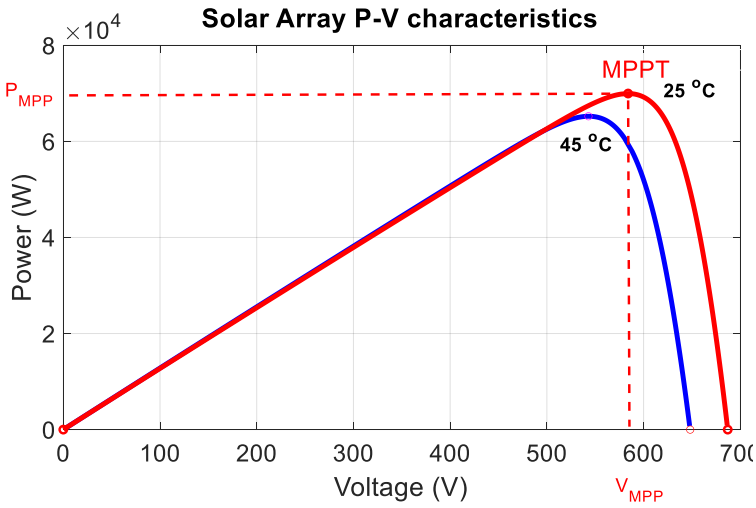

Figure 3.32. P-V characteristics of a solar array showing MPP

Real, reactive power, voltage and frequency can be controlled using local feedback applied to the inverter. From figure 3.31, real power (*P*) and reactive power (*Q*) can be approximated as:

$$P \approx \frac{3VE}{2X} sin\delta \tag{3.30}$$

$$Q \approx \frac{3VE}{2X}(V - Ecos\delta) \tag{3.31}$$

Where V and E are the voltage at the inverter and grid, respectively. The inverter controls V and the phase angle (δ_1) of the output voltage ($V\angle\delta_1$) at the inverter bus terminal. The PV system supplies power to the grid at a voltage of ($E\angle\delta_2$) through the inductor of reactance X. Under normal circumstances, $V\angle\delta_1$ leads $E\angle\delta_2$ by the angle δ, where $\delta = \delta_1 - \delta_2$. The active power ($P$) is controlled by controlling δ and the reactive power (Q) is controlled by controlling V. The inverter is used to control the local frequency, voltage, and current. PV inverters can produce maximum power when the power factor is at unity and not constraint. This assumes that the inverter capacity is matched to the rated PV capacity.

Figure 3.33 is the schematic diagram of the reactive power control system of a typical PV system. Active power generated by the PV array is represented by P , which feeds the MPPT control system. Then, the output power range is generated from the active power of the PV generator, P_{PV} ,which determines the margin of the inverter capacity, *S*. The optimal scheduling reactive power reference, Q^*_{PV} adapts the range of the reactive power for the PV generator. The active and reactive powers of the PV generator are estimated by the *"dq"* to "*abc*" conversion. The three-phase voltage reference (*abc*) is the input of a voltage source

inverter, and the inverter delivers the active P_{PV} and reactive power Q_{PV} to the distribution networks.

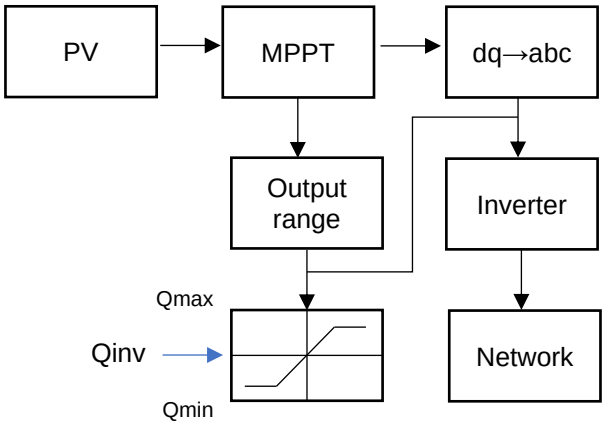

Figure 3.33. Reactive power control system for the PV (Funabashi, 2015)

Various PV inverter control strategies have been proposed in the literature (Zhao, Wang & Zhang, 2018). Two of the most common DG inverter strategies are power factor control and voltage adaptive control, which are discussed are below:

3.4.1.1 Power Factor Control (PFC)

DER inverters can be operated in unity power factor (UPF) or constant power factor (CPF) (Zhao, Wang & Zhang, 2018).

- Unity PF - UPF does not provide any reactive power output. Maximum active power is provided by the inverter when the power factor is set at 1.0. Most DG inverters operate at unity power factor during normal conditions. Any variation in real power will not have an impact on the reactive power. Constant PF can regulate the reactive power dynamically throughout the day by tracking the changes in the active power. According to the South African Grid Connection Code (SAGC) of 2012, DER with output power of 0-100kVA shall operate above 0.98 PF or at unity PF (SAGC, 2012). The PF should be improved to unity, where PF control at the PCC is possible. The PF control, illustrated in figure 3.34, is used to control reactive power (Q) proportional to the active power (P) at the connection point. For DER output power between 100 kVA and 1 MVA and operating between 20% and 100% of rated power, PF range should be 0.95 lagging and 0.95 leading (SAGC, 2012).

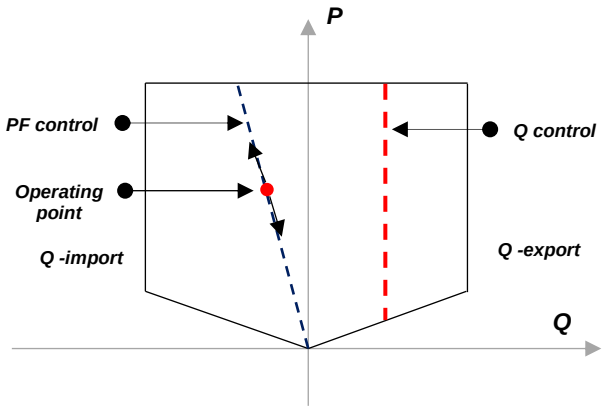

Figure 3.34. DG reactive power control function (SAGC, 2012)

- Constant/Fixed PF - power factor is kept constant and provides a constant ratio between active and reactive power. The reactive power output is proportional to the real PV power. Inverters were historically designed to operate at unity PF and feed active power into the grid. Recently, smart inverter power factor can be adjusted to change the reactive power output. Reactive power is limited however to the value of its real power. The obvious disadvantage is generation of reactive power at night when there is no PV generation. Another option is to schedule the power factor during the day to coincide with high generation but high low demand.

  Figure 3.35 shows the capability curve of an inverter with active and reactive power output, which shows that the inverter is capable of absorbing and injecting reactive power. The reactive capacity of the inverter can be used when required for voltage regulation.

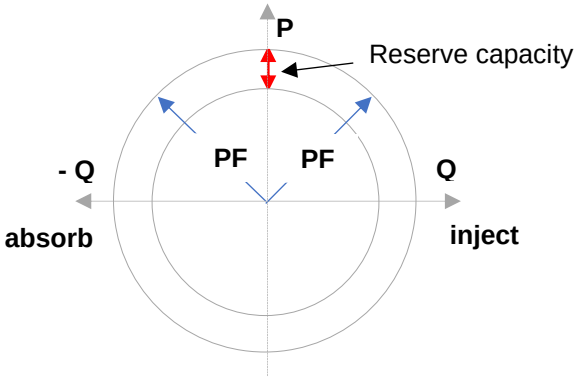

Figure 3.35. PV inverter capability curve (Bansal, 2017)

The equation for determining the reactive power (Q) is given by:

$$Q_{DG} = \pm \frac{\sqrt{1-(PF)^2}}{PF} P_{DG} \quad (3.32)$$

where:

Q_{DG} = DG reactive power

P_{DG} = DG active power

PF = Power Factor

3.4.1.2 Voltage Adaptive Control (VAC)

The control strategy using the PV inverter to automatically regulate reactive power within a given tolerance based on the PCC reference value, is referred to as adaptive voltage control (Zhao, Wang & Zhang, 2018). The strategy includes Q/V and P/V droop control. Droop control is a well-known control strategy that has been used to control the active and reactive power of DER.

- Q/V Droop control - The Q/V control curve is shown in figure 3.36, which shows the 6-points ($A, B, V_{min}, V_{max}, C$ & E), where the vertical axis represents negative and positive reactive power being absorbed and injected, respectively The horizontal axis represents the per unit voltage. Reactive power is injected by the inverter when the voltage falls outside of the reference voltage point of common coupling (PCC) but is restrained by the power factor (PF). Inverters use these curves to respond to local voltage measurements. V_{min} & V_{max} represent the dead zone, where no reactive power regulation takes place. The inverter carries out reactive power compensation outside the band. In the case below, B & C is set to be 0.9p.u. and 1.1p.u. respectively.

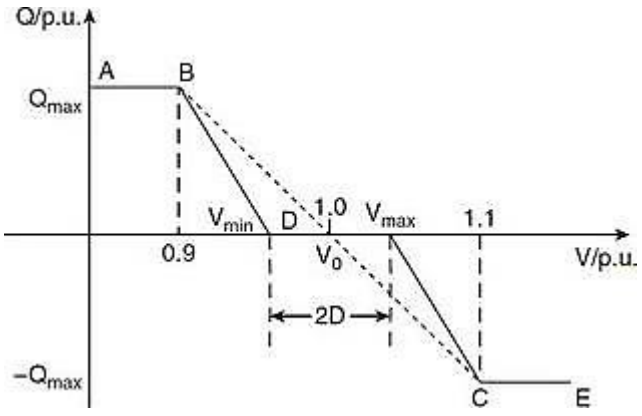

Figure 3.36. DG inverter reactive voltage control curve

From the Q/V control curve above:

$2D = 2[V_{max} - V_0]$ = dead zone, where regulation is not required

$B \ \& \ C$ = minimum and maximum voltage set points, set to corresponding droop curves

based on above, the reactive power (Q) is derived:

$$Q = \begin{cases} \frac{V}{|V|} Q_{max} & V < 0.9 \ or \ V > 1.1 \\ 0 & 1 - D \leq V \leq 1 + D \\ \frac{Q_{max}}{0.1 - D} (-V + 1 + D) & 1 + D < V \leq 1.1 \\ \frac{Q_{max}}{0.1 - D} (-V + 1 - D) & 0.9 \leq V < 1 - D \end{cases} \quad (3.33)$$

$$\begin{cases} Q_{max} = & Ptan(\varphi_{max}), & P \in [P_{cut}, P_1] \\ Q_{max} = & \sqrt{(S_{max})^2 - (P)^2}, & P \in [P_1, P_{max}] \\ P_1 = & S_{max} \cos(\varphi_{max}) \end{cases} \quad (3.34)$$

where:

φ_{max} = maximum power factor angle of the inverter

P = Active power of the inverter

Q = Reactive power of the inverter

S_{max} = capacity limited

P_{max} = maximum power available to be regulated

P_{cut} = cut in power of the inverter

- P/V Droop control - For P/V droop control, the reference PV inverter active power is set based on the upper limit voltage at the PCC. The mathematical formula is given by:

$$P = \begin{cases} P_{\max i, -k_i}(V_i - V_{crit,i}) & \forall V \geq V_{crit,i} \\ P_{max,i} & \forall \ V < V_{crit,i} \end{cases} \quad (3.35)$$

where:

i = number of PV inverters

k_i = droop coefficient

V_i = voltage

$V_{crit,i}$ = upper limit of at the PV set point

$P_{max,i}$ = maximum active power of the ith inverter

3.5 Conclusion

In this chapter a mathematical overview is given of voltage control in power grid by controlling reactive power flow. The chapter started with an overview of the computation of voltage drop in a conventional network. Thereafter, a mathematical overview was given of voltage control using conventional devices and inverter-based DER. Conventionally, devices such as OLTC transformers and shunt capacitors are used at the substation based on a centralised control strategy. For feeder-level control, shunt capacitors and step voltage regulators are used on long overhead lines. The simulation shows that a time-based or voltage-based controlled capacitor switching strategy can be effective to regulate the voltage at the busbar on long feeders and reduce the number of OLTC tap switching. The response time to voltage caused by load fluctuations and intermittent DER devices is a drawback. For local control, inverter-based DER can be more effective in providing a faster response time to voltage fluctuations. Whilst DER connected to the grid raise the network voltage, a control strategy can be used to mitigate the latter. Power factor and voltage adaptive control strategy were introduced as a possible solution. For the former, unity, fixed and scheduled PF was presented. For the latter, a mathematical overview of Q/V and P/V droop control was presented.

CHAPTER FOUR
DEVELOPMENT OF AN OFF- LINE SIMULATION PLATFORM FOR VOLTAGE CONTROL

4.1 Introduction

In this chapter, a test feeder for an off-line simulation platform is developed. Firstly, the selected software and solver are briefly discussed. Secondly, a testbed or simulation platform, which is based on the IEEE 13-bus test feeder is developed. The original unbalanced feeder is modified to a balanced system. The original components i.e., voltage source, OLTC transformer, distribution lines and SCs are described and modelled using the selected software. Thirdly, a phasor model for the variable loads, solar PV and Wind Energy system is developed. Lastly, the simulation results are presented based on various scenarios.

4.2 Software selection

4.2.1 MATLAB®

MATLAB® is a matrix-based programmable platform used by engineers in various engineering applications. It is a simulation tool that uses programming language to express problems and solutions in a mathematical notation (Colgren, 2007). Simulink®, which is an add-on programme to MATLAB®, is a block diagram environment with an interactive, graphical environment. Both programmes were used to model, simulate, and analyse dynamic systems such as the developed test feeders in this study. Both software programs are products of MathWorks™ Inc. Both environments are integrated as one, which allows the user to update a model in either environment (Karris, 2011). The programs were selected based on their wide scientific and engineering application, ranging from automotive, aerospace, electronics, and telecommunications (Karris, 2011). Simulink® is started from the main MATLAB® window by either typing Simulink® in the command window or clicking on the Simulink® block in the top ribbon. The program has a graphical interface that uses block diagrams that are divided into various subsystems to represent and simulate dynamic systems (Beucher & Weeks, 2006).

4.2.2 Solver selection

Simulink® offers different simulation time periods when performing power system studies. The simulation in this chapter is mainly concerned with changes in voltage and currents, which could be measured over a 24hour period. The Powergui block, which is placed in the top level of the diagram, allows the selection of different solvers. The phasor solution method with a variable step solver is used to study electromechanical oscillations for this feeder. This method solves a simpler set of algebraic equations, since we are only concerned with changes in magnitude of voltages and currents. The phasor method accelerates the simulation speed,

which makes simulation much faster to execute. A variable-step solver is selected, which varies the step size during the simulation.

4.3 Test feeder description

The test network is based on the unbalanced IEEE 13 bus test feeder but modified to include dynamic loads, residential rooftop solar PV and Wind energy systems. The network parameters are given in appendix A. Figure 4.1 is a single diagram of the model. The feeder is characterized by:

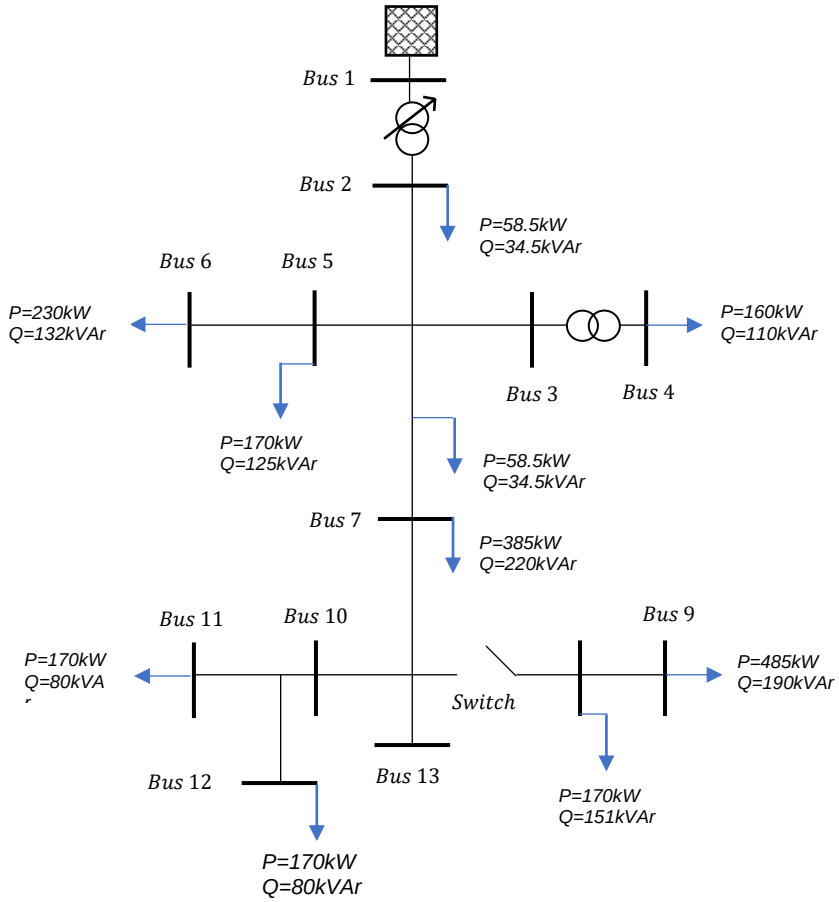

Figure 4.1. IEEE modified 13 Node Test Feeder (ieee.org)

i. Three-wire radial configuration.

ii. Three-phase $\Delta \rightarrow Y$ 115/4.16 kV OLTC transformer, which acts as the substation voltage regulating device and one $Y \rightarrow Y$ in-line 4.160/0.480 kV transformer.

iii. One spot load, four dynamic and 4 static loads, consisting of constant PQ, constant I and constant Z-type delta and star configuration. Dynamic loads are modelled as residential loads, which follows a typical residential load curve. The maximum load size is 485kW.

iv. All loads have been converted to balanced three phase loads.

v. Two feeder and one substation shunt capacitor

4.4 Modelling of the test feeder

The following section gives a detailed description and modelling of each feeder component.

4.4.1 Substation voltage regulator

- OLTC modelling - An OLTC transformer is selected for centralized substation voltage control. The simplified phasor model, which simulates the transformer and OLTC by current sources is selected as it provides a faster simulation time. The voltage regulator adjusts the taps in an upward or downward position until the input voltage (V_m) is equal to the reference voltage (V_{ref}). The standard Simulink® model is equipped with 16 taps i.e., 8 taps up and another 8 taps down. In this three-phase balanced model, the number of taps is increased from 16 to 32. The OLTC is modelled with a voltage regulator, which is shown in figure 4.2. The parameters of the OLTC transformer and regulator are shown in table 4.1.

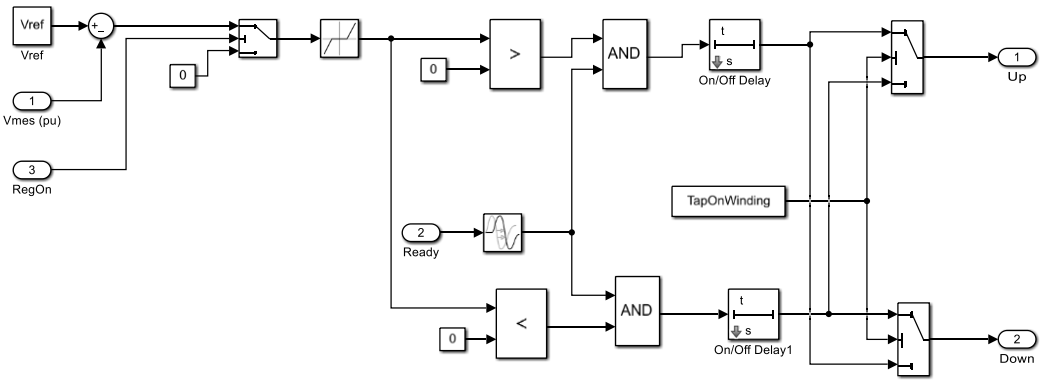

Figure 4.2. Voltage regulator block diagram

The OLTC regulates the voltage at the secondary side of the substation transformer bus by varying the primary transformer turns ratio. For this study, the positive-sequence voltage is measured at bus1, which acts as the input to the OLTC. Each tap provides a voltage correction factor of +/-0.00625pu of nominal voltage. The voltage regulator sends a signal to the tap changer to regulate the taps in the upward or downward position, depending on the load characteristic, voltage reference and dead-band.

The voltage regulation range is determined by the following formula:

$$(V_{ref}\_DB/2 \; < V < V_{ref} + DB/2) \tag{4.1}$$

where:

V_{ref} = $Reference\ voltage$

DB = $Dead - band$

The reference voltage is set to 1.05pu as the unregulated voltage at bus1 is close to 1.0pu but the voltage decreases as distance from the substation increases. This will ensure that the bus voltage at the furthest point in the network will be regulated around 1.0pu. The OLTC parameters are given in table 4.1.

Table 4.1. OLTC transformer specification

Parameter	Value
S_{base}	$5MVA$
V_{prim}	$115kV$
V_{sec}	$4.16kV$
R_1	$0.01pu$
X_1	$0.08pu$
R_2	$0.01pu$
X_2	$0.08pu$
$V_{step/tap}$	$0.0625pu$
V_{ref}	$1.05pu$
$Tap_{min/max}$	$-16, +16$

4.4.2 Distribution Lines

- Line modelling - the lines are modelled as an N-phase distributed parameter line π model where the RLC parameters are given as [N x N] matrices. The phase impedance and admittance matrix are configured based on equation 4.2 where the resistance (R), inductance (L) and capacitance (C) is given in ohms, Henries, and farads per kilometre, respectively. The line configuration is given in Appendix A.

$$[Z_c] = \begin{bmatrix} Z_{11} & Z_{12} & Z_{13} \\ Z_{21} & Z_{22} & Z_{23} \\ Z_{13} & Z_{23} & Z_{33} \end{bmatrix} \quad (4.2)$$

The equivalent circuit of the π-model is given in figure 4.3, which shows a series resistance (r_L), series reactance (jX_L), sending-end conductance and susceptance and receiving-end conductance and susceptance.

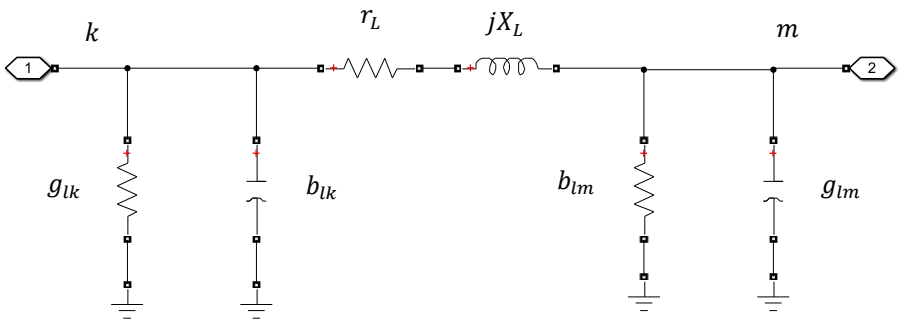

Figure 4.3. Distribution line lumped 𝛑 circuit.

4.4.3 Dynamic and static loads

- Load modelling - all the loads of the standard IEEE 13 bus network are given as static loads. The standard Simulink® RLC load mask is used to model static loads. Four static loads are converted to dynamic/variable loads. The dynamic loads can be modelled as constant PQ, current (I), or impedance (Z). Dynamic loads are time varying and can be controlled as these loads are driven by end-user behaviour. The load varies based on (i) positive-sequence voltage input or (ii) an external control, which affects active power (P) and reactive power (Q). For this study, all variable loads are externally controlled by changing P&Q over a 24hour period. The active power (P) and reactive power (Q) are given by the following equations:

$$P = Po\left(\frac{V}{V_o}\right)^{np} \tag{4.3}$$

$$Q = Qo\left(\frac{V}{V_o}\right)^{nq} \tag{4.4}$$

where:

V_0	= initial positive sequence voltage
P_0 and Q_o	= initial active and reactive powers at the initial voltage
V	= positive-sequence voltage.
n_p and n_q	= exponents, which determine the nature of the load. By selecting 0,1 or 2, constant PQ, I or Z load can be obtained, respectively.

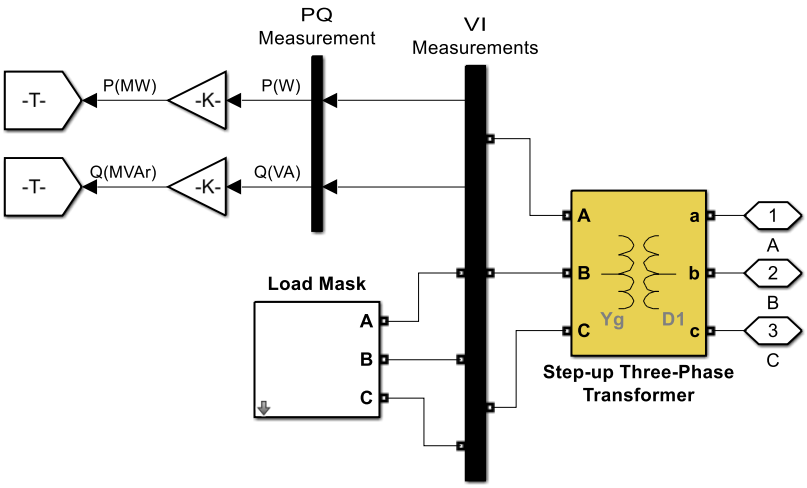

a) Load block

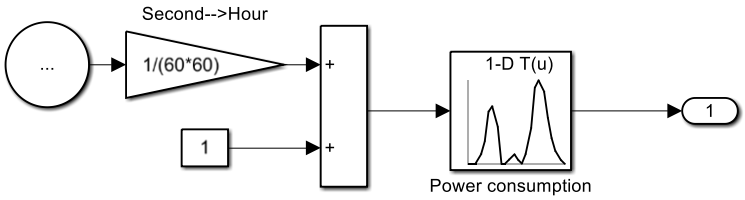

b) Power consumption input blocks

Figure 4.4. Simulink variable load model

The load block in figure 4.4, which includes the load mask, represents the phasor model of the aggregated dynamic load. The load block consists of the load mask, voltage, current, power measurement and step-up transformer. The load is modelled as a controlled current source, which is shown in figure 4.5. The input to the controlled current source is fed by a 1-D look-up table. The look-up table map inputs to an output value by looking up a table of load and time values. The controlled current source block converts the Simulink® input, which is fed by a 1-D look-up table signal into an equivalent current source.

Figure 4.4 (b) is a representation of the load block, which shows the power consumption input blocks. The input parameters of the load mask are (i) nominal power and (ii) power factor. The balanced three-phase loads are modelled as constant PQ loads. All the loads connected at the various buses are aggregated residential loads, which form a residential cluster. The load profiles are based on actual residential load data. The input parameters are given in table 4.2.

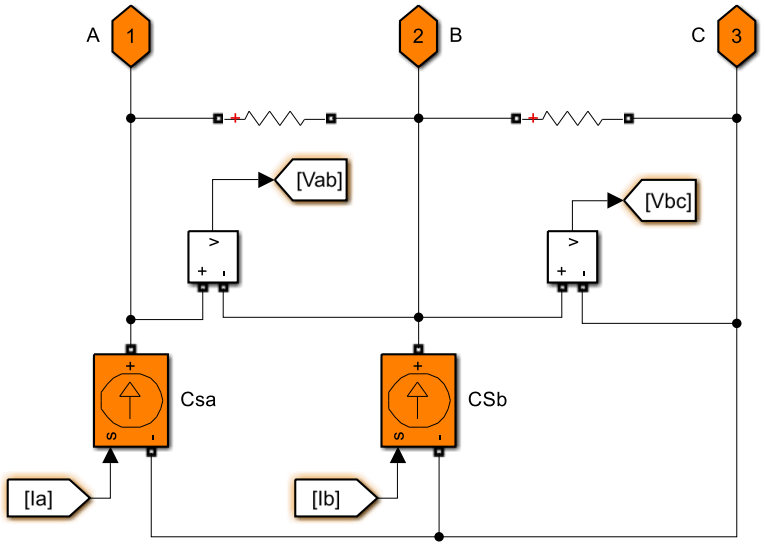

Figure. 4.5. Controlled current source

Table 4.2. Variable load mask input parameters for load 1

Parameter	Unit
$Active\ Power$	$160kW$
$Power\ Factor$	1.0
$Reactive\ Power$	$0kVAr$

Figures 4.6 and 4.7 shows the load and power factor profile of the feeder, respectively, which is measured at the substation. The profiles of the variable loads is given in Figure 4.8. The power factor at load 1 has been improved to unity by installing additional shunt capacitors close to the transformer.

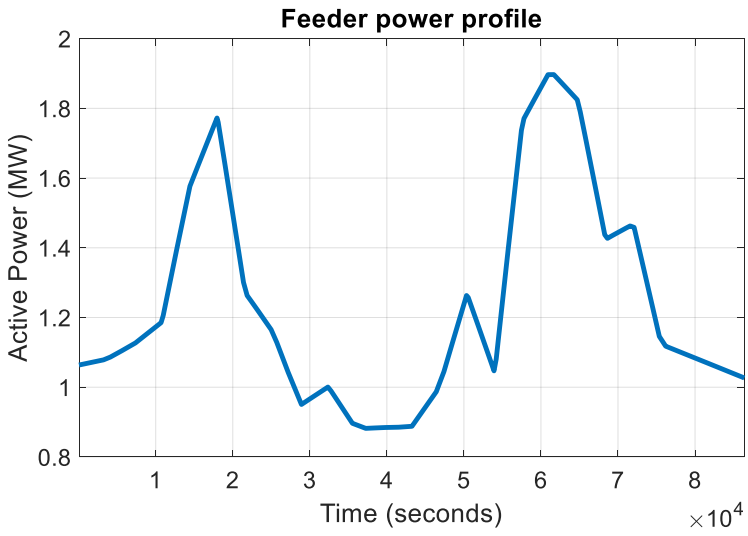

Figure 4.6. Feeder profile

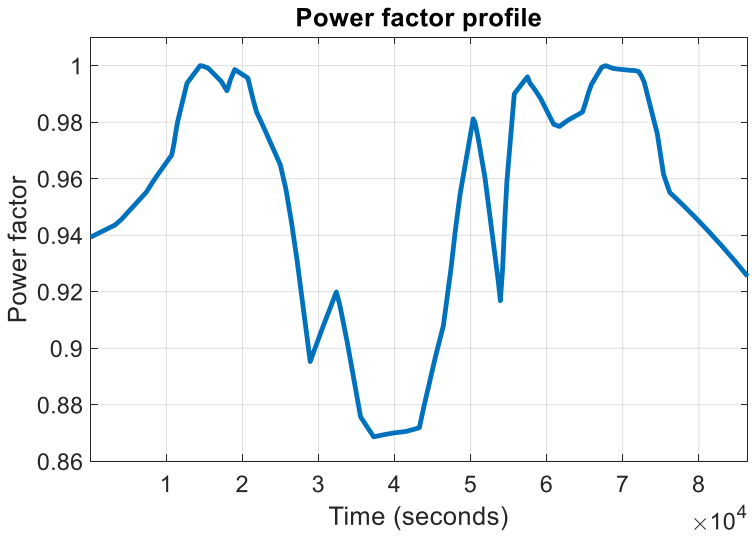

Figure 4.7. Power factor profile

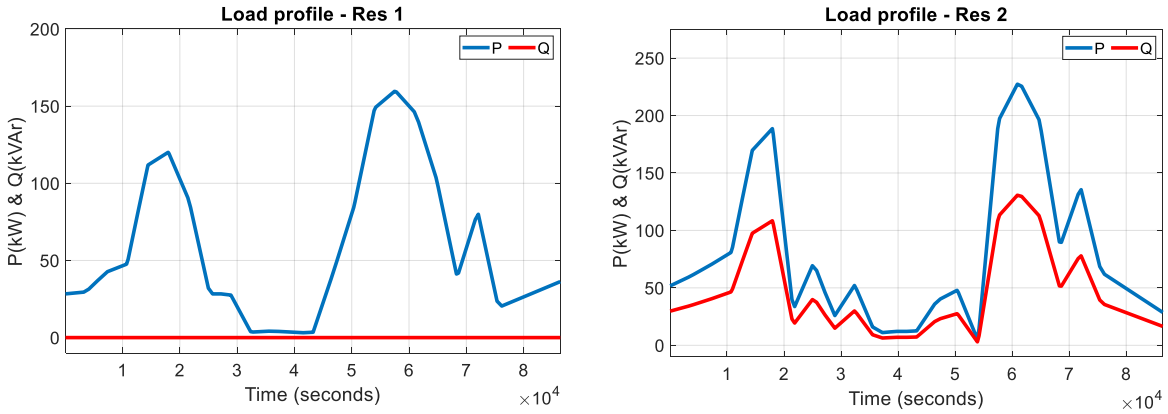

a) Residential 1 - load profile

b) Residential 2 - load profile

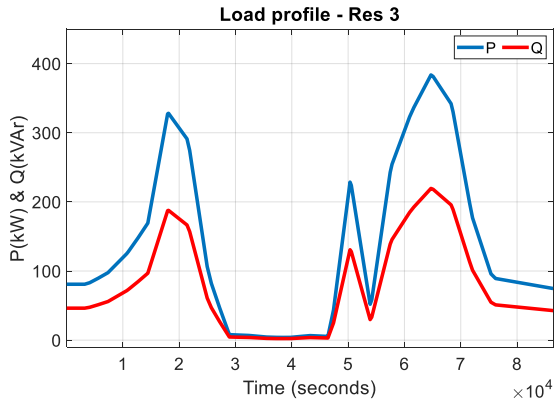

c) Residential 3 - load profile

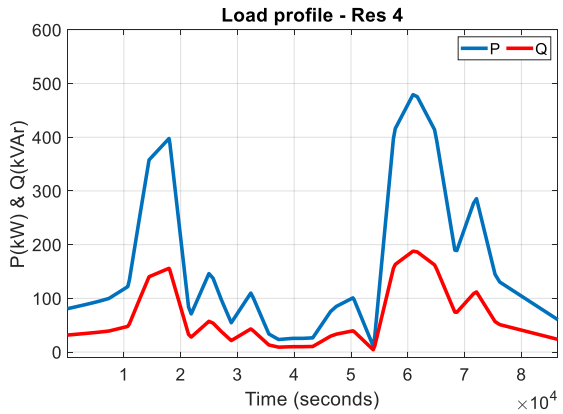

d) Residential 4 - load profile

Figure 4.8. Residential load profiles

4.4.4 Solar PV

- Solar PV modelling - figure 4.9 shows the block representation of the phasor model developed in Simulink®. The solar PV mask is modelled as a control current source, like the variable load mask. The controlled current source block converts the Simulink® input signal, which is fed by two 1-D look-up tables as illustrated in figure 4.10, into an equivalent current source. The look-up tables map inputs to an output value by looking up a table of irradiance and ambient temperature values over a 24hour period. The input parameters to the solar PV mask are (i) solar panel total area (ii) overall system efficiency and (iii) power factor. The product of the total area and the system efficiency is used to calculate the active PV output power. The power factor input block is used to calculate the reactive power supplied into the grid by the inverter.

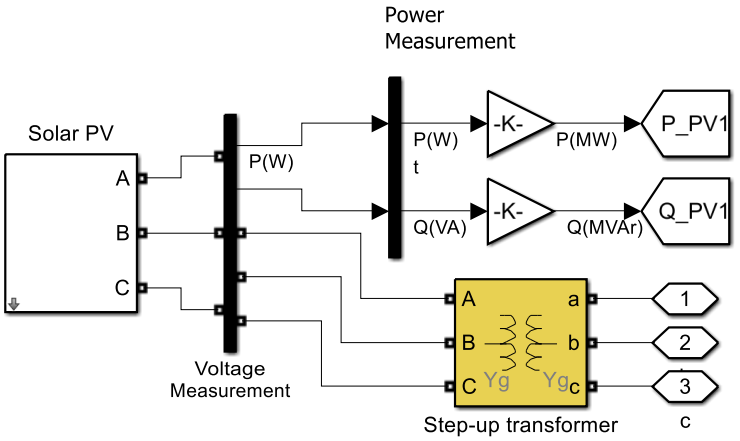

Figure 4.9. Solar PV block

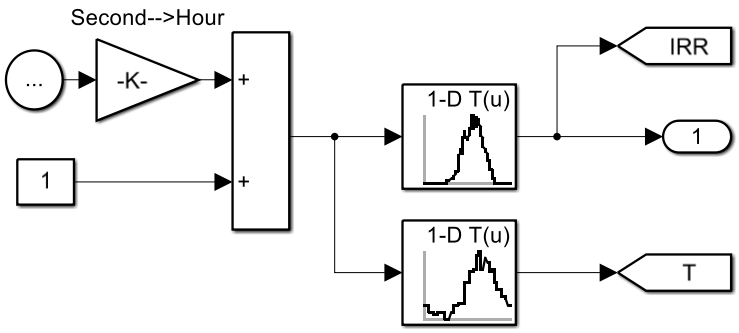

Figure 4.10. Irradiance & temperature input blocks

Figure 4.11 shows the irradiance and temperature curves on a specific day. The irradiance data was measured at 5minute intervals. The irradiance curves show actual vs an ideal irradiance measurement. The solar PV system generates active power

during 06h00 and 19h30, with maximum generation recorded at 13h30. The temperature curve, shown in Figure 4.12, was measured at 1hour intervals. The performance of the PV array is influenced by irradiance and temperature, which fluctuates during the day.

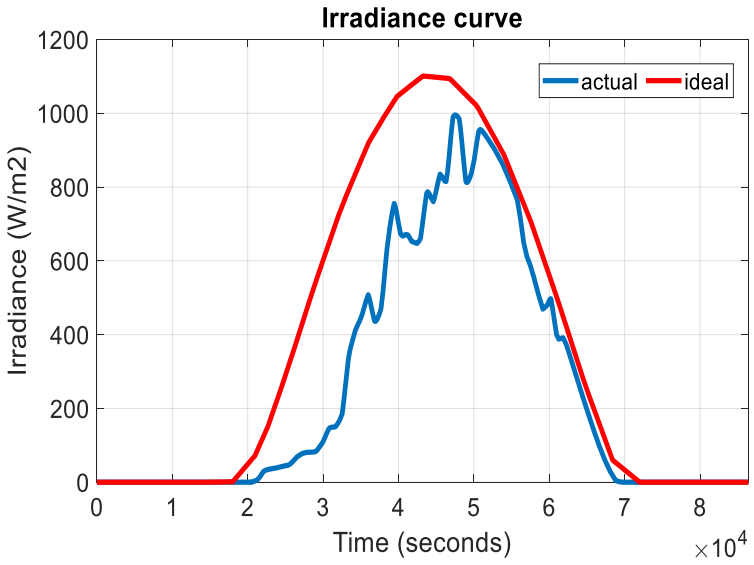

Figure 4.11. Solar irradiance curve (14 January, 2014)

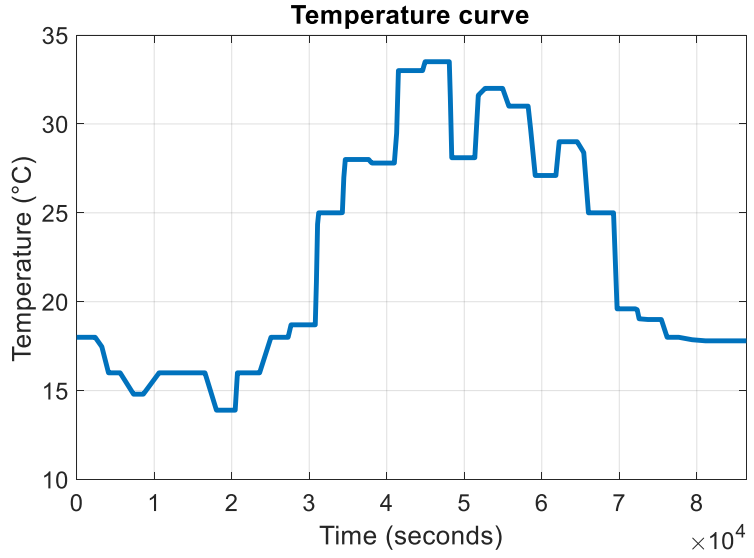

Figure 4.12. Temperature curve (14 January 2014)

The input parameters to the solar PV block are summarized in table 4.3. The active power, which is measured at the PCC, is the product of (i) solar panel total area and (ii) system efficiency. The reactive power profile is a product of the latter and the power factor input. When the power factor is set to one, no reactive power is generated by the PV system. To speed up the simulation time, the residential rooftop PV is aggregated. The combined neighbourhood load is 160kW, which consists of thirty-two, 5kW residential loads. The rooftop PV system is

sized at 5kW to match a typical residential load. The PV array is sized roughly 30% greater than the inverter, which is 6.5kW. The input data in table 4.3, represents six, 6.5kW PV rooftop systems at 25% PV penetration at unity PF.

Table 4.4 shows the aggregated rooftop PV array for all the scenarios compared to the actual load.

Table 4.3. PV array input parameters

Parameter	**Unit**
Panel area	300m^2
System efficiency	15%
Power Factor	1.0
Peak Active Power	43kW
Peak Reactive Power	0kVAr

Table 4.4. Aggregated Rooftop PV array

Bus no	**Load Size**	**Aggregated PV (kW)**		
	kW	25%	50%	75%
2	117	29.25	58.5	87.75
4	160	40	80	120
5	170	43	85	130
6	230	60	115	175
7	385	100	195	290
8	170	43	85	130
9	485	125	245	365
12	128	32	64	96
11	170	43	85	130

4.4.5 Wind Energy

Wind energy modelling – wind is generated when the sun heats up the Earth's surface unevenly and results in a difference of air pressure. This air pressure, which moves from high to low, results in wind. Wind turbines are used to convert this wind into electricity. The turbine consists of the rotor, blades, nacelle, and generator. The turbine's blades capture the kinetic energy of wind, which causes a rotating action. This rotating action drives the generator to produces electrical energy (Kiprakis, 2005). The power generated by the wind stream can be calculated by the following formula:

$$P_{wind} = \frac{1}{2}\,\rho\, A\, V_{wind}^{3} \tag{4.5}$$

where:

P = $Power\ in\ watts$

ρ = $air\ density\ in\ kg/m^3$

V_{wind} = $instantenous\ wind\ in\ m/s$

A = $swept\ area\ of\ the\ blades\ in\ m^2$

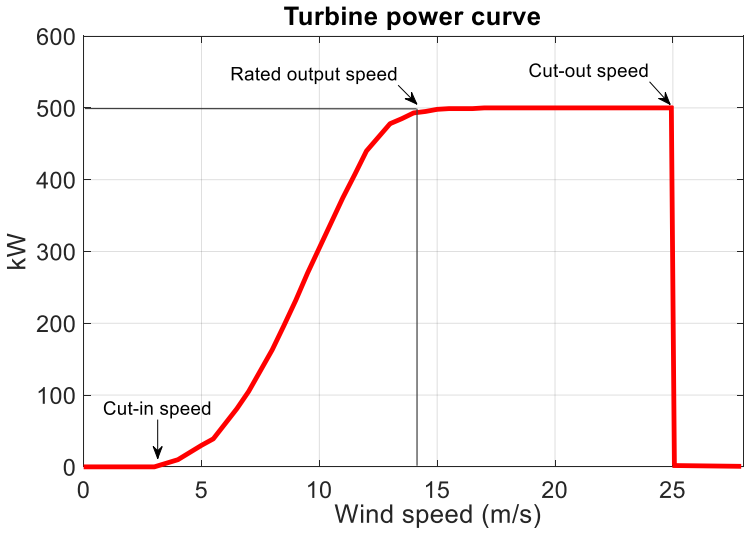

Figure 4.13. Wind turbine power curve

Figure 4.13 shows a typical 500kW wind turbine power curve. The turbine starts to operate at the cut-in speed, which is at 3.5m/s. Based on the windspeed, the power output increases until the wind speed reaches the rated speed at 14m/s. At this point, the turbine begins to operate at its rated power, which is 500kW. To prevent damage to the rotor, the rotor is stopped when the wind speed exceeds the cut-out speed, which in this case is 25m/s.

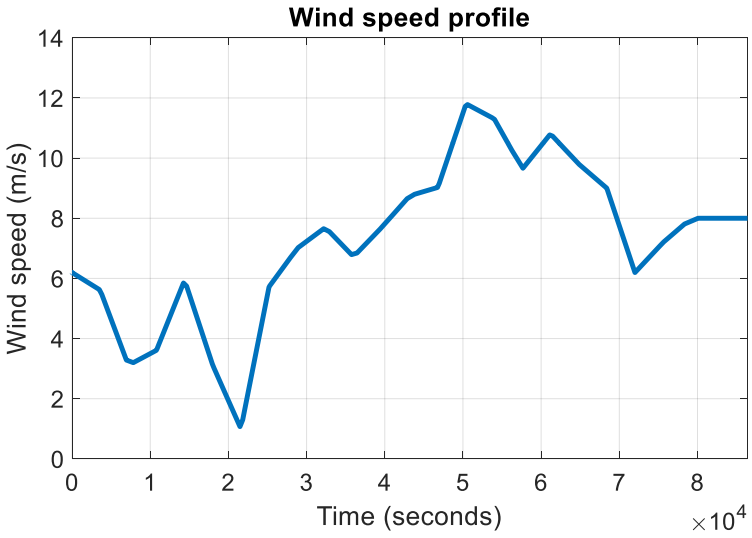

Figure 4.14. Daily wind speed curve (14 January, 2014)

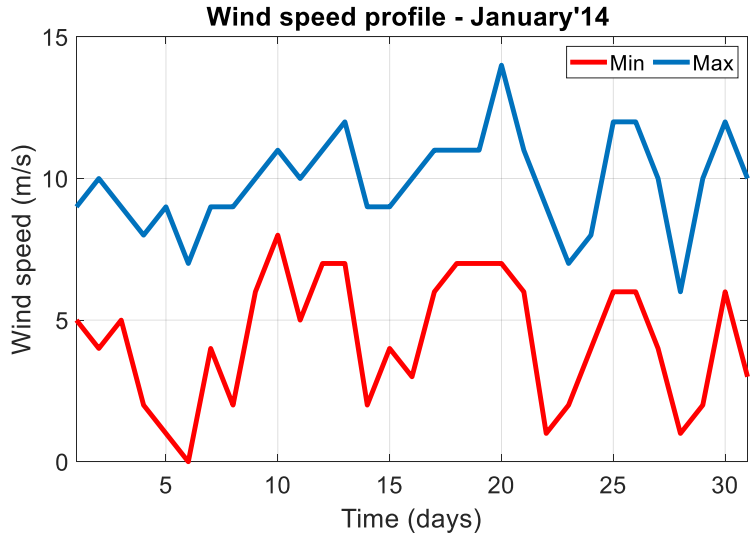

Figure 4.15. Monthly wind speed curve

Figure 4.14 shows the daily wind speed curve measured on 14 January 2014. The monthly curve in figure 4.15 shows the minimum and maximum wind speed in January 2014.

Wind energy is modelled as a controlled current source as well. Figure 4.16 shows the block representation of the phasor model in Simulink®. As with the solar PV block, the controlled current source block converts the Simulink® input signal, which is fed by a 1-D look-up table into an equivalent current source. The input parameters to the Wind mask are (i) nominal power, (ii) nominal speed (m/s), (iii) maximum wind speed (m/s) and (iv) power factor. The product of the nominal power and nominal wind speed determines the active power of the wind system. The power factor input block is used to calculate the reactive power supplied into the grid by the system. Figure 4.17 shows

the blocks of the wind energy system with nominal wind speed input data supplied by 1-D look-up table.

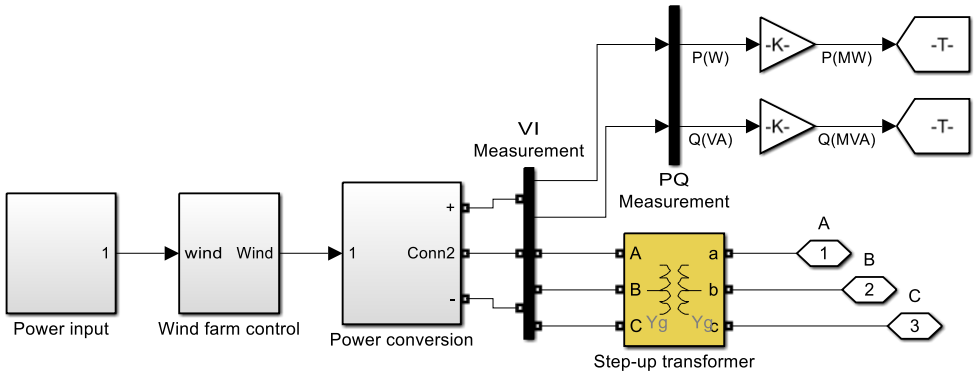

Figure 4.16. Wind Energy block

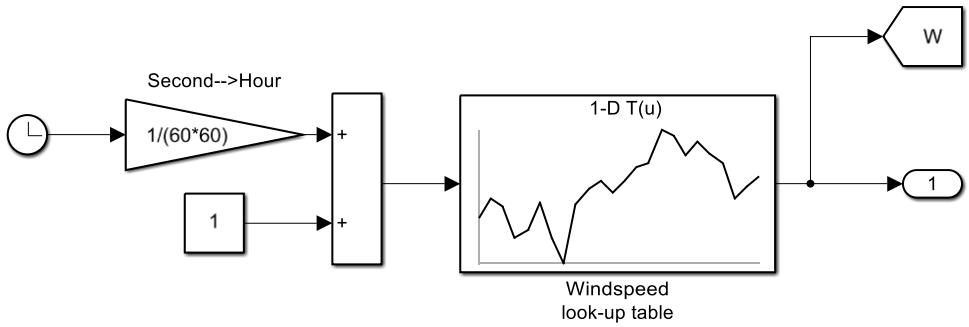

Figure 4.17. Wind mask with 1-D look-up table

4.5 Simulation results

4.5.1 Conventional control without DER

The traditional method to control voltage on the distribution feeder is controlling reactive power by shunt capacitors at the substation. The method has been used for several decades to compensate for the voltage drop from the substation and along the feeder due to the varying load current. Below are the results based on actual load data and fixed shunt capacitor.

- **Shunt capacitors (SC)** – Table 4.5 is a summary of the feeder shunt capacitor positioning and size with corresponding minimum and maximum bus voltage. Figure 4.18 shows the voltage profiles at all the buses with only feeder shunt capacitors connected at the specified location.

Table 4.5. Selected buses with feeder SCs

Bus location	Shunt capacitor		Voltage (pu)	
	Size	Position	minimum	maximum
01	-	-	0.953	1.027
11	100kVAr	1	0.925	1.027
09	200kVAr	1	0.925	1.030

From figure 4.18, all except the substation bus exceeded the lower limit. To raise the voltage within the network, a 100kVAr shunt capacitor is installed at the substation. The effect on the corresponding bus voltages is illustrated in table 4.6.

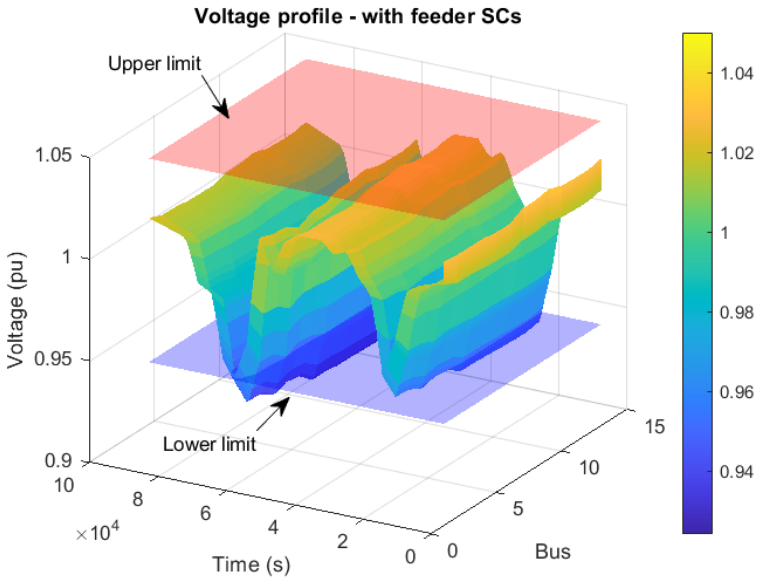

Figure 4.18. Voltage profiles with feeder SCs

Table 4.6. Selected buses with substation and feeder SCs

Bus location	Shunt capacitor		Voltage	
	Size	Position	min (pu)	max (pu)
01	100kVAr	1	0.975	1.048
11	100kVAr	1	0.948	1.048
09	200kVAr	1	0.949	1.051

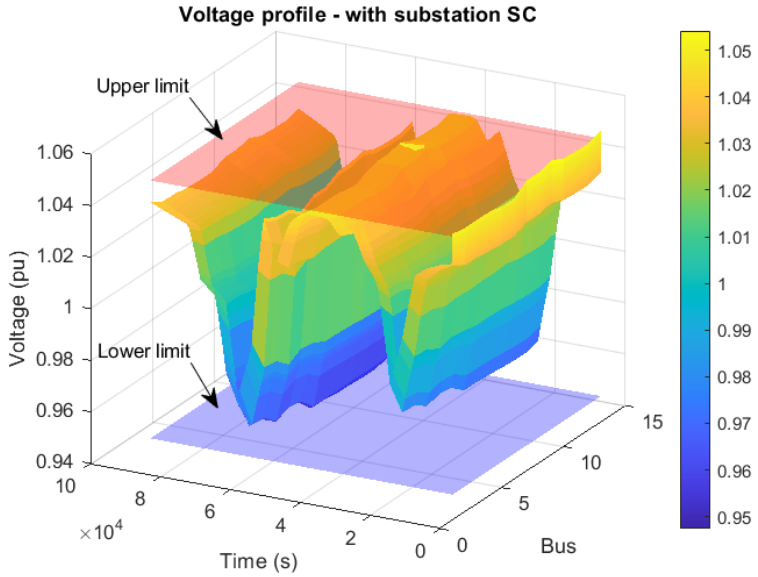

Figure 4.19. Voltage profile at substation bus

Figure 4.19 shows the profile at all the buses in the network after the connection of the substation and feeder SCs. The bus voltages are raised to the required level i.e., between 1.05pu and 0.95pu. Figure 4.20 shows the effect on the substation profile after installing one 100kVAr substation shunt capacitor.

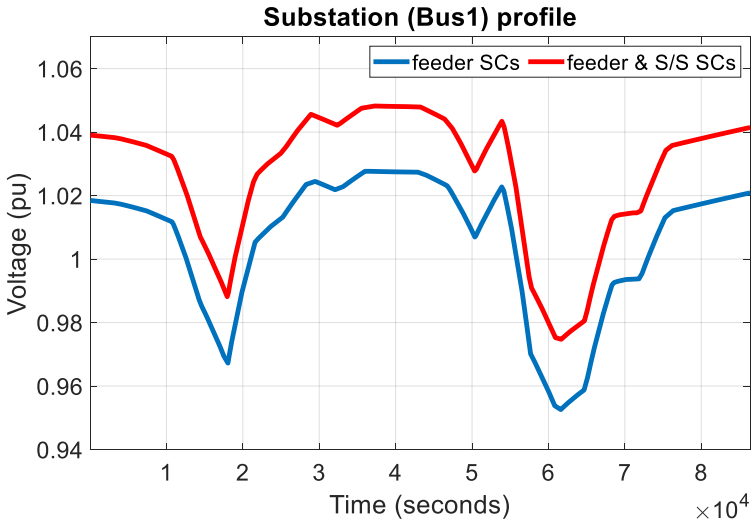

Figure 4.20. Substation profile after compensation

- **On-load Tap changer** – the OLTC is switched on to provide additional control at the substation. The reference voltage (V_{ref}) at the substation is set to 1.05pu, which regulates the other bus voltages close to 1.0pu. Figure 4.21 shows the baseline with the initial tap position, which is set to -4. Based on equation 4.1, the taps move in an upward and downward position to regulate the voltage (V) at or close to the reference voltage. The taps change 34 times during the 24hour period.

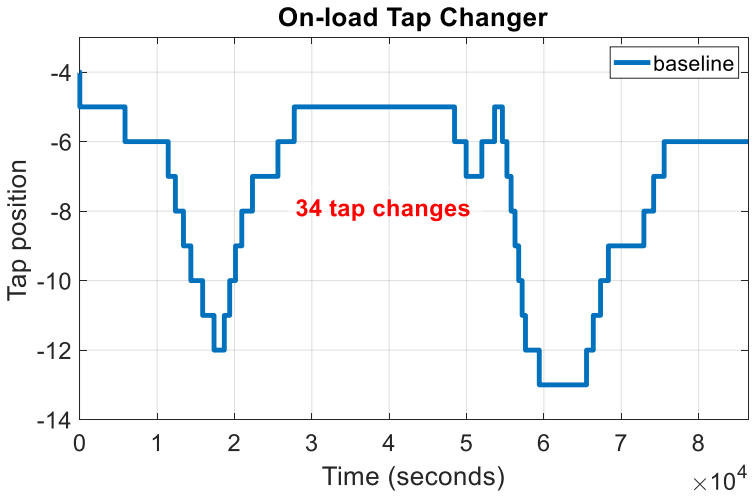

Figure 4.21. On-load tap changer profile

Figure 4.22 shows the baseline and regulated profile at the substation bus. The voltage is regulated at around 1.05pu with the voltage correction factor of +/-0.00625pu of nominal voltage. Table 4.7 gives a summary of the voltage profiles at the selected buses based on SC and OLTC control.

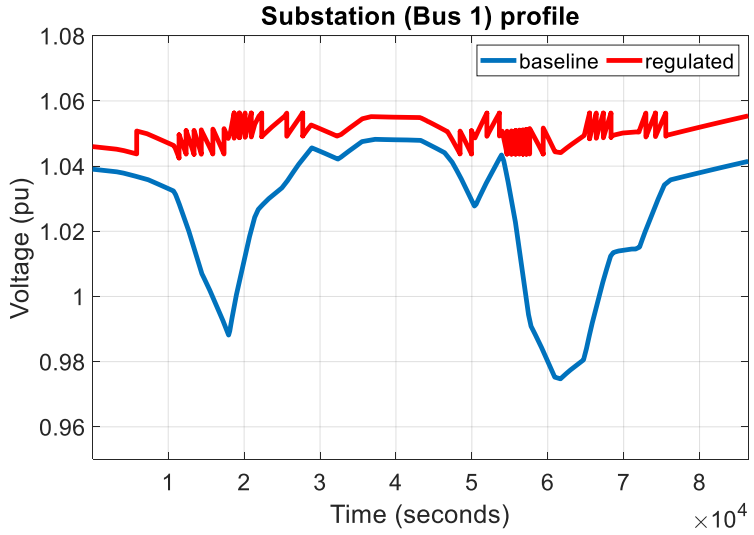

Figure 4.22. Regulated substation bus profile

Table 4.7. Selected buses with substation and feeder SCs

Bus location	Shunt capacitor		Voltage	
	Size	Position	min (pu)	max (pu)
01	100kVAr	1	1.043	1.056
11	100kVAr	1	1.020	1.055
09	200kVAr	1	1.021	1.057

4.5.2 Control with inverter-based DER

Inverter-based DER will raise the voltage at the PCC by injecting real power and/or reactive power according to equation (3.22). The latter was discussed in the previous chapter. Modern smart inverters can inject and absorb reactive power. These devices can react much faster to voltage variations caused by variable load or intermittent solar generation. The following is the summary of the results based on existing methods of reactive power control of modern smart inverters.

4.5.2.1 Solar PV power factor (PF) control

- Unity Power Factor – DER inverter is set to unity power factor (1.0), which is the default setting. Only real power is supplied with no reactive power contribution. Figure 4.23 show the Simulink® block diagram. To obtain unity power factor, the constant block is set to 1.0.

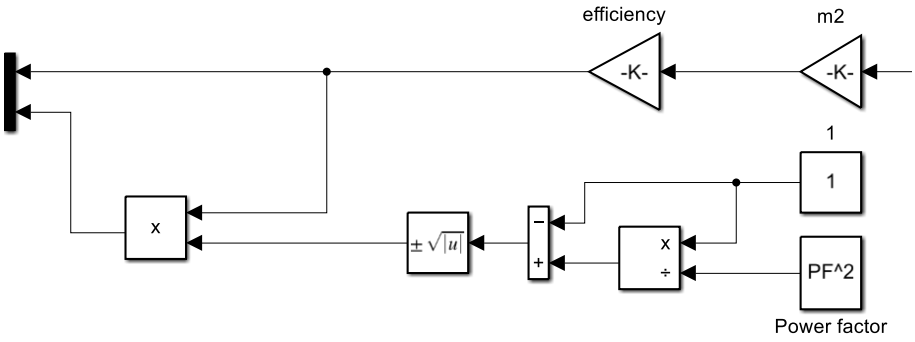

Figure 4.23. Simulink® power factor block diagram

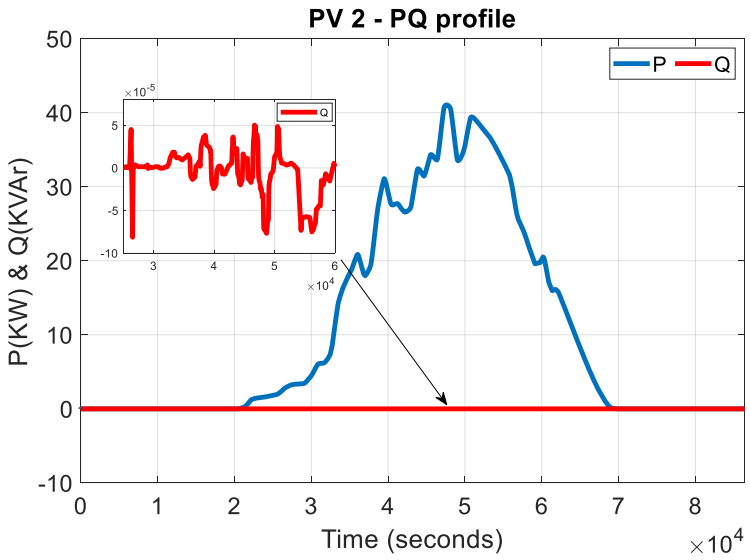

Figure 4.24. 25% PV PQ profile at unity PF

Figure 4.24 show the PQ profile of the solar PV system connected at bus 4. The power factor of the inverter is set to 1.0, which leads to zero reactive power generation when the inverter produces active power during the day. Figures 4.25 and 4.26 shows the voltage profile at all the buses with 25% PV and 50% PV penetration at unity PF, respectively. The voltage violations are depicted in yellow. At 25% PV, the upper limit at some buses have been exceeded. At 50%, most of the buses have exceeded 1.05pu.

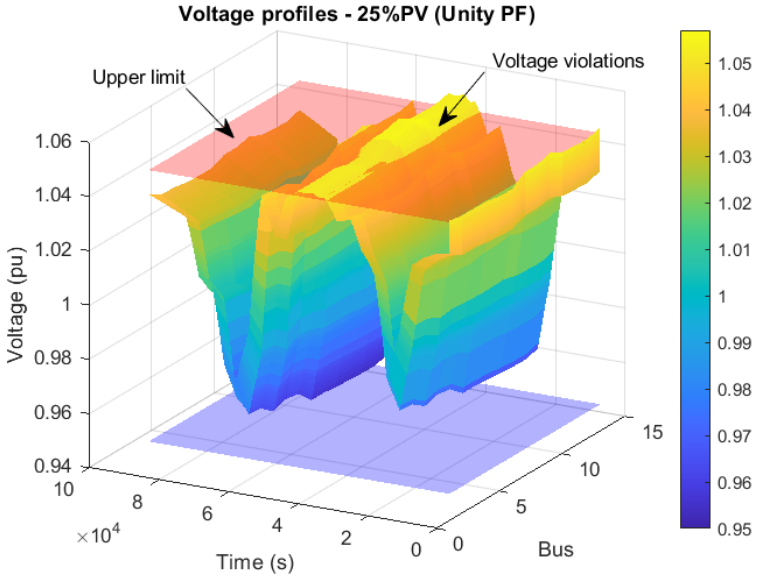

Figure 4.25. Voltage profiles with 25% PV (unity PF)

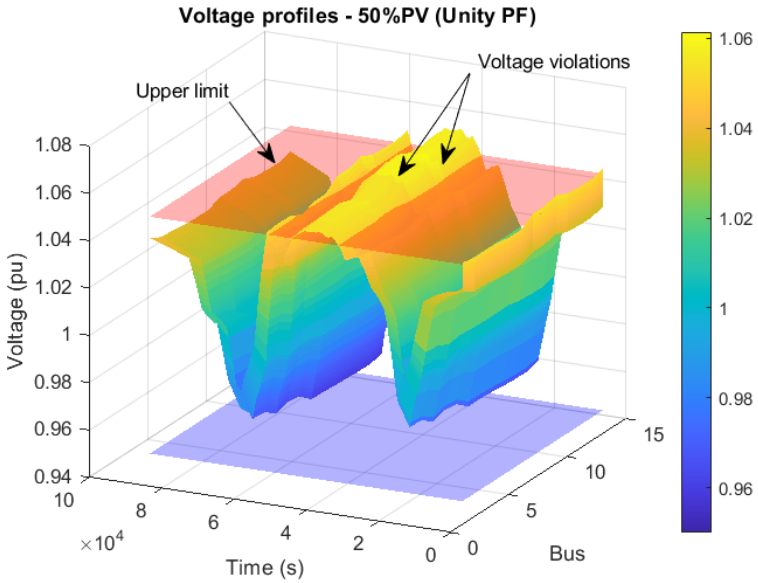

Figure 4.26. Voltage profiles with 50% PV (unity PF)

- Fixed/Constant Power Factor - DER inverter is adjusted to operate at a constant power factor. The reactive power is proportional to the active power generated by the inverter and can be expressed as.

$$Q_{PV} = P_{PV} \tan(\theta) \tag{4.6}$$

where:

$$P_{PV} \leq S_{PV} \cos(\theta) \tag{4.7}$$

The real power does the actual work, while reactive power energizes the magnetic field but does no actual work. The power factor is the ratio of the real to the apparent power. The current grid connection code in South Africa does not allow any controlled functionality for solar PV inverters less than100kVA as discussed in chapter 2. Only power factor control is allowed for generation greater than 100kVA. The results below are based on different levels of PV penetration based on the projected demand until 2050 by the Department of Energy in South Africa (DOE). For constant PF, the inverter is set to lagging and leading to inject or absorb reactive power, respectively. To achieve a lagging PF, the constant block in figure 4.20 is set to positive value, less than 1.

For the first scenario, aggregated solar PV is based on 25% penetration. The power factor of all inverters is set to 0.98 and 0.95 lagging, respectively. Figure 4.27 shows the PQ profile of the solar PV system connected at bus 4. The reactive power generated during 06h00 and 19h30 is proportional to the active power based on equation 4.4.

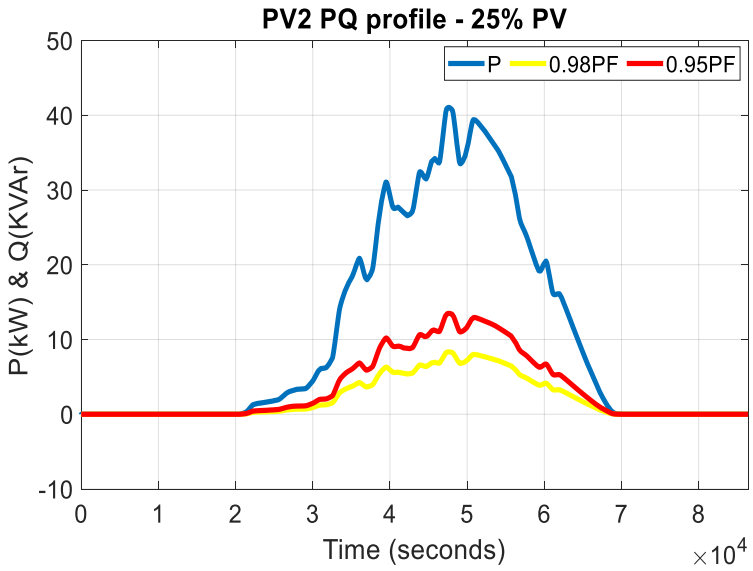

Figure 4.27. PV PQ profile with constant PF

The effect of unity and constant PF on the substation voltage profile is illustrated in Figure 4.28. It shows the baseline voltage profile with no solar PV connected in blue compared to the voltage profile with various PF scenarios. Table 4.8 gives a detailed summary of the voltage at the substation without and with 25% solar PV penetration. The scenario with PV assumes that only 25% of all residents have installed solar PV on available roof space.

At unity PF, only active power is generated during the day. This raised the voltage by 0.4% during the peak generation period. The voltage at the substation is still within the required limit, however. Reactive power is generated when the inverters are set to 0.98PF, which flows towards the PCC and the substation busbar. The voltage at 0.98PF is raises by 0.81% at the substation. The voltage exceeds the upper limit when all the inverters are set to 098PF. At 0.95PF, the voltage depicted in red exceeded the upper limit during peak generation.

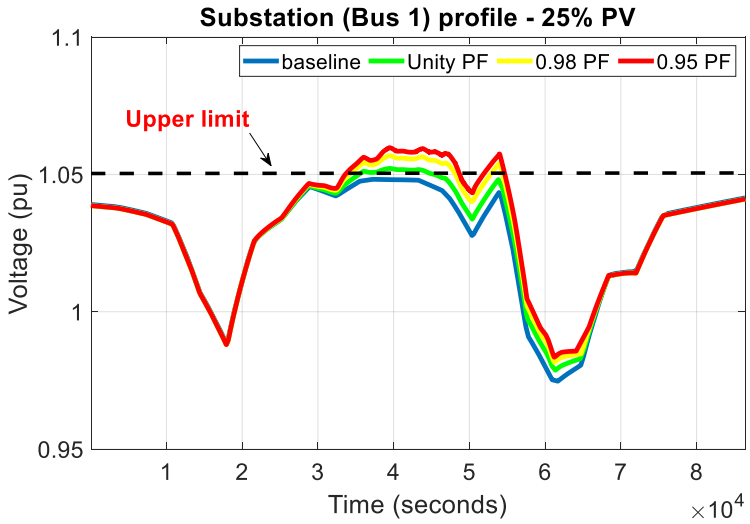

Figure 4.28. Substation profile with 25% PV penetration

Table 4.8. Voltage profile at substation with 25% PV penetration

Power factor	Baseline – no PV		25% PV		ΔV	
	Voltage (pu)				%	
	min	max	min	max	min	max
Unity	0.975	1.048	0.979	1.052	0.41	0.38
0.98	0.975	1.048	0.983	1.057	1.12	0.85
0.95	0.975	1.048	0.985	1.060	1.02	1.13

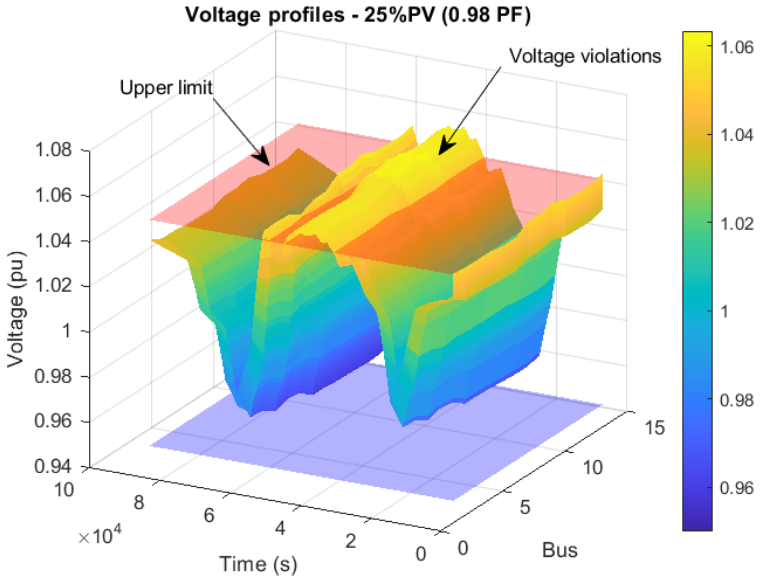

Figure 4.29. Voltage profiles with 25% PV (0.98 PF)

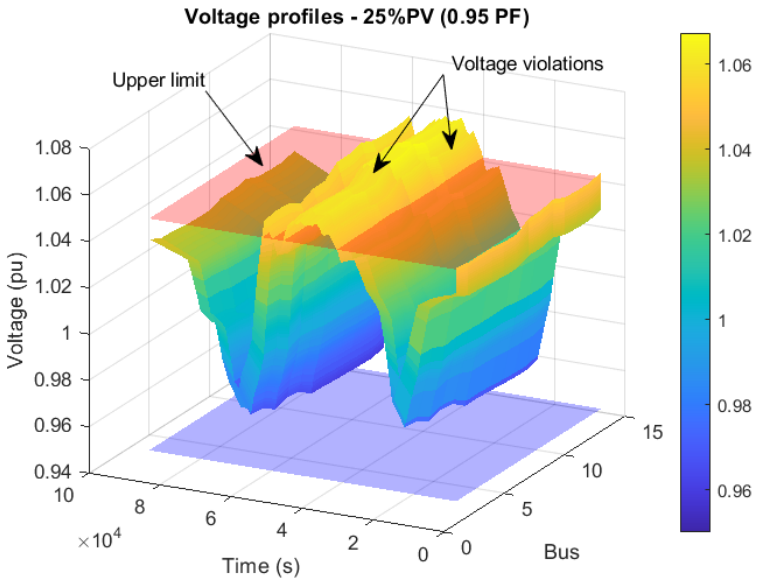

Figure 4.30. Voltage profiles with 25% PV (0.95 PF)

Figures 4.29 and 4.30 show the voltage profile at all the buses with 25% PV penetration at 0.98PF and 0.95PF, respectively. At these settings, the upper limits of all the buses except for the substation bus, have been exceeded.

Figure 4.31 is a summary of the voltage variations at all the buses based on different PF setpoints. The highest voltage variation occurs when the solar PV inverter is set to 0.95PF. This is expected as the biggest amount of reactive power is generated at 0.95PF.

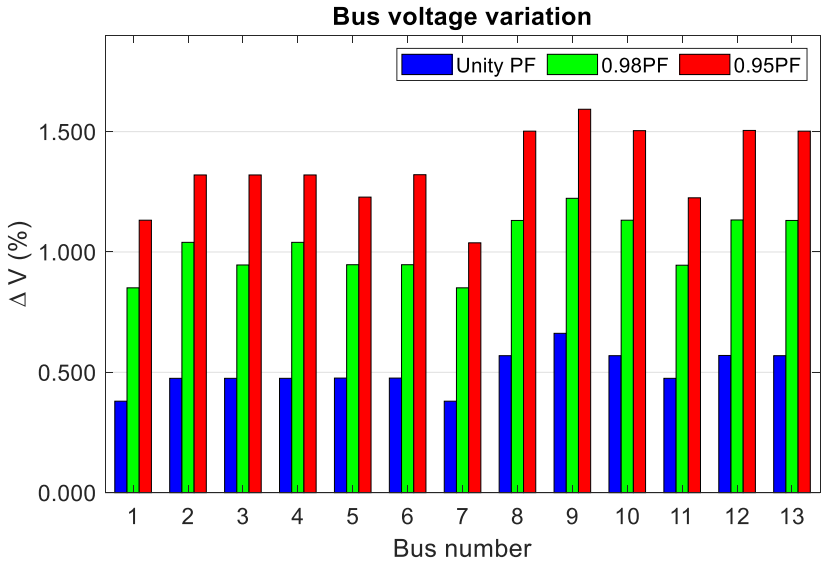

Figure 4.31. Bus voltage variations with 25% PV

For the second scenario, the aggregated solar PV is based on 50% penetration. The power factor of all inverters is set to 0.98 and 0.95, respectively. Figure 4.32 shows the PQ profile of the PV system at bus 4. It is assumed that 50% of residents have installed solar PV on available roof space. The power factor of the inverter is set to 1.0, which produces no reactive power. Reactive power is produced when the inverter power factor is set to 0.98 and 0.95, respectively. The latter is illustrated below.

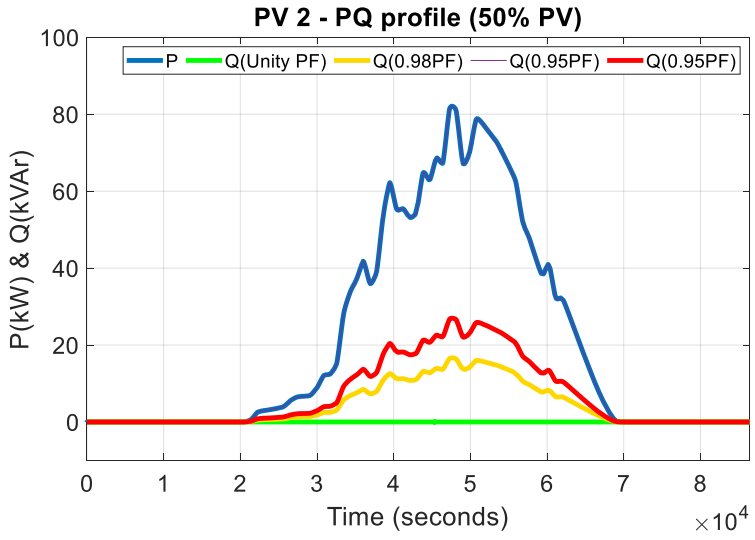

Figure 4.32. PV PQ profile with various PF scenarios

Figure 4.33 and 4.34, show the voltage profiles of all the buses with 50% PV penetration based on 0.98 and 0.95PF, respectively. All the bus voltages in the network have exceeded the upper limit. What is evident is that the voltage profile at the lower limit increased.

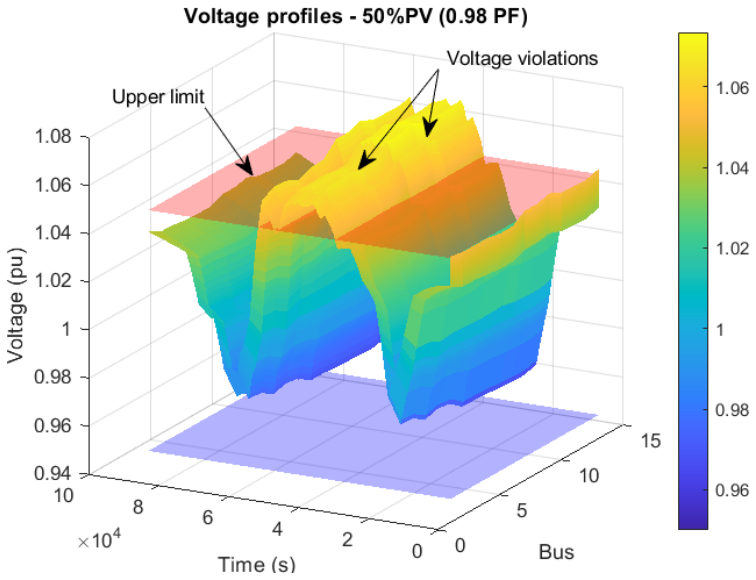

Figure 4.33. Voltage profiles with 50% PV (0.98 PF)

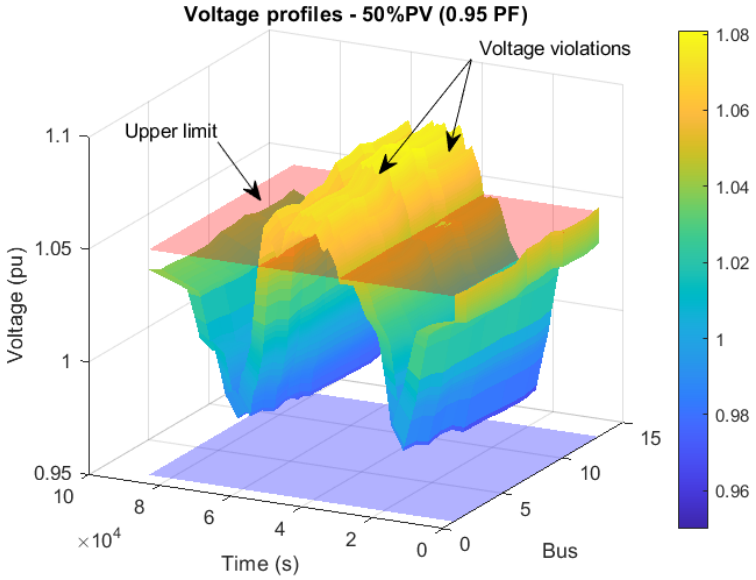

Figure 4.34. Voltage profiles with 50% PV (0.95 PF)

Figure 4.35 shows the comparative voltage profile at the substation with 50% PV penetration. At 0.98PF and 0.95PF, depicted in yellow and red, respectively, the upper limit has been exceeded.

Figure 4.36 provides a summary of the bus voltage variations based on different PF scenarios. As with the previous case, the biggest variation occurs when the PF of inverter is set to 0.95. This causes the voltage during peak hours to rise to 1.08pu. The voltage variation between the baseline and 0.95PF is significant.

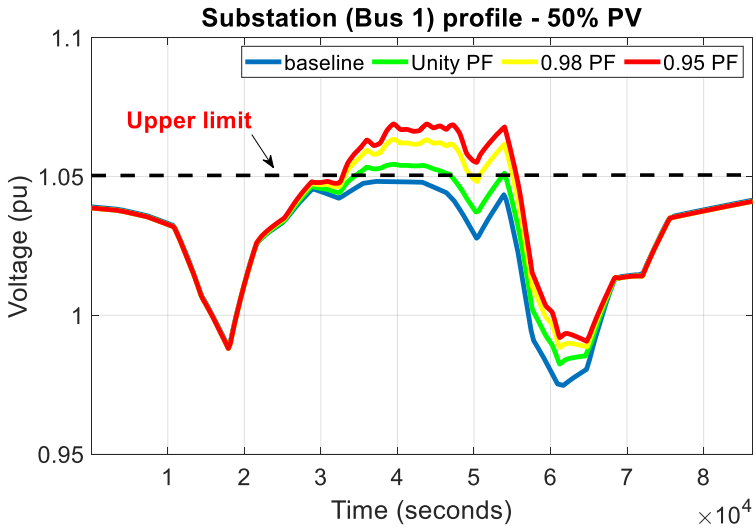

Figure 4.35. Substation profile with 50% PV penetration

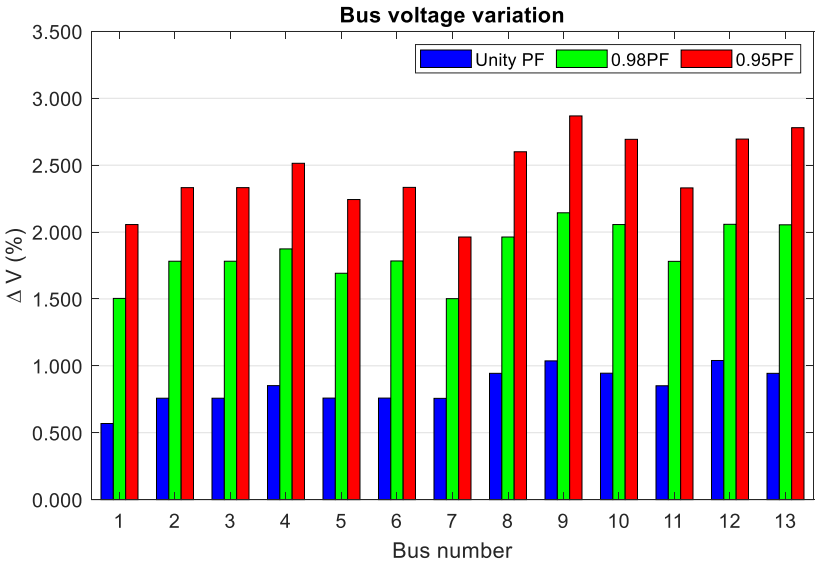

Figure 4.36. Bus voltage variations with 50% PV

- Leading PF control - Active power curtailment is potential solution to mitigate over and undervoltage problems, but this may not be in the best economic interest of the solar PV system owner. The smart inverter has the capability to absorb reactive power, which is a potential solution to voltage control. To absorb reactive power, the constant block in Figure 4.23 is set to -1.0 and the parameter of the solar PV block is set to -0.98 and -0.95, respectively. This setting allows the inverter to absorb reactive power, based on equation (4.4). Figure 4.37 shows active and reactive power generated and absorbed by the solar PV inverter, respectively.

For the scenario below, solar PV penetration is based on 25% but all inverters are set to 0.98PF and 0.95PF leading, respectively. Figure 4.38 shows the PQ profile of the PV system at bus 4.

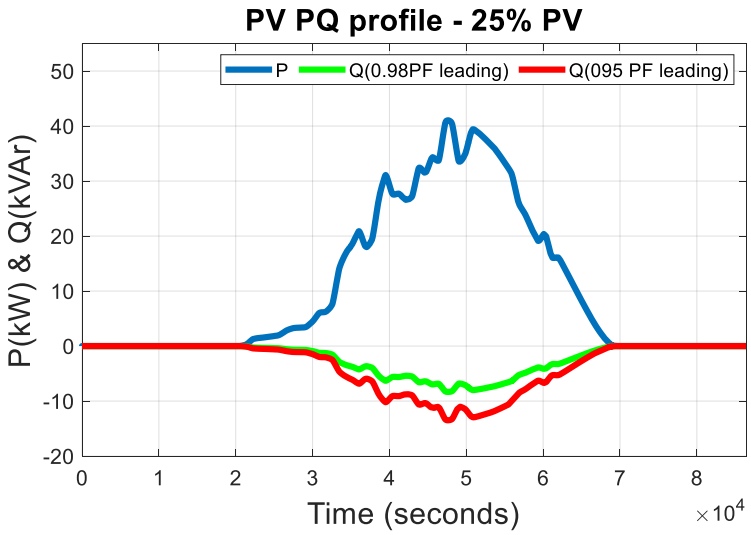

Figure 4.37. PV PQ profile with leading PF

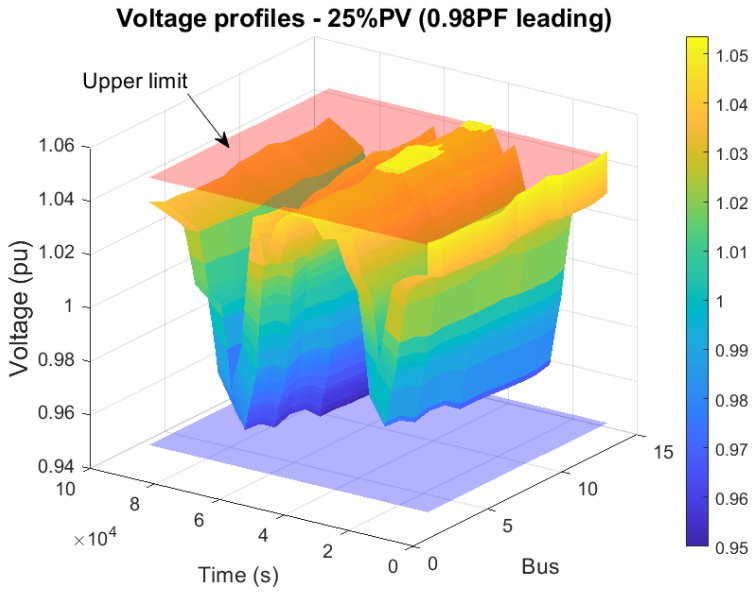

Figure 4.38. Voltage profiles with leading 0.98PF

The voltage profiles in figure 4.38 show an improvement without compromising the active power generation during the peak period. The results for 0.95 leading PF are shown in figure 4.39. All the bus voltages are within the desired upper limit; however, a few buses have exceeded the lower limit.

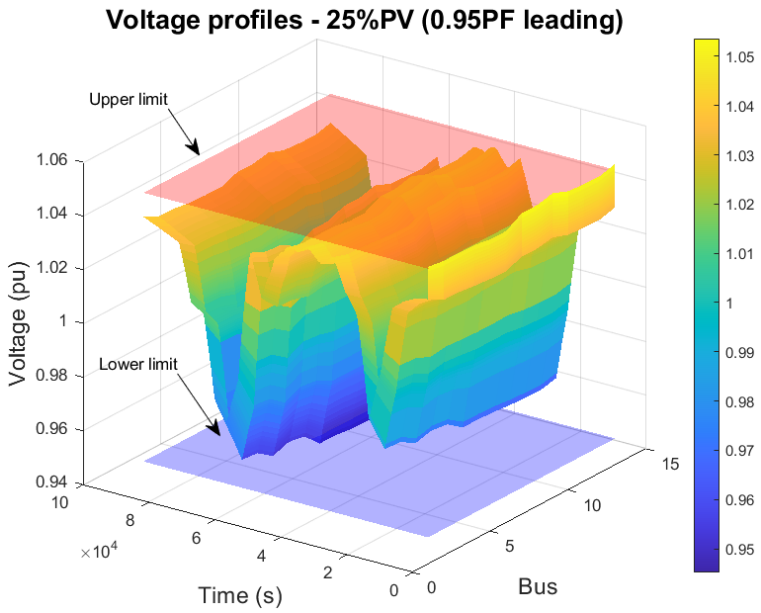

Figure 4.39. Voltage profiles with leading 0.95PF

A comparative analysis of the substation voltage profile is given in figure 4.40. Setting all the inverters to leading power, improves the voltage at the substation bus. Compared to lagging PF, where the voltage exceeded the upper limit, leading power factor, which absorbs reactive power, improves the voltage profile during the peak generation period.

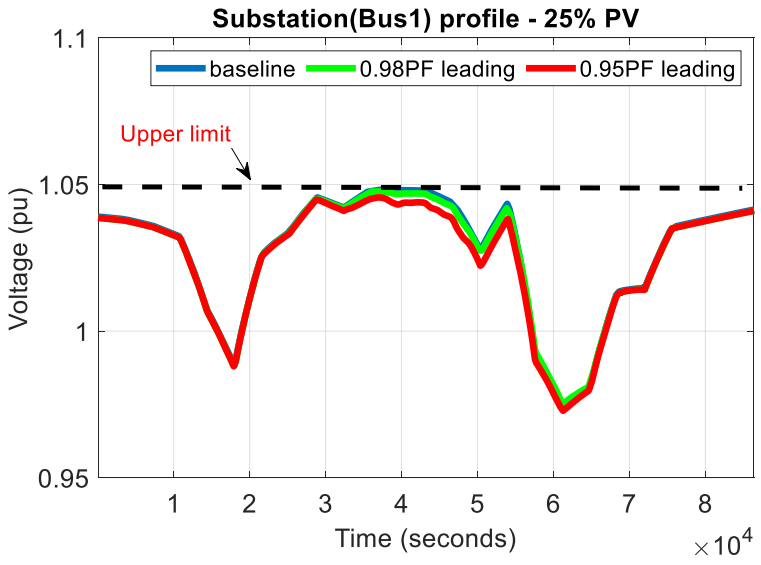

Figure 4.40. PV PQ profile with leading PF

A summary of the bus voltage variations based on different lagging and leading PF scenarios is given in figure 4.41. The biggest variation occurs when the PF of the inverter is set to 0.95 lagging PF. Leading PF is depicted in yellow and red shows a negative value, which results in an improvement in the voltage profile.

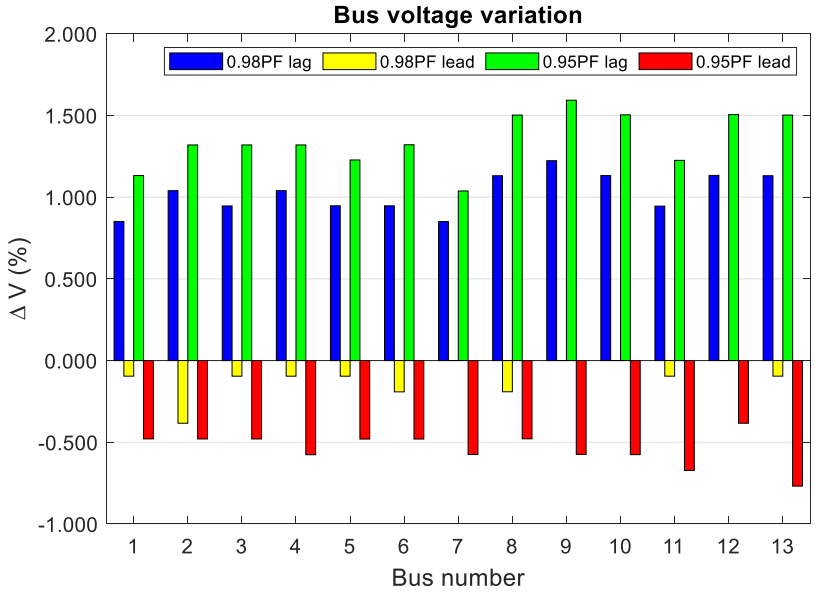

Figure 4.41. Voltage variation with 25% PV

For the fourth scenario, solar PV penetration is based on 50% but all inverters are set to 0.98PF and 0.95PF leading, respectively. Figure 4.42 shows the PQ profile of the PV system at bus 4 with 50% PV penetration.

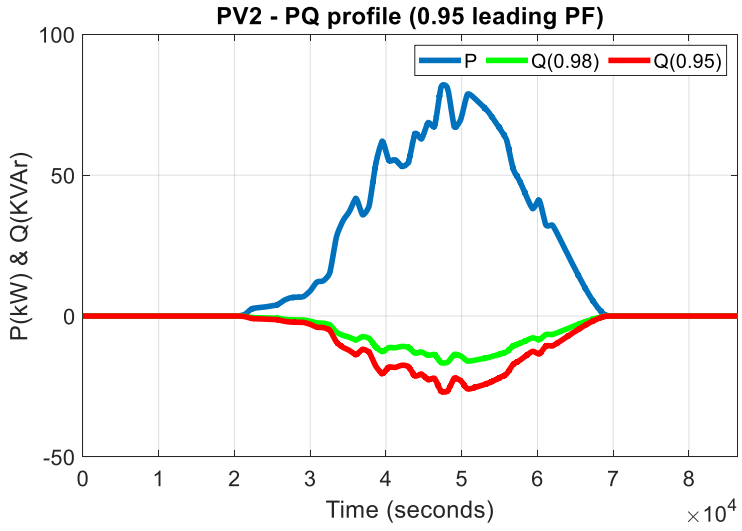

Figure 4.42. 50% PV PQ profile with fixed PF

Figure 4.43 show the voltage profiles when the inverters are set to 0.98 leading PF. The voltage profile at the upper and lower limit at all the buses show an improvement. When the inverters are set to 0.95 leading PF, the upper limit shows an improvement but the lower limit at some buses have been exceeded.

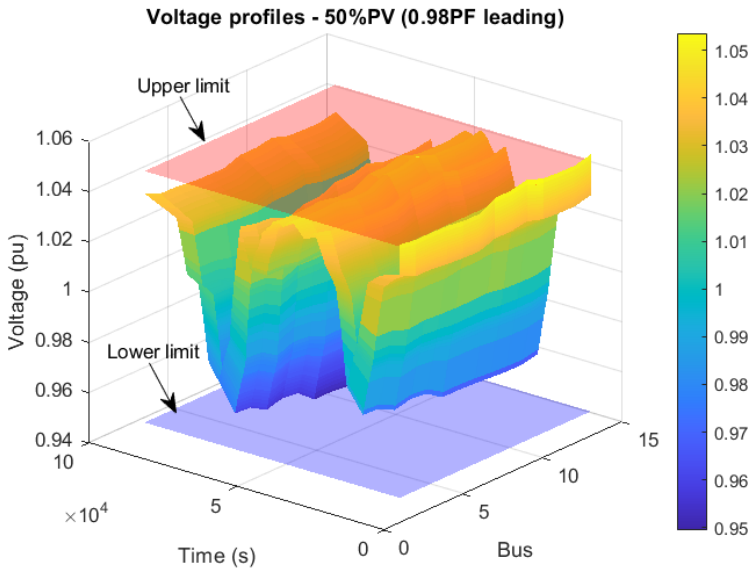

Figure 4.43. Voltage profile with 0.98 leading PF

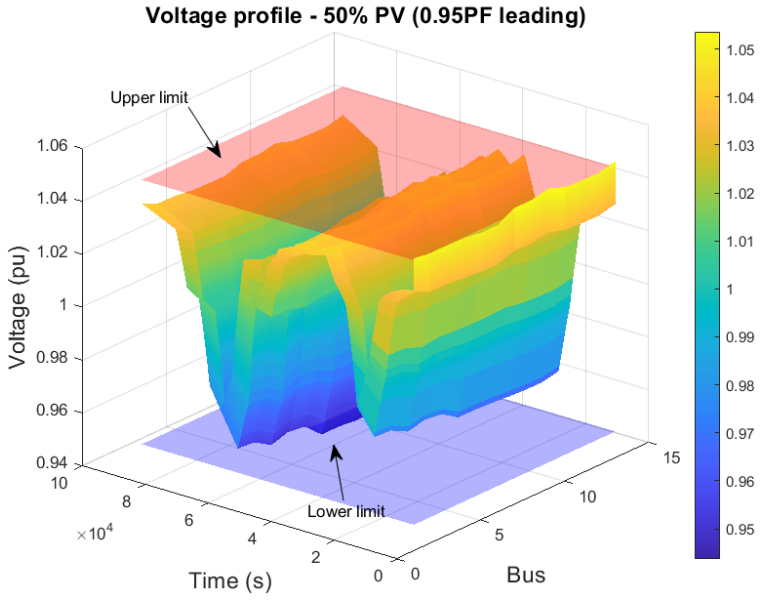

Figure 4.44. Voltage profile with 0.95 leading PF

Figure 4.44 shows the bus voltage variation based on 50% PV penetration at lagging and leading PF. As with the previous scenarios, 0.95 lagging PF shows the greatest variation. A summary of the bus voltage variations based on different lagging and leading PF scenarios is given in figure 4.45. The biggest variation occurs when the PF of the inverter is set to 0.95 lagging.

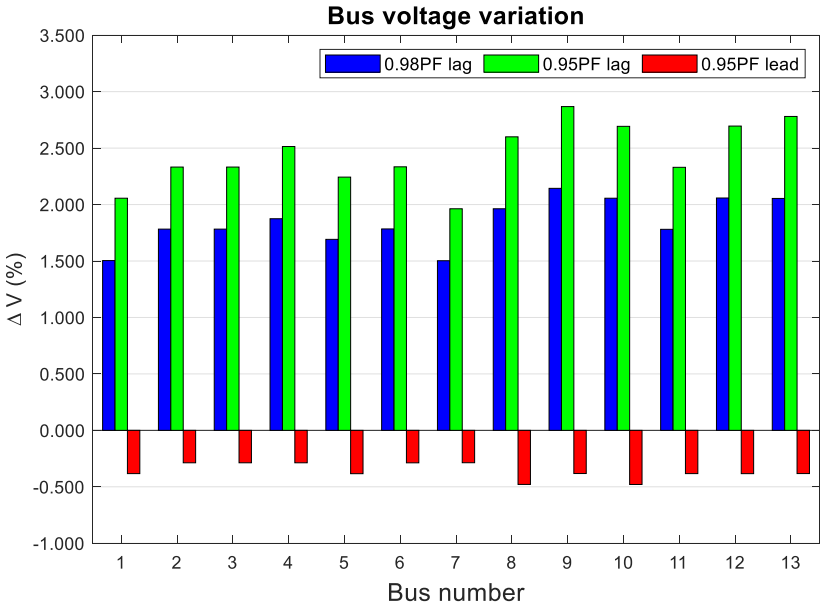

Figure 4.45. Voltage variation with 50% PV

- **Scheduled Power Factor** - DER inverter power factor is scheduled during the active power generation period based on forecasted demand. The power factor is scheduled to regulate the voltage at the substation and or local bus. The regulation is achieved by switching the inverter PF controller on or off at specific times based on the required voltage regulation. Figure 4.46 shows the profile when reactive power is absorbed for a specific time during the day.

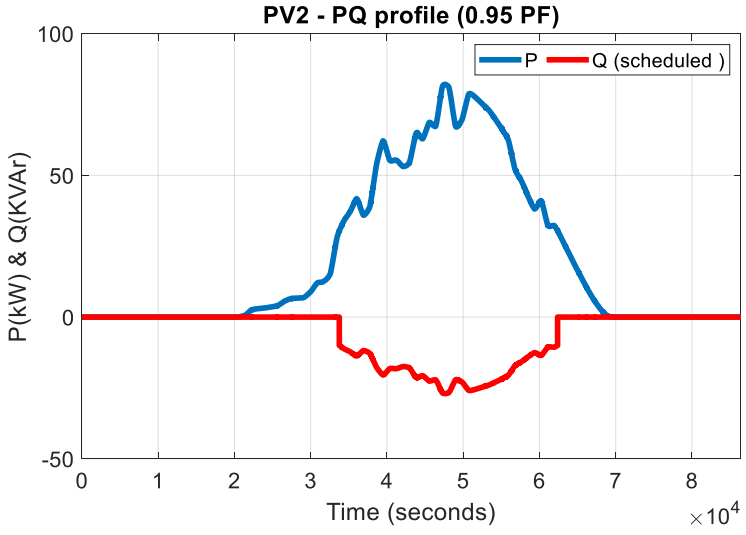

Figure 4.46. Scheduled power factor profile.

Figure 4.47 show the results of 0.98 scheduled PF. The voltage at the lower limit shows an improvement, but the voltage during peak production is still exceeding the upper limit. For the next scenario, the power factor is adjusted to 0.95 to determine the effect

on the bus profiles. Figure 4.48 show an improvement in the lower and upper voltage profiles. The voltage is within the statutory limits.

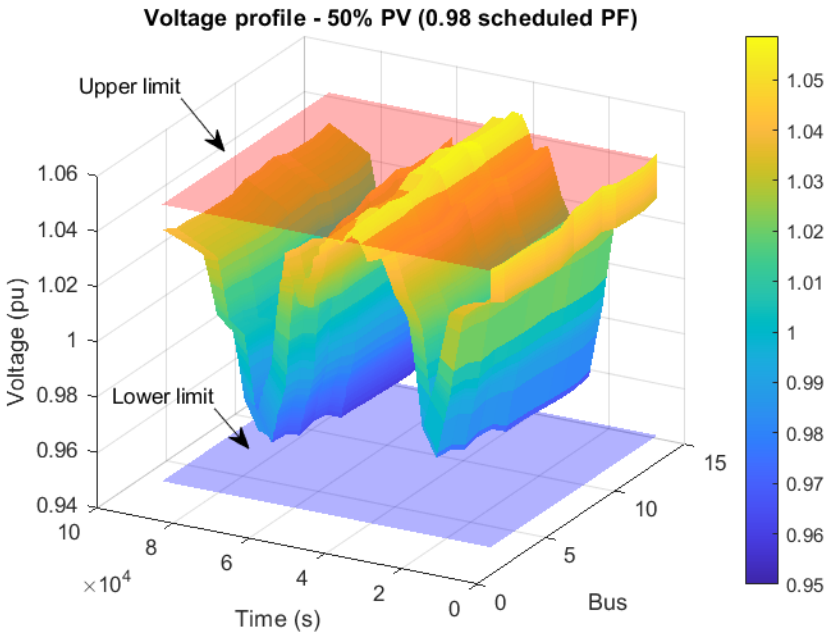

Figure 4.47. Voltage profile with 0.98 leading scheduled PF

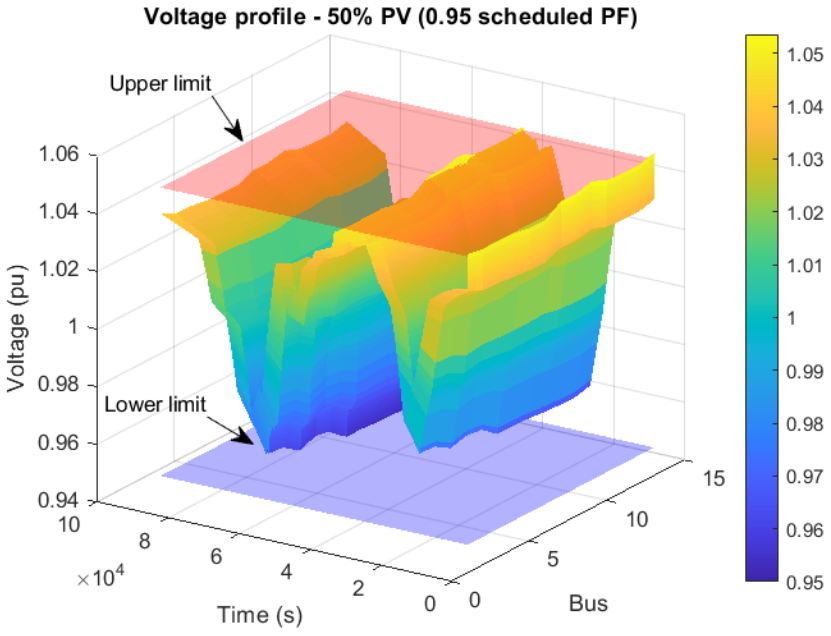

Figure 4.48. Voltage profile with 0.95 leading scheduled PF

4.5.2.2 Wind Energy PF control

According to the grid connection code of South Africa, DER with an apparent power capacity between 100kVA and 1MVA is restricted to PF control. For the latter, control is restricted between 0.95 lagging and 0.95 leading PF. The simulation is based on 2 scenarios i.e., 25% and 50% but restricted to the PF control guidelines as published in the grid connection code of South Africa. The study is based on (i) constant and (ii) scheduled PF.

Table 4.9 shows the sizes of the wind system connected at bus 13.

Table 4.9. Aggregated Wind Energy

Bus connection	**Load Size**	**Aggregated Wind Energy (kW)**	
	kW	25%	50%
13	2000	500	1000

- Constant (lagging) PF – DER inverter is set to 0.98 and 0.95 lagging PF, respectively. Figure 4.49 shows the PQ profile of the wind system connected at bus 13. For the first case, wind penetration amounts to 25% of the active load. The peak wind generation coincides with the peak load profile in the evening. The reactive power generated is proportional to the active power generated.

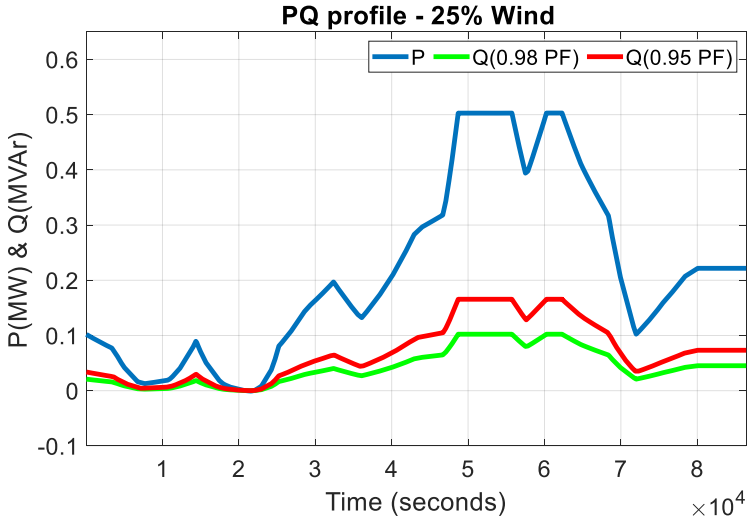

Figure 4.49. 25% Wind PQ profile with lagging PF

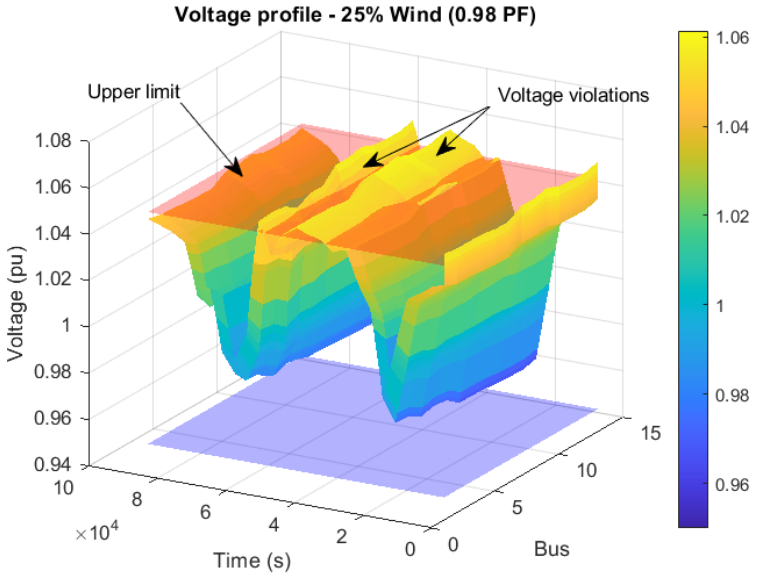

Figure 4.50. Voltage profile - 0.98 lagging PF (25% Wind)

Figure 4.50 and 4.51 show the bus profiles based on 25% wind penetration with lagging PF. Compared to the baseline, all the bus voltages exceeded the upper limit. The peak generation during the early evening hours raised the voltages at all the buses. Figure 4.52 shows the voltage profile at the substation bus, which illustrates the latter.

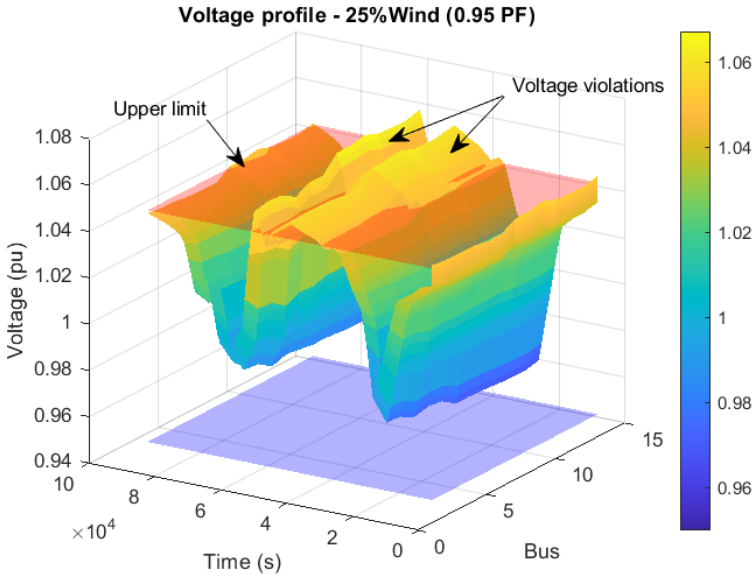

Figure 4.51. Voltage profile - 0.95 leading PF (25% Wind)

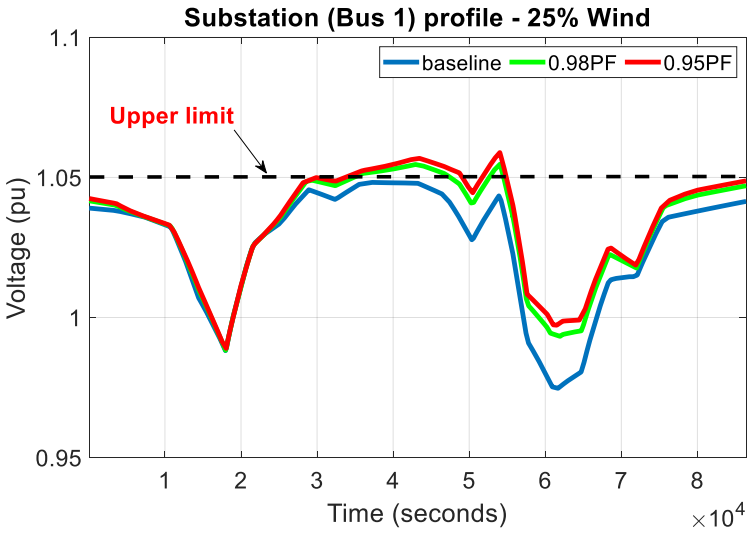

Figure 4.52. Substation bus profile with 25% Wind

For the second scenario, the wind system is increased to 50% of the feeder's active power. The PQ profile in figure 4.53 shows the active power and reactive power generated based on 2 PF scenarios.

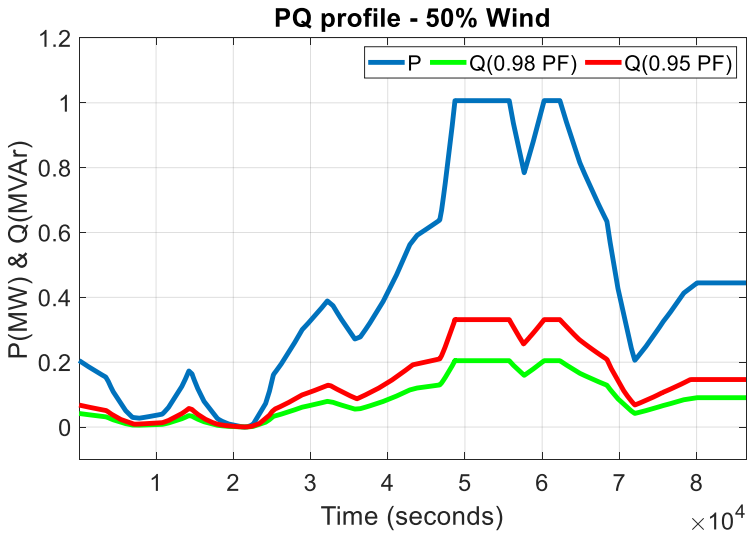

Figure 4.53. 50% PV PQ profile with various PF scenarios

A summary of the voltage profiles based on 50% wind energy with lagging PF is given in figure 4.54 and 4.55. What is evident is the major improvement in bus profiles during the peak wind generation period. What is striking is the impact on the profile during the middle of the day. Even at 0.98 lagging PF, all the bus voltages exceeded the upper limit.

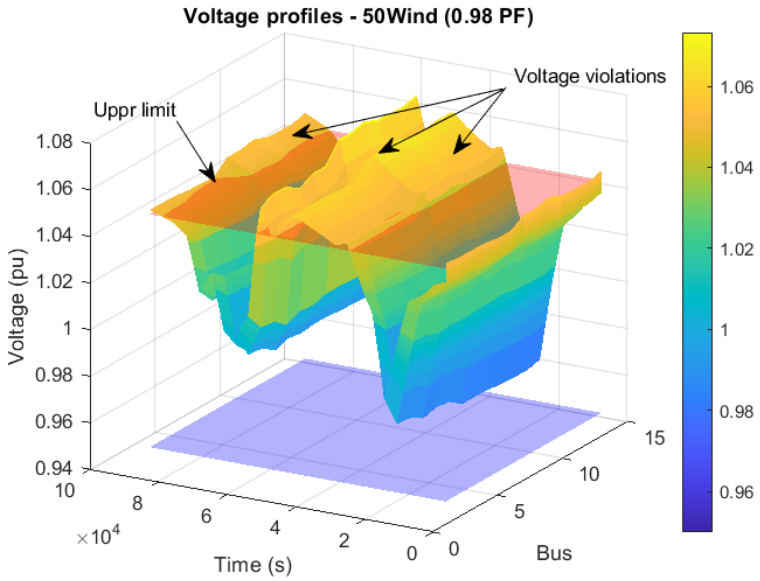

Figure 4.54. Voltage profile - 0.98 lagging PF (50% Wind)

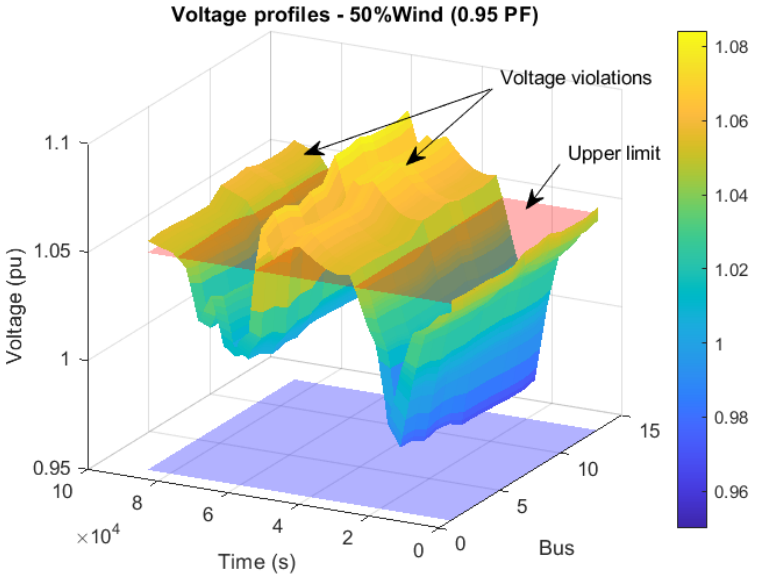

Figure 4.55. Voltage profile with 0.95 lagging PF (50% Wind)

- Constant (leading) PF – DER inverter is set to 0.98 and 0.95 leading PF, respectively. Figures 4.56 and 4.57 show the wind system PQ profile at bus 13, with 25% and 50% leading PF, respectively. Reactive power is being absorbed during the peak wind production hours.

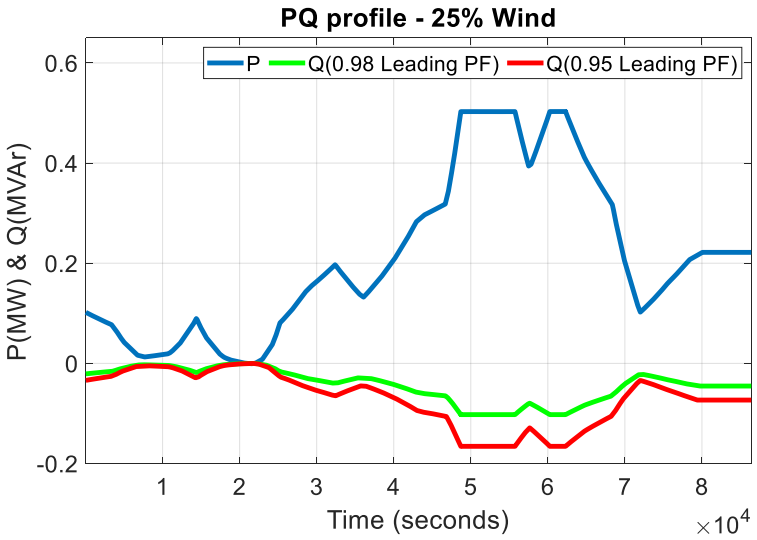

Figure 4.56. 25% Wind PQ profile with leading PF

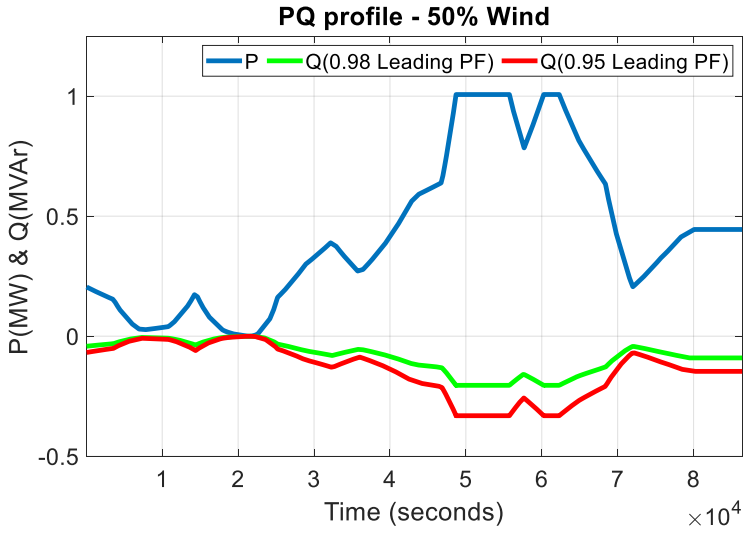

Figure 4.57. 50% Wind PQ profile with leading PF

The effect of reactive power absorption based on the specific wind pattern on the bus voltage is shown in Figures 4.58 and 4.59. The profile at the upper limit for both scenarios have been improved but the lower limit at some buses has been exceeded. A potential solution to address this problem is to inject reactive power when off peak and absorb reactive power during the peak loads. As with solar PV, Wind energy power factor can be scheduled to coincide with the fluctuating load demand.

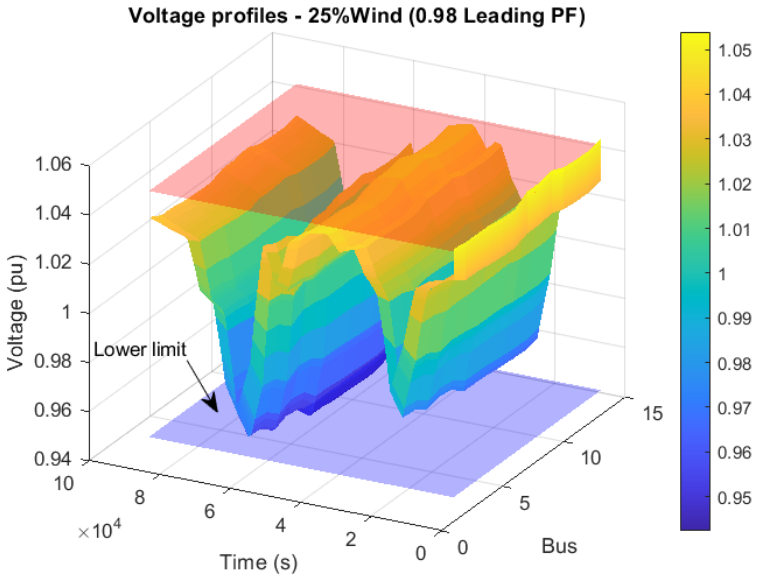

Figure 4.58. Voltage profile - 0.98 leading PF (25% Wind)

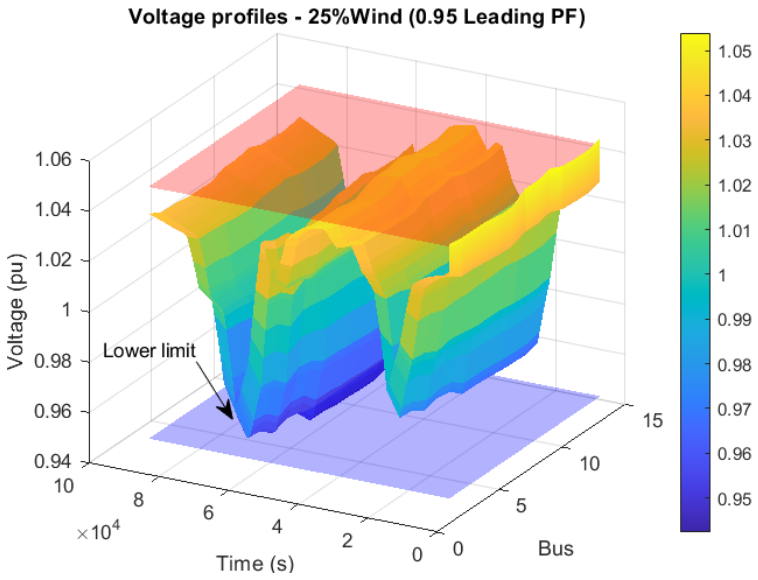

Figure 4.59. Voltage profile - 0.95 leading PF (25% Wind)

- Scheduled leading PF – to mitigate the shortcomings of fixed leading power factor, especially with Wind Energy, the PF is scheduled over the 24hour period. Wind energy, like solar PV has the disadvantage of being intermittent. This subsection presents the impact of scheduling PF on voltages profiles at the substation and various other buses in the network. The first study will be limited to 25% and 50% penetration based on 0.98 and 0.95PF, respectively.

Figure 4.60 shows the PQ profile of the Wind system based on 25% penetration. The reactive power is injection during the morning when the first part of the peak load is experienced. During the afternoon, the wind reached its maximum speed, which produces the peak energy. Currently, only a part of the maximum reactive power is injected to prevent the voltage falling below its minimum level. Figure 4.61 and 4.62 show the impact of scheduling the PF on the voltage profiles. Both scenarios show an improvement in the upper and lower boundaries.

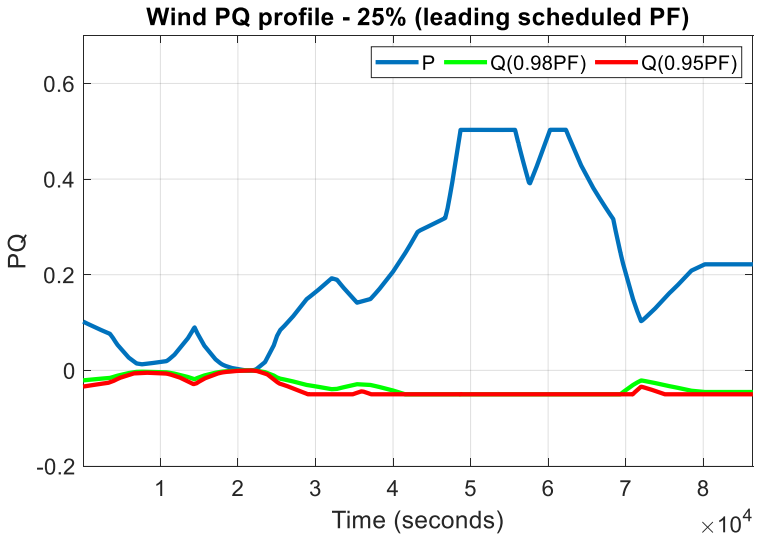

Figure 4.60. Wind PQ profile - 0.95 scheduled PF

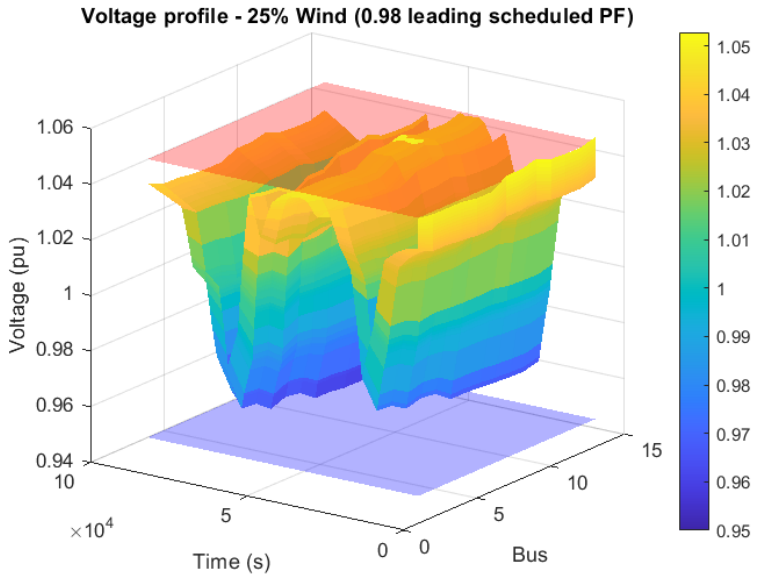

Figure 4.61. 25% Wind PQ profile - 0.98 scheduled PF

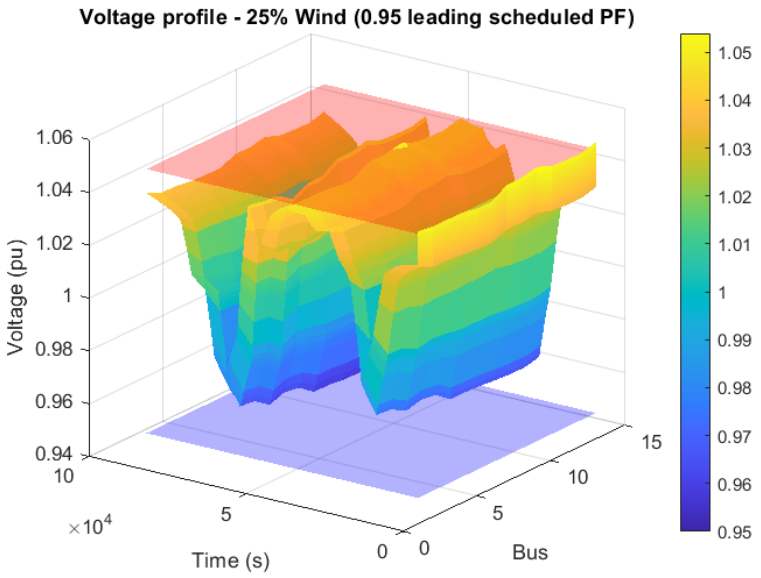

Figure 4.62. 25% Wind PQ profile - 0.95 scheduled PF

For the last scenario, the Wind system is increased to 50% of the active power. Figure 4.63 shows the PQ profile based on 50% penetration. As with the previous scenario only 0.98 and 0.95PF will be considered, which is based on the grid connection code of South Africa for connection of DER.

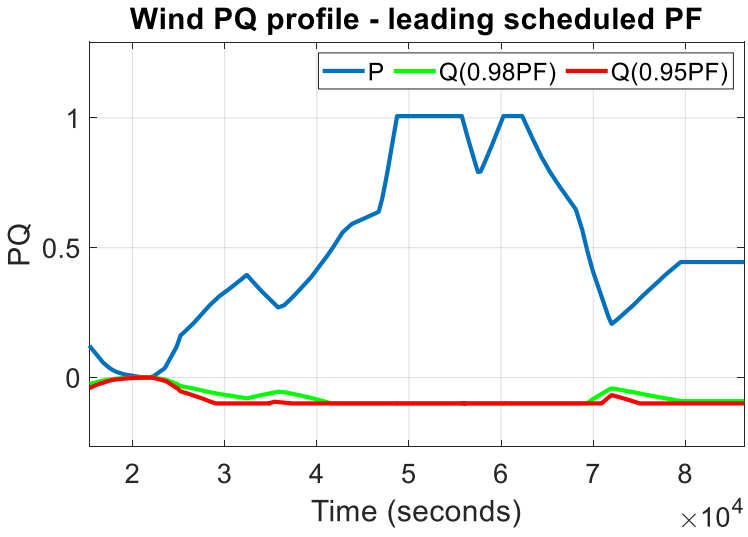

Figure 4.63. Wind PQ profile - 0.95 scheduled PF

The results given in figures 4.64 and 4.65 show an improvement in the lower limit.

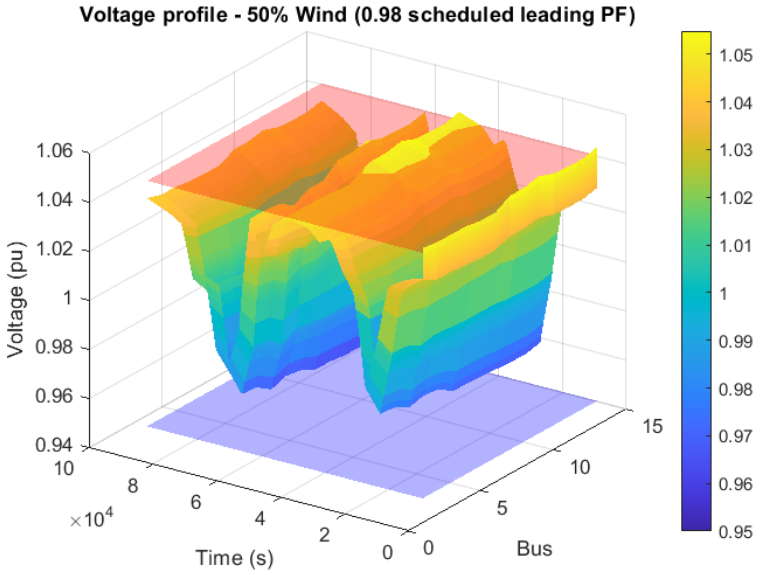

Figure 4.64. Wind PQ profile - 0.98 scheduled PF

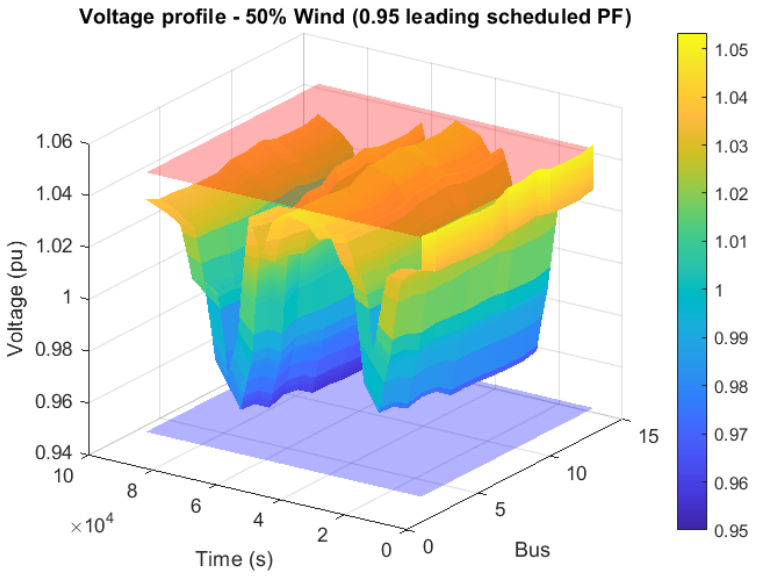

Figure 4.65. Wind PQ profile - 0.95 scheduled PF

4.5.2.3 On-load Tap changer control with DER

Simulation results with conventional control without DER was given in section 4.4.1. The results below show the impact of inverter-based DER on the substation voltage regulating device. The study is limited to 50% solar PV and Wind energy only with additional limitation to 0.95 leading and lagging PF.

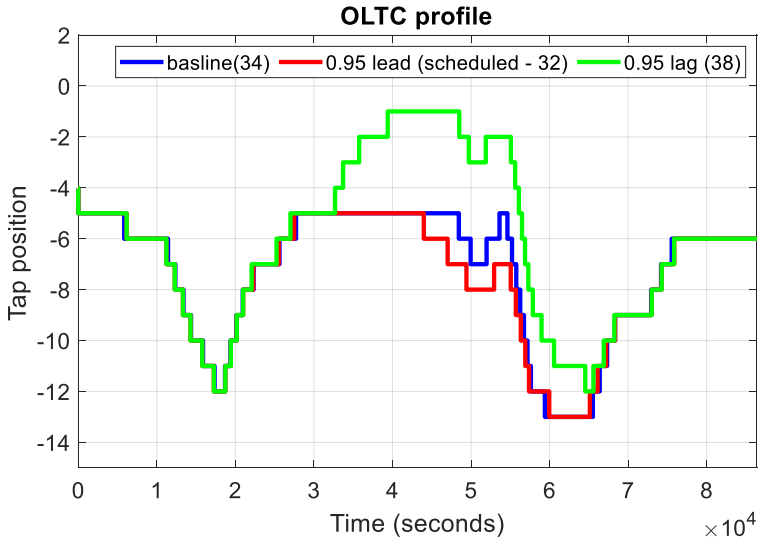

Figure 4.66. OLTC profile – solar PV

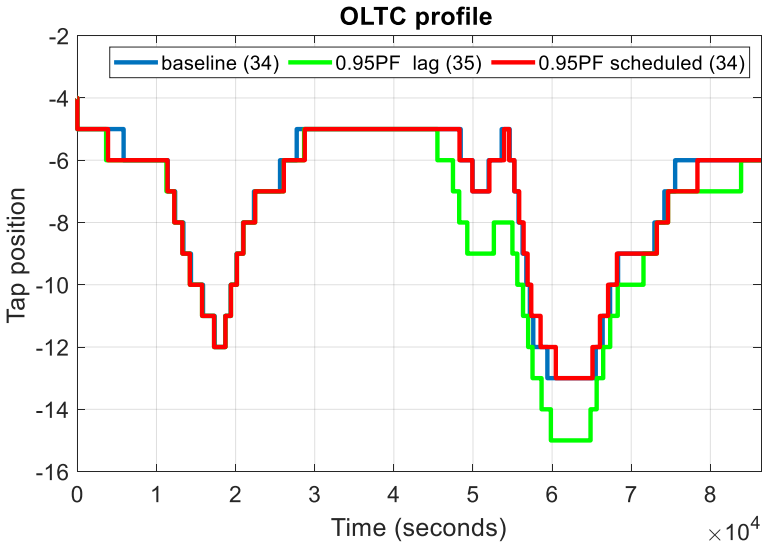

Figure 4.67. OLTC profile – Wind Energy

Figure 4.66 shows the baseline profile compared to the scenarios 0.95 lagging and scheduled PF. The scenario is based 50% PV and shows a decrease in the OLTC tap switching. Based on table 4.10 a 10.5% improvement can be seen. Figure 4.67 shows the OLTC with 50% Wind penetration. No improvement in the tap switching can be seen compared to the baseline.

Table 4.10. Effect on OLTC taps

	Number of tap changes			% Variation	
	Baseline	0.95 PF lagging	0.95 scheduled leading	0.95PF lagging	0.95 scheduled leading
50% PV	34	38	32	10.5	-6.25
50% Wind	34	35	34	2.8	0

4.6 Summary

In this chapter, a test feeder for an off-line simulation platform was developed. MATLAB® was selected to perform the power simulation based on its wide of application in the engineering and academic fields. Phasor models for the loads, solar PV and Wind energy was developed. The phasor solution with a variable step solver was selected as the study were concerned with the changes in current and voltage magnitudes only. For the first part of the simulation, the impact on the substation and other bus voltage profiles were examined based on conventional reactive power controlling devices. The results showed that voltage control can be achieved by OLTC transformers and shunt capacitors at the substation thereby regulating the voltage at a central point. Feeder-level control can be achieved by shunt capacitors and step voltage regulators on long distribution lines. The disadvantage of these devices is their slow response time to load fluctuations. In the second part of the simulation, the impact of inverter-based DER was used to control the voltage at the substation and local buses. The study was limited to PF control. The results show that DER cause the feeder voltage to rise during peak generation. It showed that PF control can be used to inject or absorb reactive power thereby controlling the voltage within the network. The final part showed that by controlling the PF, the number of taps of the substation OLTC transformers can be reduced.

CHAPTER FIVE
DEVELOPMENT OF A REAL-TIME SIMULATION PLATFORM FOR VOLTAGE CONTROL

5.1 Introduction

In this chapter, the development of a simulation platform to perform real-time testing is described. Firstly, a test feeder is developed, which is based on IEEE 37-bus test feeder. The test feeder is modified to include five static loads and a residential-sized solar PV system at one selected bus. Only a specific part of the network is developed and simulated based on the limitations of the real-time target. Secondly, the software and hardware are selected to perform real-time simulation. Thirdly, the test feeder, which includes the solar PV array is described. The PV array, which includes the design of a typical 6.5kW residential system is modelled using the selected software. Lastly, the results are presented.

5.2 Test feeder description

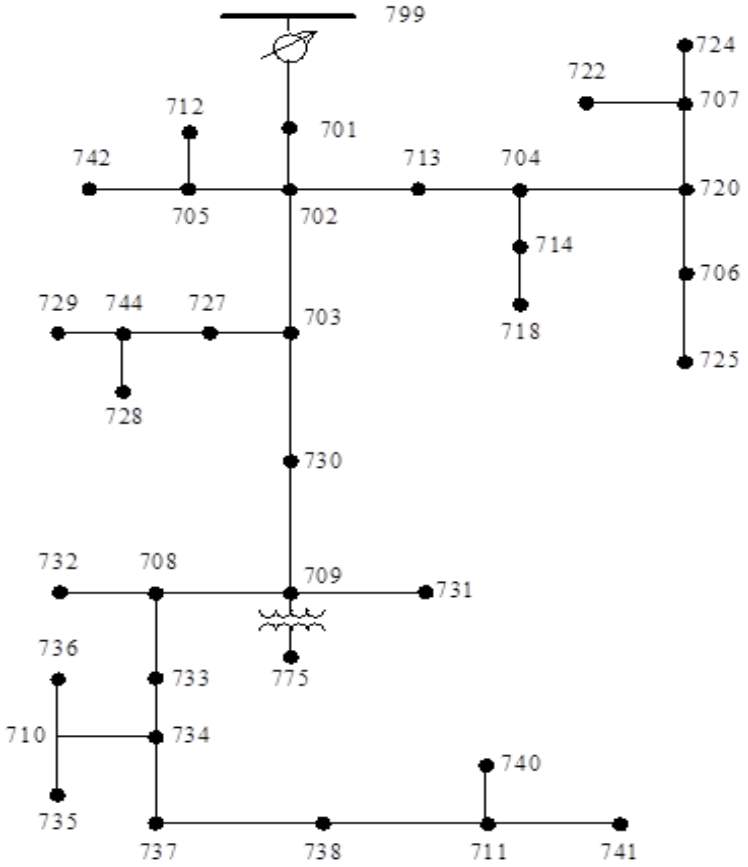

Figure 5.1. IEEE 37-bus test feeder

The selected network is based on IEEE 37 bus test feeder, which is a delta configured feeder with an operating voltage of 4.8 kV. It is characterized by an underground delta configuration. Figure 5.1 is an illustration of the model. The detailed parameters are summarized in Appendix B.

The feeder is characterized by:

i. Three-phase Δ→ Δ 230/4.8 kV substation transformer and one Δ → Δ in-line 4.8/0.480 kV transformer.
ii. Spot loads, consisting of constant PQ, constant I and constant Z-type delta configuration. The load at bus 742 has been changed to 400kW.
iii. Converted, balanced three phase loads.

5.3 Modelling and simulation of the feeder

5.3.1 Balanced and unbalanced loads

The standard three phase dynamic load model block in Simulink® library is used to model the dynamic load. The load block has an external control PQ control function, which allows the load to be controlled by feeding P & Q data, which is driven by 1-D lookup tables.

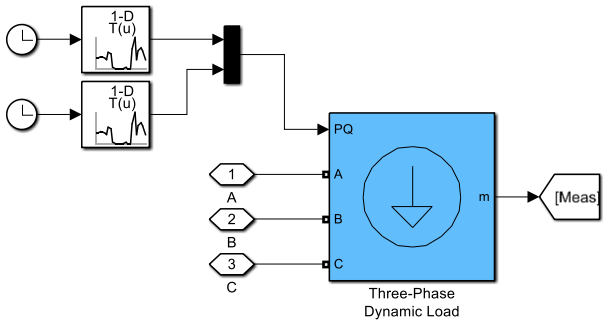

Figure 5.2. Three phase load model

The dynamic load can be modelled as constant PQ, I, or Z. The load varies based on (i) positive-sequence voltage input or (ii) an external control, which affects active power (P) and reactive power (Q). The active power (P) and reactive power (Q), which can be externally controlled, is given by the following equations:

$$P = Po\left(\frac{V}{V_o}\right)^{np} \tag{6.1}$$

$$Q = Qo\left(\frac{V}{V_o}\right)^{nq} \tag{6.2}$$

where:

V_0	= initial positive sequence voltage.
P_0 and Q_o	= initial active and reactive powers at the initial voltage V_o.
V	= positive-sequence voltage.
n_p and n_q	= exponents, which determines the nature of the load. By selecting 0,1 or 2, constant PQ, I or Z load can be obtained, respectively.

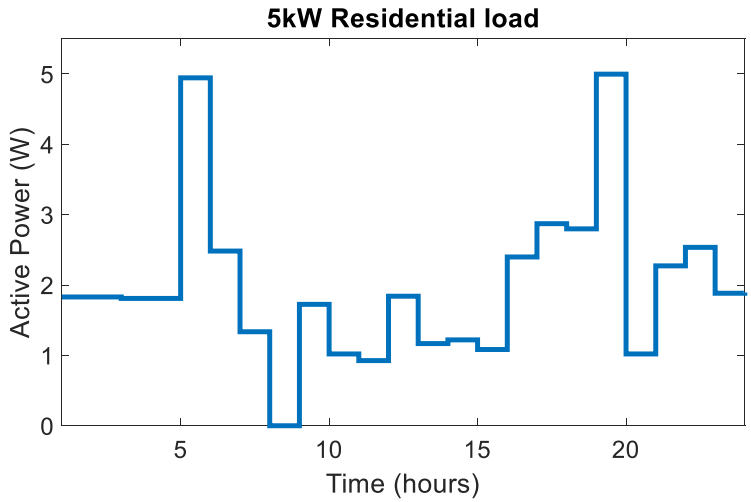

Figure 5.3. 5kW Residential load profile

5.3.2 Solar PV system (two stage power conversion)

A review of the voltage control methods using inverter-based DER was done in chapter 3. The primary control functions for a DER unit are (i) voltage and frequency and (ii) and/or active/reactive power control. For voltage control at the point of common coupling (PCC), a voltage-sourced converter (VSC) is used for a current-controlled strategy. The VSC uses a “d” and “q” reference controller. For VQ and PQ control, a reactive and active power controller is used to supply a reference signal to the VSC. No reactive power will be generated if the reactive power reference $Q(ref)$ is set to zero. The following is a detailed description of the solar PV system, which consists of several 6.5kW systems.

- Single diode PV cell (equivalent model) – SunPower’s SPR-E20-327-BLK PV panel, which consists of 96 Monocrystalline Maxeon Gen II solar cells is selected based on its efficiency. Figure 5.4 shows the equivalent single diode model, which consists of a

current source driven by the sunlight in parallel with a diode, a shunt, and series resistor.

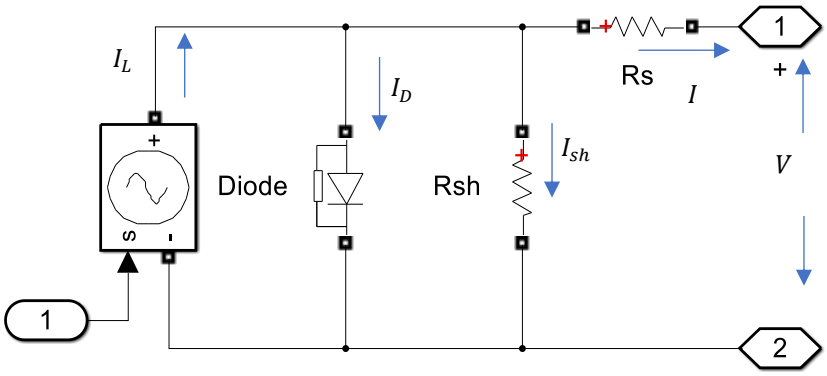

Figure 5.4. Equivalent PV module

Applying Kirchhoff's current law,

$$I = I_L - I_D - I_{sh} \tag{6.3}$$

$$I_D = I_o \left[exp\left(\frac{V + IR_s}{nV_T}\right) - 1 \right] \tag{6.4}$$

$$V_T = \frac{kT_c}{q} \tag{6.5}$$

$$I_{sh} = (V + IR_s)/R_{sh} \tag{6.6}$$

The single diode model is given by the following equation.

$$I = I_L - I_o \left[esp\left(\frac{V - IR_s}{nV_T}\right) - 1 \right] - \frac{V + IR_s}{R_{sh}} \tag{6.7}$$

where:

I_L = $Light\ current\ (A)$
I_o = $Diode\ reverse\ saturation\ current\ (A)$
I_D = $Voltage\ dependent\ current\ loss\ (A)$
R_s = $Series\ ressitance\ (\Omega)$
R_{sh} = $Shunt\ resistance\ (\Omega)$
n = $Diode\ ideality\ factor$
V_T = $Termal\ voltage\ (V)$
n = $Diode\ ideality\ factor$

k = $Boltzmann\ constant$

q = $Elementary\ charge$

- PV array – The combined neighbourhood load is 200kW, which consists of 40, 5kW residential loads. The rooftop PV system is sized at 5kW to match the load shown in Figure 5.3. The PV array is sized roughly 30% greater than the inverter, which is 6.5kW and 5kW, respectively. The data for the PV array in table 5.1 is based on SunPower's SPR-E20-327-BLK module. The voltage and current at maximum power point is 54.7V and 5.98A, respectively. The input variables to the PV module are irradiance and ambient temperature and is defined as a scalar in W/m^2 and °C (negative or positive value), respectively. The array in figure 5.5 consists of 10 series connected strings of modules with 2 strings connected in parallel. The Signal Builder block is used to create a non-linear signal, which defines the irradiance and temperature output waveforms. Figure 5.6 shows the power vs voltage (P-V) characteristic curve, which illustrates the maximum power point (MPP) of the simulated model.

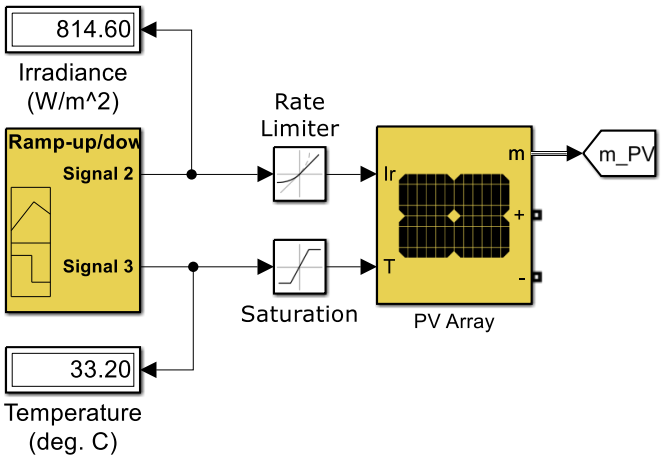

Figure 5.5. PV array model in Simulink® library

Table 5.1 – PV module data

Description	Data
Maximum Power (W)	327
Cells/module	96
Voltage at maximum power point Vmp (V)	54.7
Current at maximum power point (A)	5.98
Temperature coefficient at V_{oc} (%/°C)	-0.25
Temperature coefficient at I_{oc} (%/°C)	0.04

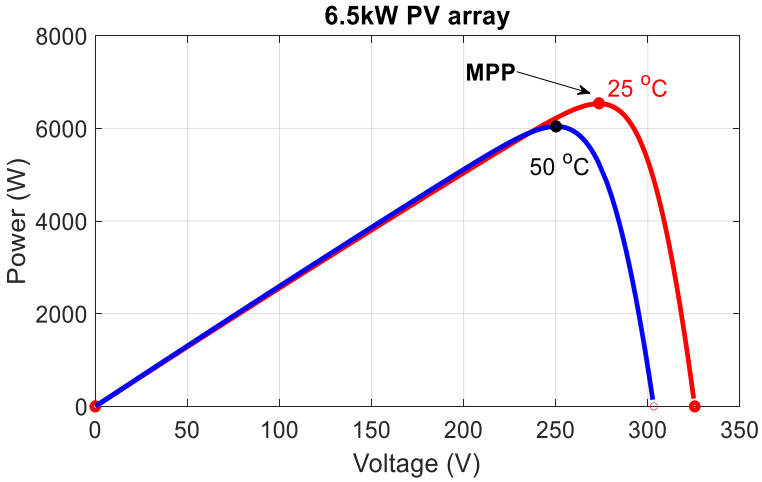

Figure 5.6. *P–V* characteristic of a 6.5kW PV array

The performance of PV cells is affected by (i) irradiance and (ii) ambient temperature. An increase in temperature reduces the performance of the PV cells. (Dubey, Sarvaiya & Seshadri, 2013). The maximum efficiency will be reached at or just below an irradiance level of 1000 W/m^2, which will lead to an increase in current and power output. The effect of variable ambient temperature on output power and voltage is illustrated in figures 5.7 and 5.8.

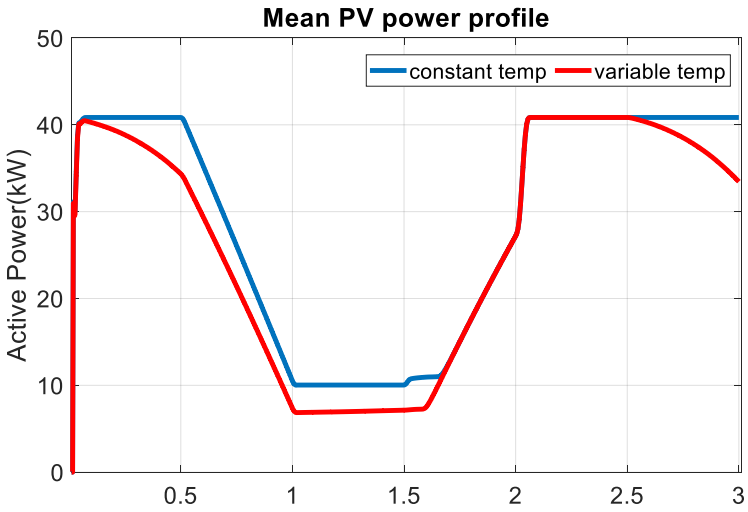

Figure 5.7. Effect of temperature of PV power profile

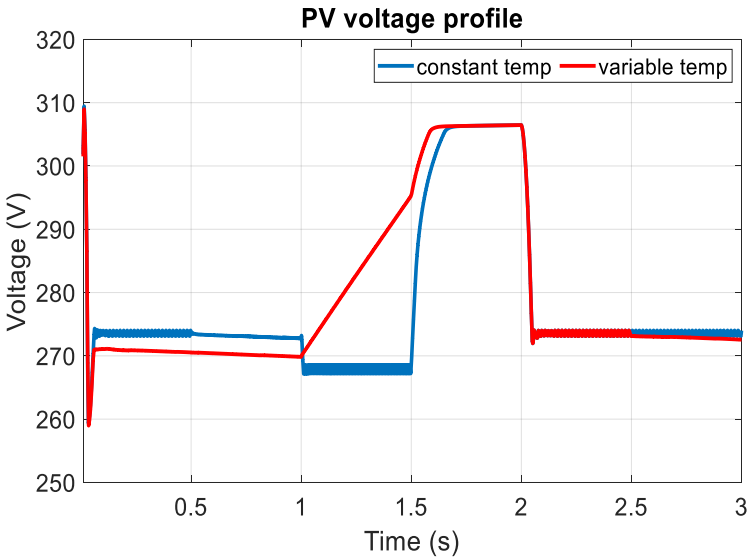

Figure 5.8. Effect of temperature of PV voltage profile

- DC-DC boost converter with Perturb and Observing (P&O) MPPT control algorithm – Sunpower's SPR-E20-327 module has a maximum power point voltage of 54.78V as per table 5.1. In this study, the PV modules are assembled in series–parallel combinations to increase the voltage rating to 273.5V. A DC-DC boost converter, which consists of capacitors, inductors, IGBTs, and diodes is used to increase this voltage to 500V.

  The converter incorporates a maximum power point tracking (MPPT), which maximizes the power generated by the PV system by adjusting the peak power of the PV panel as shown on the curve in Figure 5.6. For this system, a P&O control algorithm is implemented to achieve the latter. The P&O algorithm, which is the simplest method, is based on the observation of the array output power and the perturbation (increment or decrement) of the power based on increments of the voltage or current as illustrated in Figure 5.9. The output power of the solar module changes based on the change in solar insolation level and the atmospheric temperature. These input variables are factored into the algorithm to ensure maximum power generation.

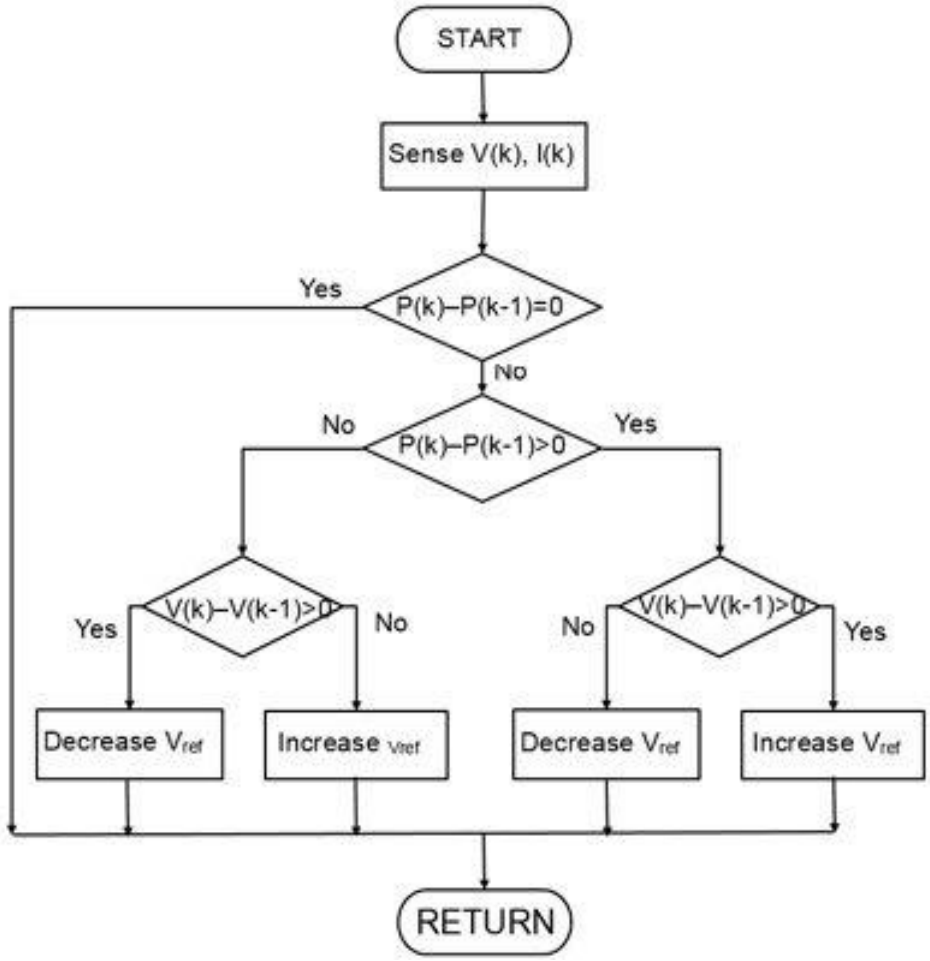

Figure 5.9. Perturb and Observing MPPT control algorithm flowchart

The step-by-step calculation of the converter input parameters are given below and summarized in table 5.2.

$$V_o = V_{bus\_ref} = 500V \tag{6.8}$$

$$V_{in} = V_{mpp} = 273.5V \tag{6.9}$$

$$D = 1 - \frac{V_{in}}{V_o} \tag{6.10}$$

$$D = 1 - \frac{273.5}{500}$$

$$D = 0.453$$

$$Lb = \frac{(1-D)^2 x\ D\ x\ V_o^2}{2\ x\ f_{sw}\ x\ P} \tag{6.11}$$

$$Lb = \frac{(1-0.453)^2 x\ 0.453\ x\ 500^2}{2\ x\ 5000\ x\ 6500}$$

$$Lb = 0.521mH$$

$$C_{min} = \frac{D\ x\ P}{V_o^2\ x\ \%_{ripple}\ x\ f_{sw}} \tag{6.12}$$

$$C_{min} = \frac{0.453\ x\ 6500}{500^2\ x\ 0.01\ x\ 5000}$$

$$C_{min} = 235uF$$

$$L_f = \frac{0.1V^2}{2\pi f P_a} \tag{6.13}$$

$$L_f = \frac{0.1x\ 480^2}{2\pi x\ 60x\ 6500/3}$$

$$L_f = 25mH$$

Table 5.2 – Converter parameters

Description	Data
$V_i = Input\ Voltage$	273.5V
$V_o = Output\ Voltage$	500V
$L_b = Boundary\ Inductor$	$0.521mH$
$L_{boost} = 10\ x\ Boundary\ Inductor$	$5.21mH$
$C_{min} = Minimum\ Capacitor\ value$	235uF
$C_{boost} = Boost\ Capacitor$	1000uF

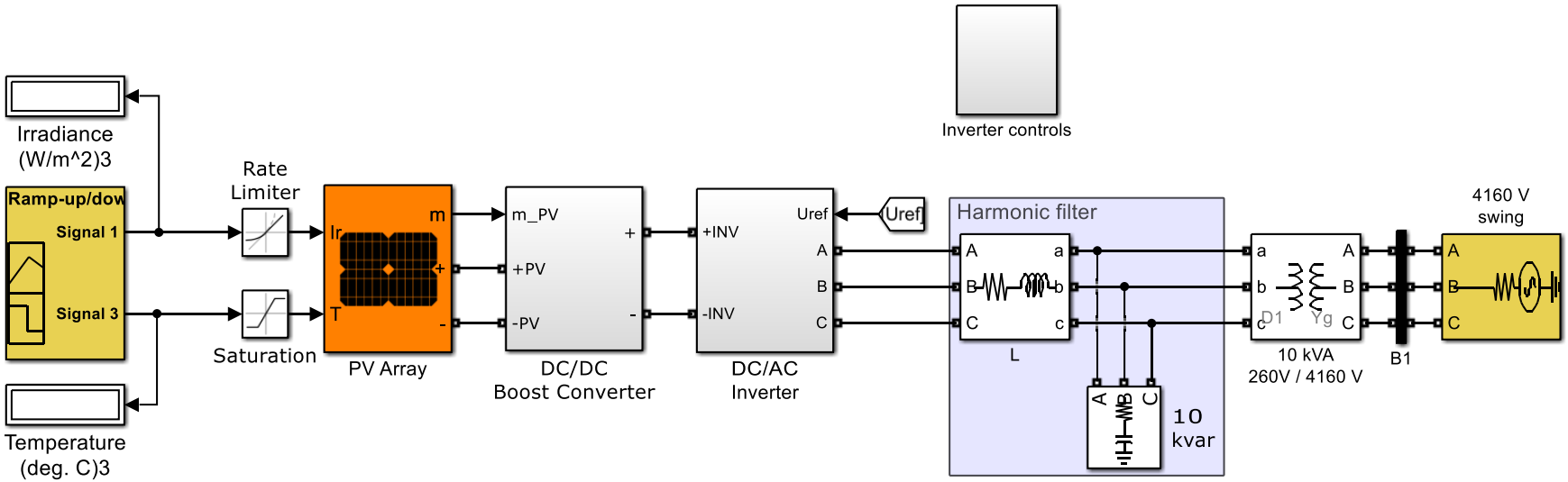

Figure 5.10. 6.5kW grid connected average PV model

- DC-AC Inverter – a two level voltage source inverter, which is found in the Simulink® library is selected to convert the voltage generated by the PV array from DC to three-phase AC. The average model seen in Figure 5.11 is used to increase simulation speed. In this study, PQ control, which controls the active and reactive power are used to track the reference currents.

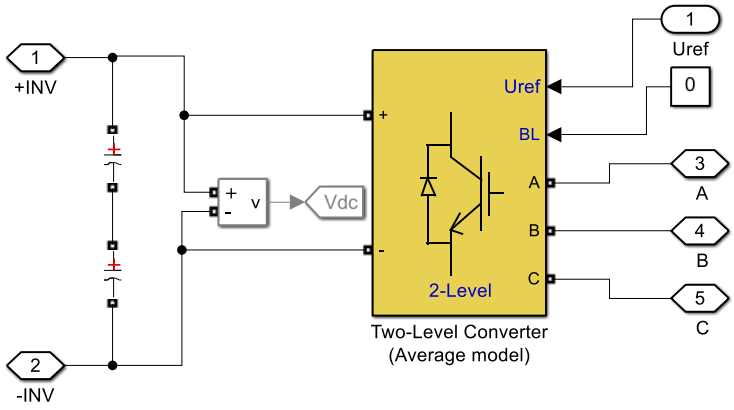

Figure 5.11. Two level (average model) voltage source inverter

- Inverter controller – the controller is designed based on a grid-following active and reactive power export strategy. It controls the DER output power based on voltage and frequency limitations. In this design, a current-controlled strategy is used to maintain constant voltage at the PCC. Figure 5.12 shows a block diagram representation of a "dq0" frame controller. The park transform is used to get the currents in "d-q" frame.

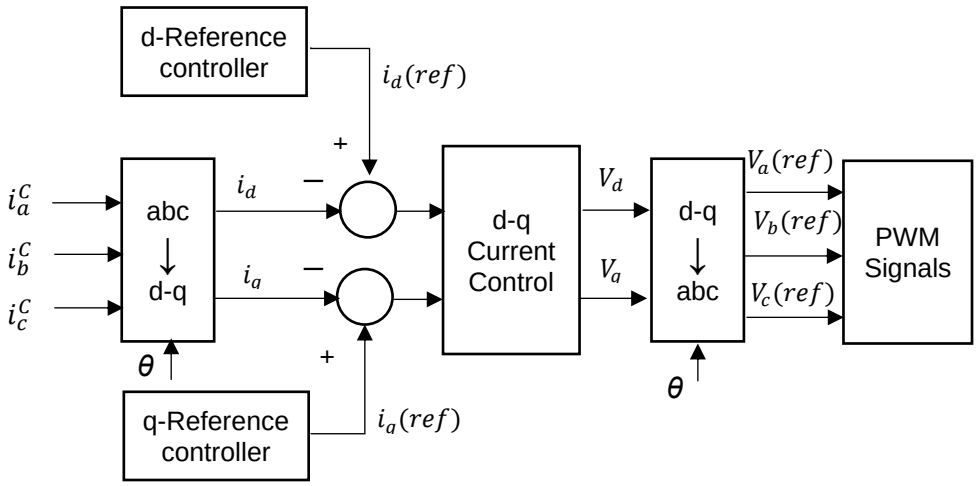

Figure 5.12. "d-q"-current control

The controller consists of a Phase Lock Loop (PLL) module, voltage, and current regulator. The PLL is used to measure the main grid phase voltage and control the PWM input to the inverter. For active power control, a PLL is used to generate the

output reference signal to the grid from the inverter, which is in phase with the grid voltage. For reactive power, the reference signal is 90° out of phase with the actual voltage. The internal diagram, which is illustrated in figure 5.13, shows a closed loop control system, where grid voltage and the inductor current are converted into the d-q frame (Park transformation) and filtered with a Mean Variable Frequency block. The PID controller keeps the phase difference to 0. The output of the controller is filtered and converted to the frequency.

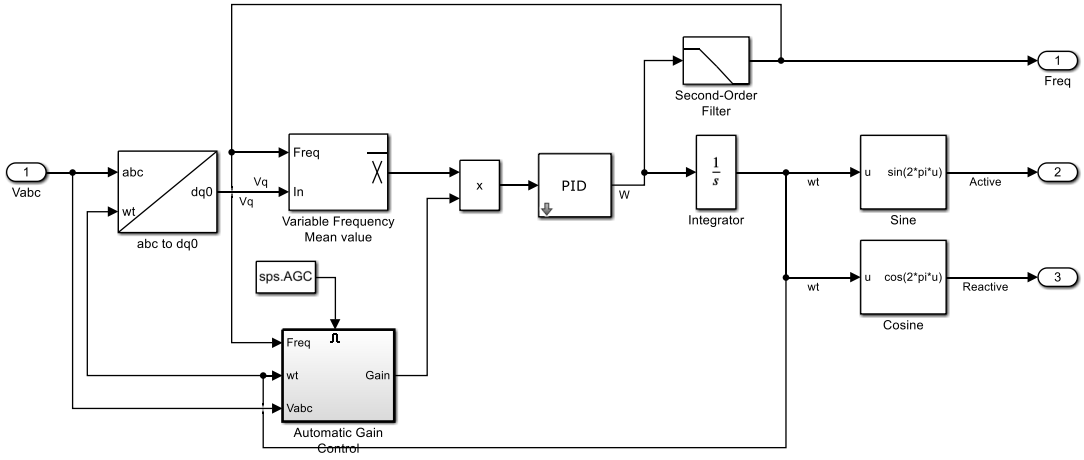

Figure 5.13. Internal diagram of the PLL

The voltage and current regulator consist of a PI controller, where proportional gain and integral gain is denoted by K_p and K_i, respectively. The output of the error signals between the measured voltage (V_{dc_meas}) and the reference voltage signal (V_{dc_ref}) is used to generate the PI actions. The input to the PI controller is mathematically given as:

$$u(s) = K_p + K_i \frac{1}{s} \tag{6.14}$$

The weighted output signal (I_{d_ref}) and ($I_{q_{ref}}$) in Figures 5.14 and 5.15 are used as input to the controllers. Id, which controls the active power gives the peak value of the current, which we want to control. “Iq” is used to control the reactive power. The controller minimizes the error. It improves the steady state response and transient response of the system.

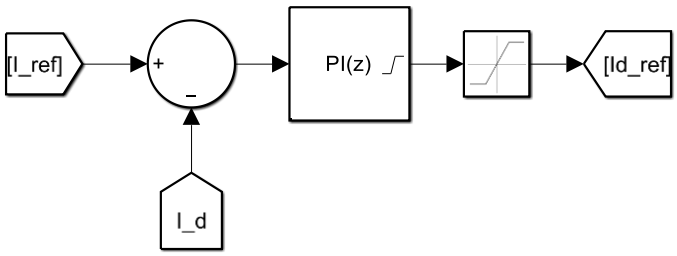

Figure 5.14. Active power control

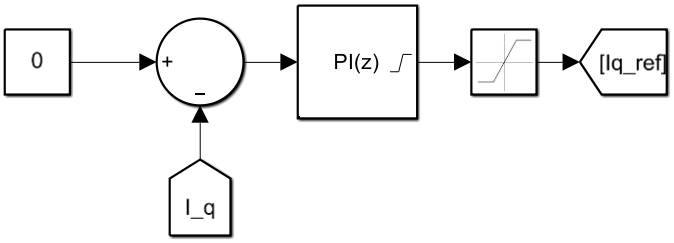

Figure 5.15. Reactive power control

Figure 5.16 is an illustration of PI controller, which is subjected to a step response. The initial nominal DC voltage or reference is set to 500V. The measured inverter DC voltage is close to 500V. After 0.2 seconds a step response is issued, which decreases the reference voltage to 450V. The result is illustrated in figure 5.17, which shown an initial overshoot, which can be manually or automatically tuned in the PI block.

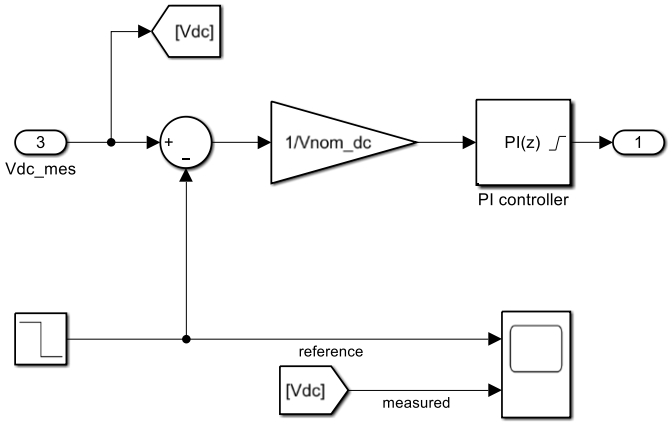

Figure 5.16. PI control

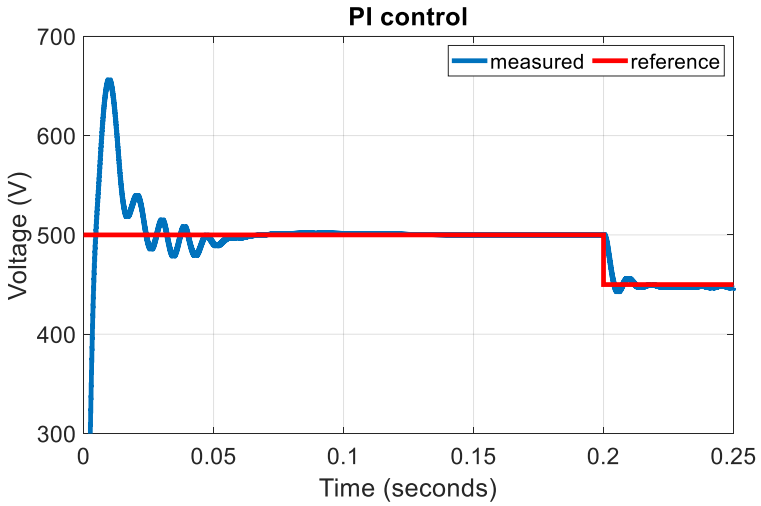

Figure 5.17. PI controller step response

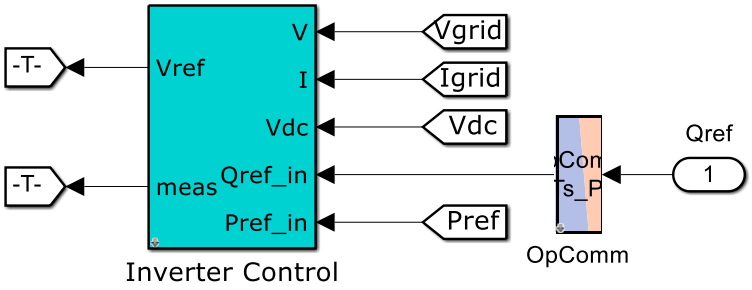

Figure 5.18. Inverter control mask

Figure 5.18 shows the inverter control mask. The inverter control consists of the voltage regulator, which regulates the dc-link voltage, active and reactive power controller.

The PV array profiles are given in figure 5.19. The results show the current, voltage and active power profile of an ideal compared to an actual irradiance input.

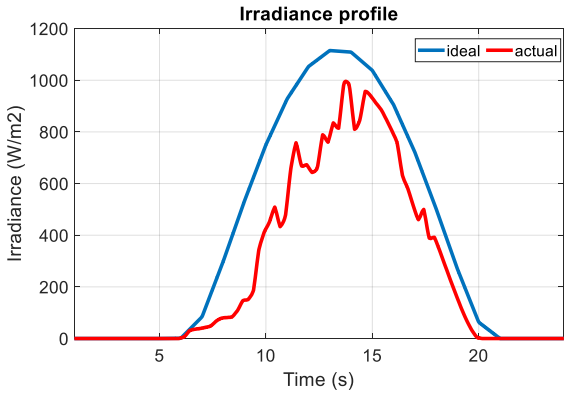

a) Irradiance profile

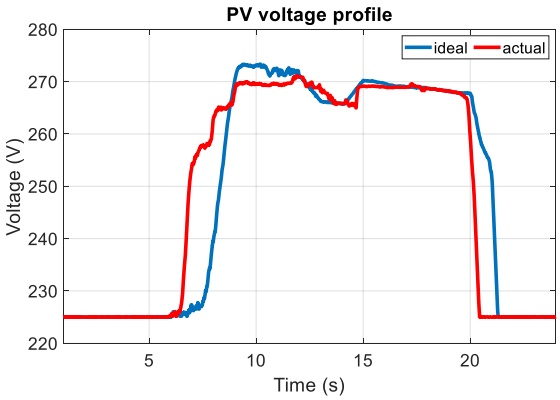

b) PV votage profile

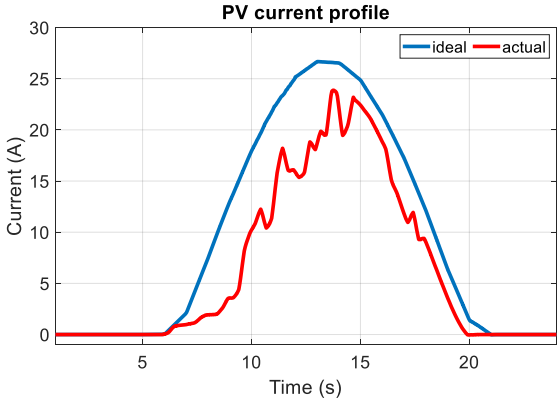

c) PV current profile

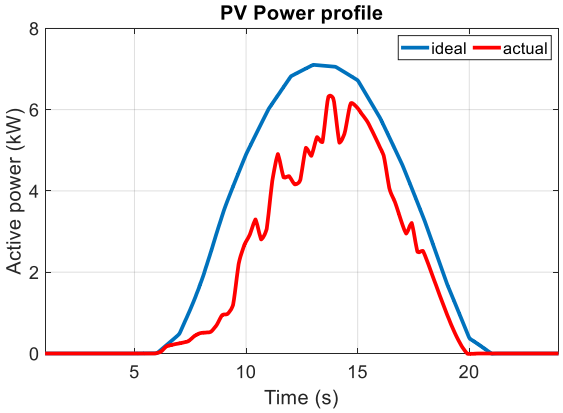

d) PV power profile

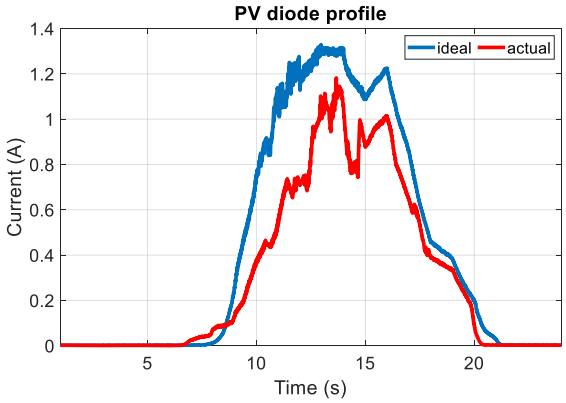

e) PV diode profile

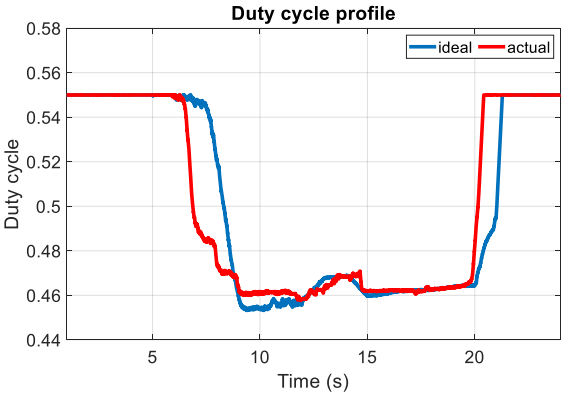

f) Duty cycle

Figure 5.19. 6.5kW PV profiles

5.4 OPAL-RT

The introduction of renewable energy resources with power electronics interface circuits is changing the operation of the distribution network. Experimental testing is usually done to validate the physical network. Actual testing of the network is not possible as it may compromise the reliability of the grid. Based on the latter, digital models are implemented to simulate real world scenarios. The digital models simulate actual electrical parameters based on the physical network.

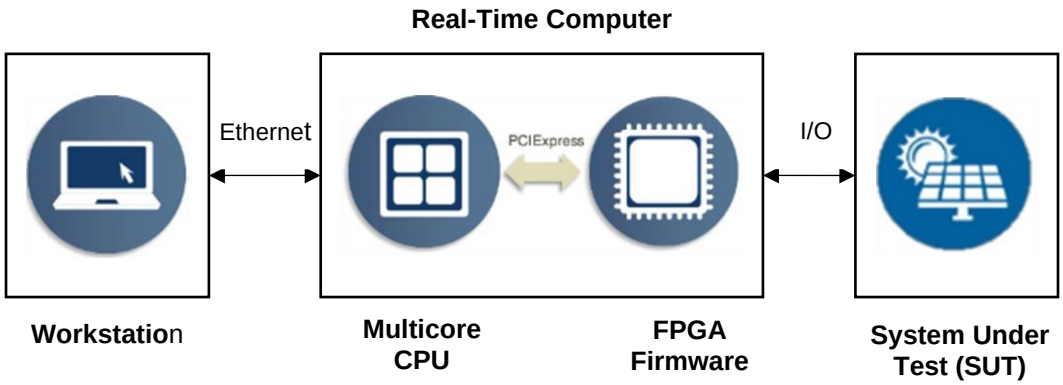

Figure 5.20. HIL process (OPAL-RT)

Simulation tools have been used for several decades for power systems design and analysis. These simulation tools have evolved in recent years based on their computational technologies. Digital real-time simulation (RTS) is commonly used in industry to validate designs prior to installation and operation as it provides reliability and security. The cost of these real-time simulators has been decreasing year-on-year, which makes it more accessible to industry and academia. Digital simulation has proven to be an efficient and effective tool for the development and testing of power systems based its reliability and accuracy and economic value. OPAL-RT Technology, which is the leading exponent in developing real-time simulators is selected to perform the simulation based on its reliable operation and performance. Traditionally, offline simulations are used, but these are slow and not able to simulate real-time conditions. Hardware in-the-loop (HIL), which is illustrated in figure 5.20 is a FPGA-based (Field-Programmable Gate Arrays) closed loop real-time simulation technique, can bridge this gap (De Farais et al, 2019).

OPAL-RT Technology, based in Canada, specialises in the development of FPGA-based real-time simulators. The hardware allows the user to run simulations in real time. RT-LAB, which is OPAL-RT's propriety real-time simulating software environment is based on modelling and is used to communicate with the hardware. The software is completely compatible with MATLAB/Simulink® environment. A developed model is divided into subsystems and

distributed to an available CPU core, which operates in parallel in real time. When simulating real world scenarios, the time to solve the functions and equations of the feeder or network must be less than the fixed step. An overrun occurs when the calculation time exceeds this fixed step.

5.4.1 Hardware (OPAL-RT)

Figure 5.21 shows OPAL-RT's OP4510 real-time (RT) simulator. The simulator used for this study is an entry level version. Table 5.3 gives a summary of the operating system and hardware used.

Table 5.3 – OP4510 operating system and hardware

Description	Specification
Platform	Linux (x86 -based)
OS version	2.6.29.6-opalrt-6.2.1
CPU speed (MHz)	3504
Number of cores	4
Number of active cores	1

The RT simulator, which interfaces with the host computer simulates the model developed in MATLAB/Simulink®. The simulator executes a physical, developed model and runs it at the same rate as the actual clock.

Figure. 5.21. OP4510 real-time simulator

Some of the key specifications of the OP4510 are summarized below.

Table 5.4 – OP4510 specification

Parameter	Description
FPGA	Kintex-7 FPGA, 325T, 326,000 logic cells, 840 DSP slice (Multiplier- adder)
Computer	Intel Xeon E3 v5 CPU (4 core, 8MB cache, 2.1 or 3.5GHz), 16G B RAM, 256 GB SSD
Software compatibility	RT-LAB multi-processors platform, LINUX, Simulink, RTW, SimPowerSystems, SimScape, ARTEMIS, RT-EVENT, HYPERSIM and several third-party software compatible with Simulink
Performance	Minimum time step of 7 microseconds for model subsystems executed on the INTEL CPU and 250 nanoseconds for models executed on the FPGA chips, 10 nanosecond timer resolution

5.4.2 Software (RT-LAB)

RT-LAB is OPAL-RT's proprietary software. It is based on MATLAB/Simulink® model-based design and allows users to build and edit graphic models in block diagram format. The software provides a real-time platform, which allows users to test dynamic models built in MATLAB/Simulink® environment.

The following is a summary of the process and procedure to run a model in RT-LAB.

- Model design - the MATLAB/Simulink® model can be opened directly from RT-LAB's main graphical interface window. Subsystems are needed to build a model. There are 3 types of subsystems as illustrated in figure 5.22. These are (i) master subsystems, noted by the prefix SM, which is the main subsystem, (ii) slave subsystem, noted by the prefix SS and (iii) the console subsystems, denoted by the prefix, SC. Console subsystems have user interface blocks like scopes and output displays. One computation block is allocated to each core of the simulator. GUI are user input and

feedback. The simulator described in table 6.3 has only one active core. This places some restrictions on the size of the simulated model.

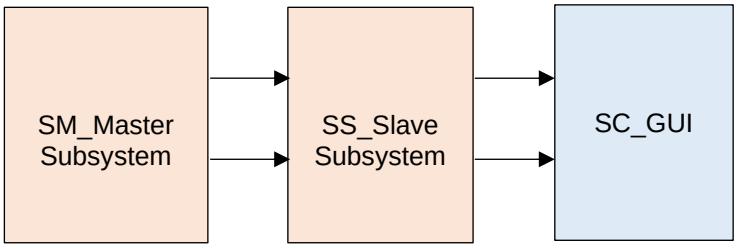

Figure 5.22. Communication link between subsystems

All inputs of subsystems must go through an OpComm block, which is used to receive real-time synchronized signals. OpComm blocks shown in figure 5.23, can accept multiple inputs.

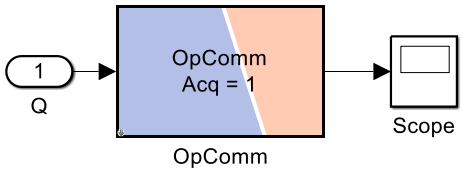

Figure. 5.23. OpComm Block with I/O port.

- Build the model -create C-code from the Simulink model and let RT-LAB compile it in the real-time target.
- Load the model - RT-LAB automatically loads the model into the different CPU cores and manages all the sequences, communication, and synchronization processes. For this study the model will be loaded onto one core.
- Execute the model - test and perform real world applications. Use graphical interface to interact with the simulation.
- Data recording – OpWriteFile

5.5 Modified test feeder.

- Simulink model - due to the limitation of the real-time simulator described in table 5.3, the 37 bus IEEE test feeder has been modified. The network parameters remain the same as previously described but feeder has been reduced to a seven-bus network. The load at bus 742 has been increased to 200kW. This load forms a residential cluster, which is connected to a solar PV system. The solar PV system represents several 6.5kW rooftop system. For ease of simulation, the rooftop systems are modelled as 4 separate PV arrays. The composition of each system is given in Table 5.5.

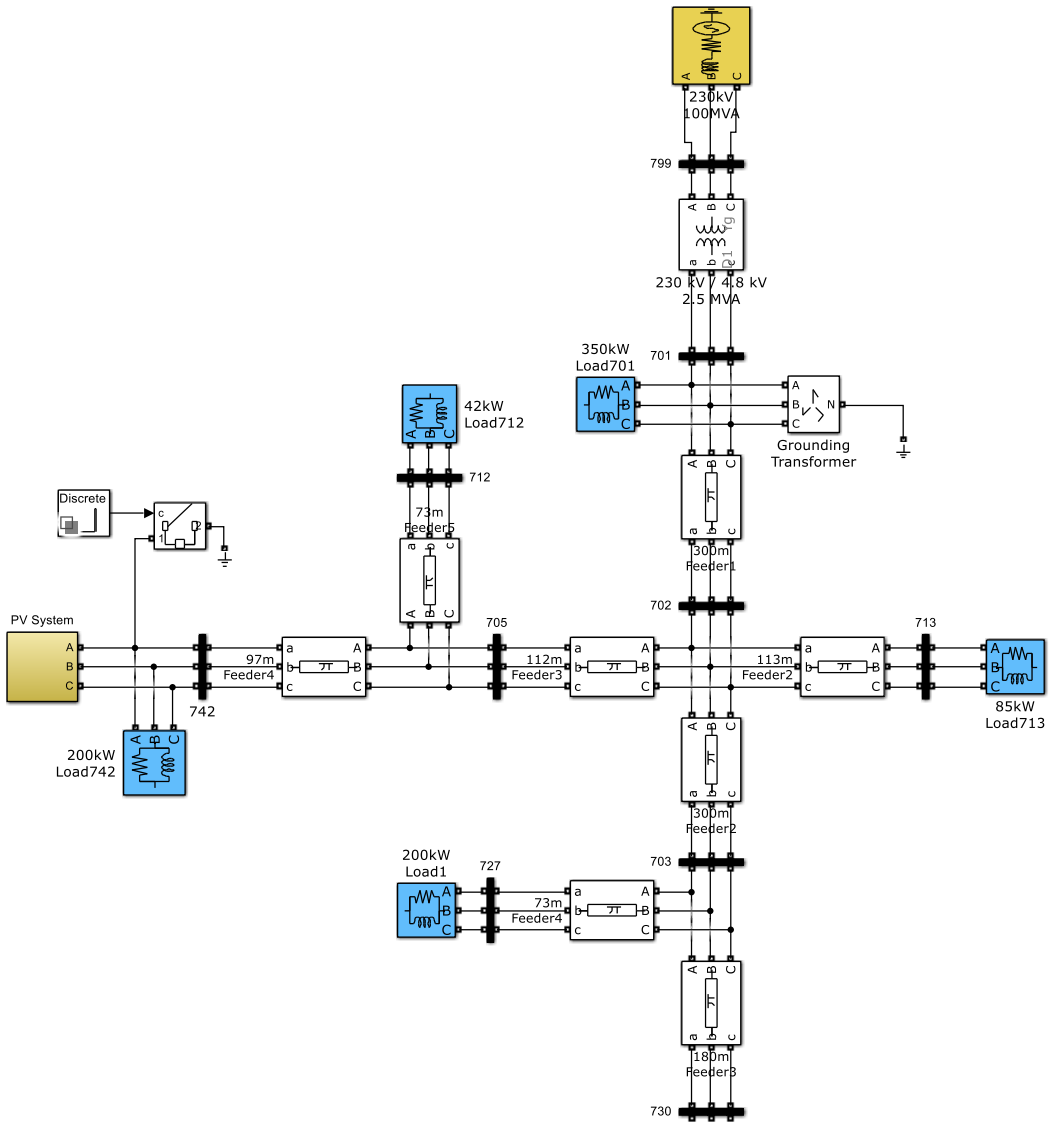

Figure. 5.24. Modified test feeder.

- RT-LAB™ model – the comprehensive 37 IEEE feeder was placed in the master subsystem and simulated in OPAL-RT™. The simulation had many overruns, which need to be corrected. The step time was reduced but the CPU was still running at

100%. The model had to be scaled down to a 10bus network to reduce the CPU usage to 58%. Table 5.6 gives a summary of the diagnostics for the comprehensive and modified feeder. Figure 5.25 shows the top-level RT-LAB™ model. The model consists of the modified feeder, which is built in the master subsystem and the measuring devices located in the console subsystem. The Powergui block is placed in the top level.

Table 5.5 – Aggregated Rooftop PV array

PV size	**Parameters**	
	Series connected modules/string	Parallel strings
26kW	16	5
13kW	8	5
40kW	24	5
21kW	13	5

Table 5.6 – OPAL-RT™ simulation diagnostics

Description	**Result**	
	Comprehensive feeder	Modified feeder
Time step	50µs	50µs
CPU core usage	100%	58%
Execution cycle (min)	281µs	40 µs
Number of overruns	3	0

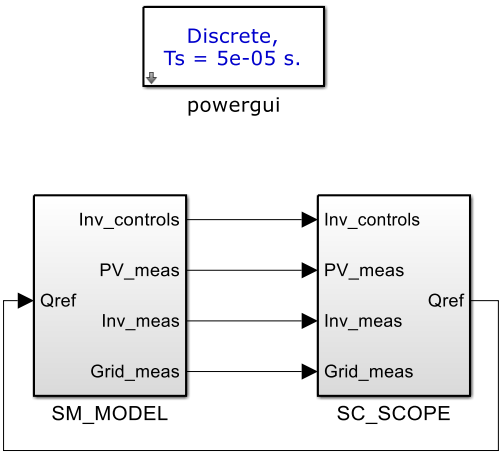

Figure. 5.25. Top Level Model of OPAL-RT™

- OpWriteFile – this block is used to write signals to a “mat. File” that can be processed in MATLAB®. The OpWriteFile is placed in the master subsystem. Figures 5.26 a, b, c and d show the measurement devices, which are placed in the master subsystem.

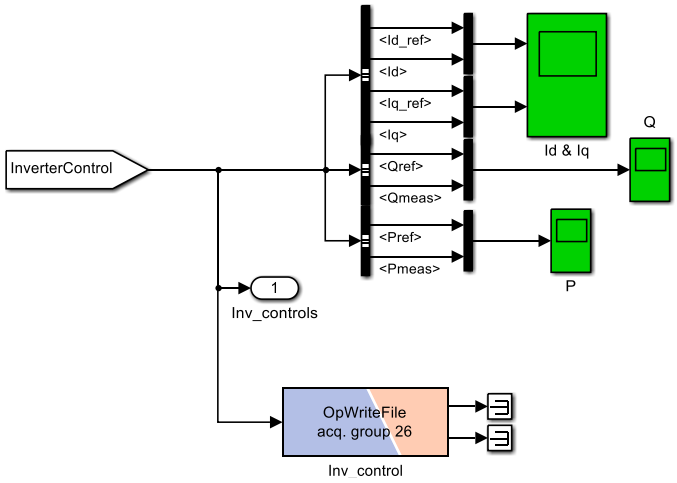

a) Inverter control measurement

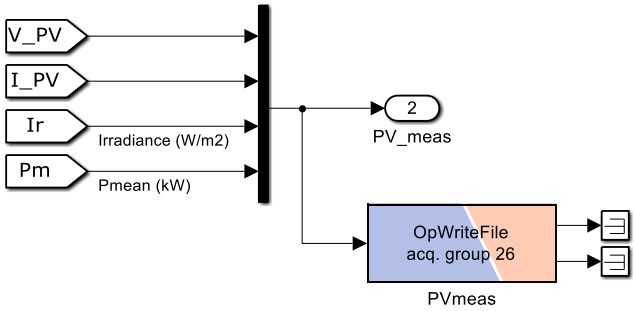

b) . PV measurement

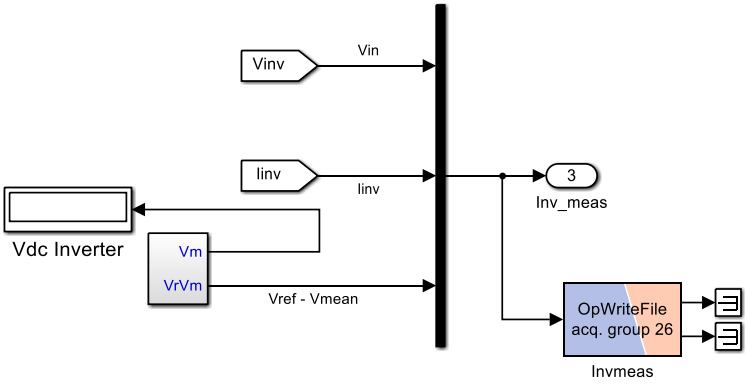

c) Inverter measurement

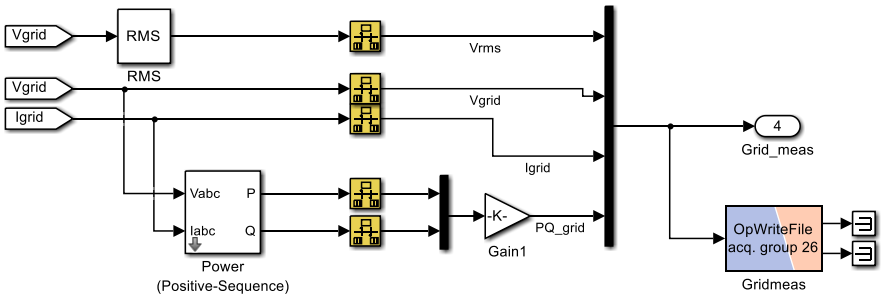

d) Grid measurement

Figure 5.26. Measurement devices with OpWriteFile blocks

- Console systems – Figure 5.27 shows the scopes inside the console system, where all signals are sent through an “OpComm” block.

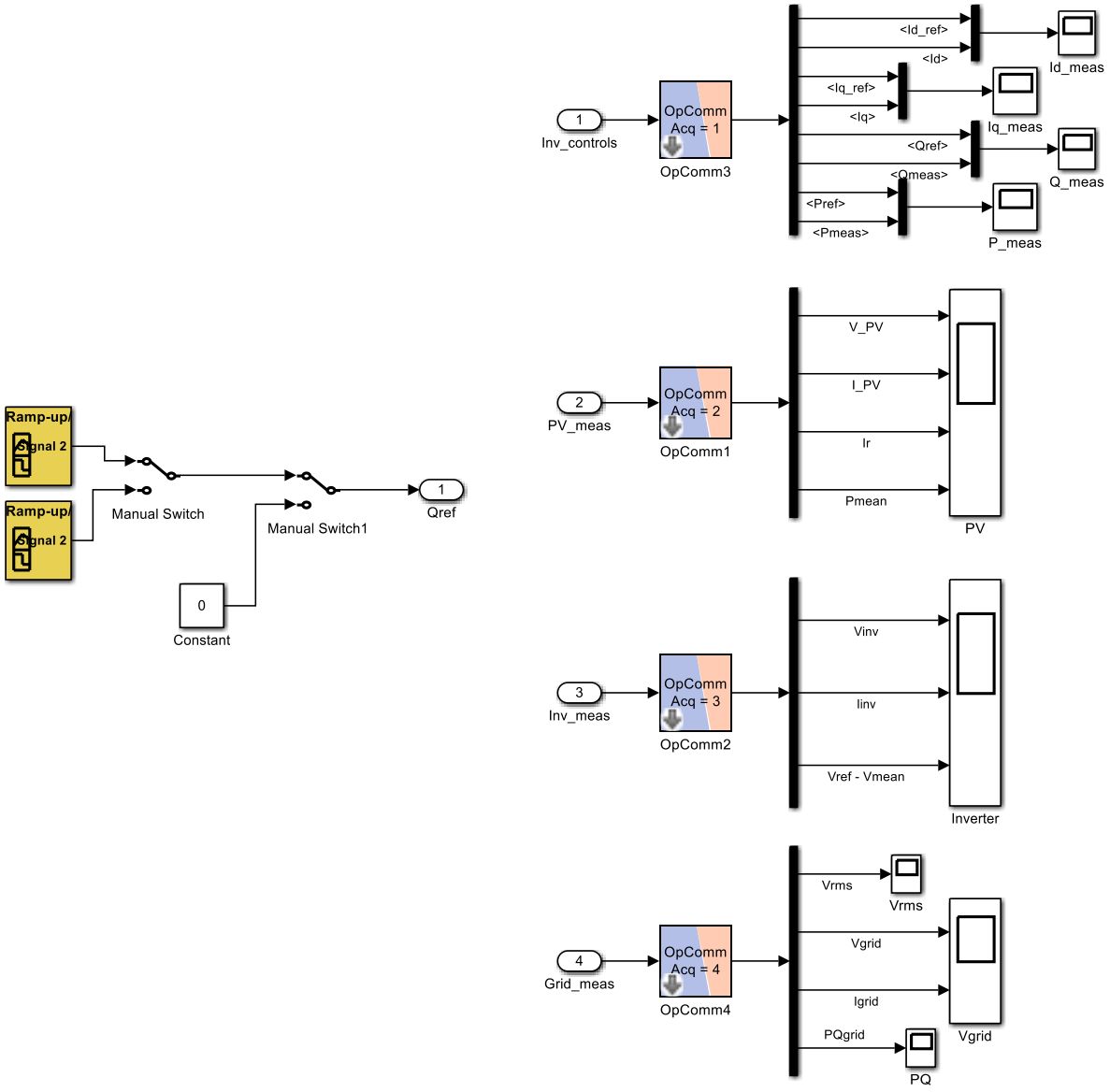

Figure. 5.27. Console subsystem

5.6 Simulation results

The ability for a network to maintain voltage under normal condition following load fluctuation is referred to as steady-state voltage stability (Viawan,2008). In this study, bus voltage analysis is done with and without solar PV to observe the effect on the steady-state voltage stability of a distribution system.

5.6.1 Conventional Network

The voltage and current profiles at bus 742 are shown in figure 5.28. The bus voltage and current, measured at the local bus is approximately 4000V and 40A, respectively. The system will maintain this voltage and current based on a steady load profile. In the absence of an increase in load, the bus measurement will be constant.

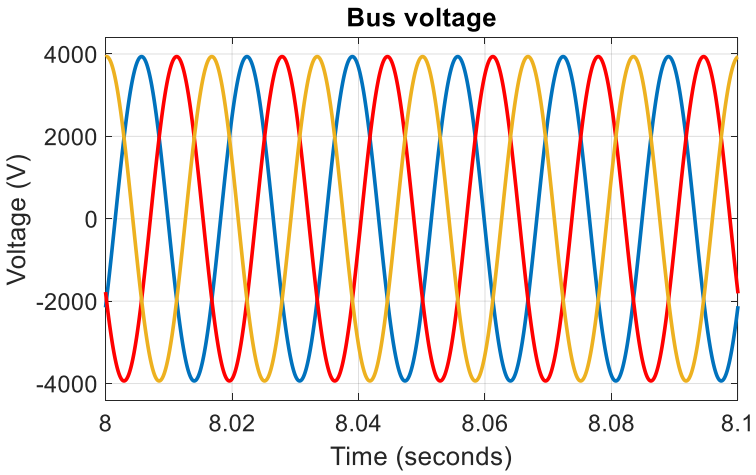

a) Bus voltage

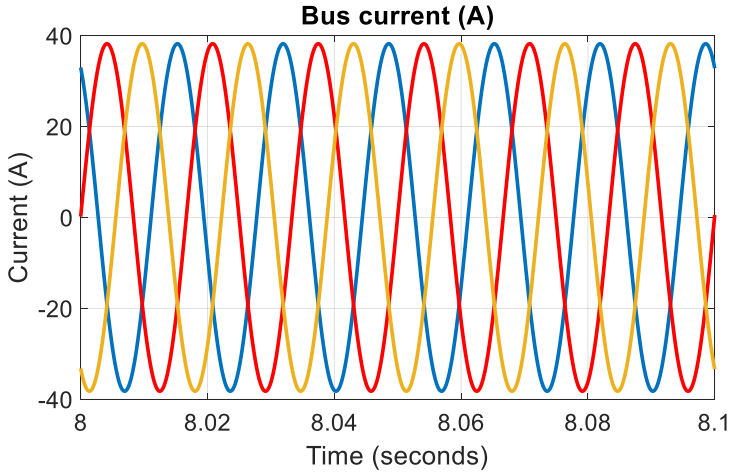

b) Bus current

Figure. 5.28. Bus voltage & current profile

5.6.2 Network with solar PV

The study focuses on the analysis of an ideal and actual irradiance profile. The simulation results are based on the reactive power export control strategy. The inverter controller in figure 5.18 consists of a DC-link voltage controller and a Q-controller. The DC-link voltage controller maintains a steady voltage based on the DC reference voltage whereas the Q-controller specifies the reference value for the q-component of the current. Unity power factor is set to zero when the reactive power reference Q(ref) is set to zero. The simulation explores the impact on the local bus voltage when the PF is varied. The reactive power reference value is based on 0.95 leading and lagging PF. It compares the results based on ideal and actual irradiance inputs.

5.6.2.1 Ideal Irradiance

The first scenario is based on an ideal irradiance output. The simulation running time is 24 seconds but mimics the irradiance over 24 hours in that period.

- DC (PV) measurements

The solar PV residential cluster consists of 4 PV arrays that are controlled by one inverter. The arrangement is for ease of simulation. Figure 5.29 shows the power profiles of PV arrays.

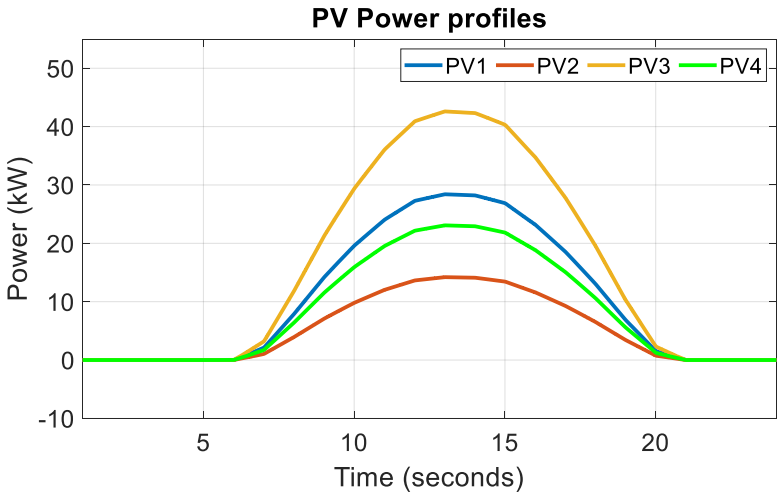

Figure 5.29. Ideal PV profiles

- AC (Inverter) measurement

The AC measurement, which are measured at the inverter busbar is given in Figures 5.30 and 5.31. The DC-link controller maintains a steady voltage by controlling the “Id” inverter current to balance the power flow from the grid of the DC link. In this way the voltage is kept at a constant output by controlling the inverter current. For the first case, PF is set to 0.95 lagging.

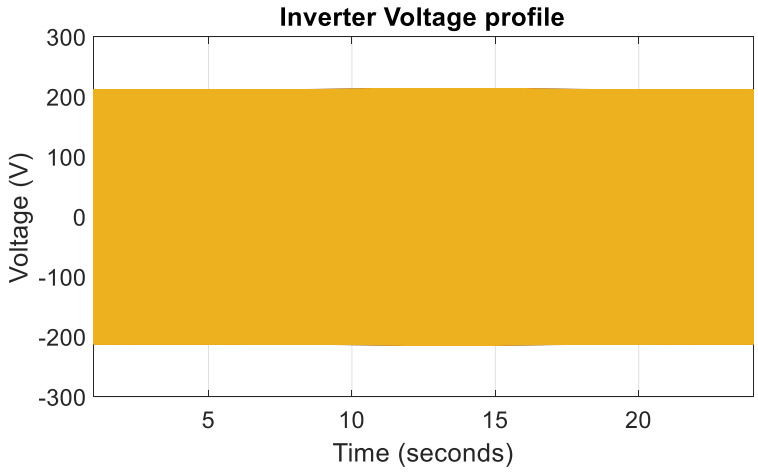

a) **Inverter voltage profile**

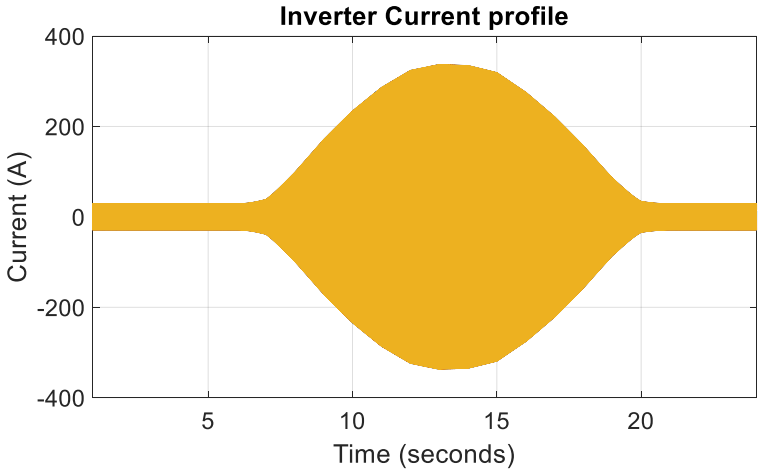

b) Inverter current profile

Figure. 5.30. Bus voltage & current profile with PV

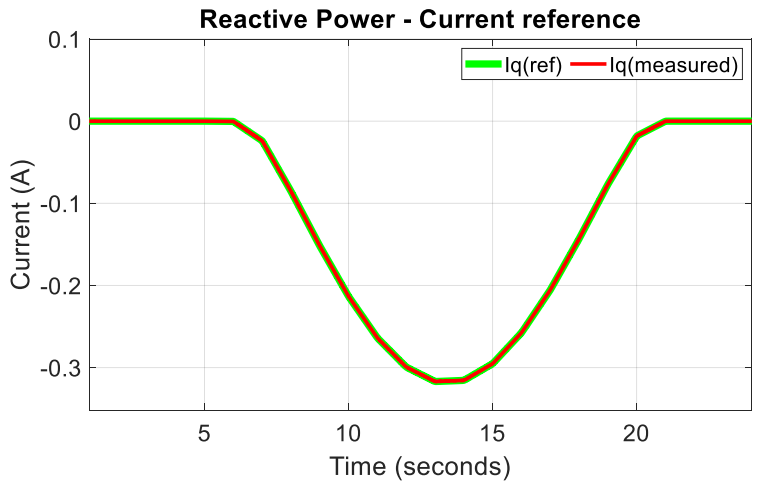

a) **Reactive current reference**

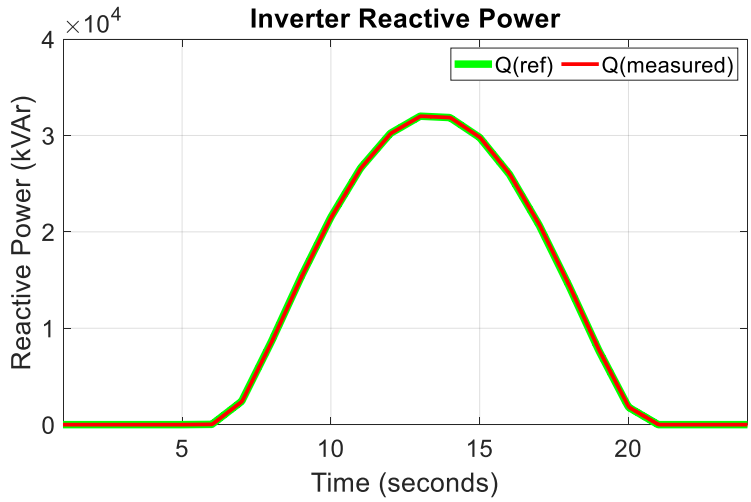

b) Inverter reactive power

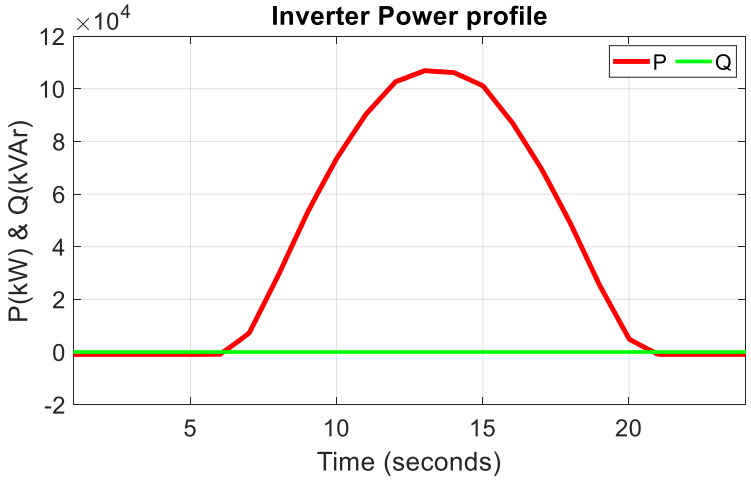

c) Inverter power profile

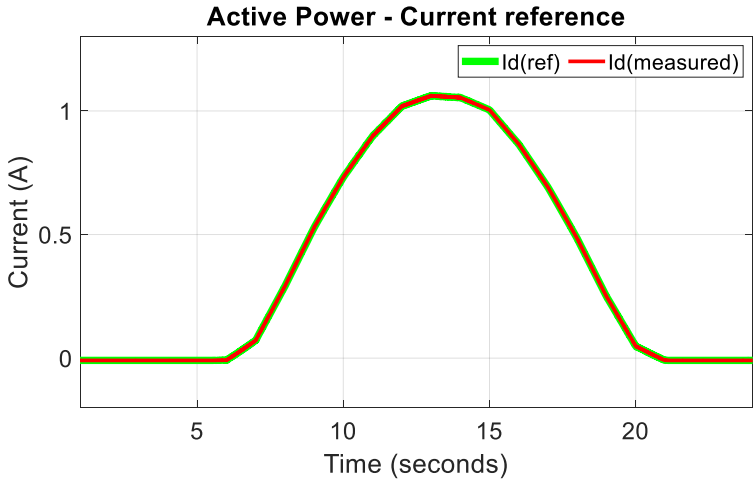

d) **Active Power – current reference**

Figure. 5.31. Inverter measurement - ideal irradiance

- PCC (local bus) measurement

Figure 5.32 shows the measured data at the local busbar. For this scenario, Q(ref) is set to 32kVAr, which is based on 0.95PF. The inverter produces a maximum active output power of 100kW. A snapshot is taken of the voltage profile at midday, which shows that voltage is maintained around 4000V, but the current decreases based on the active power produced by the PV system.

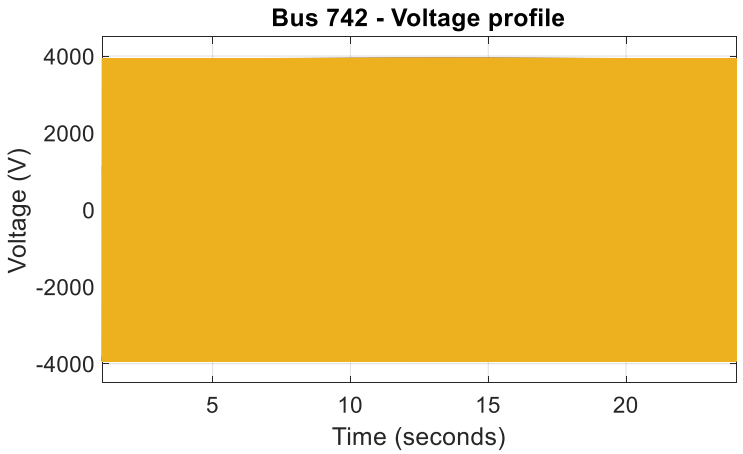

a) Bus 742 voltage profile - ideal

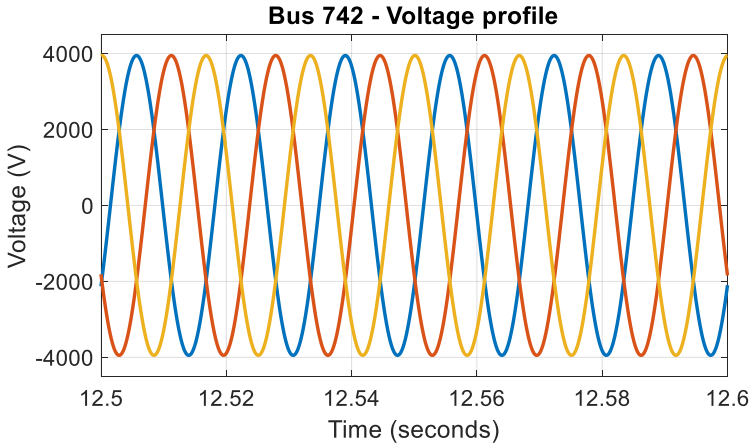

b) Detailed bus voltage profile - ideal

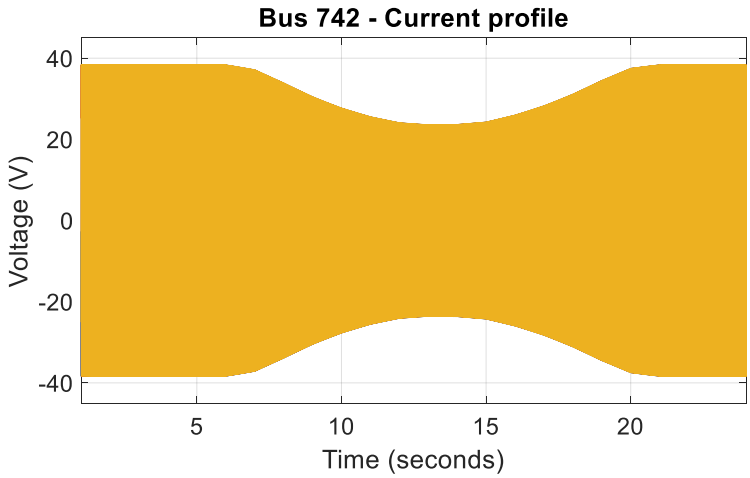

c) Bus 742 current profile - ideal

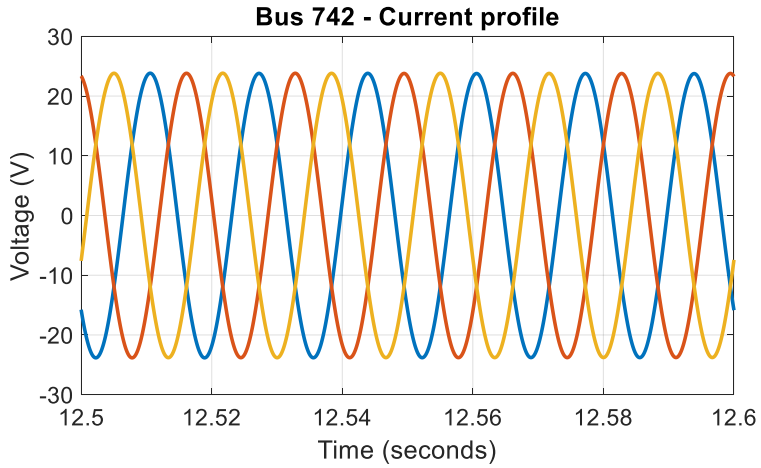

d) Detailed bus current profile - ideal

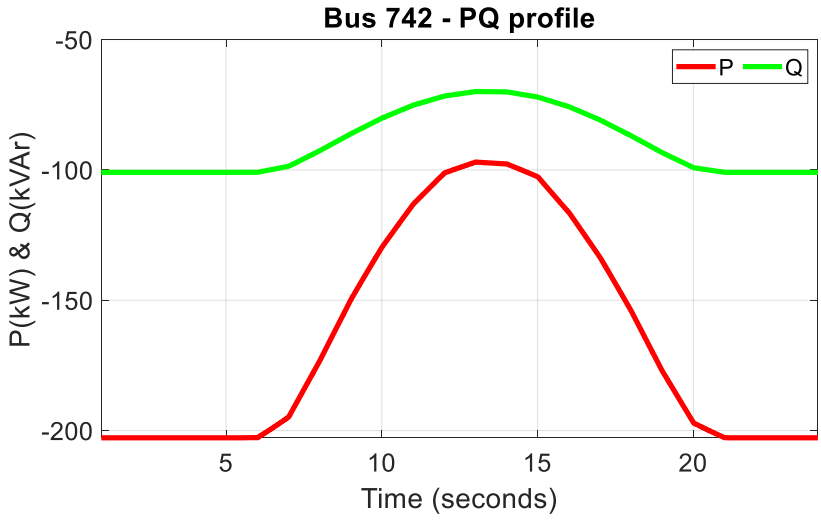

e) Bus 742 – Ideal PQ profile

Figure. 5.32. Local bus measurement

Figure 5.33 (a) shows the RMS voltage at the local bus. The baseline voltage is compared to the voltage at 0.95 lagging PF. An increase in the bus voltage can be observed. Figure 5.33 (b) shows the bus voltage profile in per unit measurement. An increase of 0.5% is observed compared to unity PF. This understandable given the connected PV represents a small part of the feeder load demand.

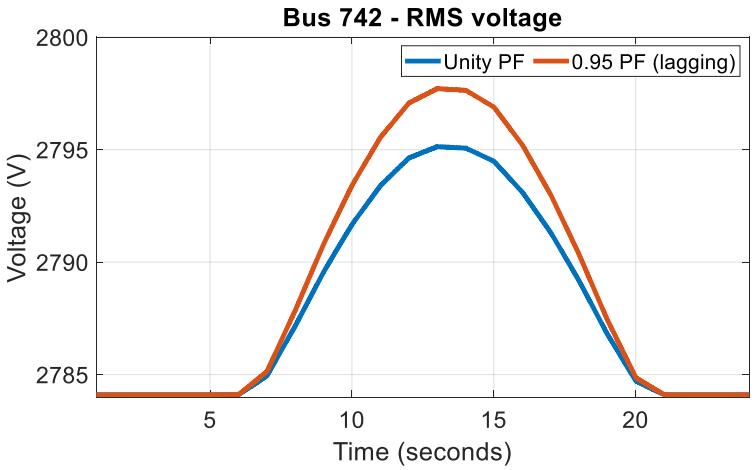

a) RMS voltage profile - ideal

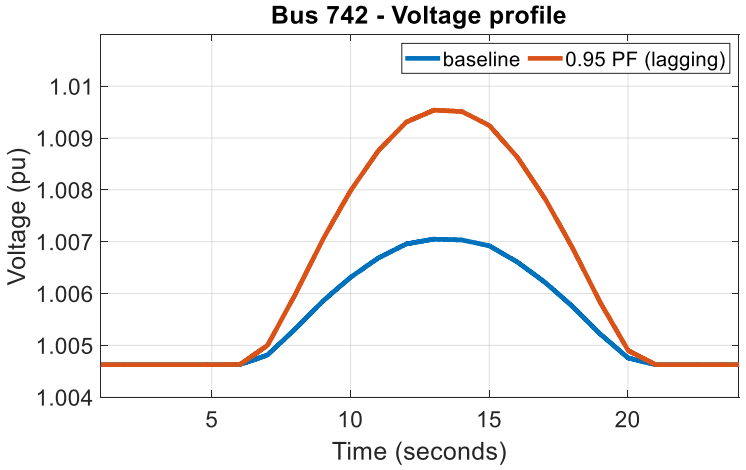

b) Bus voltage profile - ideal

Figure. 5.33. Local bus voltage measurement - ideal irradiance

5.6.2.2 Actual Irradiance

The second scenario is based on actual irradiance output. The PV active power profiles are given in Figure 5.34.

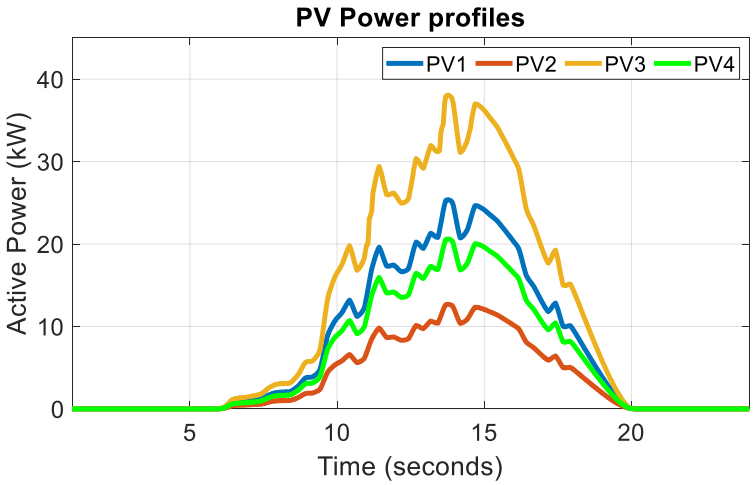

Figure 5.34. Actual PV power profiles

- Reactive Power Injection

The results below are based on reactive power injected into the network. This is achieved by supplying the Q-controller with a reference value or series of values. In this case, the reference input is based on the active power, which is based on the solar irradiance and temperature input into the PV array. The signal was constructed using the signal builder in Simulink®. To inject reactive power into the grid, the input signals must have a positive value. Figure 5.35 (a) shows the DC bus voltage based on an actual solar irradiance profile. As with the ideal profile, the measured DC voltage tracks the reference voltage. The inverter PQ profile, based on 0.95PF is shown in figure 5.35 (c). Figure 5.35 (d) shows the measured reactive power, which follows the reference reactive power.

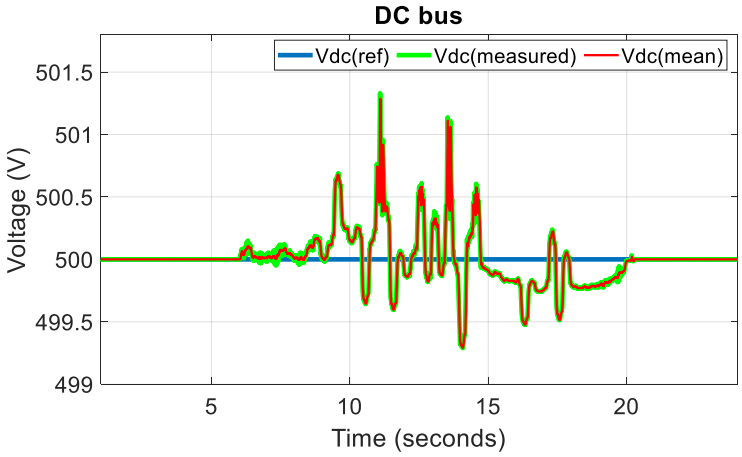

a) DC bus voltage

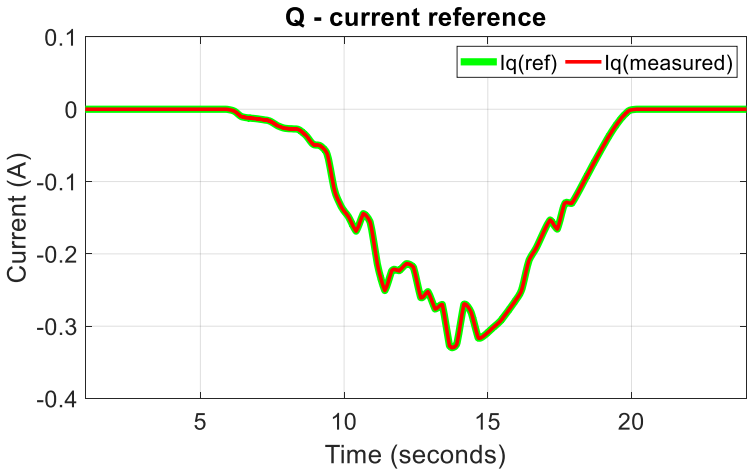

b) Reactive power current measurement

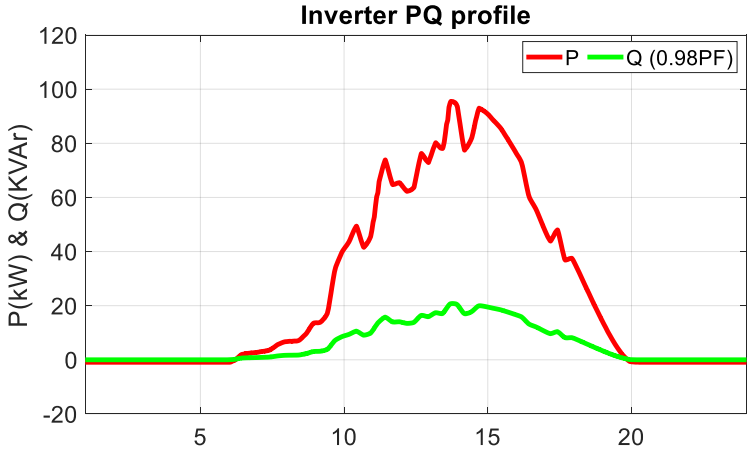

c) Inverter PQ profile

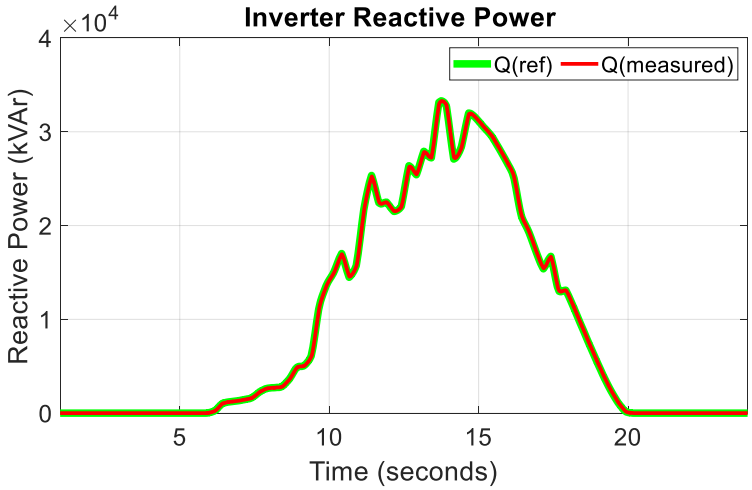

d) Inverter Q measurement

Figure. 5.35. Inverter measurement - actual

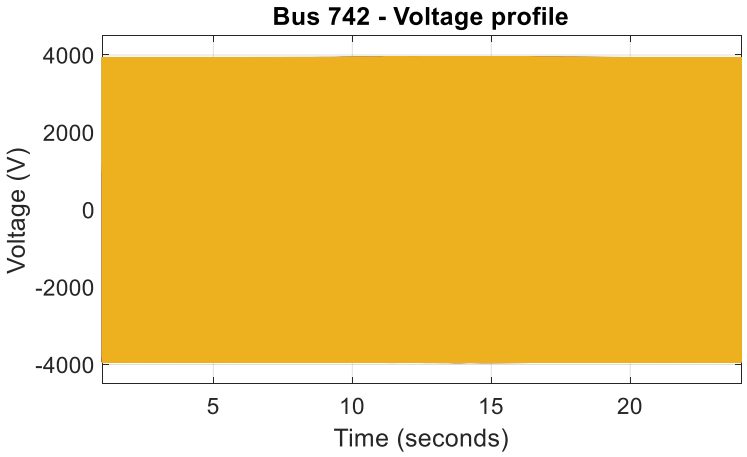

a) Bus 742 – voltage profile (actual)

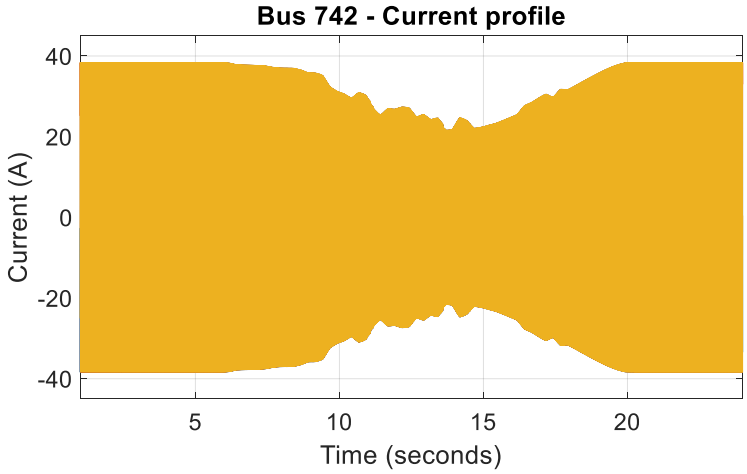

b) Bus 742 – current profile (actual)

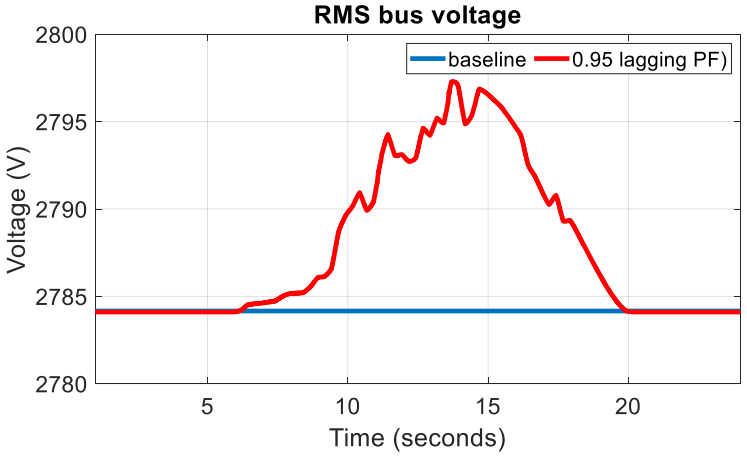

c) **Bus** RMS voltage (actual)

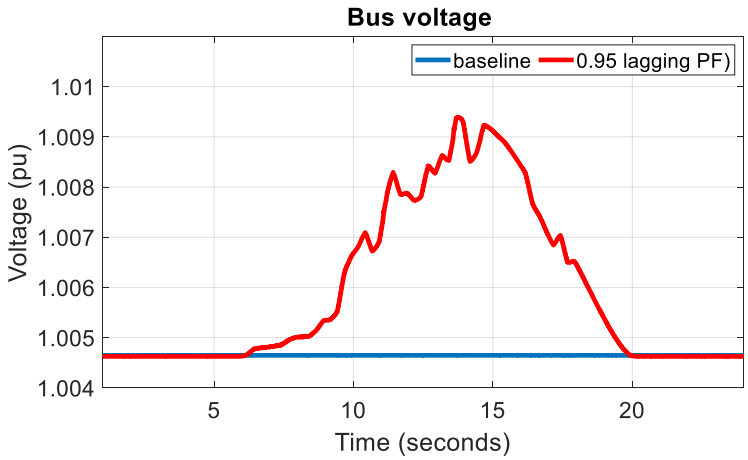

d) Bus Voltage profile (actual)

Figure. 5.36. Bus measurement - actual irradiance

Figure 5.36 shows results of the measurement taken at the local bus. The profiles show a marginal increase of 0.5% compared to the baseline voltage. As illustrated before, the results are expected due to the amount of reactive power injected by the solar PV system compared to the actual network active power.

- Reactive Power absorption

To simulate reactive power absorption, the input to the Q-controller is set to a series of negative values. As with Q injection, the input values into the Q-controller are based on the active power profile. The signal was constructed using the signal builder in Simulink®. To inject reactive power into the grid, the input signals were set to negative values. Figure 5.37 shows the reactive measurements. For this case, 32kVAr is absorbed based on 0.95 leading PF.

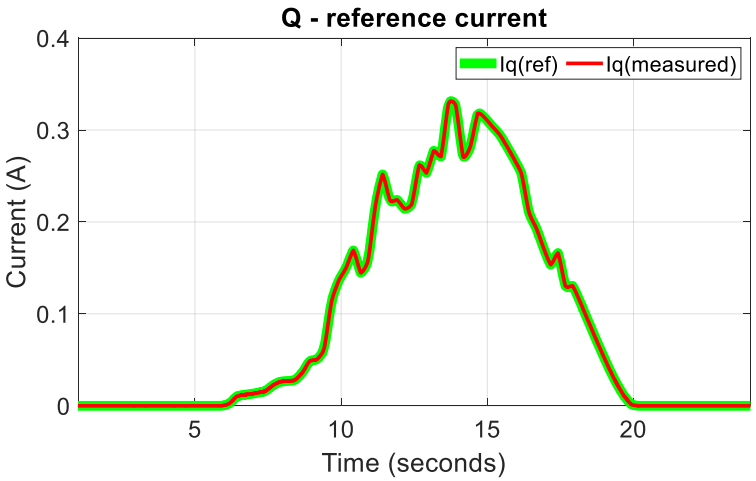

a) Q – reference current

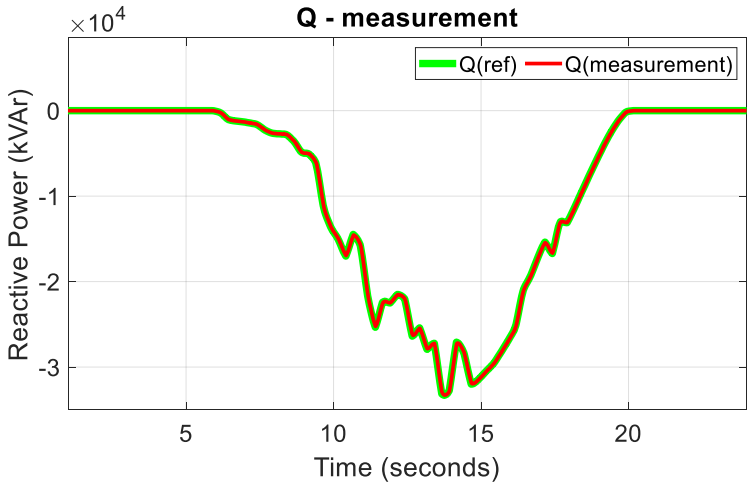

b) Q measurement

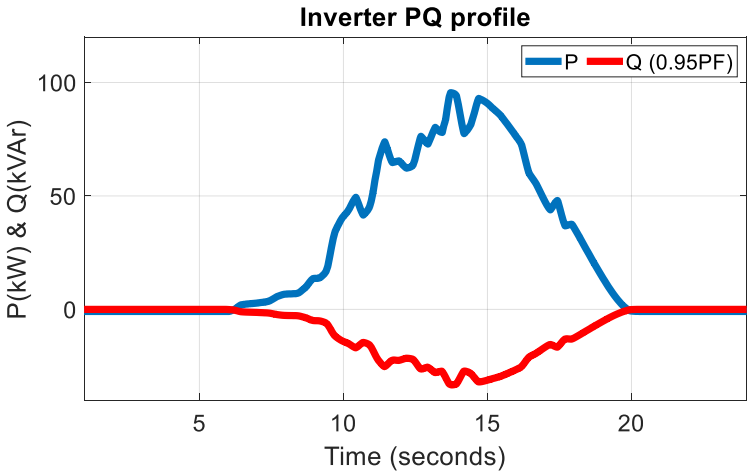

c) Inverter PQ profile

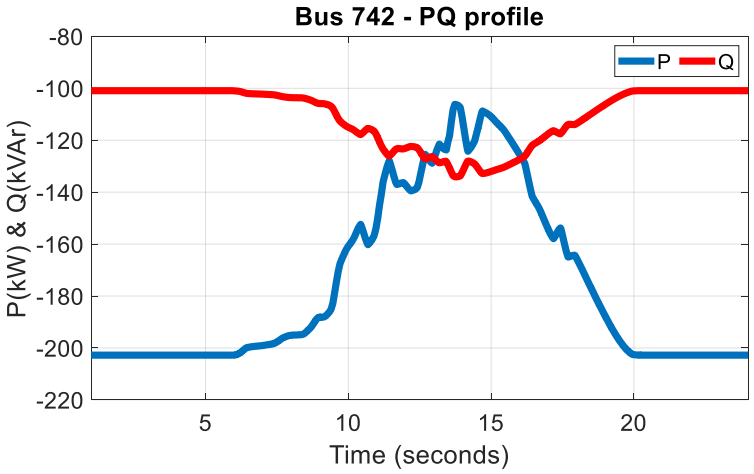

d) Bus PQ profile

Figure. 5.37. PQ measurement - actual irradiance

The measured reactive power current signal “Iq” (measured) and Iq (ref) are shown in Figure 5.37 (a). It shows how the measured signal followed the reference signal. This ensures that the measured reactive power, which is based on the reference reactive power Q(ref) is produced by the inverter and supplied to the grid. Figure 5.37 (c and d) shows the inverter PQ profile and bus PQ profile, respectively.

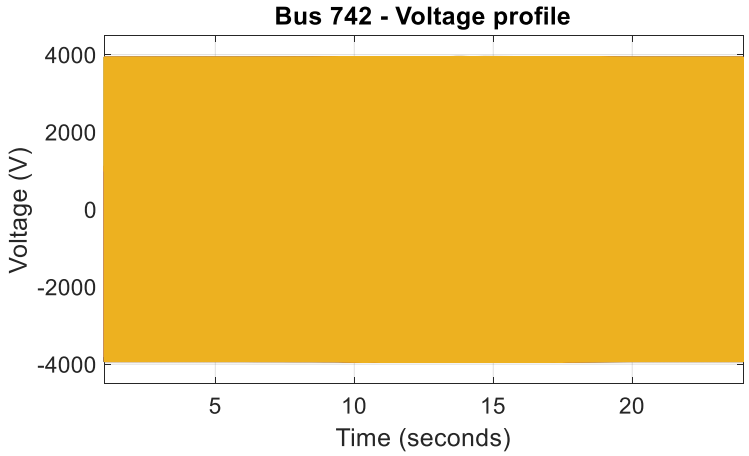

a) Bus voltage profile

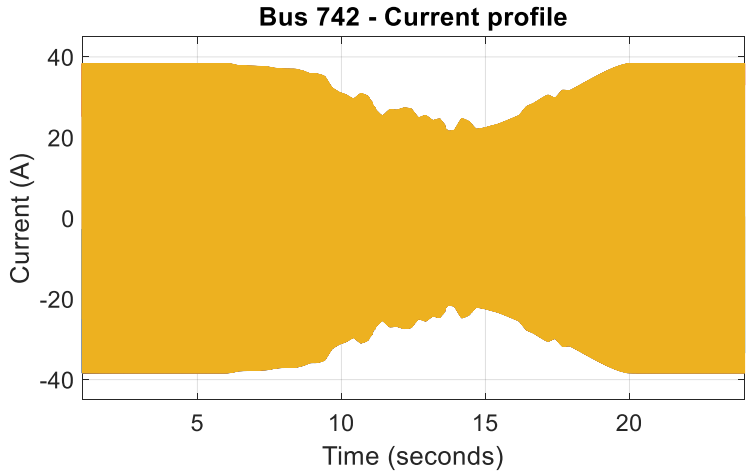

b) Bus current profile

Figure. 5.38. Bus profiles - actual irradiance

The bus voltages are shown in Figure 5.39. It shows the RMS and per unit voltage profile at the local bus (bus 742) based on 0.95 leading PF. By absorbing reactive power, voltage profiles can be improved.

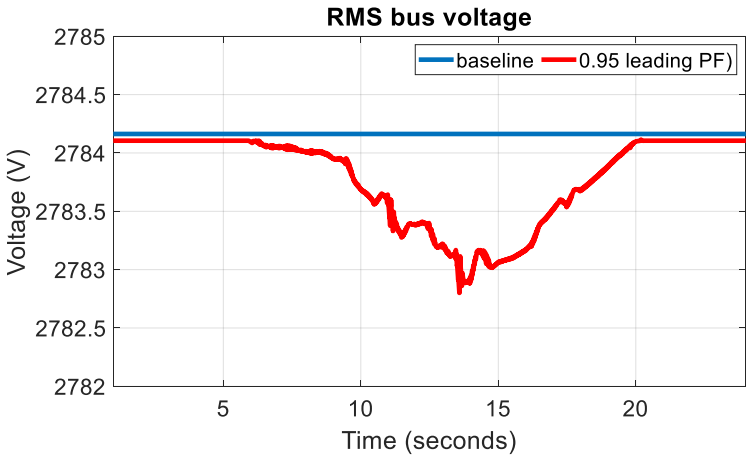

a) RMS voltage – 0.95 leading PF

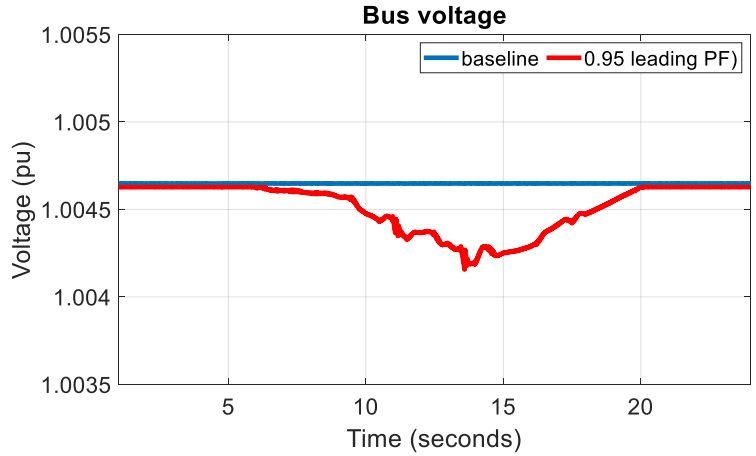

a) Bus voltage – 0.95 leading PF

Figure. 5.39. Bus voltage profiles - actual irradiance

5.6.3 Transient voltage stability analysis

The final part of this study, transient voltage stability in the time domain will be observed. The ability of the network to control and maintain voltages after a fault is referred to as transient voltage stability (Viawan, 2008). A single-phase fault was initiated at t = 8 seconds on bus 742 and the fault is cleared at 8.5 seconds.

Figure 5.40 shows the voltage profile on the DC bus. An increase in the DC bus measured voltage can be seen when the fault is initiated at 8 seconds. Figure 5.41 shows the RMS voltage at bus 742. The yellow phase voltage collapses to zero whilst decrease in the red phase can be observed. Figures 5.42 and 5.43 show the voltage and current waveforms where the impact on the yellow and red phases can be observed.

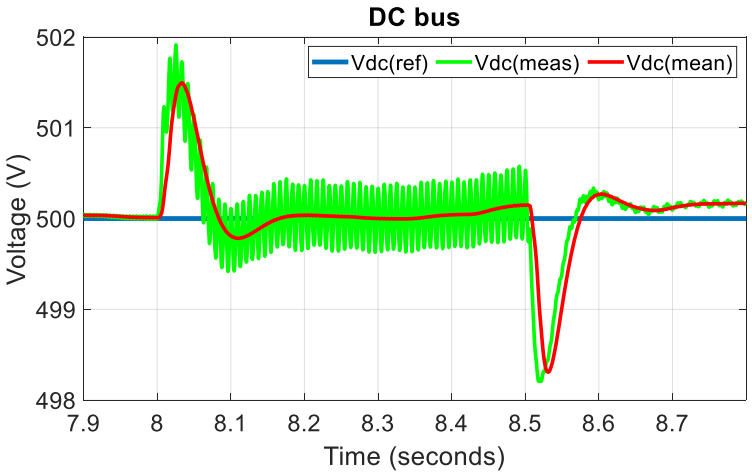

Figure 5.40. DC bus voltage

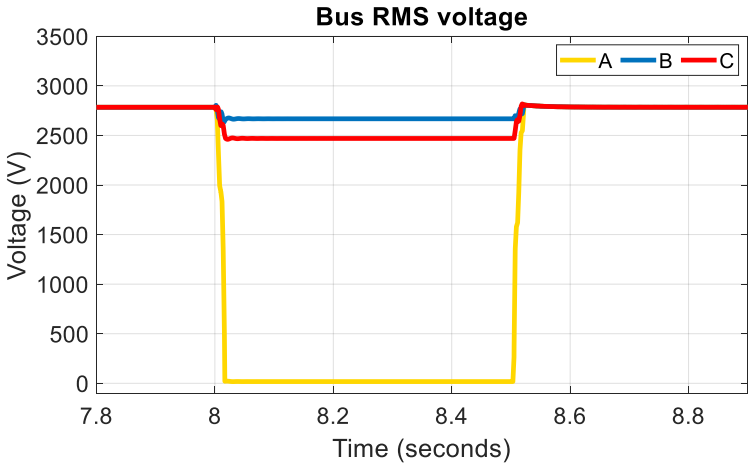

Figure 5.41. Bus 742 – RMS voltage

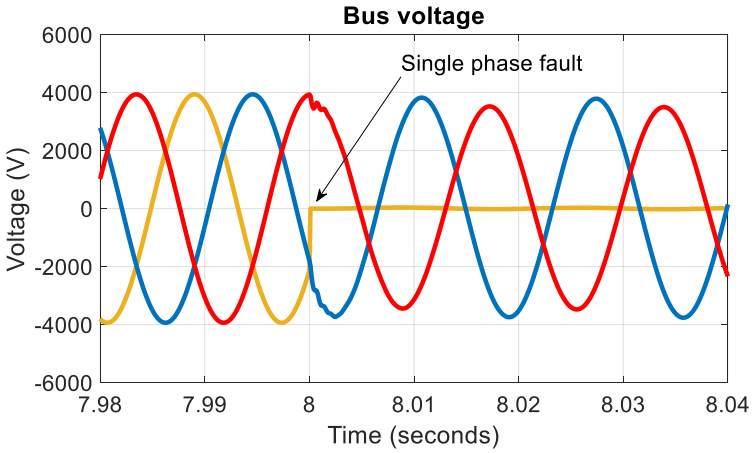

Figure 5.42. Bus 742 - voltage profile

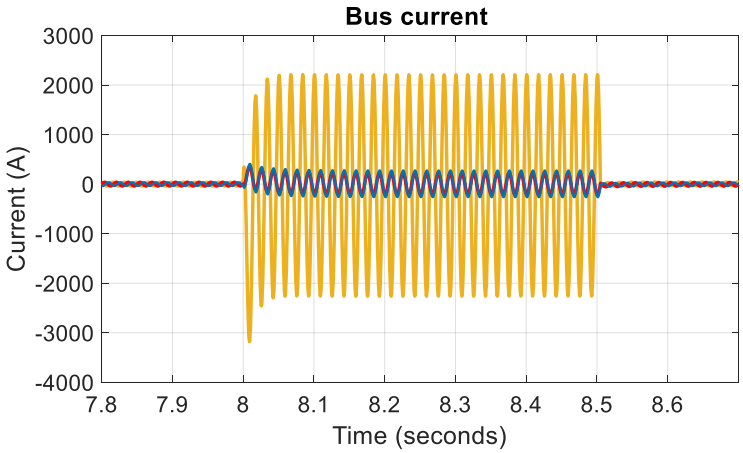

Figure 5.43. Bus 742 – current profile

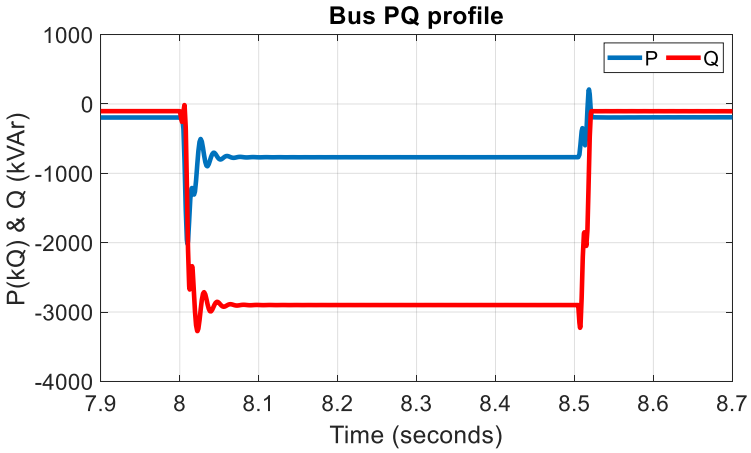

Figure 5.44. Bus 742 – PQ profile

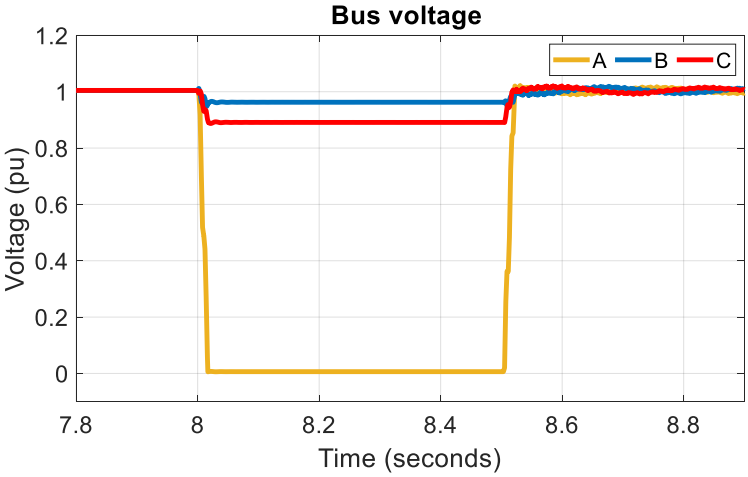

Figure 5.45. Bus 742 – voltage profile (pu)

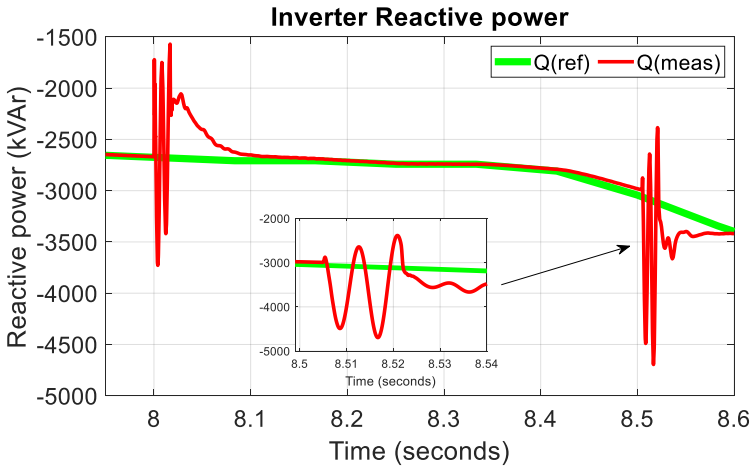

Figure 5.46. Inverter reactive power profile

To maintain the refence voltage, the inverter, produces reactive power as illustrated in Figure 5.46 to compensate for the drop in active power.

5.7 Summary

In this chapter, the development of a simulation platform to perform real-time testing was described. A residential 6.5kW solar PV rooftop model was developed and modelled in Simulink®. The standard 37 IEEE test feeder was selected to test the developed PV system, but due to constraints was reduced to a 10 buses system. The modified feeder, which includes one solar PV consisting of several 6.5kW systems was modelled in Simulink®. The selected real-time software and hardware were presented and discussed. The modified feeder was developed in OPAL-RT, the selected real-time simulation tool. The results, which focused on voltage control at the local bus using the real-time simulator was presented based on steady state and transient voltage stability analysis.

CHAPTER SIX
DISCUSSION, RECOMMENDATION & CONCLUSION

6.1 Thesis summary

The thesis started with a statement regarding the projected demand for electricity by 2050 and the need for alternative energy sources to meet this demand. It highlighted the importance of RE adoption but questioned the current infrastructure in South African distribution networks to deal with technical challenges that will be imposed by the future network. It was hypothesized that technical challenges such as voltage control problems, which is caused by DER can be mitigated by using its reactive power capability. A summary of each chapter is given below.

Chapter 1 introduced the study. An awareness of the research problem and rationale was given. It was assumed that the voltage control problem, which will be created by DER adoption can be mitigated by a coordinated operation and integration of these devices in the future. The aim and objectives were defined, which form the basis of this study. The chapter concluded with the thesis contribution and the chapter outline.

Chapter 2 presented a comprehensive review of voltage control in distribution networks based on control techniques, strategies, and optimization methods. The chapter starts with an overview of distributed energy resources. Voltage control strategies, which include centralized, decentralized, and local strategies were discussed. A comparison between centralized and decentralized control suggests that there are merits in using both. In South Africa, the control strategy is predominantly centralized with no distribution level control. Inverter-based DER, especially solar PV below 100kVA has zero control functionality. The chapter concluded with a summary of the reviewed literature.

Chapter 3 presented a mathematical description of the voltage control problem in conventional distribution networks and distribution systems with DER. It started with a mathematical illustration of a simple voltage drop calculation in distribution networks, followed by a centralized system using OLTC transformers at the substation. Feeder-level control with shunt capacitors and step voltage regulators were presented with an illustration of the effect of these devices on the voltage profile. Lastly, mathematical formulae were presented based on local control with DER. Two methods of local control i.e., power factor and voltage adaptive control were reviewed. The chapter concluded with a summary of conventional control with VVC devices compared to inverter-based DER.

Chapter 4 presented the development and simulation of a test feeder for an off-line simulation platform. The chapter started with the selection of the software for the simulation followed by the description of the test feeder. The phasor solution method was selected as the study was mainly concerned with changes in magnitude and phase of all voltages and currents. Phasor models of variable loads, solar PV and Wind Energy were developed and tested on the modified IEEE 13-bus feeder. Power factor control for solar PV and Wind energy was selected to inject or absorb reactive power based on the voltage profile at the substation or the local bus. These were based on unity, 0.98 and 0.95PF. The simulation results were presented based on various power factor scenarios. The impact of controlling reactive power on the OLTC transformer was presented.

Chapter 5 presented the development of a simulation platform for real-time testing. A test feeder was developed based on IEEE 37-bus test feeder. This feeder included the development and testing of a typical 6.5kW residential solar PV rooftop system. OPAL-RT, who is the leading exponent of real-time simulation was selected to perform real-time simulations. Due to the target's constraints, only a section of the original network was modelled. This reduced the CPU usage from 100% to 58% and the overruns to 0. The simulations were conducted, and conclusions presented.

Chapter 6 gives a summary of the thesis, includes a discussion of the aim and objectives, and draws the overall conclusion.

6.2 Aim and objectives-based discussion.

The aim of this research was to develop a testbed to study existing and improved voltage control strategies in real-time based on future scenarios in local distribution networks. To accomplish this, a few objectives were outlined, which considers existing control strategies based on the Grid Code for interconnecting DER. The study sought, found to and recommended improved voltage control strategies based on future scenarios in local distribution networks.

Objective 1 - literature review on voltage control in active distribution networks with respect to control techniques, strategies, and optimization methods.

A total of 151 references were considered for the review of which 96 scientific papers specifically dealt with the voltage control problem. The literature reviewed was divided into 3 sub-sections i.e., control strategies, control with demand-side resource and optimization methods. The control strategies were classified as communication-based or autonomous, where the former is reliant on a communication link and the latter on a local decision-making

strategy. Prior to the development of smart technologies, most utilities used a central control strategy, where control was executed at the substation using conventional devices such using OLTC transformers and shunt capacitors. Centralized control, was the focus of most of the reviewed literature. The last decade saw the deployment of DER, which shifted the focus to a decentralized strategy. Conventional devices are mechanical with time delays, which have a slower response time to voltage fluctuations than electronic-based devices. Optimization methods were classified as conventional and intelligent or heuristic. Heuristic-based techniques were used to deal with the inefficiencies of conventional methods. Various studies used PSO based on its simplicity and shorter computational time with a fast conversion rate. The algorithm was highly effective in dealing with large-scale non-linear optimization problems. The literature showed that voltage control can be achieved using demand-side resources. These were subdivided into distributed generation, distributed storage, and demand response. Most of the papers used solar PV or wind or a combination of both. Reactive power control or active power curtailment proved to be a common method to deal with the voltage control problem. It was proven that placement of reactive power devices at predetermined locations in distribution systems, especially along the feeder or at the end of the feeder, prevents voltage instability. Twenty-three papers dealt with voltage control, using demand response. From the reviewed papers, it was proven that DR could be an effective tool to deal with voltage control problems but depends on 2-way communication between the utility and the customer. Most of the studies used a centralized control strategy. For storage devices, most of the reviewed papers, focused on active and reactive power set points for voltage control. Various studies used storage devices for peak load shaving and to regulate voltage through active power injection and absorption.

The work in this chapter resulted in the publication by the author, titled "Voltage control in future electrical distribution networks" published in Renewable and Sustainable Energy Reviews, Volume 146, August 2021.

Objective 2 - Give an overview of local control strategies. Identify specific gaps and opportunities in the current control strategy in the South African distribution grid.

The South African transmission and distribution system is characterised by a centralized unidirectional, demand driven control. Control at generation and transmission level is well defined and equipped with intelligent control. In contrast, the distribution network has no intelligent control. Control is restricted to the HV/MV substation based on a centrally controlled strategy using OLTC transformers and substation shunt capacitors. The South African Grid Code sets out the grid connection requirement for distributed energy resources. This code places restrictions on control functions for DER with a power output of less than 100kVA. This restriction limits the participation of domestic and light commercial rooftop solar PV for voltage

regulation. The code recommends that DER with a capacity less than 100kVA should operate at a power factor greater than 0.98, hence preventing the use for reactive power control and any participation in voltage regulation.

International studies show that distribution level control, where DER contribute to voltage using reactive power regulation is a realistic solution for the future grid. This proposition requires further analysis and exploration. The advancement in technology, especially smart inverters and lessons learnt from international studies makes this a viable option given the projected DER adoption rate. A decentralized control strategy, using the reactive power capability of smart inverters has been identified as a possible solution to deal with the voltage control problem in the future South African grid. This eliminates the use of communication cables, which are required for centralized control. Active power curtailment has shown some benefit but does not incentives owners of the rooftop system. By varying the power factor of smart inverters, reactive power can be injected or absorbed depending on the load fluctuation.

Objective 3 - Mathematical overview of distribution level voltage control with conventional voltage control devices and DER control.

A mathematical overview is given of voltage control in power grid by controlling reactive power flow. The chapter started with an overview of the computation of voltage drop in a conventional network. Thereafter, a mathematical overview was given of voltage control using conventional devices and inverter-based DER. Conventionally, devices such as OLTC transformers and shunt capacitors are used at the substation based on a centralised control strategy. For feeder-level control, shunt capacitors and step voltage regulators are used on long overhead lines. The simulation shows that a time-based or voltage-based controlled capacitor switching strategy can be effective to regulate the voltage at the busbar on long feeders and reduce the number of OLTC tap switching. The response time to voltage caused by load fluctuations and intermittent DER devices is a drawback. For local control, inverter-based DER can be more effective in providing a faster response time to voltage fluctuations. Whilst DER connected to the grid raises the network voltage, a control strategy can be used to mitigate the latter. Power factor and voltage adaptive control strategy was introduced as a possible solution. For the former, unity, fixed and scheduled PF was presented. For the latter, a mathematical overview of Q/V and P/V droop control was presented.

Objective 4 – Development and simulation of a test feeder to study electromechanical oscillations based on the phasor solution method.

To prove the hypothesis, a test network was developed. The test network was based on the standard IEEE 13 bus test feeder but modified to include variable loads, solar PV, and Wind energy. The original test feeder is characterized by a three-wire radial configuration with a substation OLTC transformer, which acts as the substation voltage regulating device, static loads, and feeder shunt capacitors. Some of the static loads were converted to dynamic loads. The load profiles were based on actual residential measurements. The dynamic loads, solar PV and Wind energy systems were modelled as a controlled current source, which was fed by 1-D look-up tables in SIMULINK®. A power factor block was modelled and fed into the controlled current source of each dynamic component. In this way, the power factor of the solar PV and Wind system could be set to either inject or absorb reactive power. The phasor solution method was selected as the study was concerned with changes in current and voltage magnitudes only. The advantage of the phasor solution method is that a 24hour simulation period can be executed in less than 2 minutes.

Objective 5 – Propose control strategies using inverter-based DER to regulate the voltage at the central substation and local bus. Propose solutions to the voltage control problem in the future South African network.

The simulation of the test feeder was based on conventional control i.e., at the substation with OLTC transformers and shunt capacitors and with solar rooftop PV connected at each load. The PV and Wind penetration was based on future scenarios as projected by the Department of Energy in South Africa. The first part of the simulation focused on conventional control. The load profile was based on actual residential load data and showed a peak load demand during the morning and evening. The results show that only the substation bus voltage is within the upper and lower limit, i.e., 0.95 and 1.05pu. The other buses in the network have exceeded the lower limit. Substation shunt capacitors were used to raise the voltage at the substation busbar. For additional control, OLTC transformers are used to raise the voltage to 1.05pu. This ensures that the voltage at all the buses is within the required limit. OLTC are mechanical devices with time delays and response slower to load variations. The second part focused on control with inverter-based DER. For solar PV, 25% and 50% PV penetration showed a rise in the voltage profile during the low load consumption period during the midday. This low load demand coincides with the maximum PV production. All lagging power factors scenarios show an increase in the voltage profile during peak generation and an improvement in the lower limit. To mitigate the latter, the power factor of all PV inverters was changed to leading i.e., reactive power absorption. The results show an improvement in upper limit but with 50% penetration at 0.95PF, the voltage at some buses exceeded the lower limit, especially during the evening peaks but showed a major improvement in the upper limit. The substation voltage profile was within required limits, but other buses showed several violations. Scheduled power factor was

suggested to deal with the latter. Power factor was scheduled during the day when reactive power needed to be injected or absorbed. The results showed an improvement in the voltage profile. The best result was found at 50% penetration at 0.95 leading scheduled PF. For Wind energy only 25% and 50% penetration were considered. A similar approach to PV was followed for Wind energy. At 25% penetration, the voltage profiles at all the buses at 0.98 and 0.95PF including the substation bus, exceeded the upper limit. Based on the wind profile, peak generation occurred during the evening peak load consumption. Leading PF resulted in an improvement in the upper limit but at certain buses, the lower limit was exceeded, especially during the peak generation. Scheduled power factor resulted in an improvement in the lower limit. The best results were observed at 50% penetration with 0.95 scheduled leading power factor.

Using DER reactive power to regulate voltage profiles was successfully demonstrated. Scheduling power based on the load profile, maintained voltages within statutory limits. Injecting reactive power during high load demand and absorbing during low demand proved an effective strategy to limit voltage violations and reduce OLTC tap changes, simultaneously.

Objective 6 - Develop a simulation platform based on discrete models. Develop and model a 6.5kW grid-tied solar PV system with reactive power capability, which will be tested with OPAL-RT's real-time simulator.

A two-stage power conversion 6.5kW solar PV rooftop system was developed. The size was selected based on an average 5kW South African residential house. The system was oversized to allow reactive power to be injected or absorbed. The system consisted of a PV array, which was designed based a parallel/series configuration, DC/DC boost converter with a P&O MPPT algorithm. The boost converter was used to raise the PV array voltage from 275V to 500V. A step-by-step calculation of the boost converter input parameters was done. A two-level voltage source inverter, which converts the voltage generated by the PV array from DC to three-phase AC was selected. The final step was to design the inverter controller, which provided the input signal to the inverter. The inverter controller consisted of a PLL module, which measured the main grid phase voltage and controlled the PWM input to the inverter, a voltage, current, reactive power, and active power controller. All the controllers consist of a PI controller, where the output of the error signal between the measured and the reference voltage signal was used to generate the PI actions.

The developed solar PV model was added to the standard IEEE 37-bus test feeder and simulated in real-time, using OPAL-RT's real-time simulator. The initial results showed that the CPU core was running at 100% with major overruns. Due to constraints, it was decided to

reduce the network to 10 buses with 5 static loads. This reduced the CPU core loading to 58% with zero overruns. Reactive power control was achieved by providing an input reference signal to the reactive power controller, which is based on the output power profile. The amount of reactive power that was either injected or absorbed by the inverter was based on the power factor set-point. The power factor was set to 0.98 and 0.95 lagging for the first case based on 50% PV penetration. The voltage at the dc-link was kept constant but from the results, the voltage at the local bus saw an increase of 0.5% based on 0.95PF. This was expected as only 100kW and 32kVAr was injected into the network at bus 742. For the second case, the power factor was changed to 0.98 and 0.95 leading. The results show a marginal decrease in the local bus voltage. The study showed that the voltage profile can be improved by absorbing reactive power during low load demand and injecting reactive power during high load demand.

6.3 Recommendation

Based on future projections, renewable energy will have a greater contribution to the electricity mix in South Africa. The increasing number of DER connections will give rise to technical problems like over and under voltage, which should be addressed by network planners. The adoption of DER will be limited by voltage control in the future grid if not addressed properly. The location of these DERs and customer loads is expected to have an impact on network losses in the future. One of the major challenges is to incorporate these technical challenges into an optimization problem to minimize network losses and limit voltage deviations.

- Current scenario - The South African electricity grid is highly regulated. The National Energy Regular of South Africa (NERSA) is resposnible for the approval of various technical standards, which is formulated and implemented by Eskom and various municipalities. These standards provide guidelines for the safe connection of DER to the transmission and distribution network. The grid connection code, which is approved by NERSA is used for the interconnection of DER to the grid. The current power grid is designed to operate in a centralized manner with control executed at the substation. Under current regulations, DER with a power output less than 100 kVA are not allowed to participate in reactive power, power factor or voltage control. In the current context with no LV grid intelligence and low residential Solar PV rooftop penetrations, this may be acceptable, but in the future with high DER penetartion, the status quo will have to be revised.

- Future scenario - The Department of Energy (DoE), predicts that RE will contribute 38% towards the total energy mix by 2050. The current centralized control system will require a revision to incorporate the predicted RE contribution. Continous tap changers

may become detrimental to substation transformers and voltage regulators. Optimization techiques must be applied to deal with the voltage violations in the gid. A revision of the grid code is required to allow DER to particpate in voltage regulation at the local level. Decentralized control may be preferred as it does not require expensive communication and is able to provide much faster local voltage support. Reactive power management in LV distribution networks can be used to improve local voltage profiles using DER inverters. Control strategies should be implemented based on future EV adpotion to alleviate congestion on the grid.

- Real-time simulation – Continous experimental testing should be done to validate the physical network. Actual testing of the network is not possible as it may compromise the reliability of the grid. Testing small or large parts of the distribution network is not technically and economically feasible. It is for this reason that digital models are implemented to simulate real world scenarios. The digital models simulate actual electrical parameters based on the physical network. Traditionally, offline simulations are used, but these are slow and not able to simulate real-time conditions. Hardware in-the-loop (HIL), which is a FPGA-based (Field-Programmable Gate Arrays) closed loop real-time simulation technique, can bridge this gap. HIL uses digital real-time simulators, which are connected to real devices. HIL uses real hardware that operates in real-time to validate control systems in electrical networks. One of the main advantages is that it provides results with a high degree of accuracy. The development of a simulation platform for modelling a large network can be time consuming.

- Voltage control using Demand Response - DR programs could be an effective strategy implemented by local utilities to deal with peak demand, grid reliability and voltage violations. DR based on price increases or price incentive from the utility is designed to decrease overall consumption, decrease peak demand, and defer investment in large power plants. In the current generation supply crisis, DR could address grid stability problems and voltage violations in the distribution grid. DR strategies are gaining increasing popularity based on technological advances in advanced metering infrastructure (AMI) and smart appliances. The evolving distribution network in South Africa is based on greater customer involvement and two-way communication, which presents opportunities for effective DR programs. DR strategies, in respect of voltage control will be a significant concept in the future.

6.4 Overall conclusion

The power crisis in South Africa is driving the widespread adoption of renewable energy. Residential solar PV have been deployed to help mitigate the loss of supply. An increase in DER deployment, could lead to stability problems within the distribution grid, which must be mitigated. In the present South African grid, no grid intelligence exists at low voltage distribution level. The existing control strategy is based on unidirectional power flow and characterized by a centralized methodology. These conventional devices will be unable to respond fast and effectively to bidirectional power flow caused by DER. Under current regulation, only DER with an output power greater than 1 MVA can contribute to voltage regulation. Globally, various control strategies have been applied depending on the supply authority. From a cost saving perspective, decentralized control could be a better option for South Africa's distribution grid, given current financial limitations. It has been proven by this research that the reactive power capabilities of DER can be used to deal with voltage control problem in distribution grids. In the future grid, a coordinated approach between distributed level generation and storage in the local distribution network will be required to deal with voltage violations.

The increased penetration of RE over the next decade will necessitate the change of existing regulations, which are highly regulated by the National Energy Regulator (NERSA). In the future, with distribution level grid intelligence, small scale generation and storage will play a very active role in the local grid.

6.5 List of publications

1. Murray, W., Adonis, M. & Raji, A.: Voltage control in future electrical distribution networks. Renewable and Sustainable Energy Reviews, Vol.146, August 2021, 111100

2. Murray, W., Adonis, M. & Raji, A.: Voltage control in distribution networks using distributed energy resources. IET Renewable Power Generation (submitted – under review)

APPENDIX A

IEEE 13 Bus network data

Line Segment Data:

Node A	Node B	Length(ft.)	Config.
632	645	500	603
632	633	500	602
633	634	0	XFM-1
645	646	300	603
650	632	2000	601
684	652	800	607
632	671	2000	601
671	684	300	604
671	680	1000	601
671	692	0	Switch
684	611	300	605
692	675	500	606

Cable configuration parameters:

```
% miles/km
mi2km = 1.609344;

% feet to km
ft2km = 0.0003048;

% micro Siemens to Farads
ms2F = 1/2/pi/60*1e-6;

% configuration 601
R_601 = [0.3465 0.1560 0.1580; 0.1560 0.3375 0.1535; 0.1580 0.1535
0.3414];
X_601 = [1.0179 0.5017 0.4236; 0.5017 1.0478 0.3849; 0.4236 0.3849
1.0348];
L_601 = X_601/2*pi*60;
B_601 = [6.2998 -1.9958 -1.2595; -1.9958 5.9597 -0.7471; -1.2595 -
0.7417 5.6386];
C_601 = B_601*1e-6/2*pi*60/2;

% configuration 602
R_602 = [0.7526 0.1580 0.1560; 0.1580 0.7475 0.1535; 0.1560 0.1535
0.7436];
X_602 = [1.1814 0.4236 0.5017; 0.4236 1.1983 0.3849; 0.5017 0.3849
1.2112];
L_602 = X_602/2*pi*60;
B_602 = [5.6990 -1.08817 -1.6905; -1.08817 5.1795 -0.6588; -1.605 -
0.6588 5.4246];
C_602 = B_602*1e-6/2*pi*60/2;
```

```
% configuration 603
R_603 = [0.00 0.00 0.00; 0.00 1.3294 0.2066; 0.00 0.2066 1.3238];
X_603 = [0.00 0.00 0.00; 0.00 1.3471 0.4591; 0.00 0.4590 1.3569];
L_603 = X_603/2*pi*60;
B_603 = [0.00 0.00 0.00; 0.00 4.7097 -0.8999; 0.00 -0.8999 4.6650];
C_603 = B_603*1e-6/2*pi*60/2;

% configuration 604
R_604 = [1.3238 0.00 0.2066; 0.00 0.00 0.00; 0.2066 0.00 1.3294];
X_604 = [1.3569 0.00 0.4591; 0.00 0.00 0.00; 0.4591 0.00 1.3471];
L_604 = X_604/2*pi*60;
B_604 = [4.6658 0.00 -0.8999; 0.00 0.00 0.00; -0.8999 0.00 4.7097];
C_604 = B_604*1e-6/2*pi*60/2;

% configuration 605
R_605 = [0.00 0.00 0.00; 0.00 0.00 0.00; 0.00 0.00 1.3292];
X_605 = [0.00 0.00 0.00; 0.00 0.00 0.00; 0.00 0.00 1.4212];
L_605 = X_605/2*pi*60;
B_605 = [0.00 0.00 0.00; 0.00 0.00 0.00; 0.00 0.00 4.3637];
C_605 = B_605*1e-6/2*pi*60/2;

% configuration 606
R_606 = [0.7982 0.3192 0.2849; 0.3192 0.7891 0.3192; 0.2849 0.3192
0.7982];
X_606 = [0.4463 0.0328 -0.0143; 0.0328 0.4041 0.0328; -0.0143 0.0328
0.4463];
L_606 = X_606/2*pi*60;
B_606 = [96.8897 0.00 0.00; 0.00 0.00 0.00; 0.00 0.00 0.00];
C_606 = B_605*1e-6/2*pi*60/2;

% configuration 607
R_607 = [1.3425 0.00 0.00; 0.00 0.00 0.00; 0.00 0.00 0.00];
X_607 = [0.512 0.000 0.00; 0.00 0.00 0.000; 0.00 0.00 0.00];
L_607 = X_607/2*pi*60;
B_607 = [889912 0.00 0.00; 0.00 0.00 0.00; 0.00 0.00 0.00];
C_607 = B_607*1e-6/2*pi*60/2;
```

APPENDIX B

IEEE 37 Bus network data

Line Segment Data:

Bus A	Bus B	Length(ft.)	Config.
701	702	960	722
702	705	400	724
702	713	360	723
702	703	1320	722
703	727	240	724
703	730	600	723
704	714	80	724
704	720	800	723
705	742	320	724
705	712	240	724
706	725	280	724
707	724	760	724
707	722	120	724
708	733	320	723
708	732	320	724
709	731	600	723
709	708	320	723
710	735	200	724
710	736	1280	724
711	741	400	723
711	740	200	724
713	704	520	723
714	718	520	724
720	707	920	724
720	706	600	723
727	744	280	723

Cable configuration parameters:

```
% miles/km
mi2km = 1.609344;

% feet to km
ft2km = 0.0003048;

% micro Siemens to Farads
ms2F = 1/2/pi/60*1e-6;

%configuration 721
R_config_721 = [0.2926 0.0673 0.0337; 0.0673 0.2646 0.0673; 0.0337
0.0673 0.2926];
X_config_721 = [0.1973 0.0368 0.0417; 0.0368 0.1900 0.0368; 0.0417
0.0368 0.1973];
B_config_721 = [159.7919 0.0000 0.0000; 0.0000 159.7919 0.0000;
0.0000 0.0000 159.7919];
R_721 = R_config_721/mi2km;
L_721 = X_config_721/mi2km/2/pi/60;
C_721 = B_config_721/mi2km*ms2F;

%configuration 722
R_config_722 = [0.4751 0.1629 0.1234; 0.1629 0.4488 0.1629; 0.1234
0.1629 0.4751];
X_config_722 = [0.2973 0.0326 0.0607; 0.0326 0.2678 0.0326; 0.0607
0.0326 0.2973];
B_config_722 = [159.7919 0.0000 0.0000; 0.0000 159.7919 0.0000;
0.0000 0.0000 159.7919];
R_722 = R_config_722/mi2km;
L_722 = X_config_722/mi2km/2/pi/60;
C_722 = B_config_722/mi2km*ms2F;

%configuration 723
R_config_723 = [1.2936 0.4871 0.4585; 0.4871 1.3022 0.4871; 0.4585
0.4871 1.2936];
X_config_723 = [0.6713 0.2111 0.1521; 0.2111 0.6326 0.2111; 0.1521
0.2111 0.6713];
B_config_723 = [74.8405 0.0000 0.0000; 0.0000 74.8405 0.0000;0.0000
0.0000 74.8405];
R_723 = R_config_723/mi2km;
L_723 = X_config_722/mi2km/2/pi/60;
C_723 = B_config_723/mi2km*ms2F;

%configuration 724
R_config_724 = [2.0952 0.5204 0.4926; 0.5204 2.1068 0.5204; 0.4926
0.5204 2.0952];
X_config_724 = [0.7758 0.2738 0.2123; 0.2738 0.7398 0.2738; 0.2123
0.2738 0.7758];
B_config_724 = [60.2483 0.0000 0.0000; 0.0000 60.2483 0.0000;0.0000
0.0000 60.2483];
R_724 = R_config_724/mi2km;
L_724 = X_config_722/mi2km/2/pi/60;
C_724 = B_config_723/mi2km*ms2F;
```

Spot load Data:

Bus	Load model	P(kW)	Q(kVAr)
701	D-PQ	350	175
712	D-PQ	85	40
713	D-PQ	85	40
727	D-PQ	42	21
742	D-Z	200	100

REFERENCES

Abdmouleh, Z., Gastli, A., Ben-brahim, L., Haouari, M., & Al-emadi, N. A. (2017). Review of optimization techniques applied for the integration of distributed generation from renewable energy sources. *Renewable Energy*, *113*, 266–280.

Abessi, A., Vahidinasab, V., & Ghazizadeh, M. S. (2016). Centralized Support Distributed Voltage Control by Using End-Users as Reactive Power Support. *IEEE Transactions on Smart Grid*, *7*(1), 178–188.

Abraham, E., Marzooghi, H., & Terzija, V. (2017). Assessment of OLTC Contributions to Voltage Controlled Demand Response Using Structural Equation Models. *2017 IEEE Manchester PowerTech*, 1–6.

Akorede, M. F., Hizam, H., & Pouresmaeil, E. (2010). Distributed energy resources and benefits to the environment, *Renewable and Sustainable Energy Reviews* 14, 724–734.

Anderson, K., & Narayan, A. (2011). Simulating Integrated Volt / Var Control and Distributed Demand Response Using GridSpice. *2011 IEEE First International Workshop on Smart Grid Modeling and Simulation (SGMS)*, 84–89.

Antoniadou-plytaria, K. E., Kouveliotis-lysikatos, I. N., Georgilakis, P. & Hatziargyriou, N. D. (2017). Distributed and Decentralized Voltage Control of Smart Distribution Networks : Models , Methods , and Future Research. *IEEE Transactions on smart Grid*, *8*(6), 2999–3008.

Arshad, A., Ekström, J., & Lehtonen, M. (2018). Multi-agent based distributed voltage regulation scheme with grid-tied inverters in active distribution networks. *Electric Power Systems Research*, *160*, 180–190.

Azzopardi, B. (2017). *Sustainable Development in Energy Systems.*Cham: Springer.

Bagher, S. M., Moshtagh, J., Shafie-khah, M., & Catalão, J. P. S. (2018). Smart distribution system operational scheduling considering electric vehicle parking lot and demand response programs. *Electric Power Systems Research*, *160*, 404–418.

Bahramipanah, M., Cherkaoui, R., & Paolone, M. (2016). Decentralized voltage control of clustered active distribution network by means of energy storage systems. *Electric Power Systems Research*, *136*, 370–382.

Bansal, R. (2017). Handbook of Distributed Generation. Cham: Springer International Publishing

Basak, P., Chowdhury, S., Halder, S., & Chowdhury, S.P (2012). A literature review on integration of distributed energy resources in the perspective of control , protection and stability of microgrid. Renewable & Sustainable Energy Reviews, 16(8):5545–5556.

Bayat, M., Sheshyekani, K., Member, S., & Hamzeh, M. (2016). Coordination of Distributed Energy Resources and Demand Response for Voltage and Frequency Support of MV Microgrids. *IEEE Transactions on Power Systems*, *31*(2), 1506–1516.

Bayliss, C. & Hardy, B. (2012). T*ransmission and Distribution Electrical Engineering*, Fourth Edition. Oxford: Newnes

Beaude, O., He, Y., Hennebel, M. (2013). Introducing Decentralized EV Charging Coordination for the Voltage Regulation, 6–10. 2013 4th IEEE PES Innovative Smart Grid Technologies Europe (ISGT Europe), October 6-9, Copenhagen.

Bedawy, A., & Mahmoud, K. (2017). *Optimal Decentralized Voltage Control in Unbalanced Distribution Networks with High PV Penetration*. Nineteenth International Middle East Power Systems Conference (MEPCON), Menoufia University, Egypt, 19-21 December 2017

Behravesh, V., Keypour, R., & Foroud, A. A. (2019). Control strategy for improving voltage quality in residential power distribution network consisting of roof-top photovoltaic-wind hybrid systems , battery storage and electric vehicles. *Solar Energy*, *182*(June 2018), 80–95.

Berger L.R., Iniewski K. (2012). *Smart Grid Applications, Communications and Security:* John Wiley & Sons: New Jersey

Beucher, O & M. Weeks, M. (2006). *Introduction to MATLAB & SIMULINK: A Project Approach*, Third Edition, Infinity Science Press.

Bode, O., Shigenobu, R., Ooya, K., Senjyu, T., & Motin, A. (2019). Static voltage stability improvement with battery energy storage considering optimal control of active and reactive power injection. *Electric Power Systems Research*, *172*(October 2018), 303–312.

Byrski, A., Kisiel-Dorohinicki, M. (2017). *Evolutionary Multi-Agent Systems*; From Inspirations to Applications. Cham: Springer.

Budka, K.C., Deshpande, J.G., Thottan, M. (2014. Communication Networks for Smart Grids: Making Smart Grid Real, London: Springer.

Cagnano, A., & Tuglie, E. De. (2015). Centralized voltage control for distribution networks with embedded PV systems. *Renewable Energy*, *76*, 173–185.

Cagnano, A., & Tuglie, E. De. (2016). A decentralized voltage controller involving PV generators based on Lyapunov theory. *Renewable Energy*, *86*, 664–674.

Calderaro, V., Conio, G., Galdi, V., Massa, G., & Piccolo, A. (2014). Optimal Decentralized Voltage Control for Distribution Systems With Inverter-Based Distributed Generators. *IEEE Transactions on Power Systems*, *29*(1), 230–241.

Calderaro, V., Conio, G., Galdi, V., & Piccolo, A. (2012). Reactive power control for improving voltage profiles : A comparison between two decentralized approaches. *Electric Power Systems Research*, *83*(1), 247–254.

Caples, D., Boljevic, S., & Conlon, M. F. (2011). Impact of Distributed Generation on Voltage Profile in 38kV Distribution System. *8th International Conference on the European Energy Market (EEM), Zagreb, Croatia*, (May,2011), 532–536

Cardona, J. E., López, J. C., & Rider, M. J. (2018). Decentralized electric vehicles charging coordination using only local voltage magnitude measurements. *Electric Power Systems Research*, *161*, 139–151.

Carter-Brown, C.G. Network planning guideline for MV shunt capacitors, DST 34-598. Eskom controlled document; 2010

Chand, J., Pramod, B., Singh, K., & Pal, N. R. (2019). *Evolutionary and Swarm Intelligence Algorithms*. Cham: Springer.

Chicco, G., & Mancarella, P. (2009). Distributed multi-generation : A comprehensive view. *Renewable and Sustainable Energy Reviews*, *13,* 535–551.

Chowdhury, S., Chowdhury, P., Crossley, P. (2009). *Microgrids and Active Distribution Networks*. London; The Institution of Engineering and Technology.

Christakou, K., Tomozei, D., & Boudec, J. Le. (2014). GECN : Primary Voltage Control for Active Distribution Networks via. *IEEE Transactions on Smart Grid*, *5*(2), 622–631.

Civicioglu, P., Beshok, A. A conceptual comparison of the Cuckoo-search, particle swarm optimization, differential evolution and artificial bee colony algorithms, Springer. 2014; 315-346

Colgren, R. (2007). *Basic MATLAB, Simulink, and Stateflow,* American Institute of Aeronautics and Astronautics, Inc.

Das, C. K., Bass, O., Kothapalli, G., Mahmoud, T. S., & Habibi, D. (2019). Overview of energy storage systems in distribution networks : Placement , sizing , operation , and power quality. *Renewable and Sustainable Energy Reviews,* 91 (2018) 1205–1230.

Davarzani, S., Pisica, I., & Taylor, G. A. (2015). Energy management in a demand response framework for efficient voltage control and distribution automation. *2015 50th International Universities Power Engineering Conference (UPEC)*, 1–6.

Davarzani, S., Pisica, I., & Taylor, G. A. (2017). Development of a Novel Multi-Agent System for Residential Voltage Control Using Demand Response based on Customer Behaviour. *IEEE Transaction on Power Systems*, 0–5.

Diaz, I., Szczesny, I., Pillai, J. R. & Bak-Jensen, B. (2016). Demand Response Control in Low Voltage Grids for Technical and Commercial Aggregation Services. *IEEE Transactions on Smart Grid*, *7*(6), 2771–2780.

DOE. (2017). Strategic National Smart Grid Vision for the South African Electricity Supply Industry. Department of Energy, Pretoria.

DOE. (2018). Integrated Resource Plan 2018. Department of Energy, Pretoria.

Dong, X., Mu, Y., Xu, X., Jia, H., Wu, J., & Yu, X. (2018). A charging pricing strategy of electric vehicle fast charging stations for the voltage control of electricity distribution networks. *Applied Energy*, *225*(92), 857–868.

Dong, Y., Xie, X., Shi, W., Zhou, B. & Jiang, Q. (2018). Demand-Response-Based Distributed Preventive Control to Improve Short-Term Voltage Stability. *IEEE Transactions on Smart Grid*, *9*(5), 4785–4795.

Dreo, J., Petrowski, A., Siarry, P., Taillard, E., H. (2006). Metaheuristics for Hard Optimization: Methods and Case Studies. Berlin: Springer.

Du, P & Lu, N. (2015). Energy Storage for Smart Grids: Planning and Operation for Renewable and Variable Energy Resources (VERs). London: Academic Press.

Dubey, S., Sarvaiya, J.N, Seshadri, B. Temperature Dependent Photovoltaic (PV) Efficiency and Its Effect on PV Production in the World A Review. Energy Procedia 33 (2013) 311 – 321

Efkarpidis, N., Rybel, T. De, & Driesen, J. (2016). Sustainable Energy , Grids and Networks Technical assessment of centralized and localized voltage control strategies in low voltage networks. *Sustainable Energy, Grids and Networks*, *8*, 85–97.

Ekanayake, J.,Wu, J., Jenkins, N., Liyanage, K., & Akihiko Yokoyama, A. (2012). Smart Grid: Technology and Applications. John Wiley & Sons © 2012

Enang, W., & Bannister, C. (2017). Modelling and control of hybrid electric vehicles (A comprehensive review). *Renewable and Sustainable Energy Reviews*, *74*(August 2016), 1210–1239.

Fallahzadeh-abarghouei, H., Hasanvand, S., & Nikoobakht, A. (2018). Decentralized and hierarchical voltage management of renewable energy resources in distribution smart grid. *Electrical Power and Energy Systems*, *100*(August 2017), 117–128.

Farina, M., Guagliardi, A., Mariani, F., Sandroni, C., & Scattolini, R. (2015). Control Engineering Practice Model predictive control of voltage pro fi les in MV networks with distributed generation. *Control Engineering Practice*, *34*, 18–29.

Fazio, A. R. Di, Fusco, G., & Russo, M. (2013). Decentralized Control of Distributed Generation for Voltage Pro fi le Optimization in Smart Feeders. *IEEE Transactions on Smart Grid*, *4*(3), 1586–1596.

Feng, C., Li, Z., Shahidehpour, M., Wen, F., Liu, W. & Wang, X. (2018). Decentralized Short-Term Voltage Control in Active Power Distribution Systems. *IEEE Transactions on Smart Grid*, *9*(5), 4566–4576.

Feshki, H. (2017). Improving voltage unbalance of low-voltage distribution networks using plug-in electric vehicles Customer Point of Connection. *Journal of Cleaner Production*, *148*, 336–346.

Funabashi, T. (2016). Integration of Distributed Energy Resources in Power Systems: Implementation, Operation, and Control. Amsterdam: Academic Press

Gers, J.M. (2014). Distribution System Analysis and Automation. Stevenage: The Institution of Engineering and Technology

Gelazanskas, L., & Gamage, K. A. A. (2014). Demand side management in smart grid : A review and proposals for future direction. *Sustainable Cities and Society,* 11 (2014) 22–30.

Gilson, G., & Ferreira, P. (2019). Review and Assessment of the Different Categories of Demand Response Potentials. *Energy*, (2019).

GreenCape. (2019). *Electric Vehicles 2019 Market Intelligence Report*. https://www.greencape.co.za/assets/Uploads/ELECTRIC-VEHICLES-MARKET-INTELLIGENCE-REPORT-WEB4.pdf

Gu, W., Lou, G., Tan, W., & Yuan, X. (2017). A Nonlinear State Estimator-Based Decentralized Secondary Voltage Control Scheme for Autonomous Microgrids. *IEEE Transactions on Power Systems*, *32*(6), 4794–4804.

Guo, D., Zheng, R., Lin, Z., & Yan, G. (2016). A game-theoretic approach to decentralized control of heterogeneous load population. *Electric Power Systems Research*, *140*, 552–559.

Guo, Y., Fang., Khargonekar, P.P. (2017). *Stochastic Optimization for Distributed Energy Resources in Smart Grids*. Cham: Springer

Haque, A. N. M. M., Nguyen, P. H., Vo, T. H., & Bliek, F. W. (2017). Agent-based unified approach for thermal and voltage constraint management in LV distribution network. *Electric Power Systems Research*, *143*, 462–473.

Hashemi, S., Aghamohammadi, M. R., & Sangrody, H. (2018). Restoring desired voltage security margin based on demand response using load-to-source impedance ratio index and PSO. *Electrical Power and Energy Systems*, *96*(October 2017), 143–151.

Hassaine, L., Olias, E., Quintero, J., & Haddadi, M. (2009). Digital power factor control and reactive power regulation for grid-connected photovoltaic inverter. Renewable Energy *34*, 315–321.

He, Y., & Petit, M. (2016). Valorization of Demand Response for Voltage Control in MV Distribution Grids with distributed generation, *IEEE Transactions on Power Systems*, (1).

Horoufiany, M. (2012). The Management of Distributed Energy Resources for Voltage Control in Smart Grids. *20th Iranian Conference on Electrical Engineering (ICEE2012)*, 462–466.

Howlader, A. M., Sadoyama, S., Roose, L. R., & Sepasi, S. (2018). Distributed voltage regulation using Volt-Var controls of a smart PV inverter in a smart grid : An experimental study. *Renewable Energy*, *127*, 145–157.

IEA (2018). World Energy Outlook 2018. International Energy Agency, Paris

Islam, S. R., Muttaqi, K. M. & Sutanto, D. (2015). A Decentralized Multiagent-Based Voltage Control for Catastrophic Disturbances in a Power System. *IEEE Transactions on Industry Applications*, *51*(2), 1201–1214.

IRENA. (2017). *Electricity Storage and Renewables: Cost and Markets to 2030.* Interntional Renewable Energy Agency, Abu Dhabi

Islam, S. R & Sutanto, D. (2015). Coordinated Decentralized Emergency Voltage and Reactive Power Control to Prevent Long-Term Voltage Instability in a Power System. *IEEE Transactions on Power Systems*, *30*(5), 2591–2603.

Jamroen, C., Pannawan, A., & Sirisukprasert, S. (2018). Battery Energy Storage System Control for Voltage Regulation in Microgrid with High Penetration of PV Generation. *2018 53rd International Universities Power Engineering Conference (UPEC)*, 1–6.

Jenkins, N., Ekakanayake, J.B., Strabac, G. (2010). *Distributed Generation*. London: The Institute of Engineering and Technology

Ji, H., Wang, C., Li, P., Zhao, J., Song, G., Ding, F., & Wu, J. (2018). A centralized-based method to determine the local voltage control strategies of distributed generator operation in active distribution networks. *Applied Energy*, *228*(June), 2024–2036.

Jiongcong, C., Nanhua, Y., Xiaoping, Z., & Xudong, S. (2014). Coordinate Voltage Control In Active Distribution Network. *International Conference on Power System Technology (POWERCON 2014) Chengdu*, (2012), 20–22.

Joelle, Lady, Torre, C. Dela, & Pedrasa, M. A. A. (2016). Decentralized Voltage Control for Distribution Networks with High Penetration of Distributed Generators. *2016 IEEE Innovative Smart Grid Technologies - Asia (ISGT-Asia)*, 636–641.

Jordehi, A. R. (2019). Optimisation of demand response in electric power systems , a review. *Renewable and Sustainable Energy Reviews*, *103*(January), 308–319.

Juelsgaard, M., Sloth, C., & Wisniewski, R. (2014). *Loss Minimization and Voltage Control in Smart Distribution Grid*. *IFAC Proceedings Volumes* (Vol. 47). IFAC.

Jung, J., Onen, A., Arghandeh, R., & Broadwater, R. P. (2014). Coordinated control of automated devices and photovoltaic generators for voltage rise mitigation in power distribution circuits. *Renewable Energy*, *66*, 532–540.

Kabir, M. N., Mishra, Y., Ledwich, G., Xu, Z., & Bansal, R. C. (2014). Improving voltage profile of residential distribution systems using rooftop PVs and Battery Energy Storage systems. *Applied Energy*, *134*, 290–300.

Kadurek, P., Sarab, M. M., Cobben, J. F. G., & Kling, W. L. (2012). Assessment of Demand Response Possibilities by Means of Voltage Control with Intelligent MV / LV Distribution Substation. *2012 IEEE Power and Energy Society General Meeting*, 1–6.

Kakran, S., & Chanana, S. (2018). Smart operations of smart grids integrated with distributed generation : A review. *Renewable and Sustainable Energy Reviews*, *81*(August 2017), 524–535.

Karthikeyan, N., Pokhrel, B. R., Pillai, J. R., Bak-jensen, B., & Frederiksen, K. H. B. (2017). Demand Response in Low Voltage Distribution Networks with High PV Penetration. *IEEE Transactions on Power Systems,* (1-6)

Karris, S. T. (2011). Introduction to Simulink with Engineering Applications, Third Edition, Orchard Publications.

Kawamura, K. (2013). Applicability of Demand Response to Voltage Control in a Distribution System with Large Integration of Rooftop PV. *2013 IEEE Energytech*, 1–6.

Kennedy, J., Ciufo, P., & Agalgaonkar, A. (2016). Voltage-based storage control for distributed photovoltaic generation with battery systems. *Journal of Energy Storage*, *8*, 274–285.

Khalid, K., Ullah, S., Lee, S., Maqsood, Z., Kashif, M., & Kim, C. (2018). Electrical Power and Energy Systems A real-time optimal coordination scheme for the voltage regulation of a distribution network including an OLTC , capacitor banks , and multiple distributed energy resources. *International Journal of Electrical Power and Energy Systems*, *94*, 1–14.

Kim, I. (2017). A case study on the effect of storage systems on a distribution network enhanced by high-capacity photovoltaic systems. *Journal of Energy Storage*, *12*, 121–131.

Kiprakis, A.E. (2005). Increasing the Capacity of Distributed Generation in Electricity Networks by Intelligent Generator Control. Unpublished PhD dissertation, The University of Edinburgh.

Komarnicki, P., Lombardi, P., Styczynski, Z. (2017). Electric Energy Storage Systems Flexibility Options for Smart Grids. Berlin: Springer.

Kraiczy, M., Fakhri, L. A., Stetz, T., & Braun, M. (2017). Do It Locally : Local Voltage Support by Distributed Generation – A Management Summary. The International Energy Agency.

Kulmala, A., & Repo, S. (2014). Coordinated Voltage Control in Distributed Networks including several Distributed Energy Resources. 2010. *IEEE Transactions on Smart Grid*, *5*(4), 2010–2020.

Kuroda, K., & Magori, H. (2015). A hybrid multi-objective optimization method considering optimization problems in power distribution systems, *Power Syst. Clean Energy (2015*) 3(1):41–50.

Lai, J., Lu, X., Tang, R., Li, X., & Dong, Z. (2019). Delay-tolerant distributed voltage control for multiple smart loads in AC microgrids. *ISA Transactions*, *86*, 181–191.

Law, Y. W., Lee, V. C., & Lo, A. (2015). Demand response architectures and load management algorithms for energy-efficient power grids : a survey. *2012 Seventh International Conference on Knowledge, Information and Creativity Support Systems*, 134–141.

Li, B., Chen, M., Cheng, T., Li, Y., Arshad, M., Hassan, S., Xu, R., Chen, T. (2018). Distributed Control of Energy-Storage Systems for Voltage Regulation in Distribution Network with High PV Penetration. *UKACC,12th International Conference on Control (CONTROL) Sheffield, UK*, 5-7 Sept 2018 5–7.

Li, C., Disfani, V. R., Pecenak, Z. K., Mohajeryami, S., & Kleissl, J. (2018). Optimal OLTC voltage control scheme to enable high solar penetrations. *Electric Power Systems Research*, *160*, 318–326.

Li, P., Ji, H., Yu, H., Zhao, J., Wang, C., Song, G., & Wu, J. (2019). Combined decentralized and local voltage control strategy of soft open points in active distribution networks. *Applied Energy*, *241*(March), 613–624.

Li, Y., Li, L., Peng, C., & Zou, J. (2019). An MPC based optimized control approach for EV-based voltage regulation in distribution grid. *Electric Power Systems Research*, *172*(July 2018), 152–160.

Lip, W., Shiun, J., Shin, W., Hashim, H., & Tin, C. (2017). Review of distributed generation (DG) system planning and optimisation techniques : Comparison of numerical and mathematical modelling methods. *Renewable and Sustainable Energy Reviews*, *67*, 531–573.

Liu, H. J., Shi, W., & Zhu, H. (2017). Decentralized Dynamic Optimization for Power. *IEEE Transaction on Signal and Information Processing over Networks*, *3*(3), 568–579.

Liu, H. J., Shi, W., & Zhu, H. (2019). Under Limited Communication Rates. *IEEE Transactions on Smart Grid*, *10*(3), 2416–2427.

Liu, Y., Qin, W., Han, X., Wang, P., Wang, Y., Lei, W. & Li, F. (2018). Distribution Network Voltage Control by Active Power / Reactive Power Injection from PV Inverters. *IEEE Transaction on Power Systems*, 543–547.

Luo, X., Wang, J., Dooner, M., & Clarke, J. (2015). Overview of current development in electrical energy storage technologies and the application potential in power system operation. *Applied Energy*, *137*, 511–536.

Mahmud, N., & Zahedi, A. (2016). An event-triggered distributed coordinated voltage control strategy for large grid-tied PV system with battery energy storage. *2017 Australasian Universities Power Engineering Conference (AUPEC),* 19-22 Nov. 2017.

Mahmud, N., & Zahedi, A. (2016). Review of control strategies for voltage regulation of the smart distribution network with high penetration of renewable distributed generation. *Renewable and Sustainable Energy Reviews*, *64*, 582–595.

Marinelli, M. (2016). Phase-wise enhanced voltage support from electric vehicles in a Danish low-voltage distribution grid. *Electric Power Systems Research*, *140*, 274–283.

Melhem, Z. (2013). Electricty transmission, distribution and storage systems. Philadelphia: Woodhead Publsihing.

Mehrjerdi, H., Lefebvre, S., Saad, M., & Asber, D. (2013). A Decentralized Control of Partitioned Power Networks for Voltage Regulation and Prevention Against Disturbance Propagation. *IEEE Transactions on Power Systems*, *28*(2), 1461–1469.

Mocci, S., Natale, N., Pilo, F., & Ruggeri, S. (2015). Demand side integration in LV smart grids with multi-agent control system. *Electric Power Systems Research*, *125*, 23–33.

Mokgonyana, L., Zhang, J., Zhang, L., & Xia, X. (2016). Coordinated two-stage volt / var management in distribution networks. *Electric Power Systems Research*, *141*, 157–164.

Mokhtari, G., Nourbakhsh, G., Zare, F., & Ghosh, A. (2013). Overvoltage prevention in LV smart grid using customer resources coordination. *Energy & Buildings*, *61*, 387–395.

Mufaris, A. L. M., & Baba, J. (2015). Dynamic Voltage Regulator Operation with Demand Side Management for Voltage Control. *2015 IEEE Eindhoven PowerTech*, 1–6.

Naidoo, P., Goko, C., Cohen, M. (2019). https://www.fin24.com/Economy/sa-has-a-sovereign-debt-problem-its-name-is-eskom-20190724 (accessed 24 July 2019).

Nasiri, B., Ahsan, A., Gonzalez, D. M., Wagner, C., Häger, U., & Rehtanz, C. (2016). Integration of Smart Grid Technologies for Voltage Regulation in Low Voltage Distribution Grids. *IEEE Innovative Smart Grid Technologies - Asia (ISGT-Asia), Melbourne, Australia*, Nov 28 - Dec 1, 2016 3–8.

NERSA, NRS 048-2-2003, Electricity Supply - Quality of Supply, Part 2: Voltage characteristics, compatibility levels, limits and assessment methods; 2003. http://www.nersa.org.za/Admin/Document/Editor/file/Electricity/IndustryStandards/NRS048%20part%202.pdf

Newbery, D., & Eberhard, A. (2008). South African Network Infrastructure Review: Electricity. Pretoria: National Treasury and the Department of Public Enterprises of South Africa

Nimpitiwan, N., & Chaiyabut, C. (n.d.). Centralized Control of System Voltage / Reactive Power Using Genetic Algorithm. *2007 International Conference on Intelligent Systems Applications to Power Systems,* 5-8 Nov. 2007.

Olival, P. C., Madureira, A. G., & Matos, M. (2017). Advanced voltage control for smart microgrids using distributed energy resources. *Electric Power Systems Research*, *146*, 132–140.

Onori, S., Serrao, L., Rizzoni, G. (2017). *Hybrid Electric Vehicles Energy Management Strategies*. London: Springer

Oshiro, M., Tanaka, K., Senjyu, T., Toma, S., Yona, A., Yousuf, A., Funabashi, T. & Kim, C. (2011). Electrical Power and Energy Systems Optimal voltage control in distribution systems using PV generators. *International Journal of Electrical Power and Energy Systems*, *33*(3), 485–492.

Ovalle, A., Hably, A., & Bacha, S. (2018). *Grid Optimal Integration of Electric Vehicles: Examples with Matlab Implementation*, Studies in Systems, Decision and Control 137. Springer

Padullaparti, H. V, Nguyen, Q., & Santoso, S. (2016). Advances in Volt-var Control Approaches in Utility Distribution Systems. *IEEE Power & Energy Society General Meeting, Boston, MA*, July 17-21, 2016

Pathipati, V. K., Shafiei, A., & Carli, G. (2017). *Integration of Renewable Energy Sources into the Transportation and Electricity Sectors*. Cham: Springer International Publishing

Paula, A., Mello, C. De, Lopes, L., & Pinheiro, D. (2017). Coordinated Volt / VAr control for real-time operation of smart distribution grids. *Electric Power Systems Research*, *151*, 233–242.

Petinrin, J. O., & Shaaban, M. (2014). Voltage Control in a Smart Distribution Network Using Demand Response. *2014 IEEE International Conference on Power and Energy (PECon)*, 319–324.

Petinrin, J. O., & Shaaban, M. (2016). Impact of renewable generation on voltage control in distribution systems. *Renewable and Sustainable Energy Reviews*, *65*, 770–783.

Pournazarian, B., Karimyan, P., Gharehpetian, G. B., & Abedi, M. (2019). Electrical Power and Energy Systems Smart participation of PHEVs in controlling voltage and frequency of island microgrids. *Electrical Power and Energy Systems*, *110*(October 2018), 510–522.

Quijano, D. A., & Padilha-feltrin, A. (2019). Electrical Power and Energy Systems Optimal integration of distributed generation and conservation voltage reduction in active distribution networks. *Electrical Power and Energy Systems*, *113*(October 2018), 197–207.

Rabiee, A. & Mohseni-bonab, S. M. (2019). Optimal Cost of Voltage Security Control Using Voltage Dependent Load Models in Presence of Demand Response. *IEEE Transactions on Smart Grid*, *10*(3), 2383–2395.

Rahman, M., Arefia, A., Shafiullaha, G. M., & Hettiwatte, S. (2018). A new approach to voltage management in unbalanced low voltage networks using demand response and OLTC considering consumer preference, *99*(January), 11–27. *Electrical Power and Energy Systems* 99 (2018) 11–27.

Rashid, M. H. (2015). Alternative Energy in Power Electronics. Butterworth-Heinemann

Rashidi, L., & Moshtagh, J. (2014). Decentralized Control For Optimal Voltage Regulation In Smart Distribution Grids. *2014 Smart Grid Conference (SGC)*, 1–7.

Rathbun, M., Rathbun, M., Rathbun, M., & Florida, C. (2018). Impact Studies and Cooperative Control for High PV Penetration. *IFAC-PapersOnLine*, *51*(28), 684–689.

Resener, M., Haffner, S., Pereira, L. A., & Pardalos, P. M. (2018). Optimization techniques applied to planning of electric power distribution systems : a bibliographic survey. *Energy Syst* (2018) 9:473–509.

SAGC, Grid connection code requirements for renewable power plants (RPPS) connected to the transmission system (TS) or the distribution system (DS) in South Africa, 2012..

Sarimuthu, C. R., Ramachandaramurthy, V. K., Agileswari, K. R., & Mokhlis, H. (2016). A review on voltage control methods using on-load tap changer transformers for networks with renewable energy sources. *Renewable and Sustainable Energy Reviews*, *62*, 1154–1161.

Sclater, N. & John E. Traister, J.E. (2003). **Handbook of Electrical Design Details, Second Edition**: New York City, McGraw-Hill Engineering

Shaoyun, G. E., Fournier, J., & Andri, I. (2019). Coordinated Voltage Control for Active Distribution Network considering the impct of Energy Storage. *Energy Procedia*, *158*(2018), 1122–1127.

Siewierski, T., Szypowski, M., & Andrzej, W. (2018). A review of economic aspects of voltage control in LV smart grids. *Renewable and Sustainable Energy Reviews* 88 (2018) 37–45.

Solanki, J., Venkatesan, N., Member, S., & Khushalani, S. (2012). Coordination of Demand Response and Volt / Var Control Algorithm using Multi Agent System. *PES T&D 2012*, 1–4.

Ssekulima, E. B., & Hinai, A. Al. (2016). Coordinated Voltage Control of Solar PV with MPPT and Battery Storage in Grid-Connected and Microgrid Modes. *2016 18th Mediterranean Electrotechnical Conference (MELECON)*, (April), 1–6.

Kraiczy, M., Al Fakhri, L., Stetz, T. (2017) (2017). Do It Locally : Local Voltage Support by Distributed Generation – A Management Summary. Management Summary of IEA Task 14 Subtask 2 – Recommendations Based on Research and Field Experience. International Energy Agency, Paris.

STATSSA. (2018). *The latest household statistics and more*. Department: Statistics South Africa, Pretoria.

Swain, K. P., & De, M. (2019). A novel electrical proximity index for voltage control in smart distribution system. *Electric Power Systems Research*, *172*(June 2018), 50–62.

Tabatabaei, N. M., Aghbolaghi, A. J., Bizon, N., Blaabjerg, F. (2017). *Reactive Power Control in AC Power Systems*: Fundamentals and Current Issues. Cham: Springer

Taghavipour, A., Vajedi, M., & Azad, N. L. (2019). *Intelligent Control of Connected Plug- in Hybrid Electric Vehicles*.Cham: Spinger.

Takahashi, N., & Hayashi, Y. (2012). Centralized voltage control method using plural D-STATCOM with controllable dead band in distribution system with renewable energy. *2012 3rd IEEE PES Innovative Smart Grid Technologies Europe (ISGT Europe)*, 1–5.

Takayama, S., & Ishigame, A. (2018). Autonomous Decentralized Control of Distribution Network Voltage using Reinforcement Learning. *IFAC-PapersOnLine*, *51*(28), 209–214.

Tanaka, K. (2009). Decentralized Voltage Control in Distribution Systems by Distributed Generators. *2009 IEEE International Symposium on Industrial Electronics*, (ISIE), 554–559.

Tengku, J., Mohamed, A., & Shareef, H. (2012). A review on voltage control methods for active distribution networks, (June 2014).

USAID (2018). https://www.usaid.gov/sites/default/files/documents/1860/South_Africa_-_November_2018_Country_Fact_Sheet.pdf (accessed 15 June 2019)

Van Zyl, S.J & C.T Gaunt,C.T. Control Strategies for Distributed Generation operation on Weak Distribution Networks, IEEE Bologna Power Tech Conference; 2003. https://doi.org/10.1109/PTC.2003.1304398

Veneri, O. (2017). *Technologies and Applications for Smart Charging of Electric and Plug-in Hybrid Vehicles*. Cham: Springer.

Viawan, F. A. (2008). *Voltage Control and Voltage Stability of Power Distribution Systems in the Presence of Distributed Generation*. Unpublished PhD dissertation, Chalmers Uiversity of Technology, Gothenburg, Sweden.

Villacci, D. (2019). A Decentralized Architecture Based on Cooperative Smart Grids. *Energies* 2019, 12, 1386.

Vovos, P. N., Kiprakis, A. E., Wallace, A. R., & Harrison, G. P. (2007). Centralized and Distributed Voltage Control : Impact on Distributed Generation Penetration. *IEEE Transactions on Power Systems*, *22*(1), 476–483.

Walling, R. A. R., Saint, R., Dugan, R. C., Burke, J. & Kojovic, L. A. (2008). Summary of Distributed Resources Impact on Power Delivery Systems. *IEEE Transactions on Power Delivery*, *23*(3), 1636–1644.

Wang, Y., John, T., & Xiong, B. (2019). A two-level coordinated voltage control scheme of electric vehicle chargers in low-voltage distribution networks. *Electric Power Systems Research*, *168*(July 2018), 218–227.

Wang, Y., Tan, K. T., Peng, X. Y, & So, P. L. (2016). Coordinated Control of Distributed Energy-Storage Systems for Voltage Regulation in Distribution Networks. *IEEE Transaction on Power Delivery*, *31*(3), 1132–1141.

World Bank. (2005). *Primer on Demand-Side Management with an emphasis on price-responsive programs*. Washington DC.

Wu, H., Huang, C., & Ding, M. (2017). Cooperative Strategy for Distributed Voltage Control in Active Distribution Feeders. *IEEE PEDS 2017, Honolulu, USA*, 12 – 15 December 2017, 125–130.

Wu, J., Rangan, S., Zhang, H. (2013). Green Communications: Theoretical Fundamentals, Algorithms and Applications, London: CRC Press.

Xie, Q. (2017). Centralized Residential Load Scheduling with Consideration of Voltage Control in Future Distribution System. *2017 2nd International Conference on Power and Renewable Energy (ICPRE)*, 301–305.

Xu, T., & Taylor, P. C. (2008). Voltage Control Techniques for Electrical Distribution Networks Including Distributed Generation. *Proceedings of the 17th World Congress The International Federation of Automatic Control Seoul, Seoul, Korea*, July 6-11, 2008 (1), 11967–11971.

Yang, X. (2014). Optimization and Metaheuristic Algorithms in Engineering. *Elsevier,* (2013), pp. 1-23

Yang, Y., Li, H. & Aichhorn, A. (2014). Sizing Strategy of Distributed Battery Storage System With High Penetration of Photovoltaic for Voltage Regulation and Peak Load Shaving. *IEEE Transactions on Smart Grid*, *5*(2), 982–991.

Yazdanian, M., S., & Mehrizi-sani, A. (2014). Distributed Control Techniques in Microgrids. *IEEE Transactions on Smart Grid*, *5*(6), 2901–2909.

Yi, J., Wang, P., Taylor, P. C., Davison, P. J., Lyons, P. F., Liang, D., Brown, S. & Roberts, D. (2012). Distributed Network Voltage control Using Energy Storage and Demand Side Response. 3*rd IEEE PES Innovative Smart Grid Technologies Europe (ISGT Europe), Berlin*, 2012, 1–8.

Yorino, N., Zoka, Y., & Watanabe, M. (2015). An Optimal Autonomous Decentralized Control Method for Voltage Control Devices by Using a Multi-Agent System. *IEEE Transactions on Power Systems*, *30*(5), 2225–2233.

Yujun, H., & Petit, M. (2013). Active Voltage Control Using Distributed Generation on Distribution Networks. *2013 IEEE Grenoble Conference*, 1–6.

Zakariazadeh, A., Homaee, O., Jadid, S., & Siano, P. (2014). A new approach for real time voltage control using demand response in an automated distribution system. *Applied Energy*, *117*, 157–166.

Zecchino, A., & Marinelli, M. (2018). Electrical Power and Energy Systems Analytical assessment of voltage support via reactive power from new electric vehicles supply equipment in radial distribution grids with voltage-dependent loads. *Electrical Power and Energy Systems*, *97*(September 2017), 17–27.

Zeraati, M., Esmail, M., Golshan, H., & Guerrero, J. M. (2018). Distributed Control of Battery Energy Storage Systems for Voltage Regulation in Distribution Networks With High PV Penetration. *IEEE Transactions on Smart Grid*, *9*(4), 3582–3593.

Zeraati, M., Esmail, M., Golshan, H., & Guerrero, J. M. (2019). A Consensus-Based Cooperative Control of PEV Battery and PV Active Power Curtailment for Voltage Regulation in Distribution Networks. *IEEE Transactions on Smart Grid*, *10*(1), 670–680.

Zhao, B., Wang, C., & X. Zhang. X. (2018). Grid-Integrated and Standalone Photovoltaic Distributed Generation Systems: Analysis, Design, and Control, New Jersey: John Wiley; 2018.

Zimann, F. J., Batschauer, A. L., Mezaroba, M., & Neves, F. A. S. (2019). Energy storage system control algorithm for voltage regulation with active and reactive power injection in low-voltage distribution network. *Electric Power Systems Research*, *174*(February), 105825.